Government of the People's Republic of Bangladesh
Bangladesh Water Development Board

River Training Studies of The Brahmaputra River

Report on Model Studies

Volume 4

Comprising

Part 9	Calibration and Verification of 2-D Morphological Model
Part 10	2-D Numerical Modelling of River Bends
Part 11	2-D Numerical Modelling of Confluence Scour
Part 12	2-D Numerical Modelling of Flow and Scour Around a Groyne
Part 13	2-D Numerical Modelling of Bifurcation and Stability of Anabranches
Part 14	2-D Numerical Modelling of River Constriction Effects due to Jamuna Bridge Embankments

March 1993

Sir William Halcrow & Partners Ltd.

in association with

Danish Hydraulic Institute
Engineering & Planning Consultants Ltd.
Design Innovations Group

HALCROW

Government of the People's Republic of Bangladesh
Bangladesh Water Development Board

River Training Studies of The Brahmaputra River

Report on Model Studies

Volume 4

Comprising

Part 9	**Calibration and Verification of 2-D Morphological Model**
Part 10	**2-D Numerical Modelling of River Bends**
Part 11	**2-D Numerical Modelling of Confluence Scour**
Part 12	**2-D Numerical Modelling of Flow and Scour Around a Groyne**
Part 13	**2-D Numerical Modelling of Bifurcation and Stability of Anabranches**
Part 14	**2-D Numerical Modelling of River Constriction Effects due to Jamuna Bridge Embankments**

March 1993

A-16

Sir William Halcrow & Partners Ltd has prepared this report in accordance with the instructions of the Bangladesh Water Development Board for their sole and specific use. Any other persons who use any information contained herein do so at their own risk.

Sir William Halcrow & Partners Ltd.

in association with

Danish Hydraulic Institute
Engineering & Planning Consultants Ltd.
Design Innovations Group

RIVER TRAINING STUDIES OF THE BRAHMAPUTRA RIVER

REPORT ON MODEL STUDIES

GENERAL CONTENTS

Part 9

Calibration and Verification of 2-D Morphological Model

RIVER TRAINING STUDIES OF THE BRAHMAPUTRA RIVER

REPORT ON MODEL STUDIES

PART 9 - VERIFICATION OF THE 2-D MORPHOLOGICAL MODEL

CONTENTS

TABLES

FIGURES

1. OBJECTIVE

The 2-D mathematical model has been developed to simulate the complex interchange between hydrodynamic (HD) flow conditions and sediment transport (ST) and derived morphological changes. The overall objectives were described in details in "Working Paper on 2-D Modelling" (BRTS 1990). The model has been set up, calibrated, and verified against field data from two test areas before simulating selected key phenomena of importance for the BRTS-study. The calibration was described in the First Interim Report (BRTS 1990). In this report, the verification phase is summarized.

2. APPROACH

Two mathematical base models were set up for Test Area 1 at Sirajganj and for a second test area at Kazipur for simulation of the particular conditions prevailing in the sharp concave bend that has developed at this location.

The calibration and verification phases are schematizised in Table 2.1. It also shows where the various calibrations and verifications are reported.

Table 2.1: Calibration and Verification Phases of the 2-D Model

Submodel	TEST AREA 1 June	July	November	TEST AREA 2 December	August
Hydrodynamics		C[1]	V[3]		V[3]
Sediment Transport		C[1]	V[3]		V[3]
Bed forms		C[1]			
Morphology	C[1]	C[1]	V[3]	V[3]	V[3]
Bank erosion	C[2]	C[2]	C[2]	V[2]	V[2]

C = Calibration V = Verification

1) First Interim report
2) Analysis of Sediment Data
3) Present Report

In Chapter 3, the verification of the hydrodynamical model and sediment transport model based on data from Test Area 1, November 1990, is described. The verification of morphology from the same period and area is described in Chapter 4. The verification phase of the various submodels based on data from Test Area 2 is dealt with in Chapter 5. In Chapter 6, the findings are summarized.

3. TEST AREA 1, HD AND ST

3.1 Objective

The HD-and ST-model was calibrated against data collected during the monsoon season of 1990. The objective of this study was to see whether the same calibration was valid for post-monsoon conditions.

3.2 Approach

The bathymetry was surveyed in November 1990 together with measurements of velocity. The discharge was determined by taking the average of discharge calculations at different cross sections. The water level was known at Shahapur (downstream d/s) and Sirajganj (upstream u/s). The calibrated HD-model was then used to simulate velocities and the slope of the water surface. The calibrated ST-model was used to simulate the concentration of suspended sediment. By comparing these results with the field measurements, the quality of the calibration of the model could be evaluated.

3.3 Description of the Model

The bathymetry shown in Figure 3.1 was used. It was based on the survey from November 1990. The bathymetry was smoothened so that the influence of dunes on the mean bed level for each grid point was eliminated. The d/s condition was a constant water level of 8.84 m at Shahapur gauge station in both anabranches. A constant discharge of 14000 m^3/s was used as the u/s boundary condition. The discharge was calculated from velocity and depth measurements in three different cross-sections. The bed resistance from the calibration of monsoon data was applied:

$$C = 74 \left(\frac{D}{D_0}\right)^{0.25} m^{0.5}/s$$

D = depth, D_o = mean depth

3.4 Results and Conclusion

The observed water level at the u/s boundary was 9.59 m. The simulated level was only 9.39 m when a mean Chezy Number of 74 m 0.5/s was used. Good agreement between observed and simulated velocities was obtained, see Figure 3.2 to 3.5. However, the velocity in the d/s West anabranch seemed to be a little too low. The reason could be that the d/s water level in the East channel should be higher. Then the u/s water level would also increase.

The simulation indicated that the bed resistance would increase outside the monsoon season. If the value

$$C = 60 \left(\frac{D}{D_0}\right)^{0.25}$$

was used instead, the simulated u/s water level would be 9.58 m (9.59 m was the observed value). This is also in agreement with the usual assumption that the Chezy number varies with the mean depth:

$C \alpha D^{\frac{1}{6}}$

The mean depth decreased from 7.0 m in July to 3.5 m in November. Hence the Chezy value should reduce by 11% according to the equation above.

In the Jamuna Bridge Project (RPT/NEDECO/BCL, Aug 1989), it was found that the Chezy Number varied between 40 $m^{0.5}/s$ for low flow and 100 $m^{0.5}/s$ for flood conditions based on BWDB discharge measurements.

The simulated concentration of suspended sediment is plotted in Figure 3.6 and Figure 3.7 for Engelund/Fredsoe MOVA model and the van Rijn model, respectively. The latter had a modified description of the Vanoni-profile as described in the First Interim Report, Annex 1. The concentration computations are compared with measurements in Table 3.1. The best agreement between observation and simulation was obtained with the Engelund/Fredsoe model with the modified Vanoni-profile where the mean difference between observed and simulated concentration was less than 11 %. For van Rijn, the simulated was about 50 % smaller than the observed value.

The study revealed that the Chezy Number must be modified depth ie. when the depth is different from the one found in Test Area 1 in July. For post-monsoon conditions, the Engelund/Fredsoe model performed very satisfactorily.

Table 3.1: **Measured Concentration (g/l) of Suspended Sediment and Simulated Values with van Rijn and with Engelund/Fredsoe Models**

No.	Measured	van Rijn	Engelund/Fredsoe (MOVA)
1	0.334	1.202	0.919
2	0.345	0.045	0.131
3	0.337	0.056	0.235
4	0.099	0.018	0.022
5	0.257	0.106	0.327
6	0.358	0.098	0.270
7	0.027	0.069	0.076
8	0.082	0.095	0.164
9	0.319	0.106	0.332
10	0.299	0.180	0.378
11	0.080	0.058	0.086
12	0.411	0.010	0.003
13	0.093	0.129	0.345
14	0.086	0.049	0.101
15	0.261	0.163	0.301
16	0.252	0.062	0.151
17	0.285	0.033	0.116
18	0.198	0.084	0.211
19	0.612	0.046	0.083
20	0.149	0.035	0.126
21	0.189	0.028	0.081
22	0.111	0.000	0.000
23	0.102	0.340	0.689
24	0.260	0.276	0.558
25	0.144	0.000	0.000
26	0.541	0.037	0.069
27	0.281	0.033	0.094
28	0.119	0.079	0.066
29	0.186	0.135	0.193
30	0.195	0.088	0.125
Mean Value	0.234 g/l	0.122 g/l	0.208 g/l

4. TEST AREA 1, MORPHOLOGY

4.1 Objective

The objective of this study was to see how sediment transport varies over the year. The regime equation for sediment transport derived in the JMB-study (RPT/NEDECO/BCL 1987) was verified by comparison between the 2-D model, measurements in the field and the regime equation

$$Q_s = 4.5 \times 10^{-6} Q^{1.38} \; m^3/s$$

4.2 Approach

It was the intention to simulate the full period from low to high flow conditions. Difficulties in describing the inundation and drying of bars and chars in the 2-D model prevented this and a revised approach had to be adopted. The different periods, each with a given discharge, were simulated separately and compared. The discharges 8000 m^3/s, 17850 m^3/s, 53750 m^3/s, and 62000 m^3/s were chosen to be representative for the seasons.

4.3 Description of the Model

The calibrated model from July 1990 was used in all simulations, see First Interim Report, Annex 3 (BRTS,1990). For each simulation, the upstream (u/s) boundary condition was the predefined discharge. The downstream (d/s) boundary condition was water levels found from 1-D model runs, see Table 4.1 below.

Table 4.1: Boundary Conditions for the Simulations

Discharge u/s	Water level West d/s	Water level East d/s
8000 m^3/s	8.5 m	8.6 m
17850 m^3/s	10.2 m	10.2 m
53750 m^3/s	13.2 m	13.4 m
62000 m^3/s	13.5 m	13.7 m

For calculation of the sediment transport the van Rijn formulation was used. The fall velocity was 0.020 m/s. The grain diameter was 0.15 mm, based on the field survey data.

4.4 Results and Conclusions

The simulations are presented in the following figures, see Table 2.

Table 4.2: Matrix for Presentation of the Results of Simulations.

Discharge	Velocity	Sediment	Comparison
8000	Fig 4.1	Fig 4.5	Fig 4.7 + Fig 4.11
17850	Fig 4.2	-	Fig 4.8
53750	Fig 4.3	-	Fig 4.9
62000	Fig 4.4	Fig 4.6	Fig 4.10 +Fig 4.11

During the dry season, the flow follows small channels formed in between the dry chars, and the thalweg will be visible. The channels meander in the river valley, see for example the South West anabranch in Figure 4.1. The velocity can still be high because of the reduction in cross sectional area.

The sediment transport rate varies significantly along the thalweg. It reflects that the bathymetry is out of equilibrium and morphological changes are on-going. It also shows that the scatter in the sediment data from the field survey is not only due to the measurement technique. A natural scatter is inherent in nature. Hence regime equations will be associated with some uncertainty.

In Figure 4.7 to 4.11, the sediment transport rate has been integrated over the width of the river. The graphs show the total transport rate at different cross sections along the river. If the bathymetry was in equilibrium, the graph would be horizontal. However, it varies significantly as mentioned above. The measured transport rate fits well with the simulated average value. The regime equation is also quite accurate for large discharges. For small discharges, the regime equation tends to overestimate the transport rate.

In Figure 4.11, the sediment transport at Q=8000 m^3/s and at Q=62000 m^3/s is compared. The difference in sediment transport is more than a factor 10 indicating that morphological changes are negligible outside the monsoon period.

5. TEST AREA 2, HD, ST AND MORPHOLOGY

5.1 Objective

Upon analysis of data from Test Area 1, it was found that this location did not include severe bend scour which is one of the main characteristics of the river at the exposed areas of the bank. Hence a second test area adjacent to Kazipur where two actively eroding bends were present was chosen for verification of the 2-D simulation of bend scour.

5.2 Approach

Data were collected with some months interval so that the rate of scour could be measured. The 2-D model was employed to calculate velocities, water levels and erosion/deposition rate.

The water levels and velocities were simulated without changing the calibration from Test Area 1. This exercise would show whether the calibration from Test Area 1 was representative for this area also. If so, the model could be used for simulations in other parts of the river where there were not sufficient field data for a proper calibration.

The sediment transport was simulated without changing the calibration from Test Area 1. The amount of sediment data from Test Area 2 was much smaller but of better quality than in Test Area 1. It was the aim of the simulation to verify whether the same concentration of suspended bed material as measured and the same development of the scourhole could be simulated by the 2-D model.

In order to assess the various assumptions which were necessary to supplement the information in the site specific data, some sensitivity runs of the uncertain parameters were also carried out.

5.3 Data Collection

Test Area 2 at Kazipur was surveyed in December/January 1991 and resurveyed in August 1991. Due to strong currents and submerged chars, it was difficult to operate inside the area and to cover the full test area during the monsoon survey. However, from the bathymetry in December 1990 and the bathymetry in August 1991, it was possible to derive the erosion and deposition in that period. The scour hole close to the bankline at Kazipur has migrated downstream by 800-1000 m and heavy bank erosion has occurred in the south west corner of the test area. For these reasons it was necessary to extend the model area of Test Area 2, see Figures 5.1 and 5.2.

The right bankline at Kazipur has been monitored at different times since December 1990 in order to estimate the bank erosion rate at different times of the year, see Figure 5.3.

Velocity was measured during the August survey at eight different stations in the west channel upstream the scour hole. Measurements were taken at different depths so that the velocity profile could be evaluated from the data. Especially it was hoped that the helical flow component could be extracted from the measurements. If so, the velocity vector at the surface should point more towards the outer bank and the

velocity vector at the bottom should be directed more towards the inner bank (the char). But it was not possible to detect such a trend.

Some float tracks were also monitored and they showed, that the velocity vector at the surface was directed outwards against the bank. This could be observed by the floats which eventually landed on the bank.

At each station, a sample of 25 l of water was pumped from a specific depth and filtered through a 0.053 mm sieve in order to remove all wash load. The filtrate (sand) was backwashed into small bottles and brought to the laboratory for analysis. From the samples, the concentration of suspended sand and the grain size were found. The mean grain size of suspended sand was 0.077 mm and the mean concentration of all samples was 0.21 g/l.

Also samples from the river bed were taken at the different stations. The mean grain size was 0.171 mm but the difference from one station to another was much greater than for the suspended material. The most coarse material was located in the middle of the deep channel whereas the fine material was found on the chars.

5.4 HD - Model

The following was needed to run the hydrodynamic model:

- bathymetry,
- downstream water level,
- upstream discharge,

and the following had to be available when the calibration was tested:

- upstream water level,
- velocity inside the model area.

For Test Area 2, the upstream discharge was estimated from velocity measurements in the middle of the Test Area. By assuming a constant resistance Manning Number across the river, the discharge was estimated at Q= 21000 m^3/s by the expression:

$$Q = K\int_0^w d^{\frac{5}{3}}\,dw$$

where w is the width of the cross section, d is the depth and k is estimated by

$$K = \left(\sum_{i=1}^{n} v_i d_i^{\frac{2}{3}}\right)/n$$

where n is number of velocity measurements and v and d are, respectively, mean velocity and depth at station number i.

Only the water level downstream was measured, see location in Figure 5.2. It was 15.41 m during the field survey in August.

The upstream water level was estimated by the 1-D model by simulating the 1988 event. On the day of the same water level (15.41 m), the water surface slope was derived from the simulation:

$$I = 12 \times 10^{-5}$$

The length of Test Area 2 was approximately 5.8 km. Hence the upstream water level should be about 16.1 m. This calculation has some uncertainty because the gradient could vary considerably between different anabranches over the cross section.

The simulated surface elevation with Q=21000 m^3/s and downstream water level 15.41 m is shown in Figure 5.4. The upstream water level is close to 16.1 m at the right bank. The simulated velocity field is shown in Figures 5.5 and 5.6 and fits reasonable well with the measured velocities.In the simulation, the Chezy Number found from Test Area 1 was used, see "First Interim Report, Annex 3, Part 2", BRTS(1990):

$$C = 74 \left(\frac{D}{D_0}\right)^{0.25} m^{\frac{1}{2}}/s$$

mean depth D_0 =7.0 m

The determination of the upstream discharge was inaccurate for which reason some sensitivity runs were carried out. If the discharge was Q=16000 m^3/s, the upstream water level would be 15.8 m and if the discharge was Q=26000 m^3/s, the upstream water level would be 16.4 m. In both cases, however, the simulated velocities would be different from the measurements. In the following, a discharge of 21000 m^3/s and the Chezy Number given above was used.

5.5 ST - Model

The required data for running the sediment transport model was

- hydrodynamics (water level and velocities)
- grain size of bed material (spatial distribution if available)
- water temperature, which influences the fall velocity of sediment particles and viscosity of the water

The fall velocity was derived from relationships between fall velocity and grain size. In order to verify the model, the following data were required:

- concentration of suspended sediment inside the area
- changes in bed level over a specific period of time

The model was calibrated by choosing the mathematical description of the sediment transport (Van Rijn, Engelund & Fredsoe, Engelund-Hansen) which was most close to the observed sediment transport rates. A refined calibration was obtained by using a factor on the sediment transport rate. This factor should not go beyond the range 0.5 to 2. Using a factor like this can be justified because all transport models

are based to some extent on empirical data. The scaling factor is used because the data from the actual site may differ from those used when the model was developed.

Van Rijn and Engelund & Fredsoe equations proved to be adequate descriptions of the sediment transport in Test Area 1, see "First Interim Report, Annex 3, Part 2", BRTS(1990). In the following, the Van Rijn model was used.

The grain size of bed material varied inside the test area from 0.1 mm in the shallow areas to 0.2 mm in the deep channels, see Figure 5.7. Different runs were carried out and compared in order to analyse the sensitivity of various assumptions. In Table 5.1 the results are summarised. The simulated concentrations seem to be a little too high in all simulations. But with a scaling factor of 0.5 on Van Rijn, the mean concentration between all stations was similar in measurements and in simulation. The concentration of suspended sediment is shown in Figure 5.8.

The next phase in the verification of the sediment model was to examine whether the 2-D model would simulate morphological changes satisfactorily.

Table 5.1: Observed and Simulated Concentration of Suspended Sediment (Bed Material).

Stn.	Observed concentration (g/l)	Simulated Concentration (g/l) 1	2	3	4	5
1	0.35	0.07	0.08	0.06	0.08	0.08
2	0.54	0.30	0.33	0.24	0.32	0.41
3	0.07	0.36	0.38	0.30	0.37	0.46
4	0.07	0.28	0.30	0.23	0.26	0.23
5	-	-	-	-	-	-
6	0.15	0.39	0.46	0.30	0.34	0.30
7	0.20	1.08	1.19	0.89	1.20	2.47
8	-	-	-	-	-	-
9	0.26	0.36	0.40	0.29	0.66	2.74
Mean	0.23	0.40	0.45	0.33	0.46	0.96

Simulation Code

1: van Rijn, constant grain size d=0.17 mm
2: van Rijn, constant grain size d=0.17 mm, viscosity v=1 10^{-6} $m^{0.5}/s$
3: van Rijn, constant grain size d=0.20 mm
4: van Rijn, varying grain size, d_{50}=0.17 mm
5: Engelund & Fredsoe, varying grain size, d_{50}=0.17 mm

5.6 Morphology Model

Sediment Transport

When the sediment transport was simulated with the bathymetry shown in Figure 5.2, it turned out that the transport rate was increasing from the upstream to the downstream end which meant that the model would erode heavily from the downstream end until the sediment transport was lowered in the whole area, see Figures 5.9 and 5.10. Figure 5.10 shows the sediment transport integrated over the width of the river as a function of distance along the thalweg at four different times: 0,7,14,21 days. If the bathymetry were in equilibrium, the graph in Figure 5.10 would be a horizontal line. This was not the case at the beginning but it is seen that the 2-D model tries to dampen out the fluctuations as it happens in the prototype. However, due to continuous changes in the flow conditions, new "waves" will be generated all the time in nature especially during sudden rise or fall in water level.

Data on the sediment inflow into the test area were not available so it was necessary to assume that the sediment transport at the boundary (k=45) balanced the capacity of the flow at a specific depth and with a specific velocity. For that reason, the sediment transport and thus the change in bed level were connected with some degree of uncertainty in the upper part of the model area. Figure 5.10 and Figure 5.13 show how much the sediment transport varied inside the model while at the upper boundary (k=45) it was maintained as constant. A second simulation (Figure 5.13), see below, was carried out in order to estimate the importance of this boundary condition.

Change in Bed Level

The simulated bathymetry after 21 days with the same discharge as in the hydrodynamic simulation (21000 m^3/s) is shown in Figure 5.11, and the difference in bathymetry over that period is shown in Figure 5.12.

The upstream boundary conditions govern how the morphology changes over a long period of time. In order to check the sensitivity, the bed level was raised at the upstream end by about 2 m to increase the sediment transport into the area. The simulated sediment transport rate, integrated across the width, is shown in Figure 5.13, the simulated bathymetry after 21 days in Figure 5.14 and the difference in Figure 5.15.

The observed changes from December 1990 to August 1991 are shown in Figure 5.16 . It can be seen that the model exhibited the same erosion pattern at least in the lower half of the area. The scour hole was migrating downstream, the char was eroded from the upper end and deposition took place further down behind the chars. As mentioned above, the simulated bathymetry in the upper half of the model was associated with some uncertainty because of the inaccurate boundary conditions at the upstream boundary. Maximum accretion was in both cases, observed and simulated, in the order of 7 to 9 m and maximum erosion about 5 to 7 m. Locally, the erosion might be much greater but the grid size of the 2-D model put a limit to the accuracy of the simulation of such local scour holes. A wedge of deposits between the main areas of erosion was seen both in the observed and in the simulated changes in the lower half of the test area.

From the curves in Figures 5.10 and Figure 5.13, the simulated migration speed of the fluctuations in sediment transport rate is found to be between 40 and 90 m/day.

When the simulated migration speed of the major bed forms, eg. the deep scour hole, is extracted from Figures 5.2, 5.11 and 5.14, the result is 25 m/day to 35 m/day.

The reason for this discrepancy between migration speed of simulated fluctuations in transport rate and migration speed of simulated major bedforms could be that in the first case only the one-dimensional case is considered whereas the latter is a direct picture of what happens in two horizontal dimensions. For instance, widening of a channel causes change in the transport rate in the direction of the current but not necessarily any change in the longitudinal profile.

In the simulation, the length of the scour hole has increased whereas the depth remained constant. The downstream movement predicted by the model was 500 m.

To assess the speed by which changes takes place, it is necessary to take into consideration that the flow varies significantly from December to August. In the simulation, a constant peak discharge of 21000 m^3/s was used whereas in the prototype, the discharge increased from low flow in December to high bank full flow in August. The migration in the prototype is the product of the varying flow from low to high flow conditions whereas high flow was applied in the 2-D model. The sediment transport and thus the migration speed is a function of flow velocity to a power of more than 3. Therefore, variations in sediment transport are more pronounced than variations in discharge, see Figure 5.17.

In the prototype, the length of the scour hole remained constant from December to August and the maximum depth increased slightly. The scour hole migrated 800 m downstream. Hence, based on the considerations described above, it is concluded that the simulated migration speed of the scour hole is in satisfactory agreement with prototype observation.

5.7 Conclusion, Test Area 2

The calibration parameters of hydrodynamics and sediment transport were maintained from Test Area 1. With this model, it was possible to reproduce the velocity pattern, the concentration field (although with a scaling factor of 0.5 on the van Rijn model), and the change in bed level to a satisfactory degree of accuracy when the available amount of calibration data from the test area is being taken into consideration. The verification gave some insight into the heavy fluctuations in sediment transport rate indicating that local areas like Test Area 2 will never be in equilibrium. The migration speed of the macro bed forms has been shown in the model and in the observations to be in the order of 20 m/day although some uncertainty was associated with the calculations and the observations.

6. CONCLUSION

The HD-model predicted the velocities with a satisfactory degree of accuracy. For post-monsoon conditions, it was necessary to increase the bed resistance to obtain the right slope of the water surface (gradient). This is in agreement with theory and with the findings from other studies (JMB).

The sediment transport formulae Engelund/Fredsoe with modified Vanoni profile and van Rijn were found to give transport rates of the correct order of magnitude. Engelund/Fredsoe performed best for Test Area 1, post monsoon, whereas van Rijn was best for Test Area 2.

Continuous simulation of morphology in Test Area 1 over one year was not possible. Instead selected events were picked out and simulated to give some insight into the variation over the year. The regime equation developed by the JMB-study (RPT,NEDECO,BCL 1989) was verified and performed well for flood conditions and less well for low flow conditions.

Simulation of the migration of the scour hole in Test Area 2 was satisfactory. The same erosion and deposition pattern was obtained if the uncertainty at the upstream boundary was neglected.

The 2-D model has proved to be capable of predicting velocities, concentration of suspended sediment and erosion/deposition rates. Furthermore, the survey data have revealed that the conditions prevailing in the Brahmaputra River are highly changeable and a large natural scatter is inherent in the system. This should be taken into consideration in the interpretation of results from the 2-D model.

7. REFERENCES

Coleman, James M - Sedimentary Geology, Volume 3, August 1969 no 2/3, 1985/126

Halcrow/DHI/EPC/DIG - River Training Studies of Brahmaputra River First Interim Report, Technical Annexes, Annex 3: Mathematical Modelling, April 1991

Halcrow/DHI/EPC/DIG - River Training Studies of Brahmaputra River First Interim Report, Technical Annexes, Annex 1: Data Collection and Analysis, April 1991

Halcrow/DHI/EPC/DIG - River Training Studies of Brahmaputra River Working Paper on 2-D Modelling, December 1990

Halcrow/DHI/EPC/DIG - River Training Studies of Brahmaputra River Second Interim Report, Technical Annexes, Annex 1: River Survey, December 1991

Halcrow/DHI/EPC/DIG - River Training Studies of Brahmaputra River Second Interim Report, Technical Annexes, Annex 2: Mathematical Modelling, December 1991

Halcrow/DHI/EPC/DIG - River Training Studies of Brahmaputra River Second Interim Report, Technical Annexes, Annex 3: Morphology, December 1991

Rendel, Palmer and Tritton/NEDECO/BCL - Jamuna Bridge Project, Phase II, Study Feasibility Report, Volume II, Annex B: River Morphology, August 1989

FIGURES

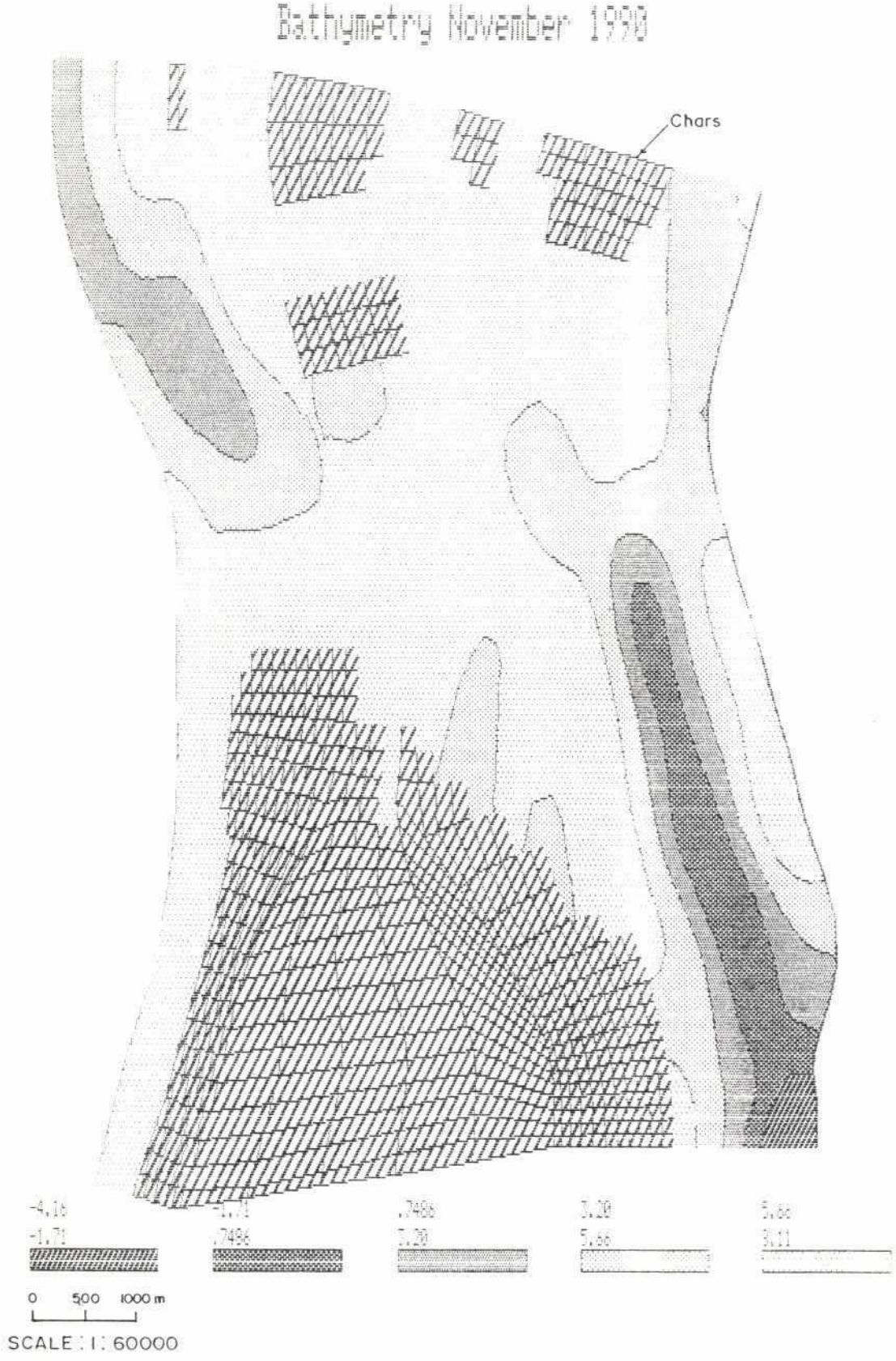

BRTS Verification of the 2-D Morphological Model

Bathymetry, Survey in Test Area 1 November 1990	Vol.3 Part 9
	Figure 3.1

South East Corner

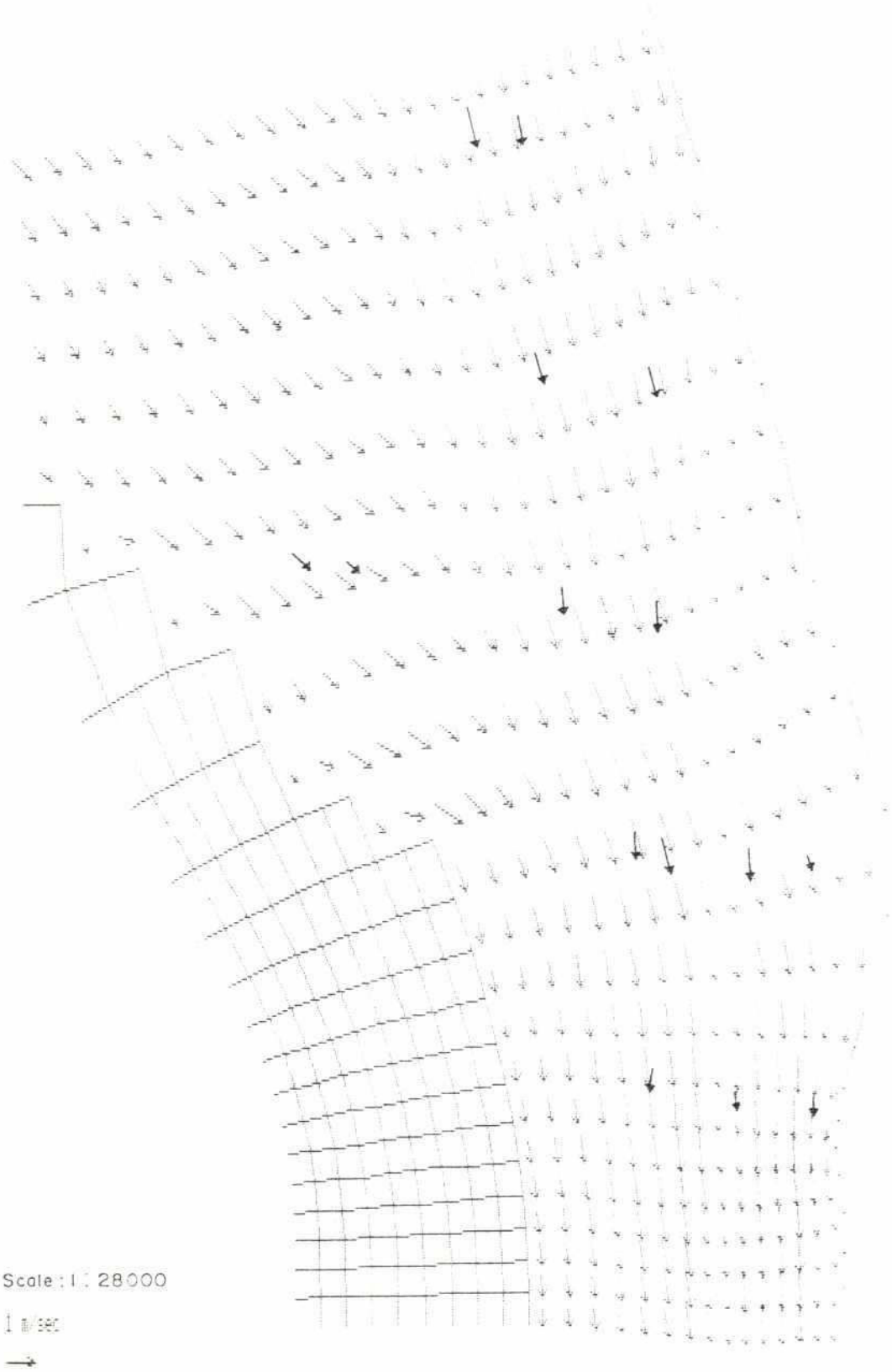

BRTS Verification of the 2-D Morphological Model

Simulated and Measured Velocity in Test Area 1	Vol.4 Part 9
	Figure 3.2

North East Corner

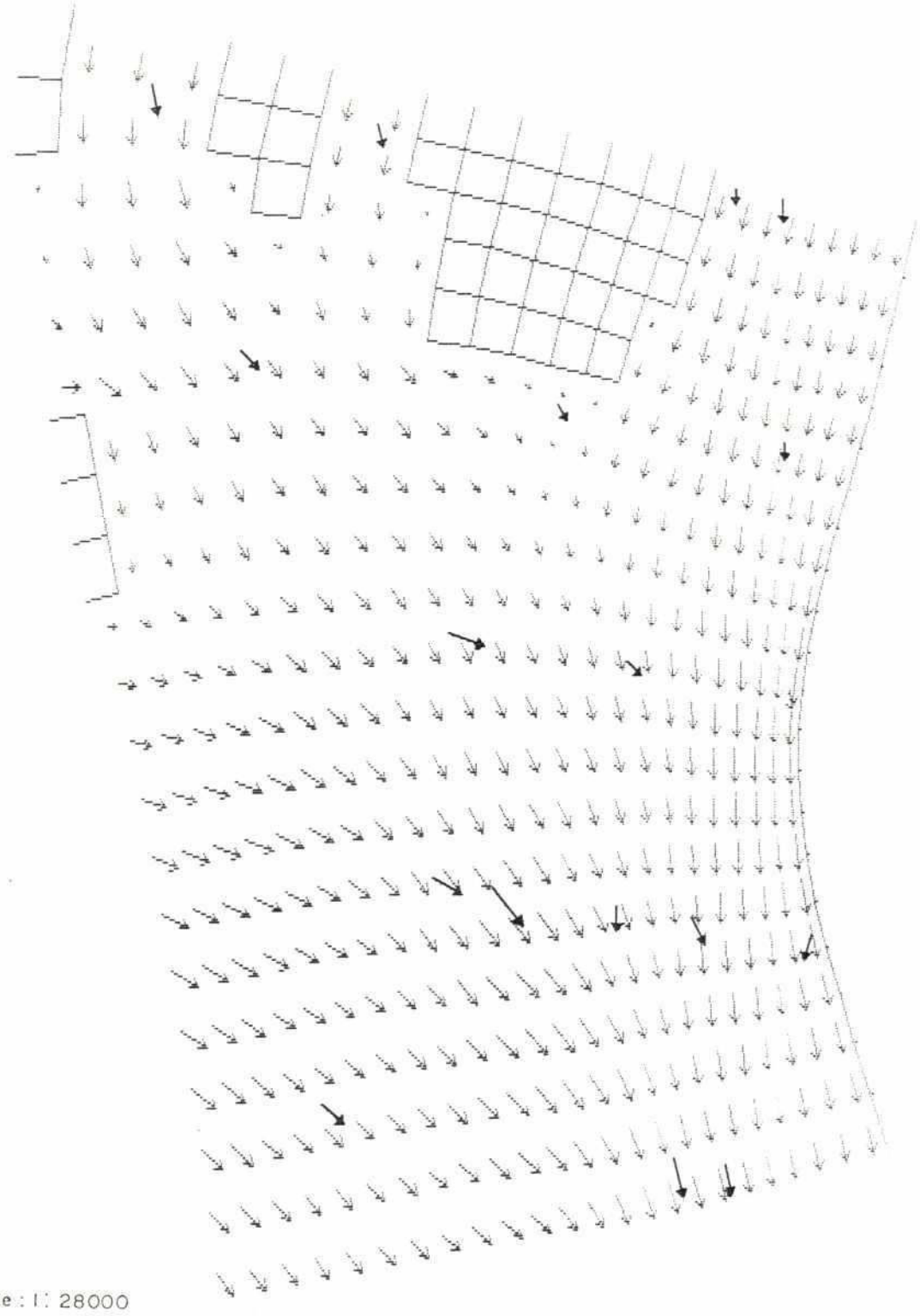

Scale : 1 : 28000

1 m/sec

BRTS Verification of the 2-D Morphological Model

Simulated and Measured Velocity in Test Area 1	Vol.4 Part 9
	Figure 3.3

South West Corner

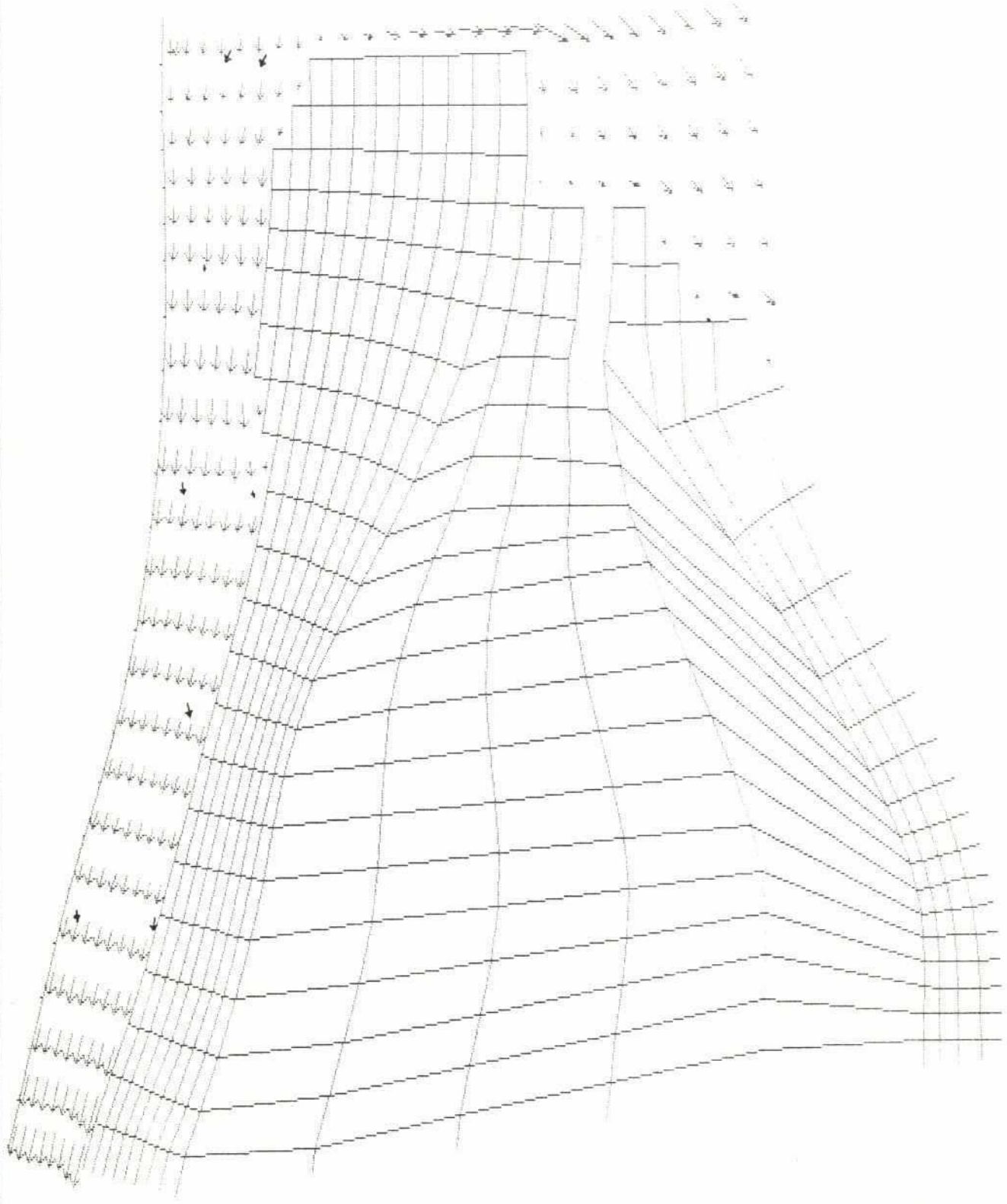

Scale : 1: 28000

1 m/sec

BRTS Verification of the 2-D Morphological Model

Simulated and Measured Velocity in Test Area 1	Vol.4 Part 9
	Figure 3.4

North West Corner

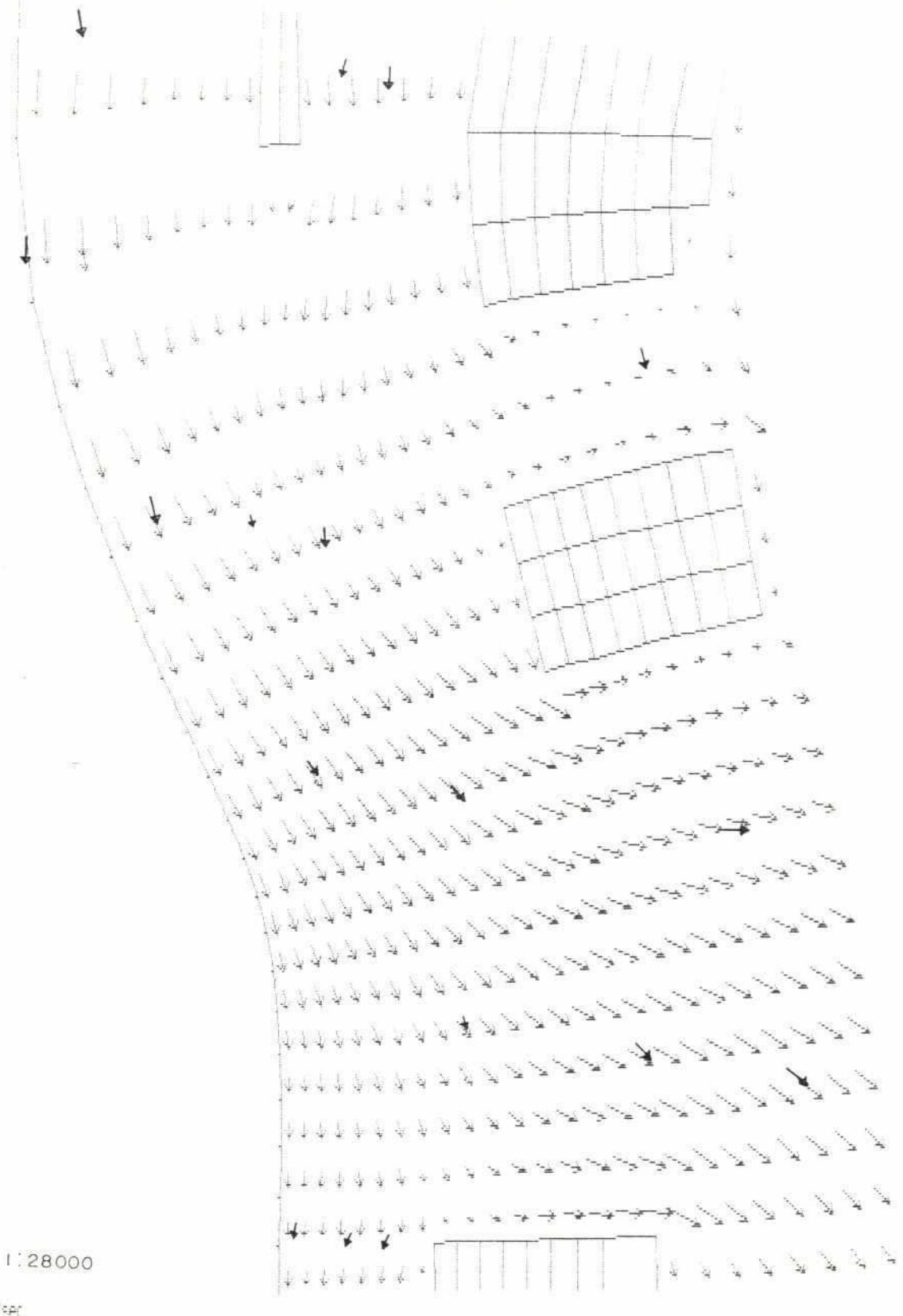

Scale : 1 : 28000

1 m/sec

BRTS Verification of the 2-D Morphological Model

Simulated and Measured Velocity in Test Area 1	Vol.4 Part 9
	Figure 3.5

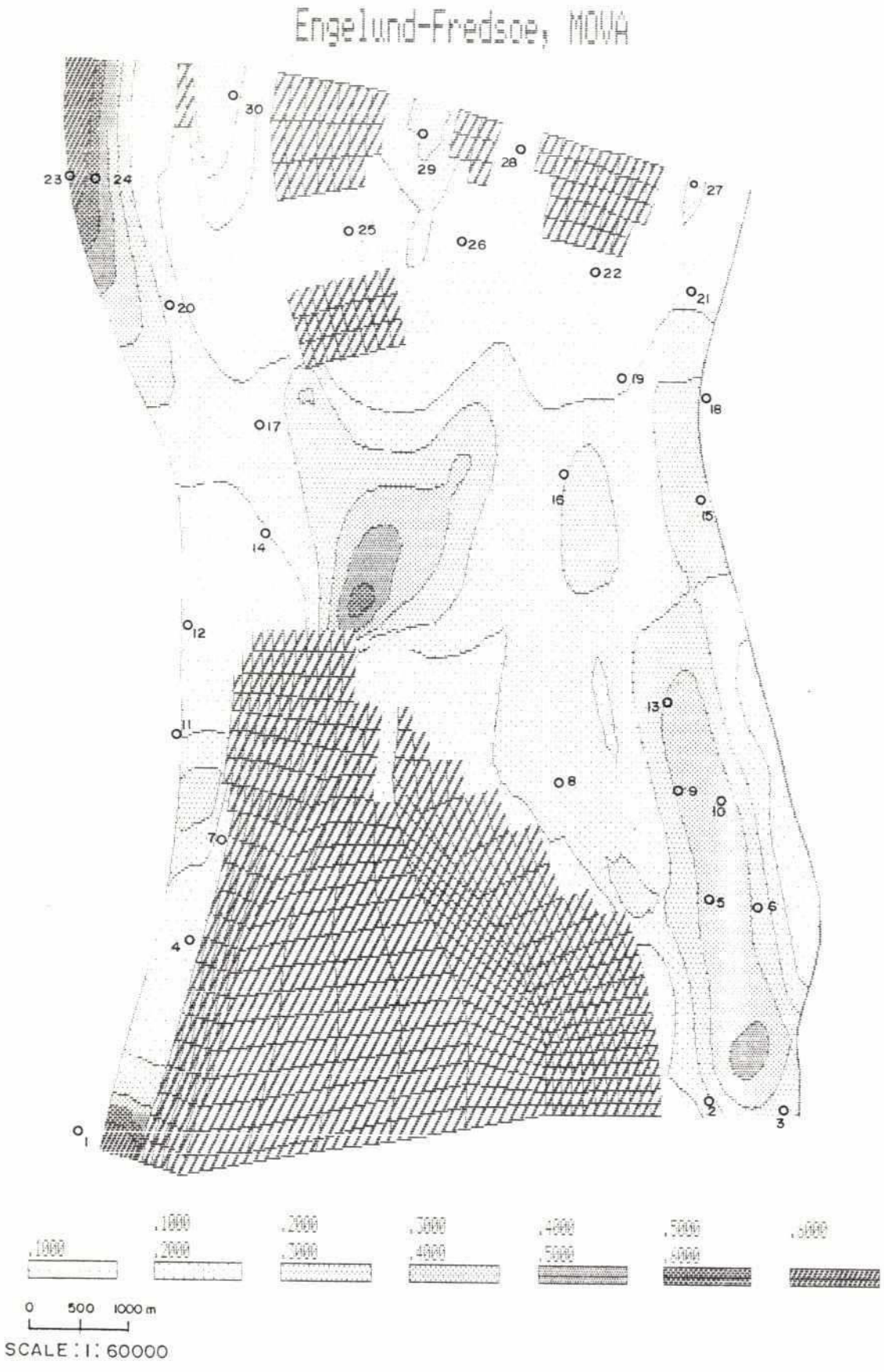

BRTS Verification of the 2-D Morphological Model

Simulated Concentration of Suspended Sediment with Englund/Fredsoe Mova Model. Sample No. of Measurements Indicated	Vol.4	Part 9
	Figure 3.6	

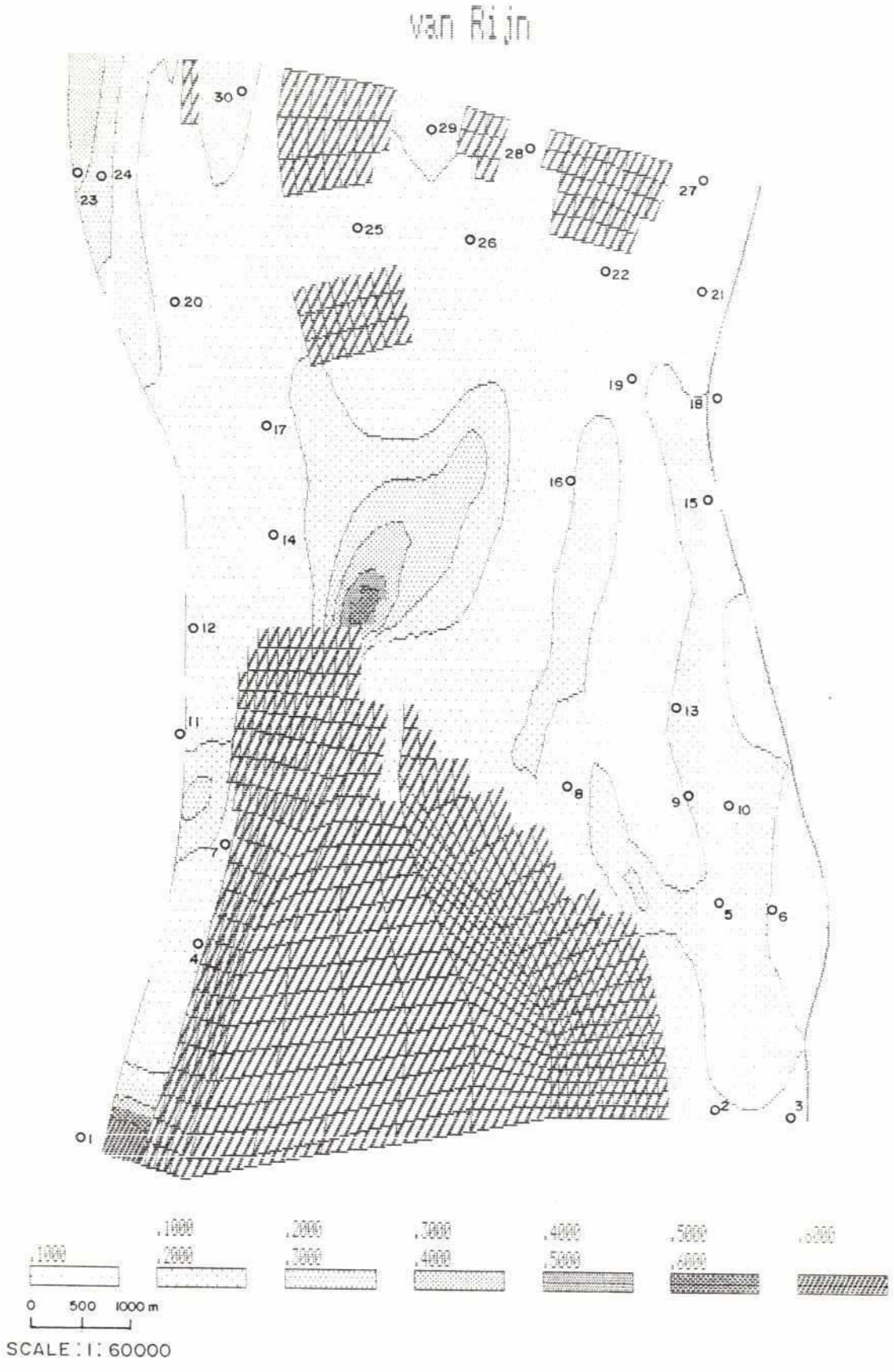

BRTS Verification of the 2-D Morphological Model

Simulated Concentration of Suspended Sediment with van Rijn Model. Sample No. of Measurements Indicated	Vol.4 Part 9
	Figure 3.7

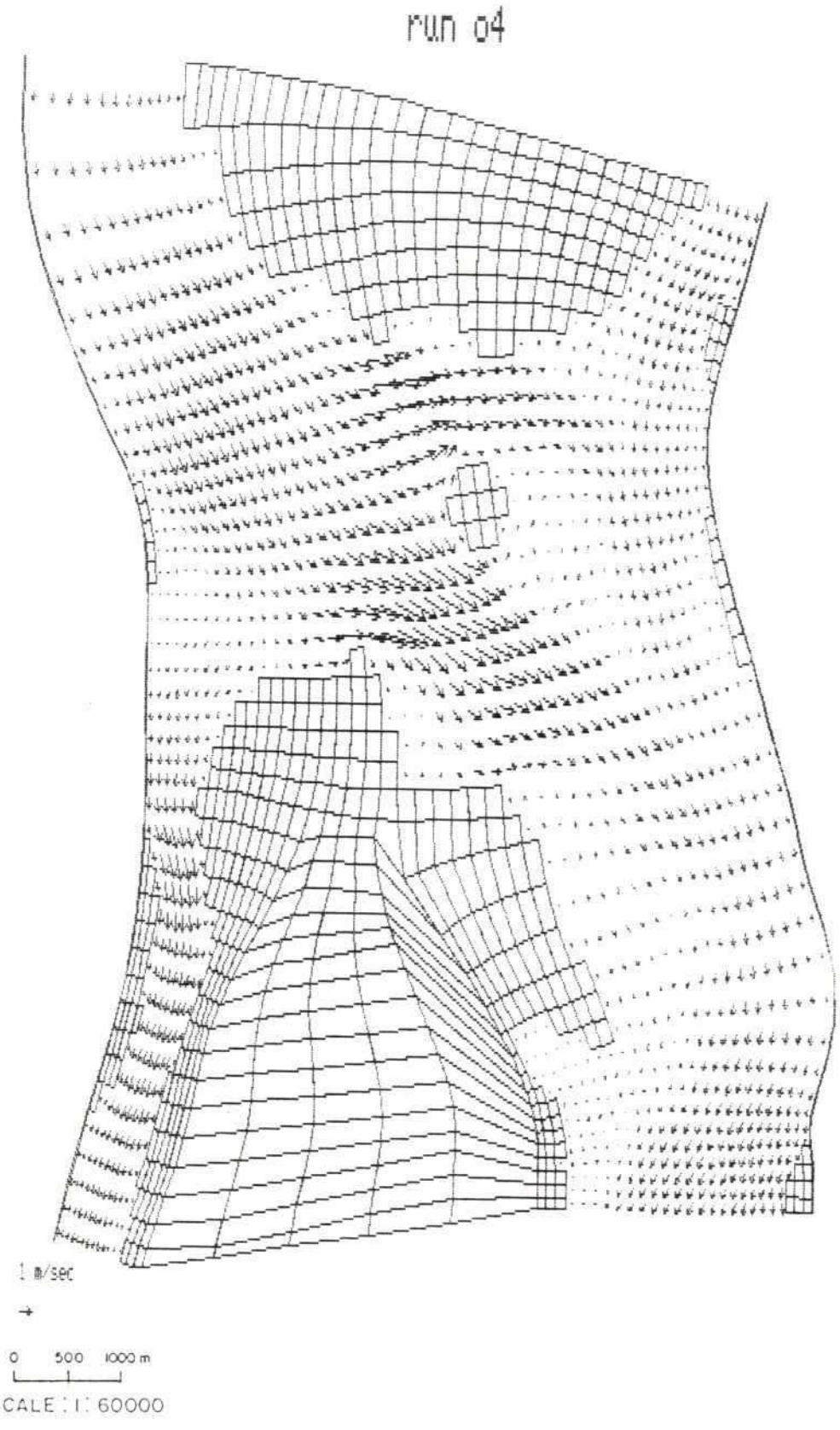

BRTS Verification of the 2-D Morphological Model

Simulated Velocity Field. Q = 8000 m^3/s

Vol.4 Part 9

Figure 4.1

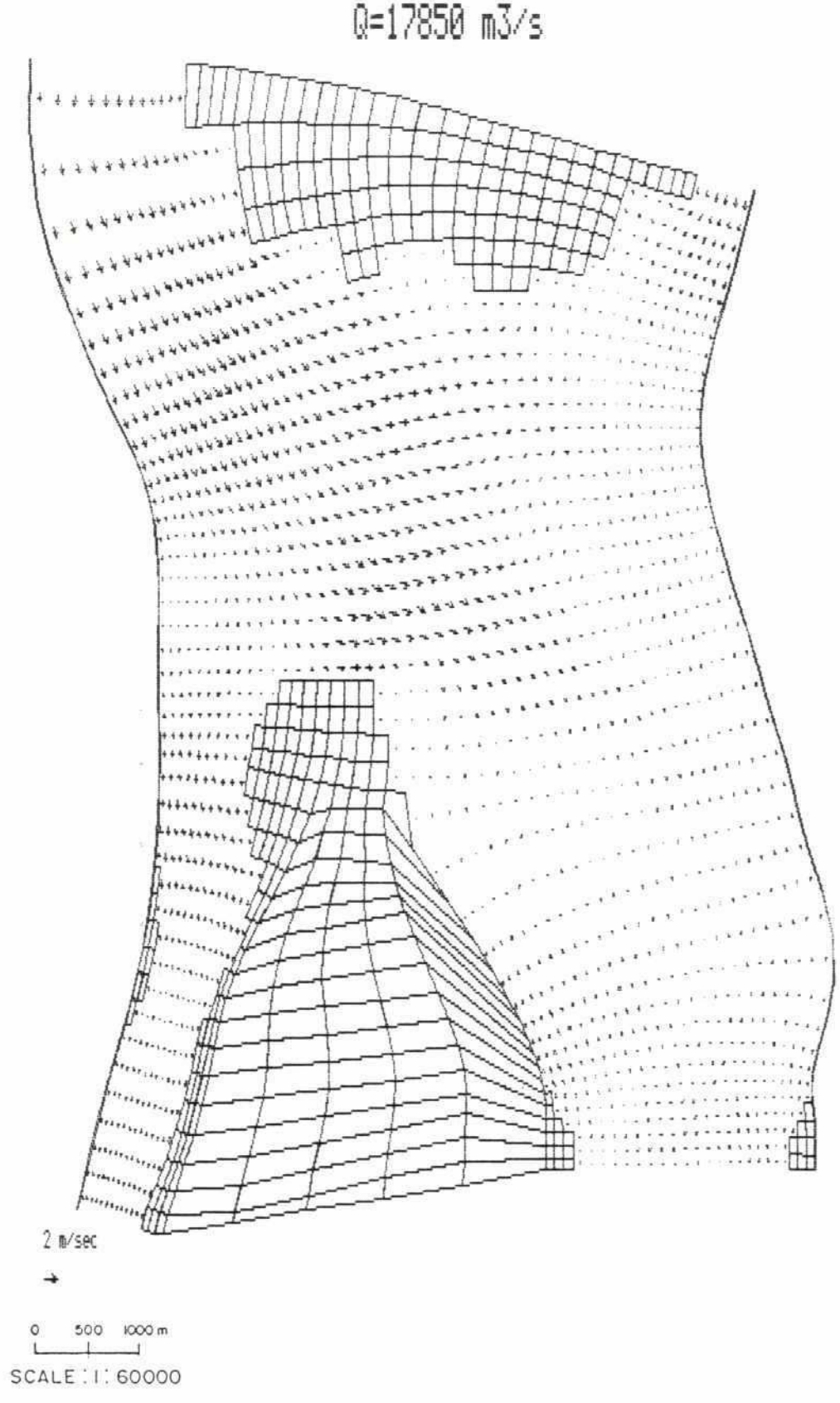

BRTS Verification of the 2-D Morphological Model

Simulated Velocity Field. Q = 17850 m^3/s

Vol.4 Part 9

Figure 4.2

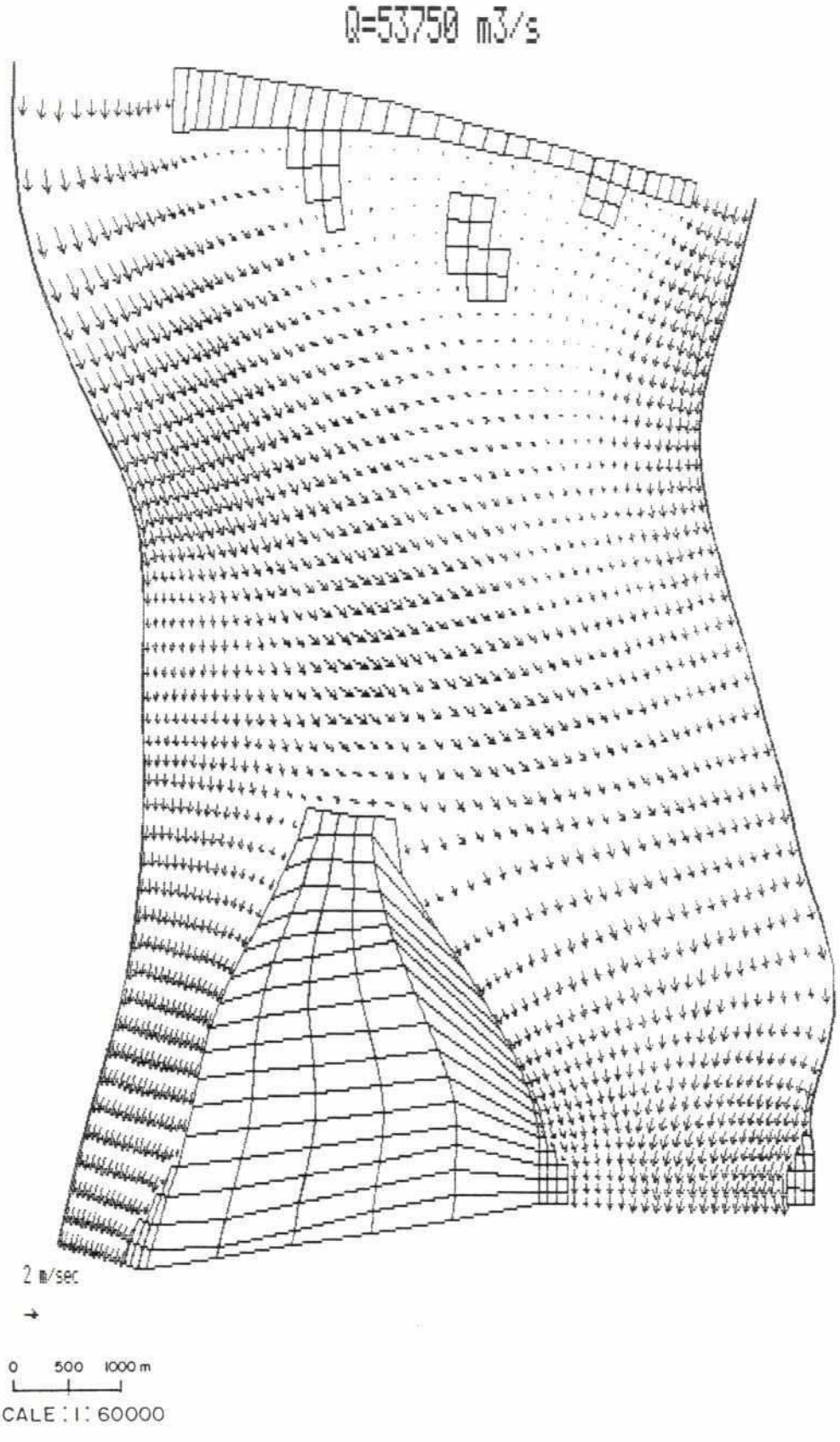

BRTS Verification of the 2-D Morphological Model

Simulated Velocity Field. Q = 53750 m^3/s

Vol.4 Part 9

Figure 4.3

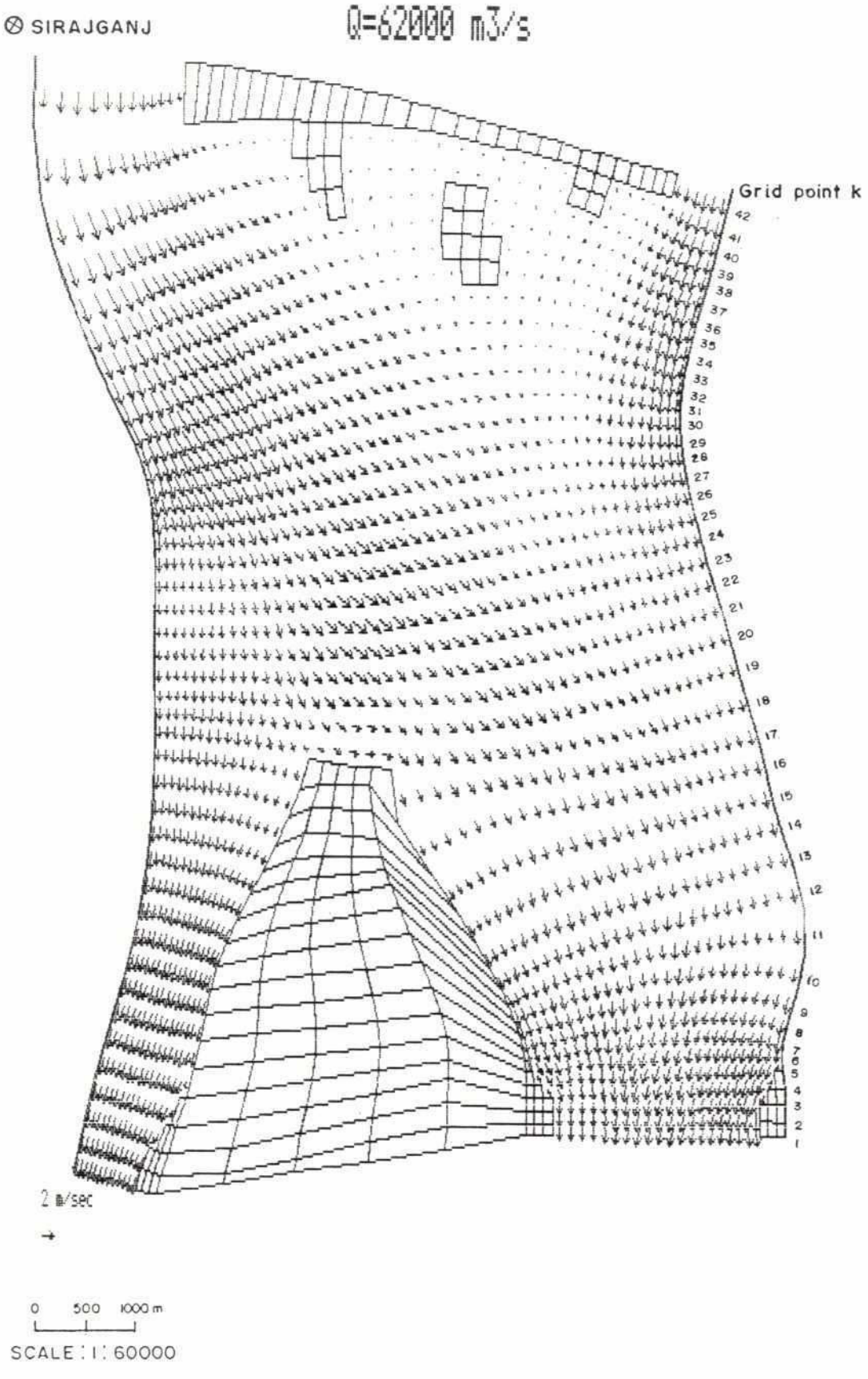

BRTS Verification of the 2-D Morphological Model

Simulated Velocity Field. Q = 62000 m^3/s	**Vol.4** Part 9
	Figure 4.4

run 04

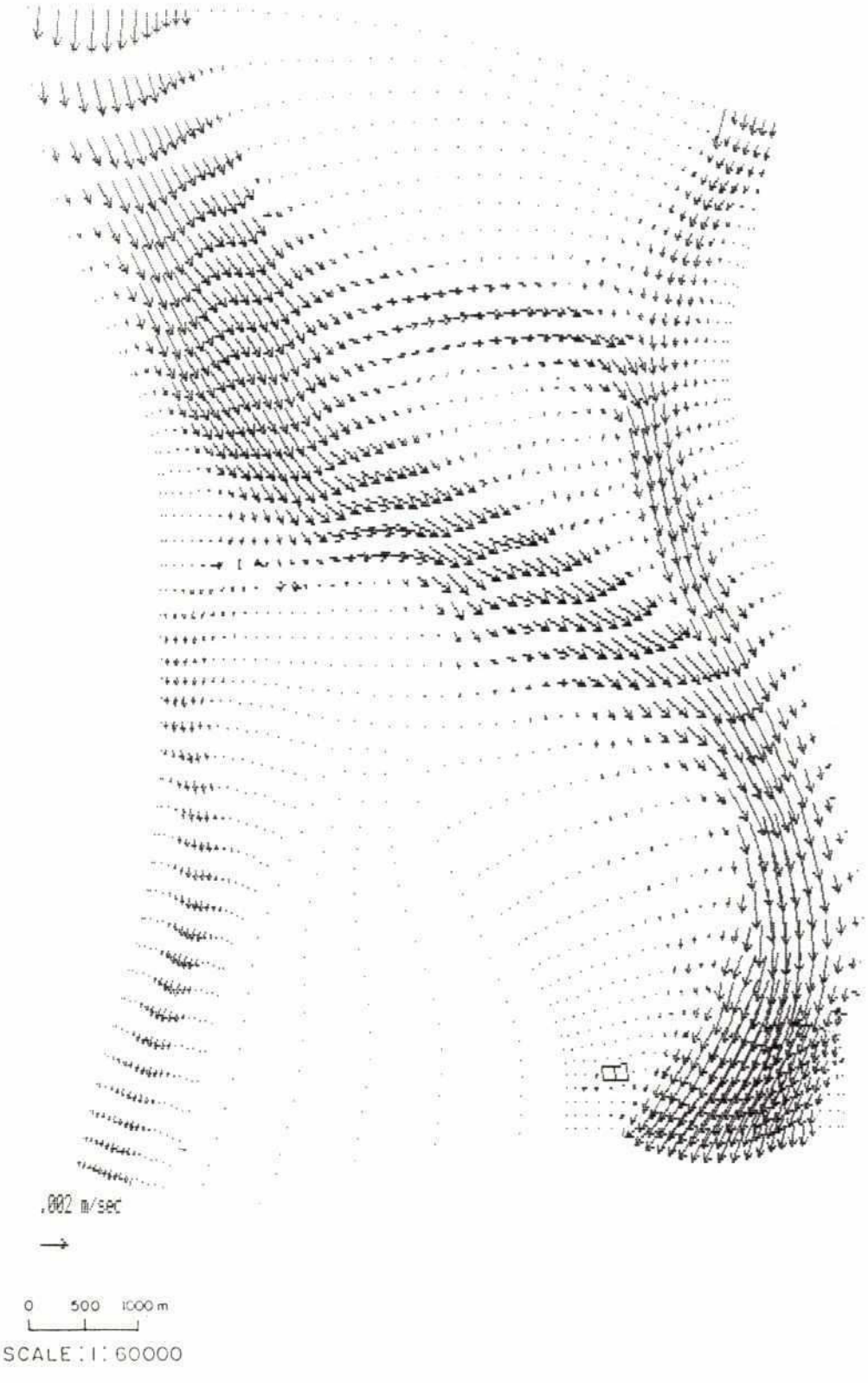

BRTS Verification of the 2-D Morphological Model

Simulated Sediment Transport Rate. Q = 8000 m^3/s	**Vol.4** Part 9
	Figure 4.5

run 03

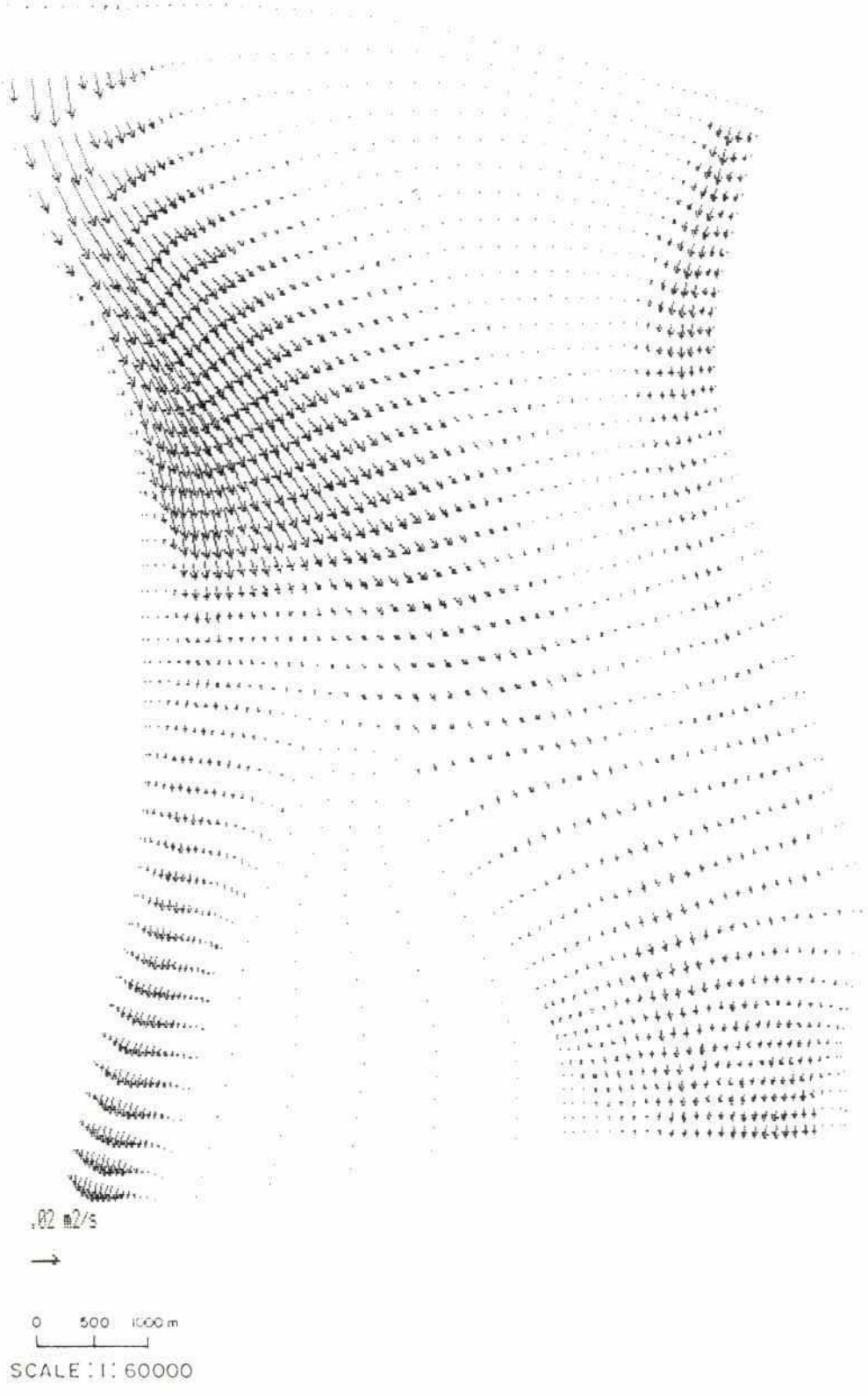

BRTS Verification of the 2-D Morphological Model

Simulated Sediment Transport Rate. Q = 62000 m^3/s	**Vol.4** Part 9
	Figure 4.6

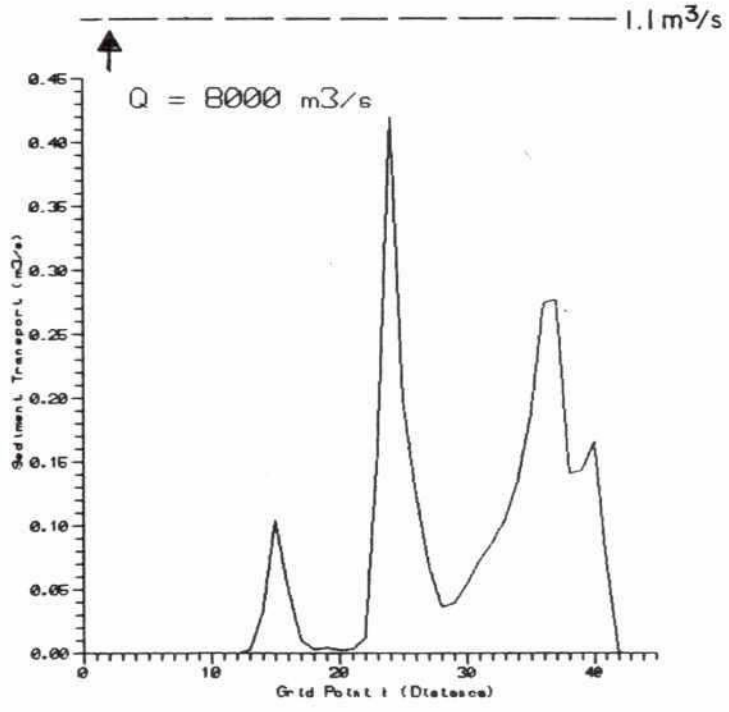

——— 2-D van Rijn

— — — Regime equation, Bahadurabad data '68-'70 (JMB)
$Q_s = 4.5 \times 10^{-6} Q^{1.38}$ m³/s

BRTS Verification of the 2-D Morphological Model

Simulated Sediment Transport (m^3/s) Over Cross Sections (k) with Q = 8000 m^3/s	Vol.4 Part 9
	Figure 4.7

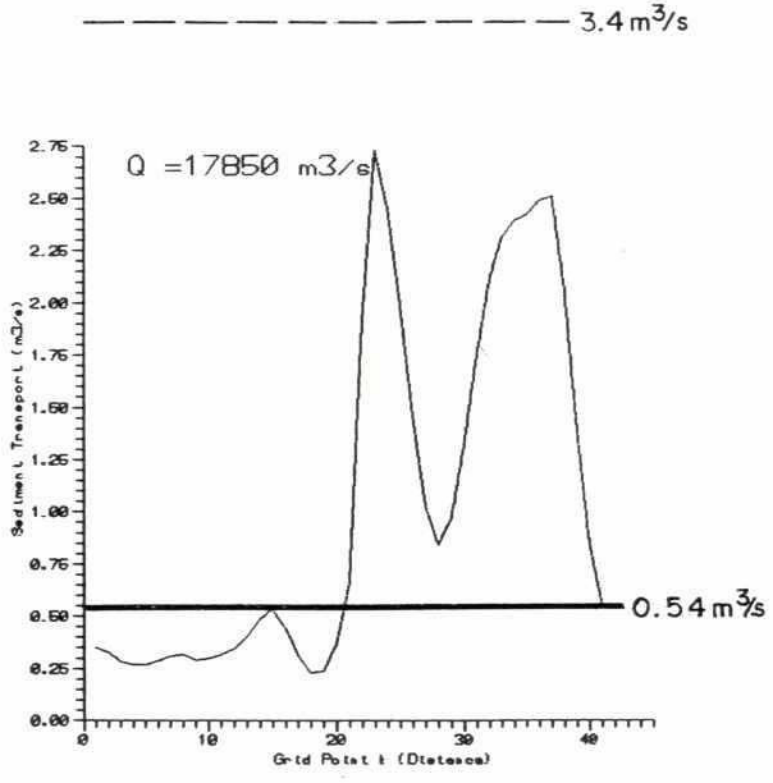

2-D van Rijn

Recorded suspended sediment transport BRTS 1990

Regime equation, Bahadurabad data '68-'70 (JMB)

$Q_s = 4.5 \times 10^{-6} Q^{1.38}$ m³/s

BRTS Verification of the 2-D Morphological Model

Simulated Sediment Transport (m^3/s) Over Cross Sections (k) with Q = 17850 m^3/s	Vol.4	Part 9
	Figure 4.8	

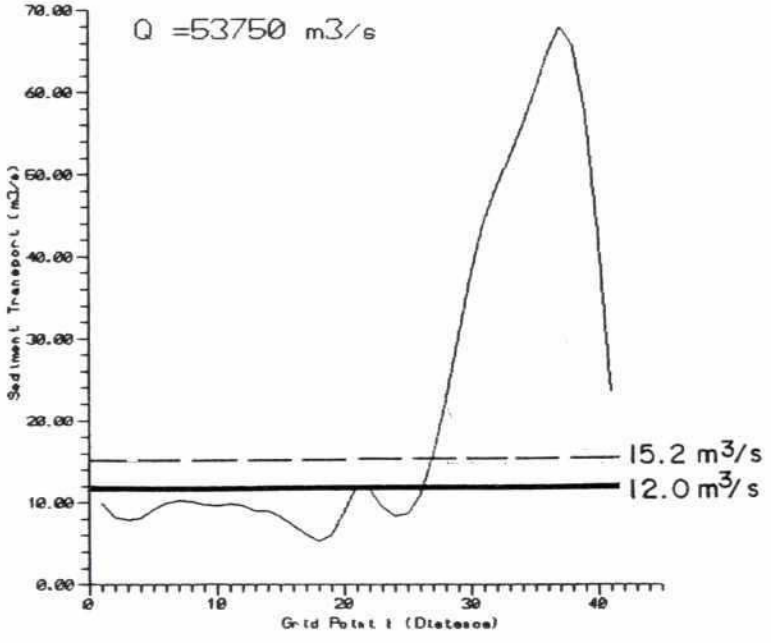

——— 2-D van Rijn

——— Recorded suspended sediment transport BRTS 1990

— — — Regime equation, Bahadurabad data '68-'70 (JMB)
$Q_s = 4.5 \times 10^{-6} Q^{1.38}$ m³/s

BRTS Verification of the 2-D Morphological Model

Simulated Sediment Transport (m^3/s) Over Cross Sections (k) with Q = 53750 m^3/s	**Vol.4** **Part 9**
	Figure 4.9

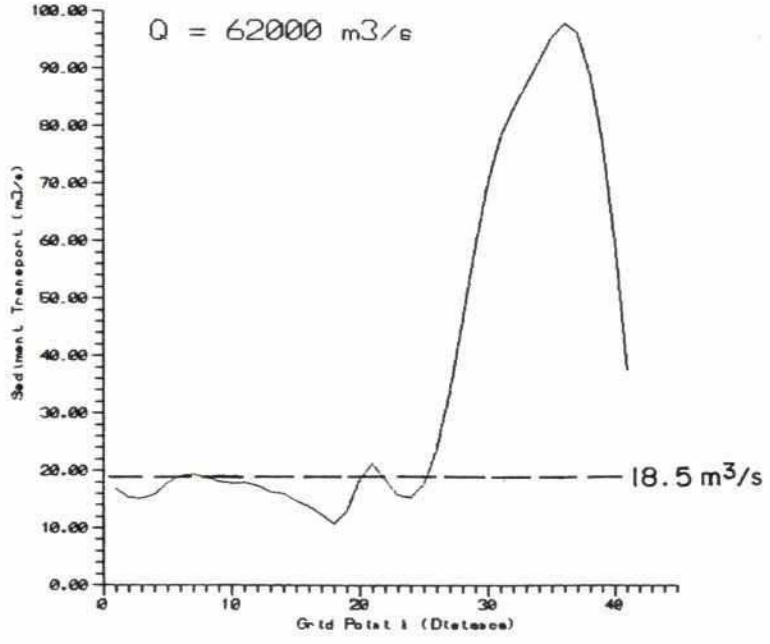

——— 2-D van Rijn

— — — Regime equation (JMB)

$Q_s = 4.5 \times 10^{-6} Q^{1.38}$

BRTS Verification of the 2-D Morphological Model

Simulated Sediment Transport (m^3/s) Over Cross Sections (k) with Q = 62000 m^3/s	Vol.4 Part 9
	Figure 4.10

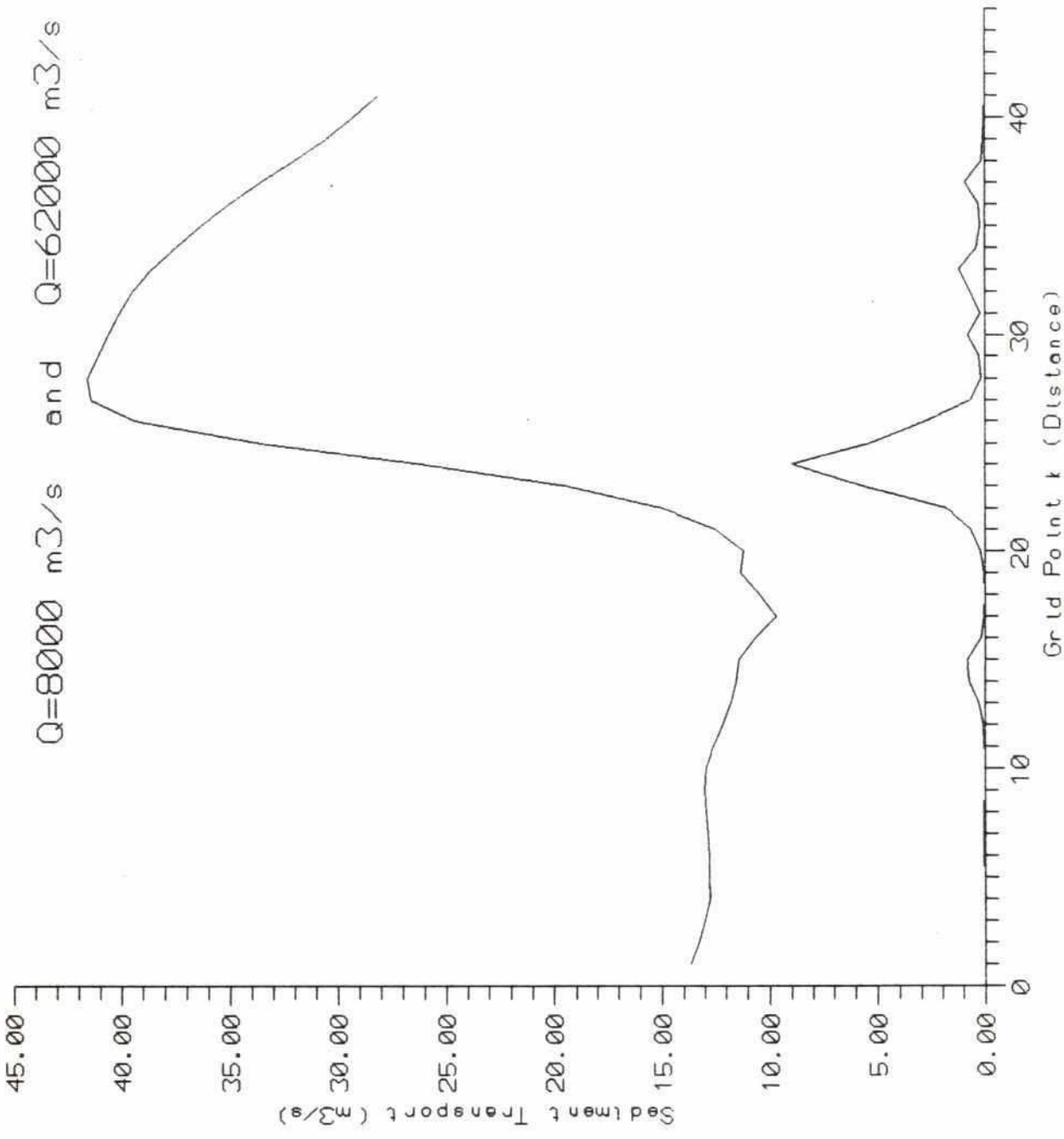

BRTS Verification of the 2-D Morphological Model

Simulated Sediment Transport (m^3/s) Over Cross Section (Grid Period k) for event Q = 8000 m^3/s and Q = 62000 m^3/s	Vol.4 Part 9
	Figure 4.11

December

BRTS Verification of the 2-D Morphological Model

Bathymetry from Test Area 2, December 1990

Vol.4 **Part 9**

Figure 5.1

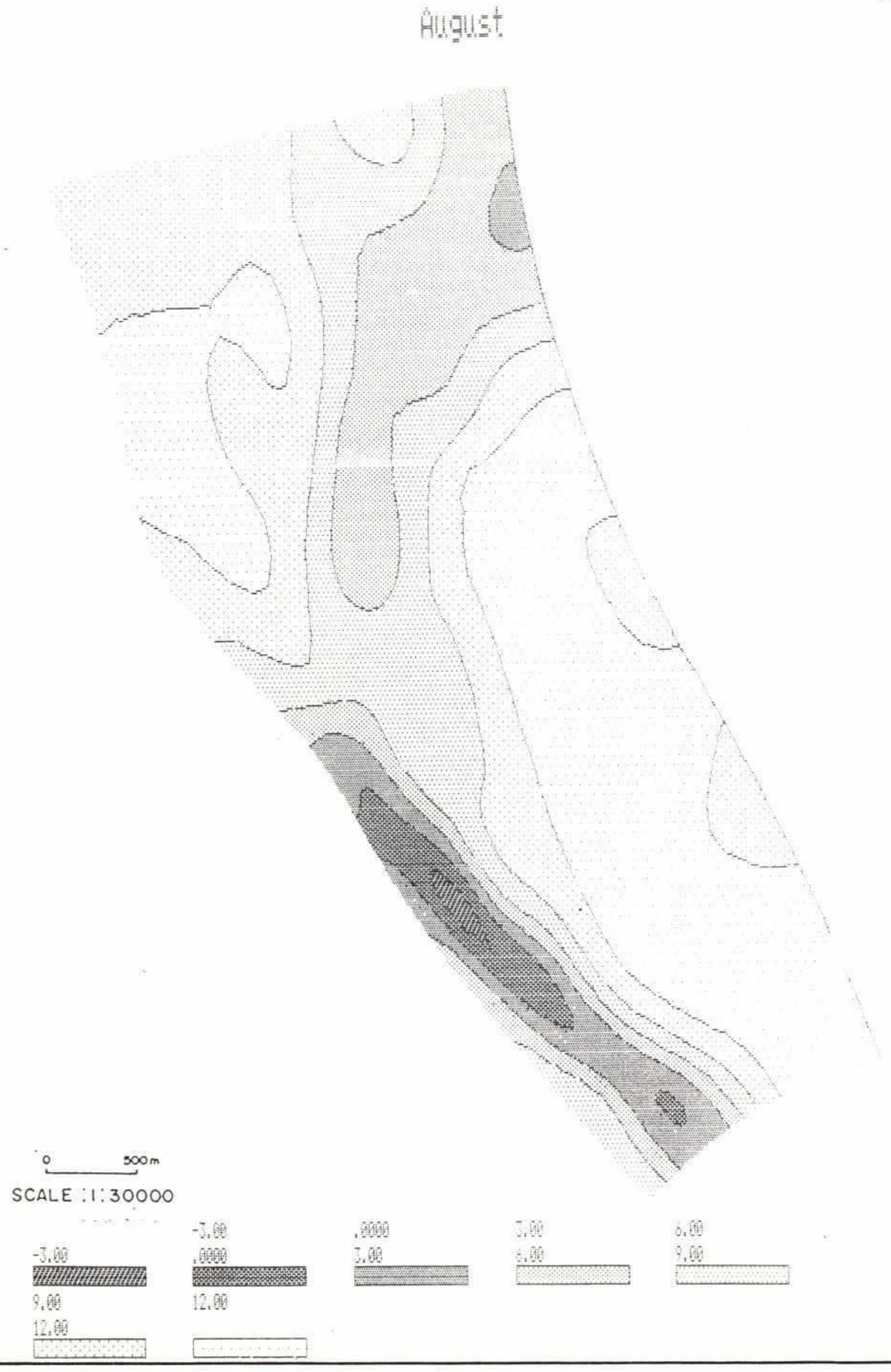

BRTS Verification of the 2-D Morphological Model

Bathymetry from Test Area 2, August 1991

Vol.4 Part 9

Figure 5.2

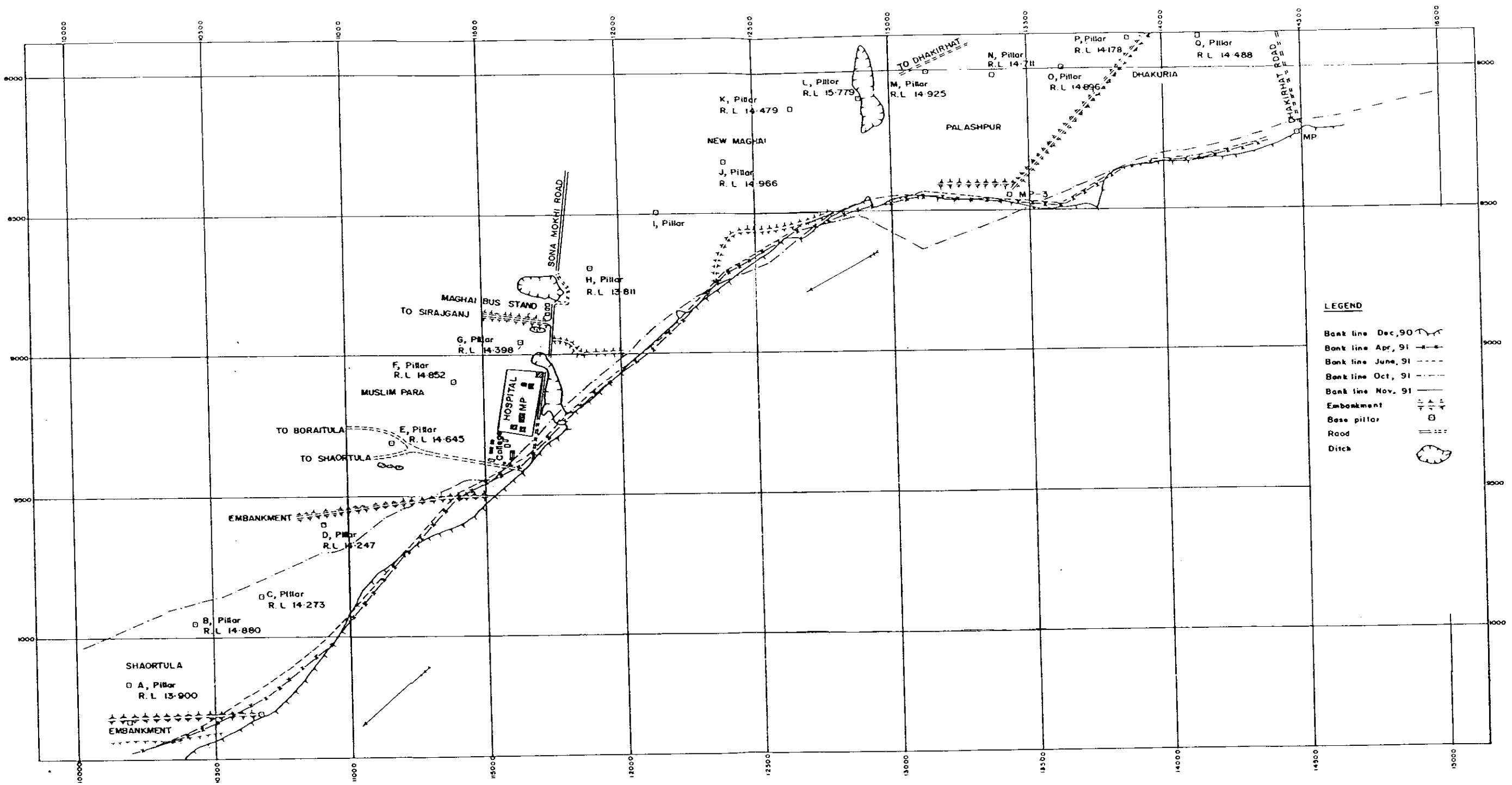

Bankline in April, June and October 1991 at Kazipur

Vol.4 Part 9

Figure 5.3

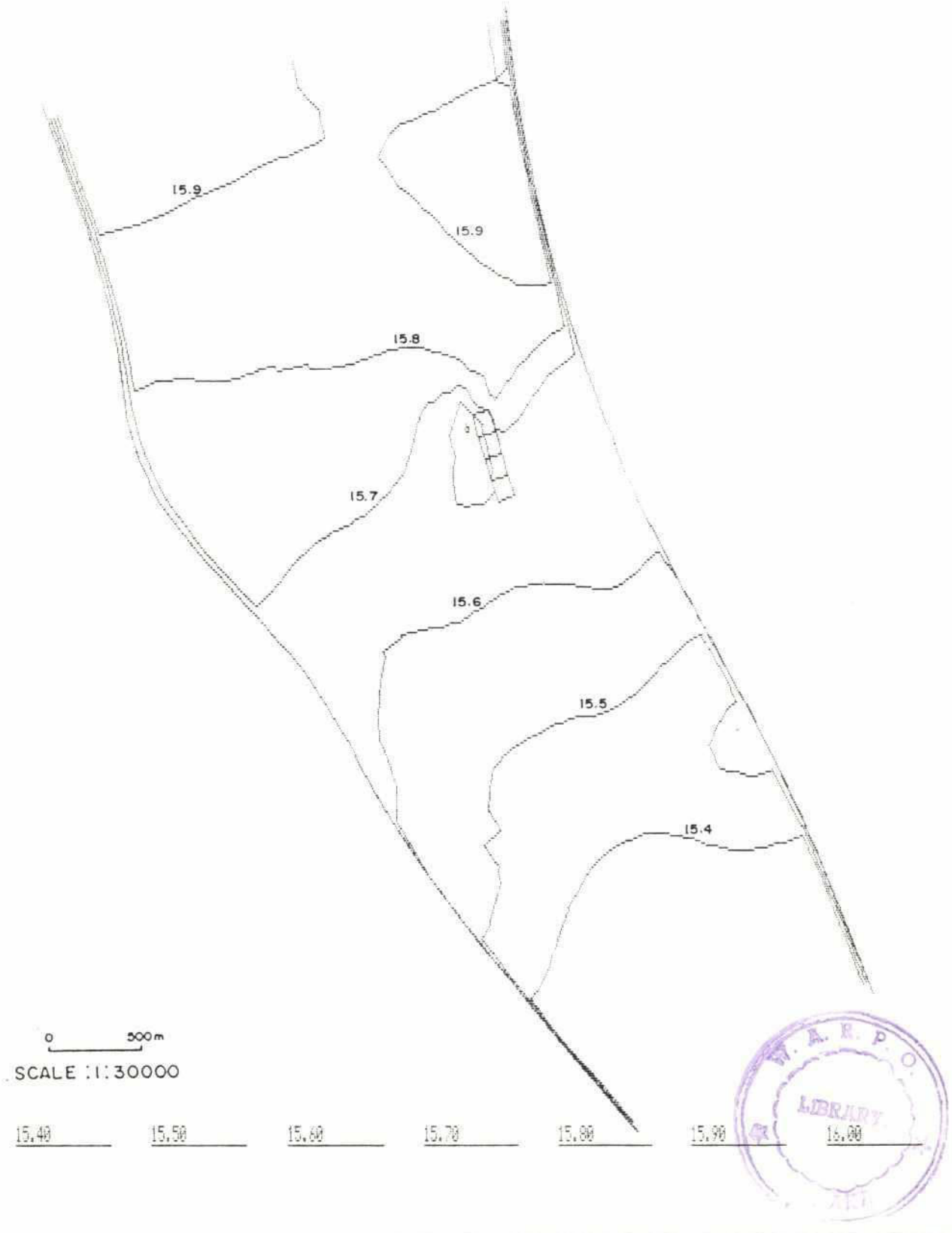

BRTS Verification of the 2-D Morphological Model

Simulated Water Level

Vol.4 Part 9

Figure 5.4

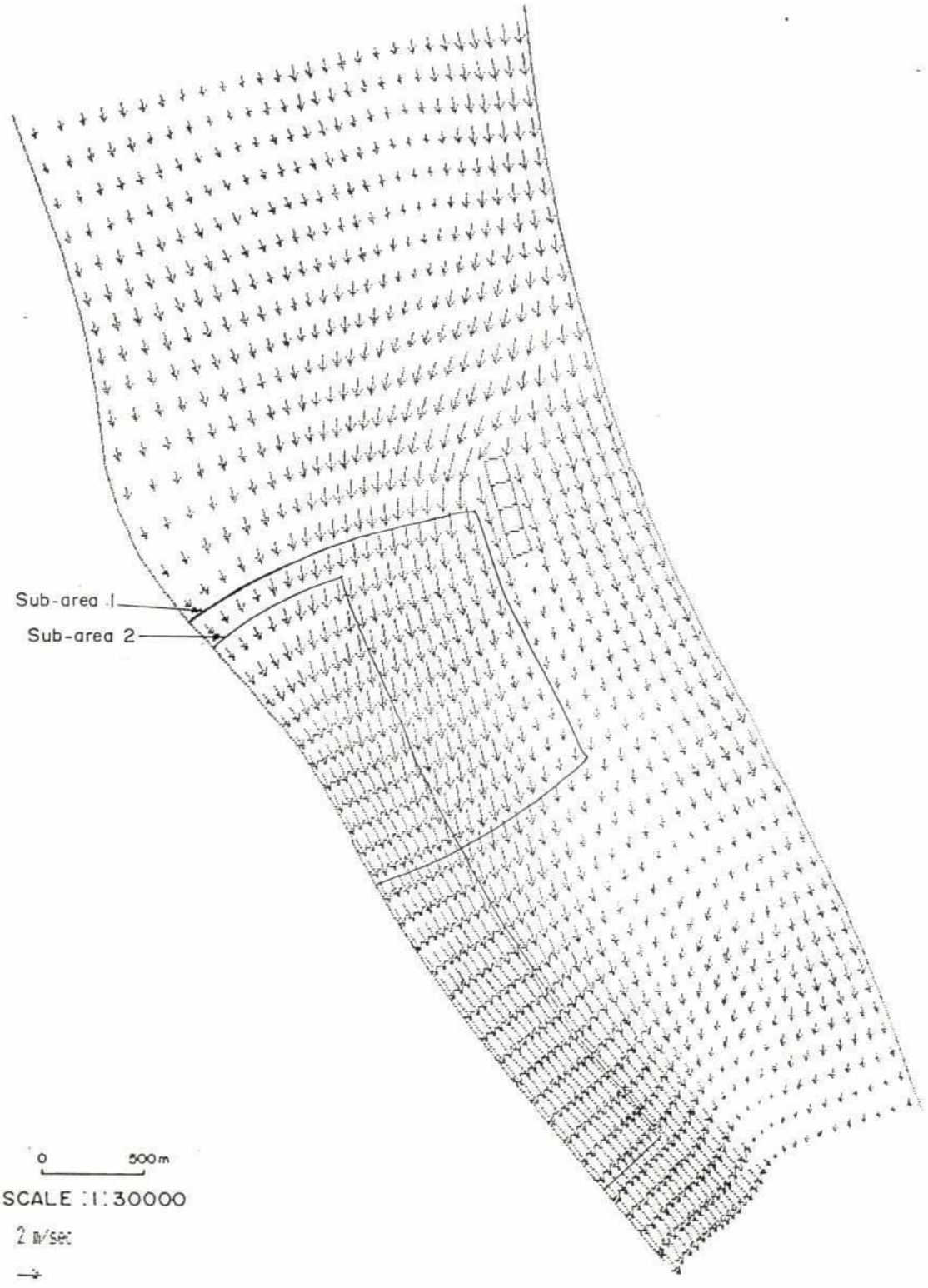

BRTS Verification of the 2-D Morphological Model

Simulated Velocities

Vol.4 Part 9

Figure 5.5

Sub-area 1

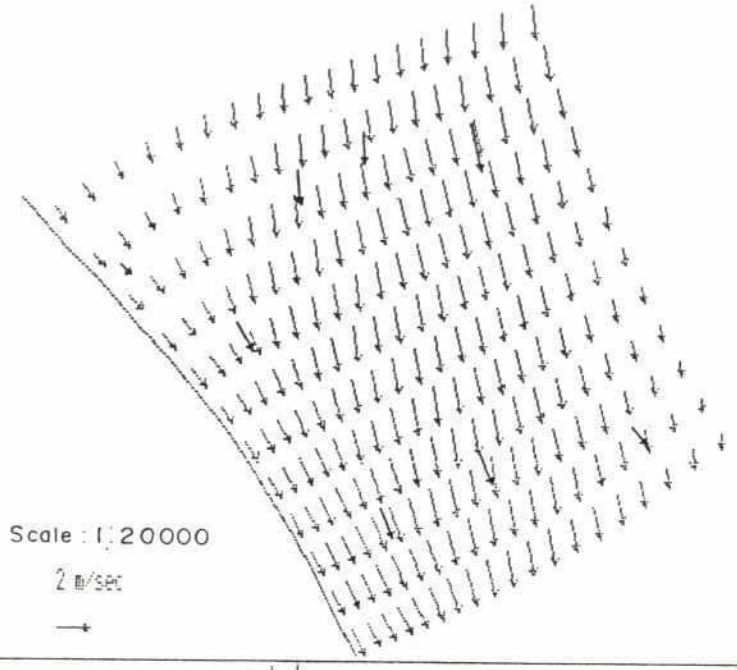

Scale : 1 : 20000

2 m/sec

Sub-area 2

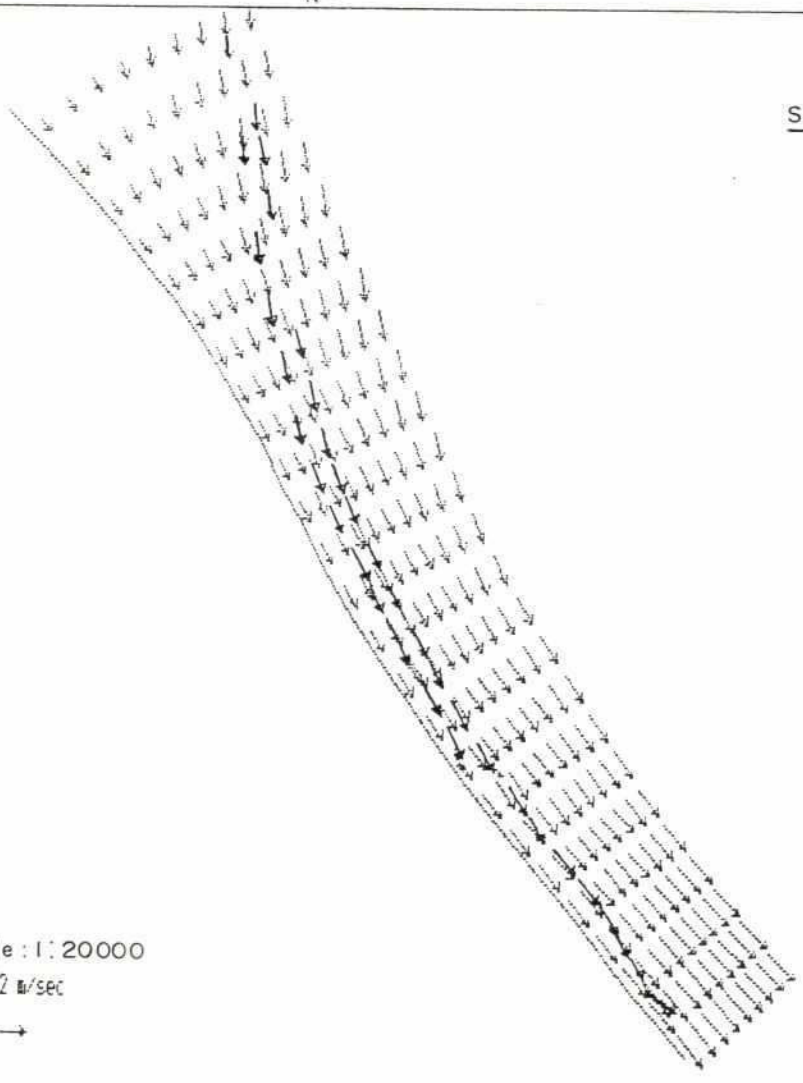

Scale : 1 : 20000

2 m/sec

Note : Locations of sub-areas shown in Figure 5.5

BRTS Verification of the 2-D Morphological Model

Simulated and Observed Velocities in Sub-areas	**Vol.4**	**Part 9**
	Figure 5.6	

Grain Diameter (mm)

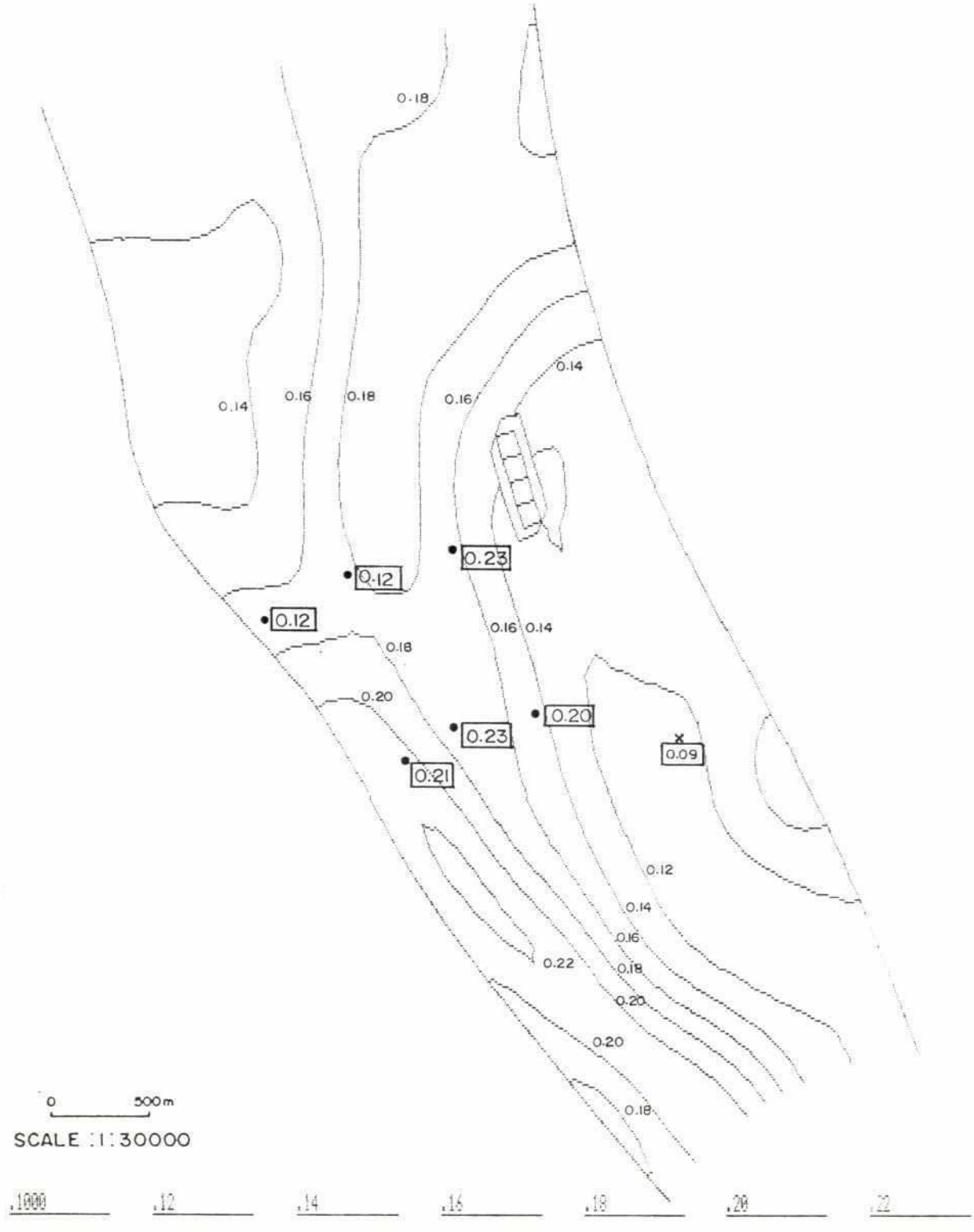

Note : Measurements of grain size in squares

BRTS Verification of the 2-D Morphological Model

Grain Diameter as Defined in 2-D Model

Vol.4 Part 9

Figure 5.7

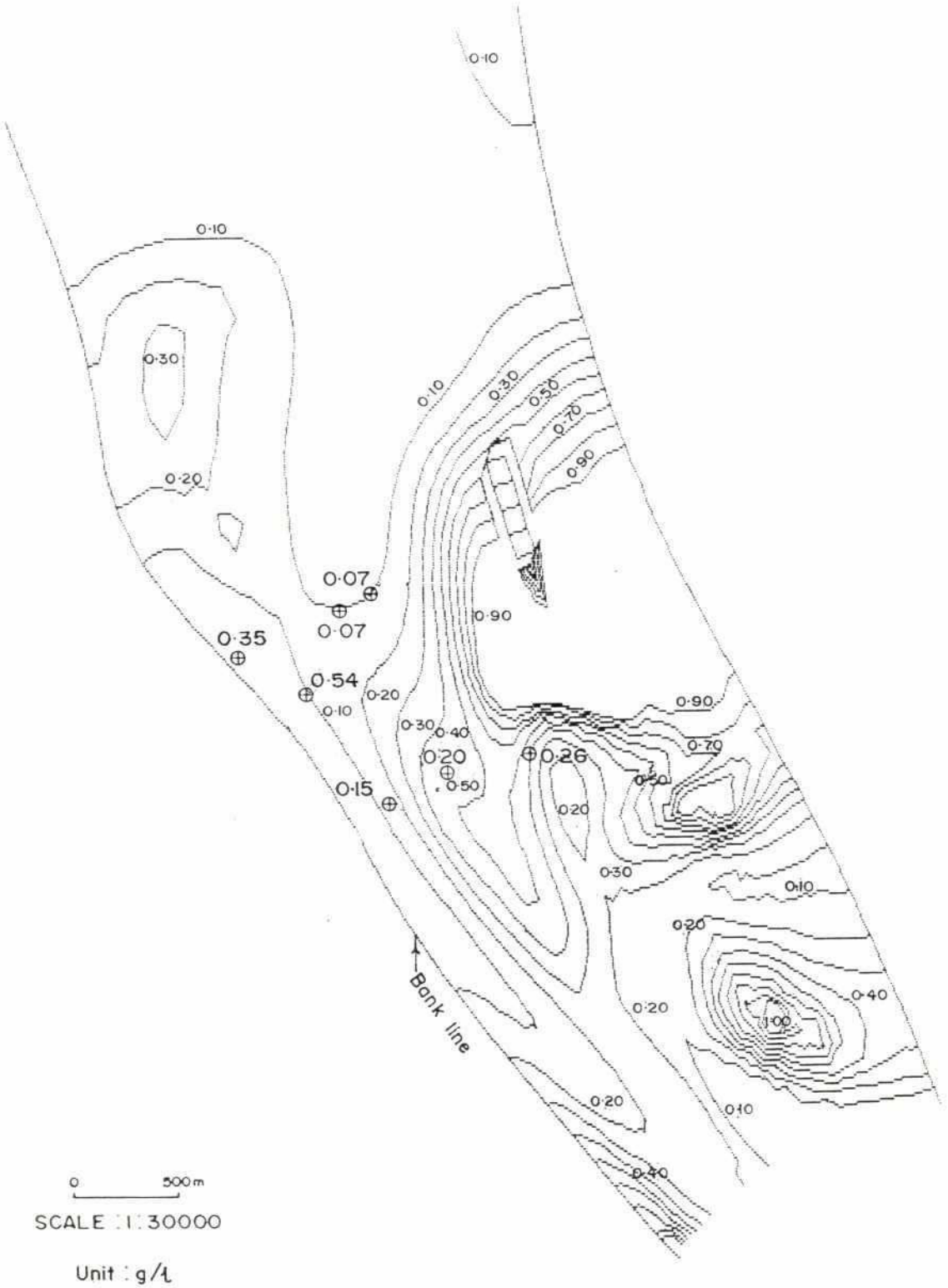

BRTS Verification of the 2-D Morphological Model

Simulated and Measured Concentration of Suspended Sediment in Test Area 2	Vol.4 Part 9
	Figure 5.8

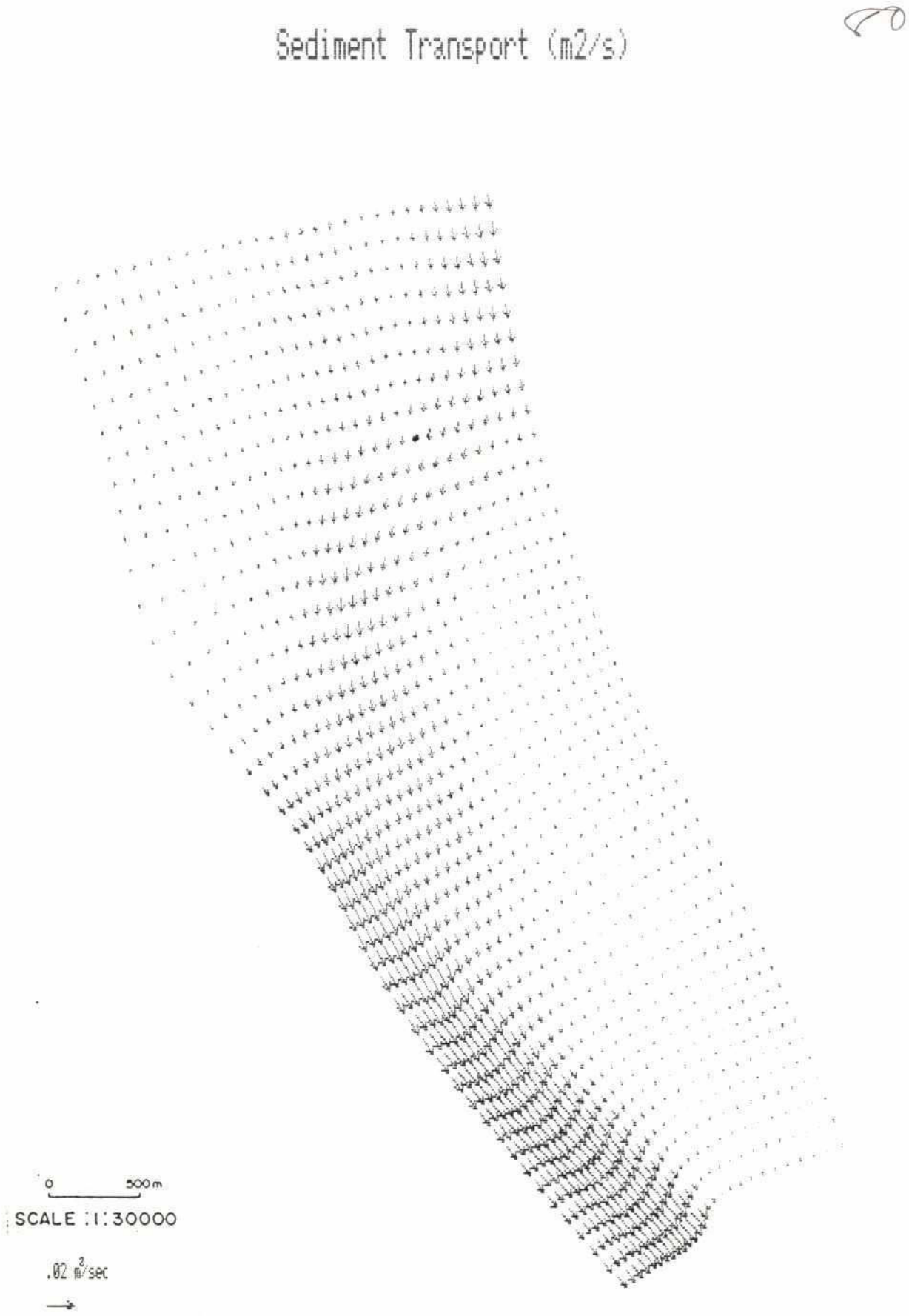

BRTS Verification of the 2-D Morphological Model

Simulated Sediment Transport Rate Per Unit Width	**Vol.4** Part 9
	Figure 5.9

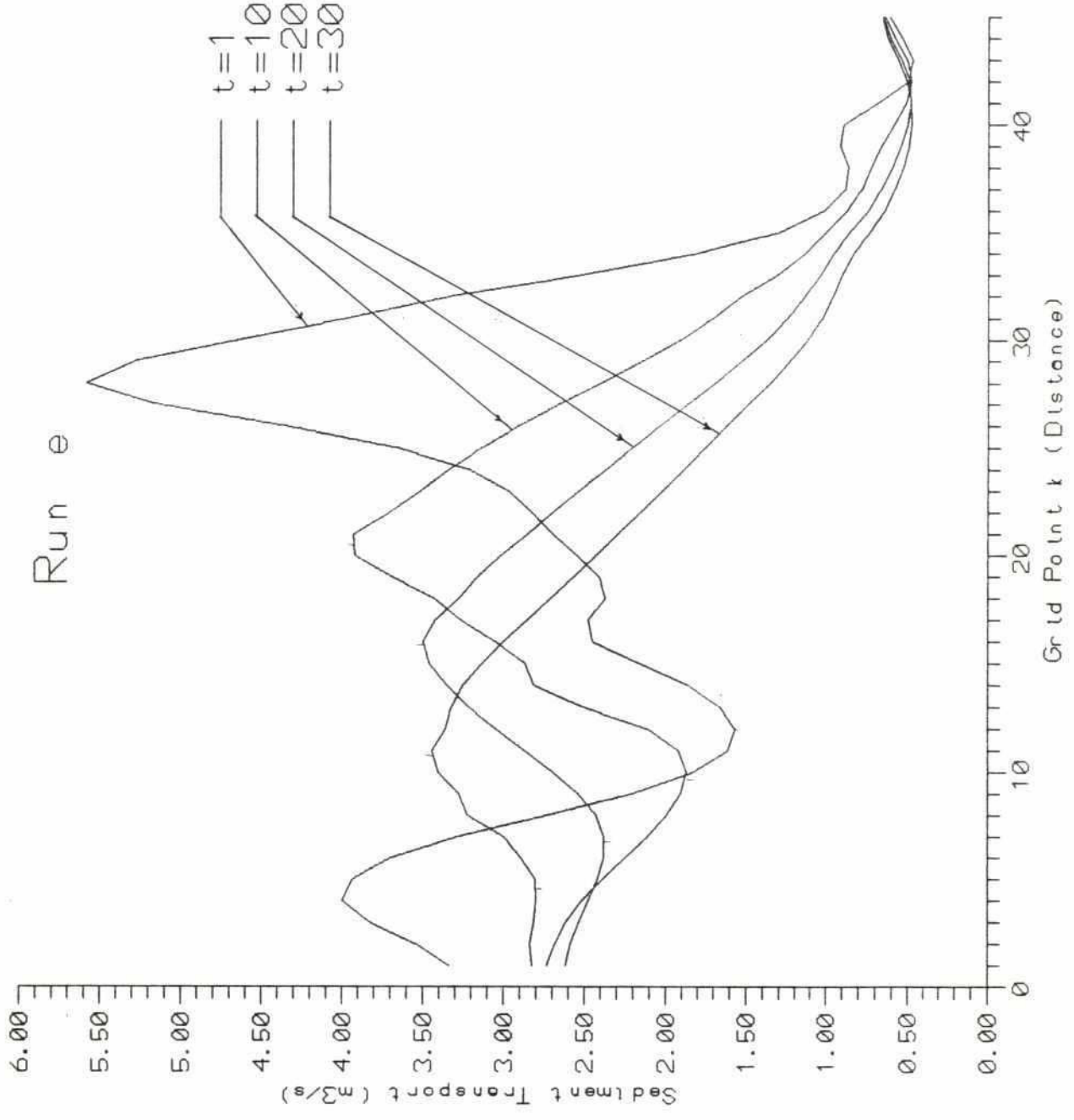

Notes : K = 0 at downstream boundary
1 time unit = 0.7 days

0 500m
SCALE : 1 : 30000

BRTS Verification of the 2-D Morphological Model

Sediment Transport Rate in Test Area 2 as a Function of Distance Along Thalweg	**Vol.4** Part 9
	Figure 5.10

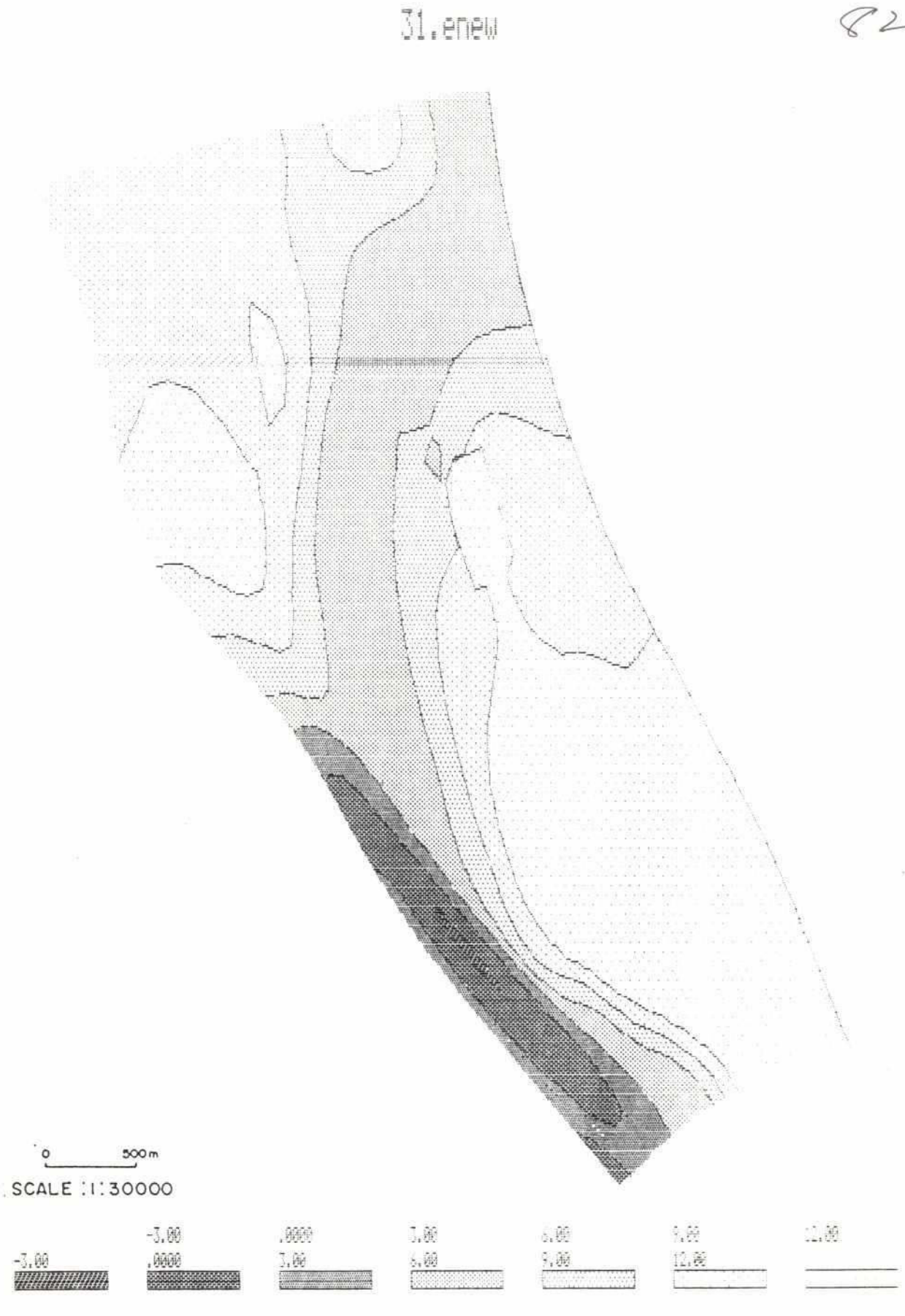

BRTS Verification of the 2-D Morphological Model

Simulated Bathymetry. After 21 Days

Vol.4 **Part 9**

Figure 5.11

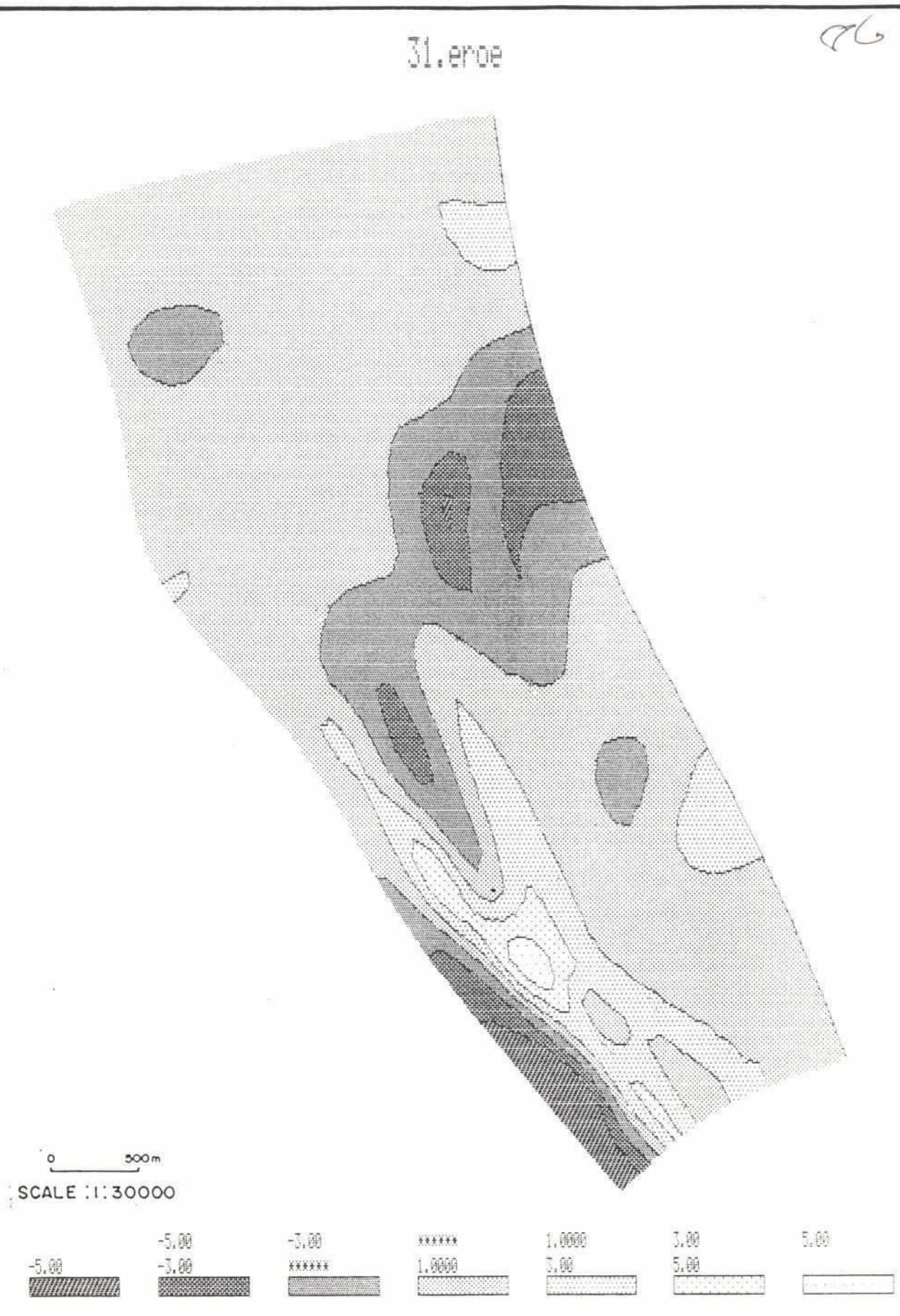

BRTS Verification of the 2-D Morphological Model

Simulated Erosion (-) and Deposition (+) After 21 Days	Vol.4 Part 9
	Figure 5.12

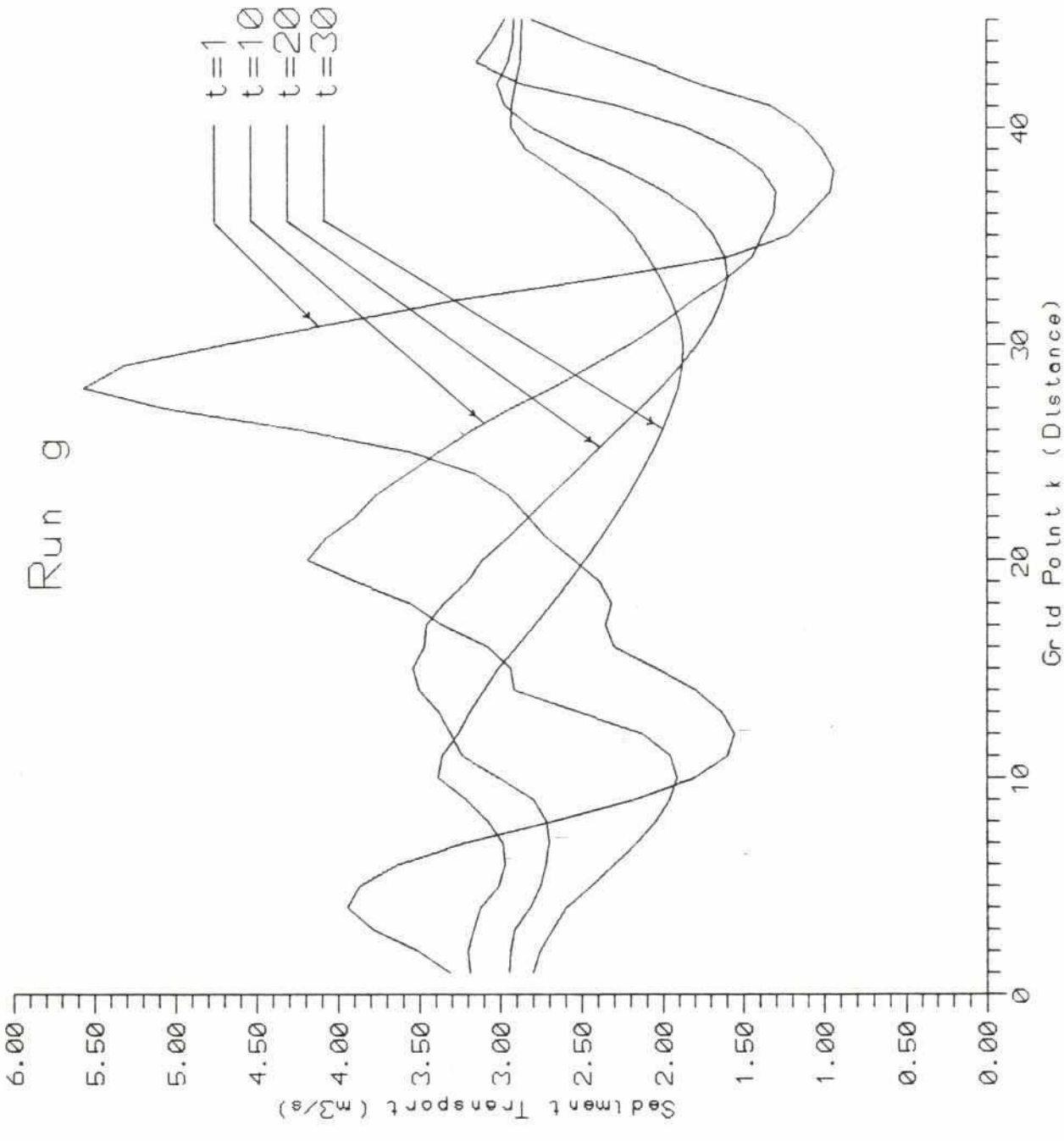

BRTS Verification of the 2-D Morphological Model

Width Integrated Sediment Transport Rate with Modified Upstream Conditions (from k = 39 to 45)	Vol.4	Part 9
	Figure 5.13	

BRTS Verification of the 2-D Morphological Model

Simulated Bathymetry With Modified Boundary Condition	Vol.4 Part 9
	Figure 5.14

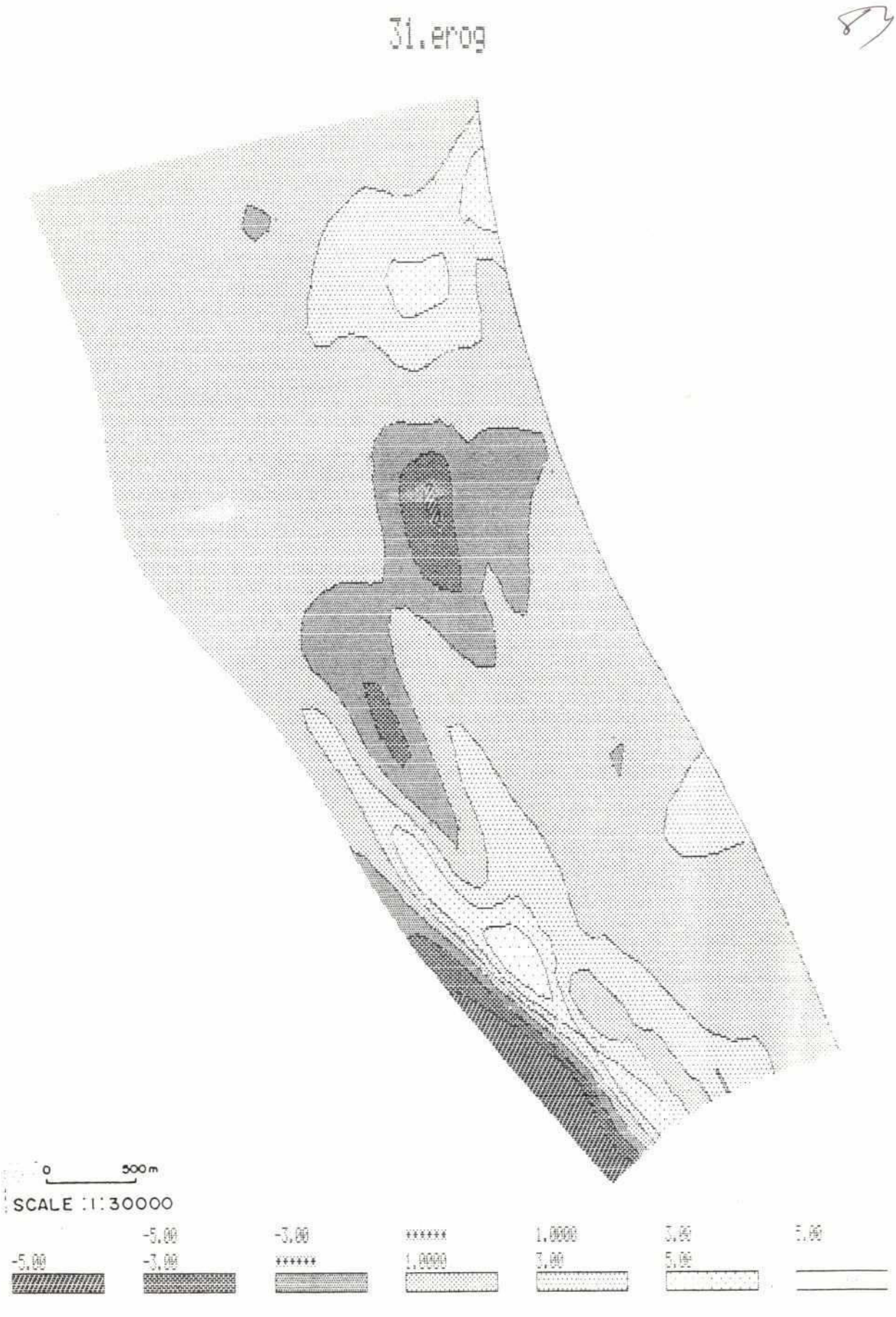

Simulated Erosion (-) and Deposition (+) with Modified Boundary Condition

Vol.4 Part 9

Figure 5.15

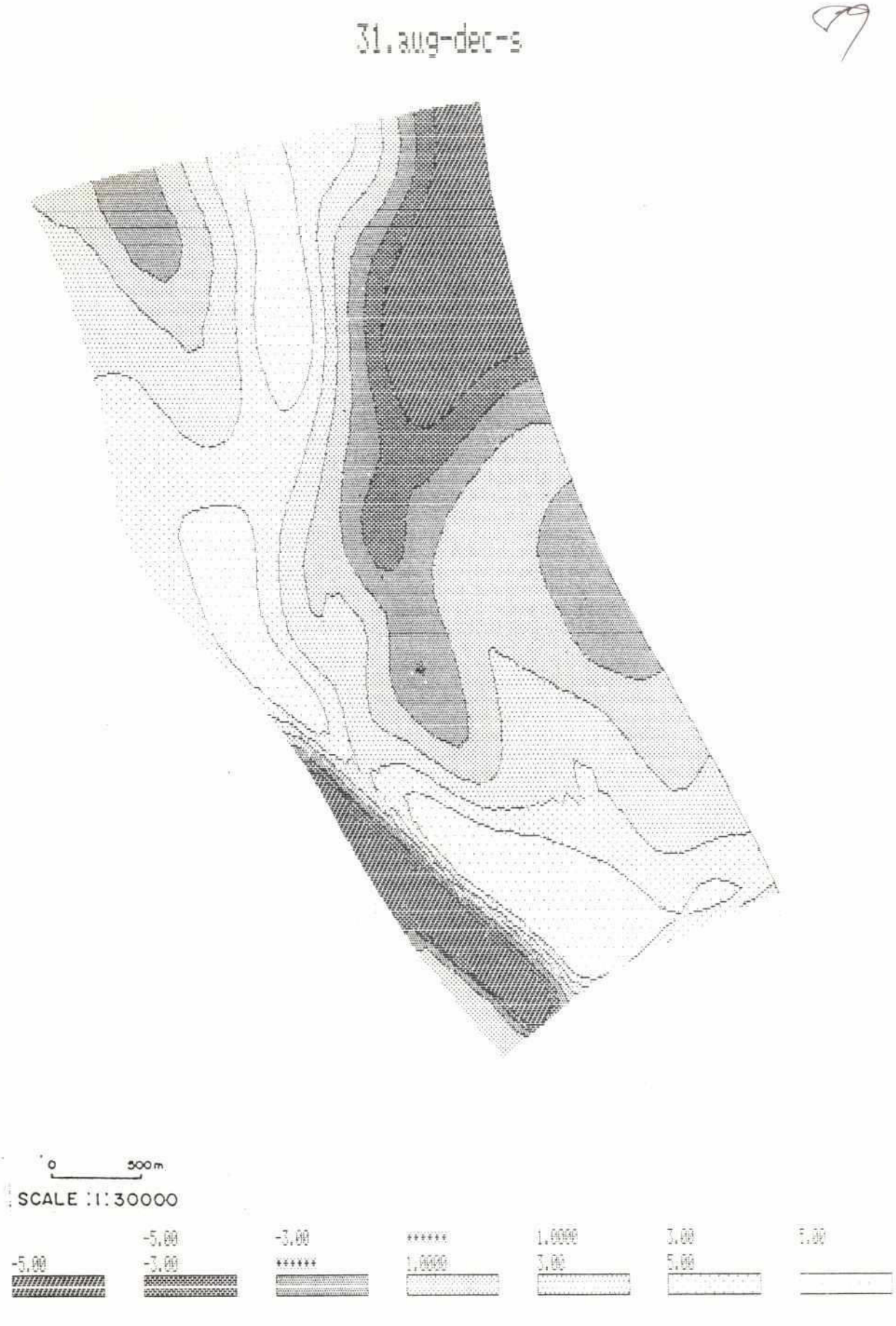

BRTS Verification of the 2-D Morphological Model

Observed Erosion (-) and Deposition (+) from December to August	**Vol.4** Part 9
	Figure 5.16

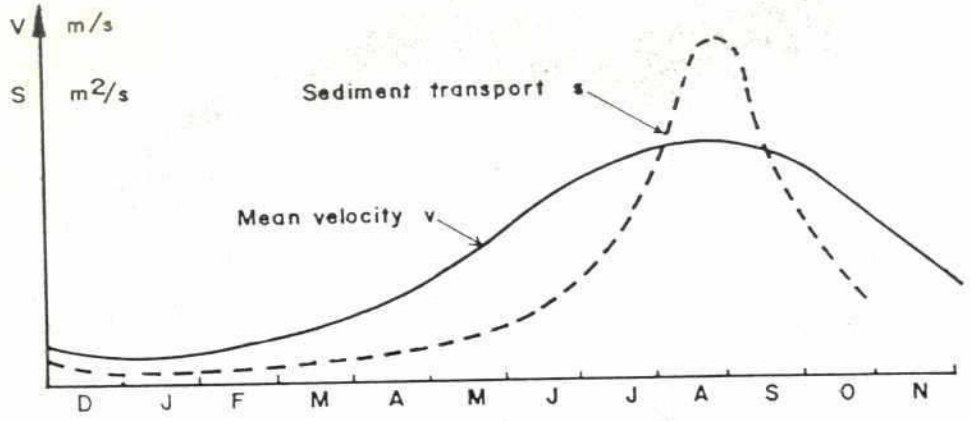

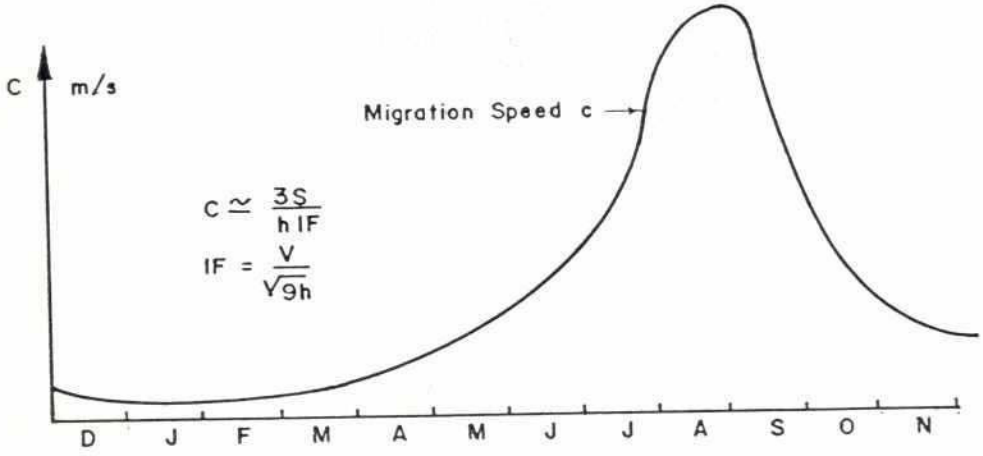

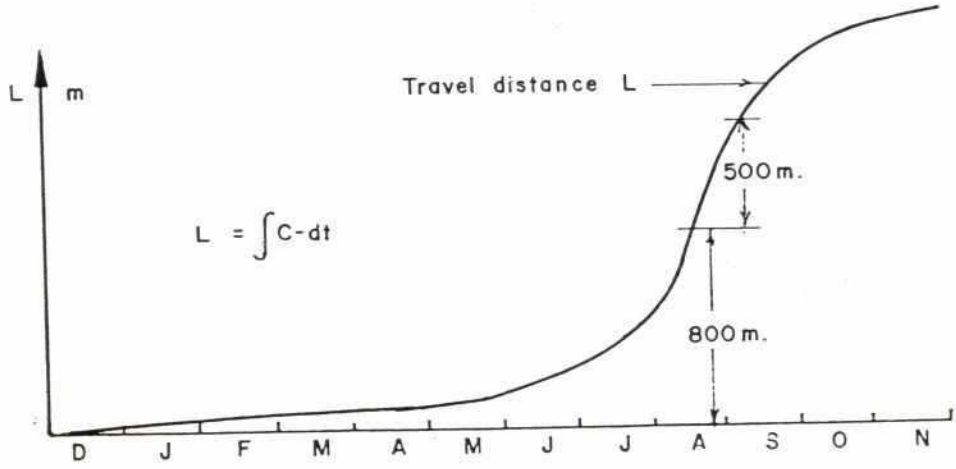

BRTS Verification of the 2-D Morphological Model

Variation in Mean Velocity, Migration Speed of Bed Forms and Accumulated Travel Distance of Bed Form Over the Year	Vol.4	Part 9
	Figure 5.17	

Part 10

2-D Numerical Modelling of River Bends

HALCROW

RIVER TRAINING STUDIES OF THE BRAHMAPUTRA RIVER

REPORT ON MODEL STUDIES

PART 10 - 2-D NUMERICAL MODELLING OF RIVER BENDS

CONTENTS

TABLES

FIGURES

1. INTRODUCTION

1.1 Objective

Some of the exposed places along the BRE with respect to erosion of the bank are along bends of anabranches. Thus, in order to provide a good foundation for outline of a master plan for protection of the BRE, it was found necessary to carry out a thorough analysis of the processes associated with river bends and bend scour. A detailed morphological assessment of bends was carried out from available maps, aerial photos and satellite imagery. Survey data has been used to establish river bend parameters. An analytical model of the equilibrium bathymetry in river bends has been applied. Finally, the 2-D model has been employed. It is capable of simulating the dynamic development of scour in river bends. Experience from the other studies was utilised in the analysis.

The objective of the river bend analysis with the 2-D model was to:

- find the most sensitive parameters for river bend development in order to assess the uncertainty attached to various predictors of maximum depth and velocity eg. mathematical and physical models
- verify the analytical BENDFLOW programme which in a simple way calculates maximum scour depth and velocity in river bends
- derive some relationships between v/v_{max}, h/h_{max}, and R/W in order to be able to verify/justify the choice of design velocity in the design of protection works along the river bank

1.2 Approach

With one specific planform geometry, a sensitivity analysis of the following parameters on the morphology was carried out:

- Time step and other model parameters
- Eddy viscosity (degree of turbulence)
- Bed resistance
- Slope of water surface
- Strength of secondary currents (helical flow)
- Bank erosion
- Grain size of bed material
- Model description of bed load and suspended load.

All simulations were compared separately to a reference simulation in order to evaluate the influence from changes in the parameters.

The BENDFLOW and the 2-D model was run in parallel with similar parameters. The calculated maximum depths and velocities were compared. The limitations of the BENDFLOW programme were assessed.

The velocity and scour depth was simulated using six different planform geometries, each with a specific ratio between the radius of curvature of the bend and the width. The maximum depth and velocity was extracted from each simulation in order to find the most critical R/W ratio.

The bathymetry would be predicted by the 2-D model. However, some simulations were carried out with predefined bathymetries with a fixed bed and maximum depth. The objective was to derive the maximum near bank velocity as a function of the near bank scour depth with maximum depth/mean depth ratios extended beyond the range predicted by the 2-D model but within the range observed in nature.

1.3 Description of the Model

The river bend in the model is limited by two fixed banks where the radius of curvature of the outer bankline decreases from infinity to the specific minimum value at the middle of the bend. The coordinates (x,y) of the bank lines are described by the expressions:

$x = R/a^2 \cosh(bt)$ $y = R/a \sinh(bt)$

in which t is the coordinate along the outer bankline, R is the minimum radius of curvature, a and b are factors determined by the length of the bends and the rapidity by which the radius changes. The width is constant along the channel axis. Figure 1.1 shows an example of the generated computational grid.

Typical values from Test Area 2 were used. The slope is relatively steep compared to the average slope of the entire river.

width	$w = 1000$ m
radius	$R = 3000$ m
mean depth	$h = 7.0$ m
slope	$I = 11 \times 10^{-5}$
mean velocity	$v = 2.0$ m/s
mean bed resistance	$C = 74$ $m^{0.5}/s$

The total length of the channel was chosen so that the boundaries would not overmuch affect the results:

length	$L = 9600$ m

The sediment transport parameters applied for Test Area 2 were reused:

grain diameter	$d_{50} = 0.17$ mm
fall velocity	$w_s = 0.018$ m/s
transport model	van Rijn (1987)

1.4 Boundary Conditions

The simulation of bend scour is very sensitive to the applied boundary conditions. Hence, a careful selection of these was required. In order to find the most critical radius of curvature, the boundary conditions should consist of a water level boundary upstream and a water level

boundary downstream. The discharge would then be determined by the water surface slope, the bed resistance and the resistance due to the plan shape of the river bend.

The morphological model requires a concentration boundary of suspended sediment at the upper boundary together with the variation in bed level at the upstream boundary. The equilibrium concentration for the specific depth and velocity at the boundary was applied. A fixed bed level at the upper boundary was assumed.

Hence, the boundary conditions were:

Upstream water level: 17.6 m

Downstream water level: 16.5 m

Upstream concentration: Locally in equilibrium

Upstream bed level: 10.5 m

1.5 Model Parameters

The grid size was chosen so that the adaptation length for inertia forces to friction forces

$= C^2h/2g$

was properly resolved. Using typical values of C and h, one finds an adaptation length of about 1100 m. The grid mesh has the dimensions 63x19 where the distance between neighbouring points in the longitudinal direction varies between 50 m and 200 m.

The mean value is

$x = 155$ m

The grid is most dense at the point of the minimum radius of curvature. Across the river, the space step is

$y = 55$ m

The time step was chosen so that the mean Courant Number,

$$(v + \sqrt{gh}) \frac{\Delta t}{\Delta x}$$

was about 5:

$\Delta t = 90$ sec

For the updating of the bed level, another time step is used:

$\Delta t_s = 10$ hours

The bed resistance and the eddy viscosity from the Test Area 2 was used:

Bed Resistance,

$$C = 74 \left(\frac{h}{h_{mean}}\right)^{0.25}$$

Eddy viscosity, E = 20 m^2/s

2. SIMULATIONS

2.1 Sensitivity Analysis

When reading the results of the sensitivity tests, it is important to note that the reference (base case) had a time step of 90 s, and an eddy viscosity of E = 20 m^2/s.

The selected bathymetry at the beginning of each simulation was the same, see Figure 2.18. The simulation time was 167 days real time in all simulations. Equilibrium was then reached in almost all cases. The development in time of the maximum scour depth is depicted for all simulations in Figure 2.2. The graph of the reference simulation is identical for the first 167 days with the graph for Radius/Width = 3 in Figure 2.13. The maximum calculated depth in the simulations is listed below in Table 2.1.

Table 2.1: Simulated Maximum Depth with Different Input Parameters.

Run No	Parameter	h_{max}	h_{max}/h_{mean}	Deepest grid point	Figure
1	Time step	13.50	1.95	(14,18)	2.3
2	Eddy visco.	17.86	2.61	(27,18)	2.4
3	Bed resist.	11.56	1.64	(2,18)	2.7
4	Surface slope	8.36	1.25	(32,18)	2.8
5	Helical flow	13.07	1.88	(13,18)	2.9
6	Bank erosion	12.79	1.84	(17,18)	2.10
7	Grain size	11.13	1.58	(2,18)	2.11
8	Sed.model	-	-	-	-
9	Reference	14.74	2.12	(9,18)	2.13

The simulations are described below.

Time step

A simulation was made with a time step of 60 s instead of 90 s. The difference in the maximum depth after 167 days was 8% less See Figure 2.3. Thus, a more accurate calculation could be obtained with a smaller time step. But the simulation becomes much more time consuming and for a sensitivity analysis, the high degree of accuracy is not crucial as long as the same time step is used in all simulations.

A simulation was undertaken with a sediment transport time step of 5 hours instead of 10 hours. The difference in the maximum depth was 0.9%.

Eddy viscosity

The eddy viscosity parameter expresses the diffusion of momentum in horizontal directions. It is a product of the vertical averaging of the flow equations in the numerical scheme and the horizontal averaging of water level and currents over one grid spacing. If the degree of

turbulence (eddies) is high, the eddy viscosity in the model must also be high. The exact values depend on the calibration because it depends on the grid size and the model bathymetry. Typical values are between 0 and 50 m^2/s in this size of model. In some cases, the eddy viscosity has no importance (in uniform flow). In other cases, a more detailed turbulence model is required. In Test Area 2, a constant value of 20 m^2/s was used in the calibration throughout the model area and the same value was used in this study with a similar layout to the one in Test Area 2.

A sensitivity simulation with E = 5 m^2/s was run. In the first 50 days, the simulations look the same, see Figure 2.2. But then there start to be large differences in velocity across the river; the change in eddy viscosity becomes significant. After 167 days, the bathymetry looks as shown in Figure 2.4. The reference simulation with E = 20 m^2/s is shown in Figure 2.12. The depth has increased from 14.74 m to 17.86 m, i.e. an increase of 21 %. Hence, according to the model, the scour should be more severe with less momentum diffusion or turbulence in the water. In reality, the increased turbulence would also influence the sediment transport capacity. The model takes that into account in the definition of the vertical dispersion coefficient of sediment particles in suspension. This coefficient determines the shape of the vertical concentration profile. It was the same in both simulations. Hence it can be concluded that the influence of the value of the eddy coefficient used in the simulation is not insignificant.

Bed Resistance

The hydraulic resistance determines the discharge and hence the sediment transport in the channel for a given surface slope. Differences in bed resistance across and along the river will occur due to differences in depth and bed forms. From the calibration of the models of Test Area 1 and 2, the Chezy Number was found to be

$$C = 74 \left(\frac{h}{h_{mean}}\right)^{0.25}$$

This means that the Chezy Number is updated as a regular procedure following the local depth. A simulation has been run where the overall mean value of the Chezy Number is the same in both simulations but where the resistance number is kept constant throughout the simulation and not updated when the bed levels (and depths) are updated in the morphological model. Figure 2.5 shows the initial bed resistance which was kept unchanged throughout this simulation. Figure 2.6 shows the simulated bed resistance (from the above equation) after 167 days in the reference simulation.

The erosion pattern is almost the same, see Figure 2.7. The maximum scour depth has decreased by 3.2 m (22 %). This is because the resistance is getting smaller where the depth is getting deeper if the Chezy Number is updated in the morphological model and thus encouraging even higher velocities in the deeper parts. The simulation demonstrates that the sensitivity of hydraulic resistance over the cross section on the scour is significant.

Surface slope

The effect of changing the water surface slope from 11 x 10^{-5} to 7 x 10^{-5}

was tested by changing the upstream water level by 40 cm. The discharge went down from 13200 m^3/s to 9700 m^3/s. The maximum scour depth went down by 6.4 m (44 %), see Figure 2.8. The impact is significant because a minor change in velocity is amplified in the sediment transport.

Strength of helical flow

The helical flow in river bends will cause a net current at the bed from the outer to the inner bank. At the surface it is reversed. When the transverse bed slope is sufficiently high, the net transport of sediment from the outer to the inner bank will be zero. This happens when the gravity forces (due to the slope) equals the secondary current forces. If this effect is neglected a simulation showed that the maximum depth would decrease by 1.7 m (11 %). Thus, the secondary flow is important in the modelling of bend scour, see Figure 2.9, but not as significant as some of the other parameters investigated in this sensitivity analysis.

Bank Erosion

The model has fixed banks. The bank erosion is included by introducing lateral inflow of sediment into the model. From Test Areas 1 and 2, bank erosion rates of up to 15 m/day were observed during the monsoon. The porosity of the bank material is about 0.4. The percentage of sand is 60%. As an extreme event, bank erosion over a stretch of 1700 m and a mean depth in front of the bank of 11 m was used. Hence the lateral inflow of sediment was 7×10^{-4} m^3/s per meter length of the bank. The simulation showed that the extension of the eroded areas had changed. The maximum scour depth was 12.79 m instead of 14.74 m. Downstream of the sediment sources, scour was less severe, see Figure 2.10. It is, however, very difficult to model the bank erosion properly because even field surveys have not given a precise answer of how the erosion rate depends on depth, velocity, slope etc. Upstream and downstream conditions are also believed to have a big importance. Heavy bank erosion is often seen when a main current runs hard on the bank and is forced to turn. The simulation shows that bank erosion is an important element in the development of bends. The maximum scour depth can increase by about 15 % if the bank is protected against erosion.

Grain Size

Bed samples from Test Areas 1 and 2 and other parts of the Brahmaputra show that the grain size of the bed material varies approximately between 0.10 mm and 0.20 mm. The most coarse material is found in the thalweg of the river. In all simulations, a constant value of 0.17 mm was used. In order to test the sensitivity of the spatial variation in grain size, a simulation was done where the grain size was updated automatically as a function of depth (see Figure 2.11).

$$d_{50} = 0.17 \left(\frac{h}{h_{mean}}\right)^{0.25} mm$$

At the end of this simulation, the grain size varied from 0.14 mm to 0.20 mm (in the scour hole), see Figure 2.12. The maximum depth was reduced by 3.6 m (24 %). The spatial grain sorting mechanism tends to "armour" the river bed when it is attacked by erosion. In areas with high velocities, more fine material will be eroded than will be deposited and only the coarser material will be in a state of

equilibrium with the local flow conditions. However, it is known from studies of the test areas that the bathymetry will probably never be in equilibrium locally. The course of the flow changes continuously and new bars and channels are created. Hence it is difficult to establish the kind of relationship between grain size and depth shown above. Field surveys have shown that there is no consistency in the size of sediment grains on the submerged chars for instance. In some places it is coarse, in other places fine. It depends on the historical development: whether the char is being built up or whether it is being eroded.

Sediment Transport Model

Most analytical models of the so-called equilibrium scour depth in river bends are based on the assumption that the sediment transport is composed of bed load only. However, only about 10% of the transport of bed material in Brahmaputra is bed load according to various sediment transport formulas (van Rijn, Engelund & Fredsoe). From the field survey, it was found that a considerable part of the total transport was going on by migration of sand dunes. More than 50% of the suspended sediment contributes to the migration of these sand waves by sediment being trapped on the lee side of the dunes.

In order to check the significance of distinguishing between bedload and suspended load, a simulation with only bedload was run. A factor was multiplied to obtain the same order of magnitude in total sediment transport along the channel. Hence, the simulation is not directly comparable with the others. But it showed that the maximum depth occurred further upstream. According to the theory, this should also be the case because there is built in a certain adaptation length and delay in the suspended sediment transport mechanism.

2.2 Comparison between Numerical (2-D) and Analytical model

The 2-D model was compared with the BENDFLOW programme in two simulations with the following parameters:

mean depth	h = 4.0 m and h = 7.0 m
width	w = 1000 m
wave length of meander	λ = 19200 m
sinuosity	p = 1.22
slope	$I = 11 \times 10^{-5}$
Min. radius of curvature	R = 3000 m

The 2-D model was run until equilibrium was reached (417 days). The results agree reasonable well on velocities while the 2-D model showed significantly larger water depths, see Table 2.2 below:

Table 2.2: Comparison between the 2-D Model and the BENDFLOW model.

Model	h_{min}	h_{max}	h_{max}/h_{mean}	v_{mean}	v_{max}	v_{max}/v_{mean}
2-D	1.46	8.09	2.02	1.53	1.94	1.26
BENDFLOW	1.79	7.15	1.79	1.51	2.01	1.33
2-D	1.47	15.07	2.17	2.03	2.53	1.25
BENDFLOW	3.12	12.51	1.79	2.00	2.61	1.31

The 2-D model is mainly based on suspended load whereas the BENDFLOW programme is based on bed load only. The bendscour tends to be more severe when most of the sediment is in suspension because the gravity force, which should counterbalance the forces due to the secondary current, is less effective in this kind of transport. Hence BENDFLOW will underestimate the scour depth. The sensitivity of the simulated scour depth in the 2-D model (see section 2.1) should also be taken into account when the results are assessed.

2.3 Critical Radius of Curvature

The study of the influence of radius of curvature on the scour depth was performed with a bend with length 9600 m. The up and downstream water level was kept constant and hence the slope along the centerline remained constant during the simulation.

The results of the simulations, which covered 417 days, are shown below in Table 2.3. Equilibrium was reached in all cases, see Figure 2.13 which shows the time development of the maximum erosion depth below the mean depth.

Table 2.3: Simulation of Scour Depth and Velocity as a Function of the Radius(R) and Width(W) Ratio.

R/W	h_{max}	h_{max}/h_{mean}	v_{max}	v_{max}/v_{mean}	Figure
2*	14.98	2.14	2.53	1.24	2.14
3	15.07	2.17	2.53	1.25	2.15
4	14.89	2.15	2.52	1.25	2.16
5	14.62	2.11	2.52	1.25	2.17
8	14.05	2.03	2.51	1.25	2.18
10	13.85	2.00	2.51	1.25	2.19

* No bend scour developed.

Six different runs were performed with radius/width ratios of 2, 3, 4, 5, 8 and 10 (see Figure 2.14 through 2.19). The smallest possible ratio where bend scour took place in the model was 3. In the simulation with a smaller ratio, scour took place at the inner bank instead indicating that the bend tried to increase the radius of curvature by taking a short-cut.

Above the critical ratio between radius and width, the maximum scour depth decreases with increasing R/W-ratio. However, the difference between R/W=3 and R/W=10 is not very large when compared to the sensitivity of other parameters (see section 2.1). The maximum depth decreased by 8 %.

Another observation is that it took some time before the equilibrium scour was reached: about 170 days. Steady conditions were assumed in the model, which seems to be a major approximation because the wet season only lasts for four months. On the other hand, when the water level falls, the velocity in a bend anabranch decreases less rapidly because the total cross sectional area reduces also.

2.4 Maximum Near Bank Velocity

The ratio between maximum velocity and mean velocity has been calculated for different values of the ratio between maximum depth and mean depth. As seen in Table 3, the 2-D model was not capable of creating max/mean depth ratios of more than about 2.4. Bend scour is not necessarily the only source for near bank scour, see later, and greater h_{max}/h_{mean} ratios can be observed in nature. Therefore the bathymetry was distorted up to the required max/mean depth ratio by using a factor on the calculated erosion pattern. The simulations were repeated with two values of the eddy viscosity: 5 m^2/s and 20 m^2/s. Results are shown in Figure 2.20.

The influence of the value of V_{max}/V_{mean} is highly significant as for an increase from 1.3 to 2.1 in this parameter, the value of h_{max}/h_{mean} increases from 2.0 to 5.5.

The simulated values of Vmax/Vmean in the 2-D model area appear on the low side compared to the values observed in physical model tests. This difference is explained by the fact that the secondary currents due to curving stream lines are not explicitly included in the calculation of velocities. Only when the sediment transport is calculated is the effect of secondary currents included.

3. CONCLUSION

The study has shown that the most sensitive parameters in the development of bend scour are the slope of the water surface, grain size, bank erosion rate, eddy viscosity representing the degree of turbulence, and the variation in bed resistance over the cross section.

The last two of these are compound parameters that are used in the process description and their values are normally best determined by calibration.

The study revealed that the dynamics in bend scour development are very sensitive and a state of equilibrium is probably never reached because the parameters mentioned above will change continuously in the Brahmaputra. One of the most important degree of freedom, the horizontal movement of a bend, was fixed in the 2-D model. Instead the bank erosion was included as a lateral inflow of sediment. The dynamic interaction between bank erosion and planform movement cannot be explored with a 2-D model at the present state of development. However, the sensitivity analysis showed the significance of bank erosion to bend scour, for instance if a revetment were constructed. The difference in maximum depth would be in the order of 2 m.

The 2-D model and the simpler analytical BENDFLOW model were compared and the results were found to be compatible when the sensitivity of the various parameters were taken into consideration.

The BENDFLOW model underestimates scour and marginally overestimates velocity amplification.

The modelling of the bed levels reached the state of equilibrium after approximately 170 days where the maximum depth would be about 15 m. The results give an indication of the time scale of bend scour development (but not planform movements) although the flow will not be steady in the whole period as assumed in the model. Another approximation was that the planform geometry was fixed.

In this connection, it is important to compare the results of the JMB-studies. Collected data on bend scour from surveys carried out by BIWTA gave depth below Low Water Level (LWL) ranging from 6 to 23 m. The mean value from 27 measurements was 13.4 m with a standard deviation of 3.6 m. The dominant discharge water level is almost 4 m higher than LWL indicating that the 2-D model simulated scour depths of the order of 10 m below LWL, which are smaller than those actually observed in the Brahmaputra.

The 2-D bend model could not simulate the development of the large scour holes at for instance Kazipur. However, from the verification of the model on Test Area 2, it was shown that the model was able to simulate the migration of the scour hole once it was there. The reason why the creation of the scour hole cannot be adequately simulated is believed to be because other modes of scour, confluence and "protrusion scour", interact with the conventional bend scour to produce the critical depths. This has been studied in more detail in the model dealing with confluence scour where this explanation was confirmed.

With fixed bed levels, the maximum near bank velocity as a function of scour depth was simulated. The BRTS physical modelling showed that a

ratio of upto about 2 between maximum and mean velocity is possible. The 2-D model predicted a similar ratio when the maximum scour depth was about 5.5 times the mean depth.

The present 2-D model has been used to simulate one of the important processes in the river morphology of Brahmaputra, namely bend scour. The study has derived valuable information on the development of bend scour and about expected maximum near bank velocities.

Part 11

2-D Numerical Modelling of Confluence Scour

HALCROW

RIVER TRAINING STUDIES OF THE BRAHMAPUTRA RIVER

REPORT ON MODEL STUDIES

PART 11 - 2-D NUMERICAL MODELLING OF CONFLUENCE SCOUR

CONTENTS

TABLES

FIGURES

1. OBJECTIVE

The purpose of this study was to assess confluence scour by use of the 2-D model and to compare the results with the simulations of river bend scour to determine which kind of scour is most severe. The simulated confluence scour was compared to the equation for prediction of scour, presented in the JMB study (RPT/NEDECO/BCL 1989). The study thus forms part of the investigation into a deterministic assessment of possible maximum water depths near hard-points and other bank protection structures.

2. APPROACH

Initially, a model with a flat bed was set up. Confluence scour was simulated for three different situations with different upstream distributions of the discharge. The effect of discharge distribution could then be evaluated. Velocity and depth were chosen so that the model became comparable to the river bend simulations described in "2-D Numerical Modelling of River Bends". The difference in confluence and bend scour could then be derived. Finally the scour was compared with the equation developed in the JMB study*:

$$\frac{h_s}{\bar{h}} = 1.292 + 0.037\ \theta$$

$$\bar{h} = \frac{h_1 + h_2}{2}$$

This equation was based on measurements from the dry period. For flood conditions, the maximum depth h_s is over-estimated with this equation unless one takes into account the increase in water level, Δh from low to high flow conditions.

$$\frac{h_{s,\,high} - \Delta h}{\bar{h}_{high} - \Delta h} = 1.292 + 0.037\ \theta$$

h_1, h_2 depth in upstream anabranches.

h_s depth at point with confluence scour

θ angle between anabranches upstream in degrees

* RPT/NEDECO/BCL
JMB project, Phase II, study Feasibility Report, Vol II
Annex B: River Morphology, August 1989

3. DESCRIPTION OF THE MODEL

3.1 Geometry

The curvilinear grid is shown in Figure 3.1. The grid is most dense where the maximum scour is expected to take place. The shape of the bank line was found by studying aerial photos of Kazipur, Sariakandi, Kamarjani and Sirajganj. The minimum width is 3000 m. This was chosen as a representative width of a major anabranch downstream the confluence of two large anabranches carrying good part of the flow discharge of the entire river. The model comprised the confluence of two anbranches carrying a total of 43,000 m^3/s, i.e about 43% of the 100 year flow of 100,000 m^3/s. The angle θ between the two approach channels, separated by a char, is assumed to be approximately 60°.

3.2 Boundary Conditions

The initial bathymetry is shown in Figure 3.2. Except at the char, the initial bed level was constant, 10 m relative to an arbitrary datum. The applied boundary conditions are listed in Table 3.1. Simulation no. 1 (results not shown) was an exploratory run. The total discharge was equal to 43000 m^3/s.

A value between the dominant and the 100 year discharge was chosen in order to get an event which is representative for the "average" annual maximum discharge over a month in the monsoon season.

Table 3.1: Boundary Conditions in Simulation Nos. 2 to 4.

Simulation No.	Upstream		Downstream Water level
	Left anabranch	Right anabranch	
2	21500 m3/s	21500 m3/s	16.5 m
3	17000 m3/s	26000 m3/s	16.5 m
4	19250 m3/s	23750 m3/s	16.5 m

Sediment grain size was taken to be 0.17 mm and the van Rijn model for sediment transport was used.

3.3 Model Parameters

The mean space step in the flow direction was 200 m and between 100 m and 300 in the transverse direction. The time step was 90 s and for sediment transport calculation it was 10 hours. The total simulation time (real time) was 650 days.

4. RESULTS

The simulated surface elevation is shown in Figure 4.1. Due to the Coriolis effect, the water level was not exactly symmetrical around the axis of symmetry.

The slope was steeper at the downstream end because the cross sections were narrower here. Hence some constriction scour would inevitably occur. The ratio between the upstream depth D_2 and the downstream depth D_1 can be expressed as a function of the ratio between the widths of the upstream and downstream cross section:

$$\frac{D_1}{D_2} = \left[\frac{W_1}{W_2}\right]^{(1 - \frac{1}{b})}$$

D_1, W_1 depth and width at cross section 1
D_2, W_2 depth and width at cross section 2
$b \simeq 3$ from sediment transport equation $s = a.V^b$

Taking the full width of the river upstream (W_2 = 5800 m) the mean depth was D_2 = 5 m here. For b = 3 and with downstream width W_1 = 3000 m, one finds D_1 = 7.8 m.

The initial depth downstream was 7.0 m. Hence the effect of constriction scour was negligible.

The maximum scour was reached after 600 days where a state of equilibrium was found. In simulation no. 2, the minimum bed level was -10.12 m corresponding to a maximum depth of 26.70 m.

The depth h of the two channels was approximately 7.5 m which corresponds approximately to prototype conditions around dominant discharge (water level is close to bank full conditions). The angle between the two anabranches was 60°. Hence, the expected confluence scour was:

$$h_s = \overline{h}\ (1.292 + 0.037\ \theta)$$

$$\overline{h_s} = 26.3\ m$$

The simulated scour in the three simulations was as listed in Table 4.1.

Table 4.1: Simulated Confluence Scour.

Simulation No.	V m/s	Vmax m/s	Vmax v	max erosion m	min bed level m	max depth m	Figure No.
2	1.50	2.32	1.55	20.12	-10.12	26.70	4.2 + 4.5
3	1.33	2.65	1.99	28.02	-18.02	34.60	4.3 + 4.6
4	1.38	2.39	1.73	25.66	-15.66	32.51	4.4 + 4.7

The simulated scour holes are depicted in Figures 4.2 to 4.4. Enlargements of the scour holes are shown in Figures 4.5 to 4.7. Finally, the velocity field at equilibrium is shown for each simulation in Figures 4.8 to 4.10.

5. CONCLUSIONS

The simulated value of confluence scour agreed surprisingly well with data collected and analysed in the JMB study. In the simulation with equal distribution of discharge, the difference between the simulated scour depth (26.70 m) and the predicted scour depth with the JMB relation was less than 2%. The analysis of field data shown in Figure 5.1 (from RPT/NEDECO/BCC 1987 survey) reveal that the standard deviation on the observed confluence scour is large, around 4 m for h = 7 m.

When the distribution of discharge at the upstream boundaries is changed from a 50/50 % distribution, the erosion pattern becomes very different. Using a 40/60% distribution, the scour hole would move to the bank and increase to 34.60 m. With 45/55%, the scour depth was 32.5m. In both cases, the scour hole moved to the bank, and a combined effect of confluence and bend scour seemed to be active in creating the scour hole. This appears a very important observation as it shows that in nature the uneven distribution of flow will almost always adhere to one of the banks downstream of the confluence of the major anabranches.

Maximum bend scour predicted by the 2-D model was 8.1 m (water depth 15.07 m) with mean velocity v = 2 m/s and mean depth h = 7 m. Thus confluence scour can be much more severe.

In the exercise, the JMB equation for confluence scour was verified. It was shown that confluence scour tends to be more severe than bend scour. A combined effect of the two was obtained when the upstream boundary conditions were slightly changed. Hence the maximum design water depth close to a bank line would be a result of combined confluence and bend effects with the effects of confluence playing the largest role.

The field studies performed by BRTS have shown that the deepest scour was found near Kazipur. It has not previously been possible to explain the occurrence of the deep scour holes. However, the present 2-D simulation of confluence scour presents such explanation, as the situation upstream of Kazipur closely resembles the bathymetry conditions simulated. Such a deep scour hole can thus occur when a well developed bend is cut off in such a way that the angle of incidence of the two channels is relatively large and both remain active and the flow distribution is critical. For full development this combination must be sustained for more than one season.

Thus it is not enough for two channels to meet (confluence). It is also required that the upstream bathymetry of the two channels remains almost stable for a considerable time. The 2-D model showed that 600 days are required for equilibrium to develop. The real conditions in nature and the seasonal changes in water level and discharge would probably disturb the development as one flood/monsoon season is only of about 4 months duration at the maximum (120 days). The maximum water depth of about 35m (relative to the water level at dominant discharge, close to bank full water level) is thus considered close to the maximum possible upper limit that can develop. However, the instability and changes of the upstream flow channels in the meandering portion of the river will almost always prevent this from happening.

FIGURES

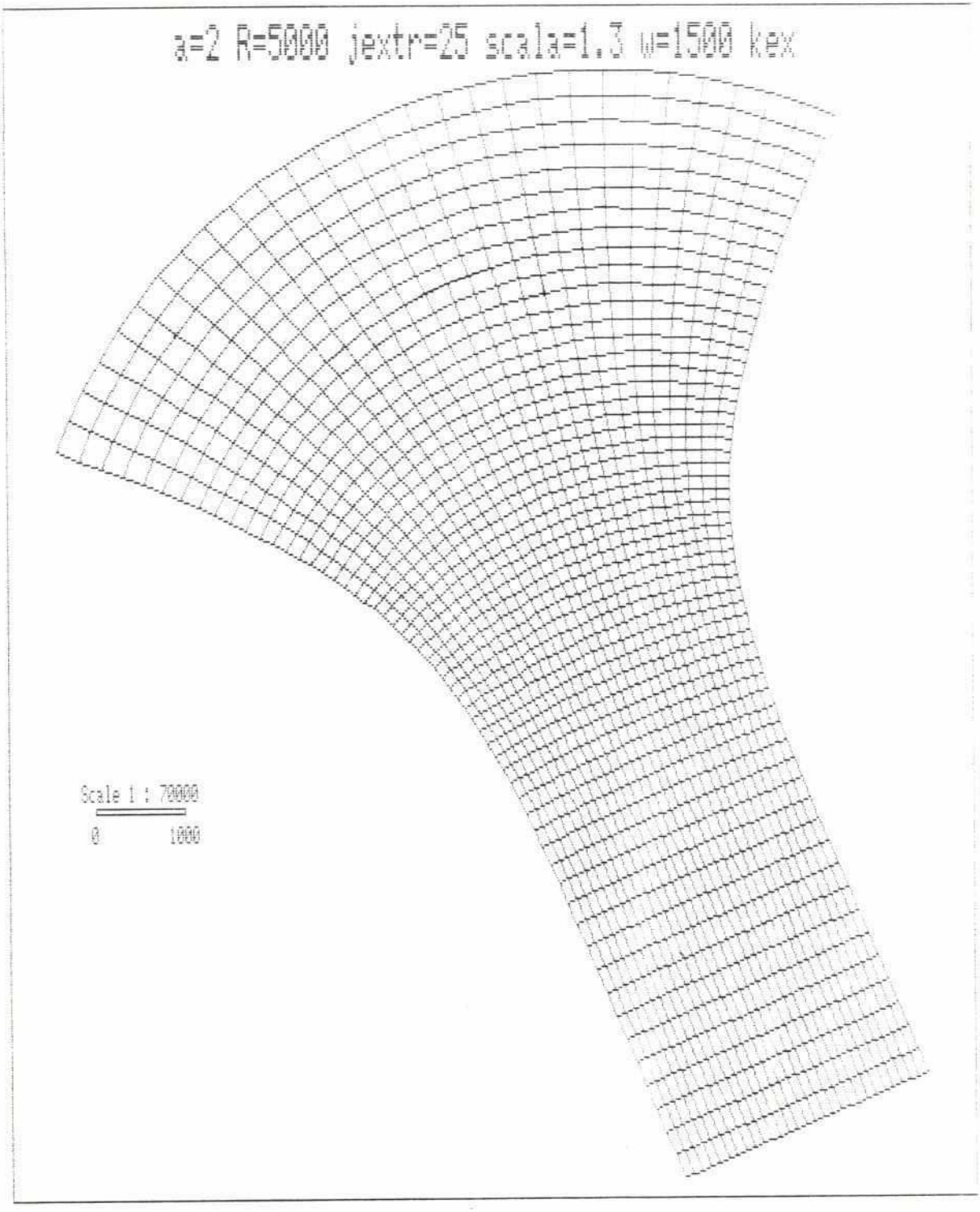

BRTS 2-D Numerical Modelling of Confluence Scour

Computational Grid	Vol.4 Part 11
	Figure 3.1

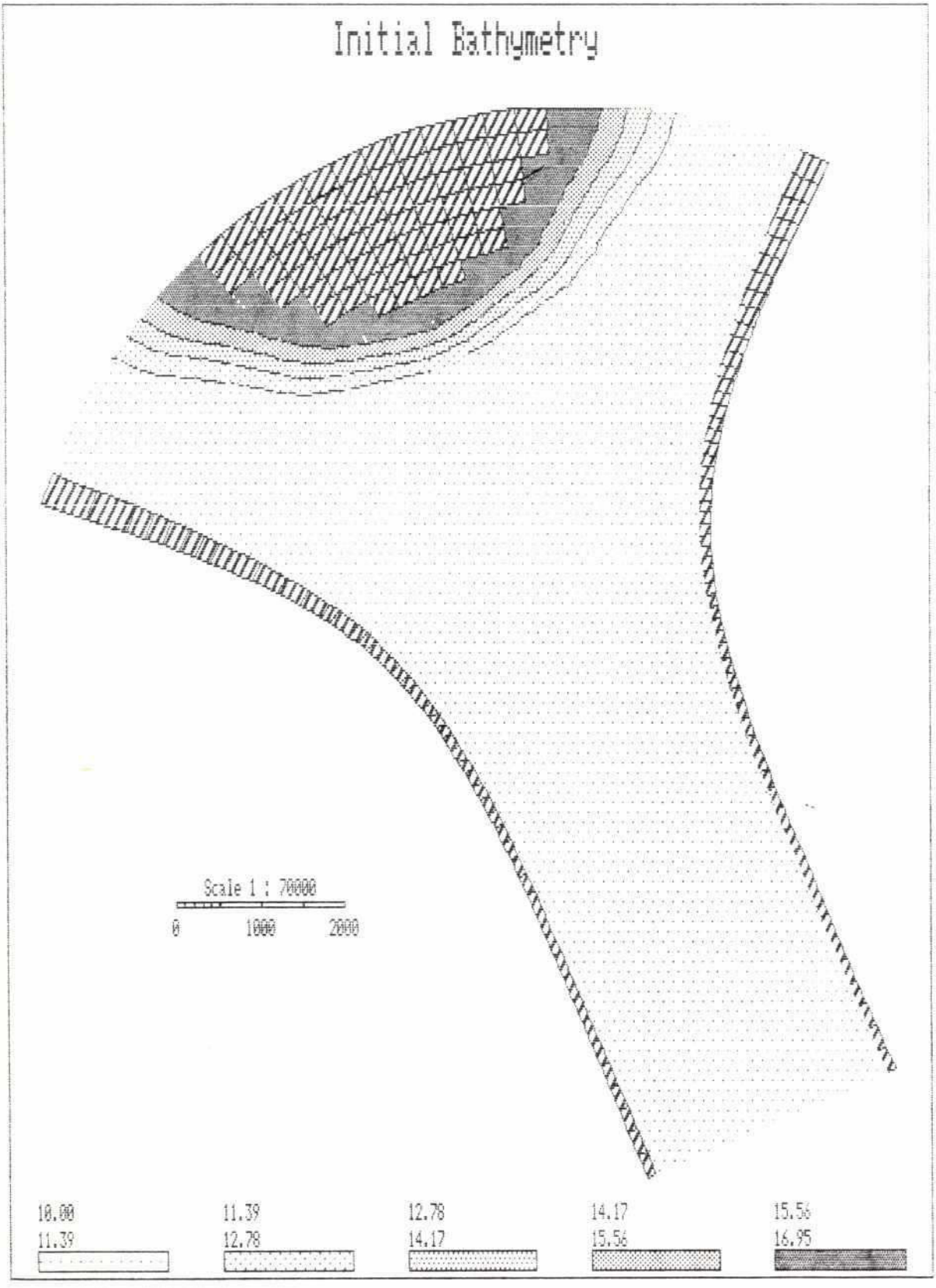

BRTS 2-D Numerical Modelling of Confluence Scour

Initial Bathymetry

Vol.4 **Part 11**

Figure 3.2

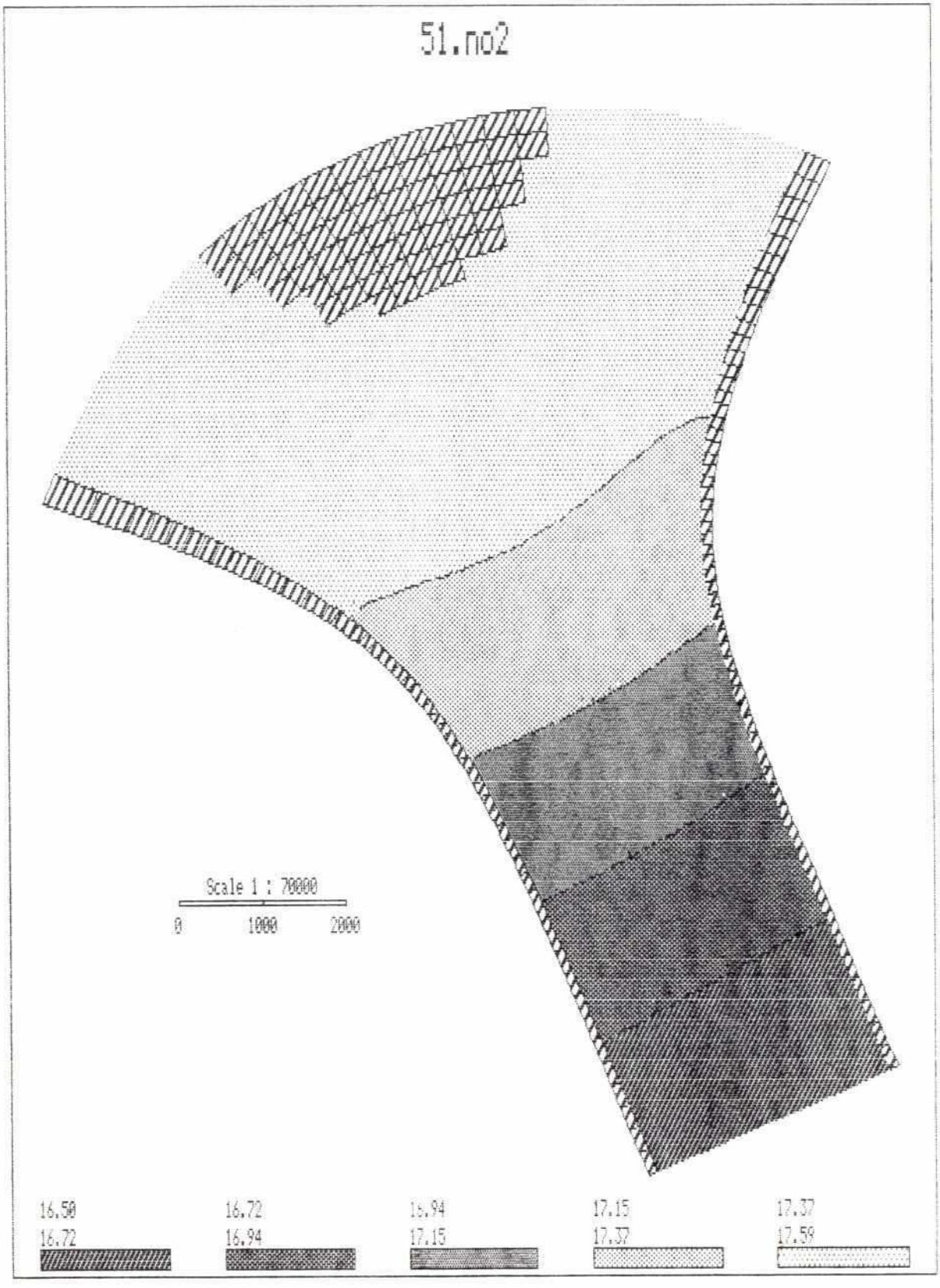

BRTS 2-D Numerical Modelling of Confluence Scour

Surface Elevation

Vol.4 **Part 11**

Figure 4.1

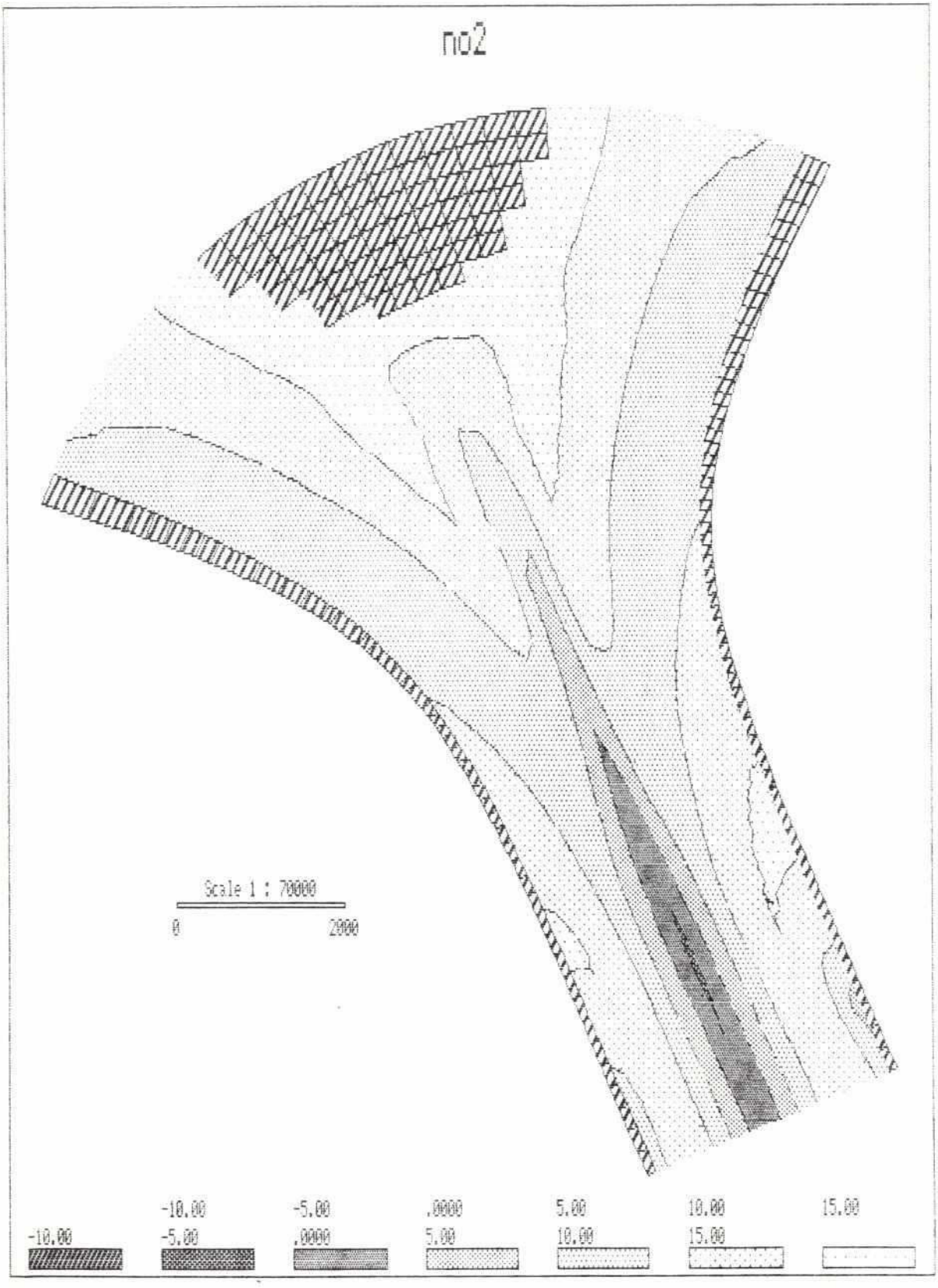

BRTS 2-D Numerical Modelling of Confluence Scour

Simulated Bed Level, Simulation 2

Vol.4 **Part 11**

Figure 4.2

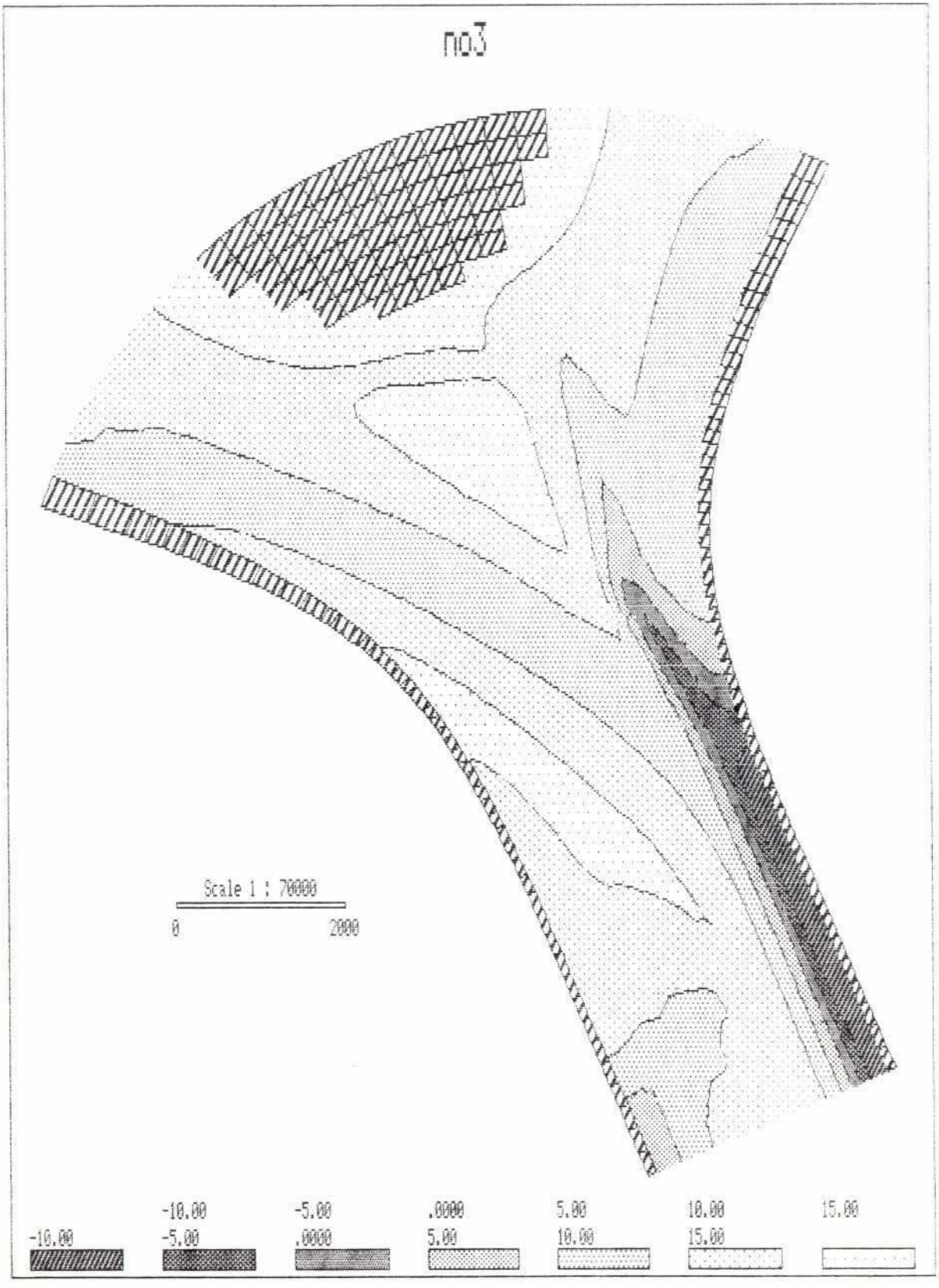

BRTS 2-D Numerical Modelling of Confluence Scour

Simulated Bed Level, Simulation 3

Vol.4 **Part 11**

Figure 4.3

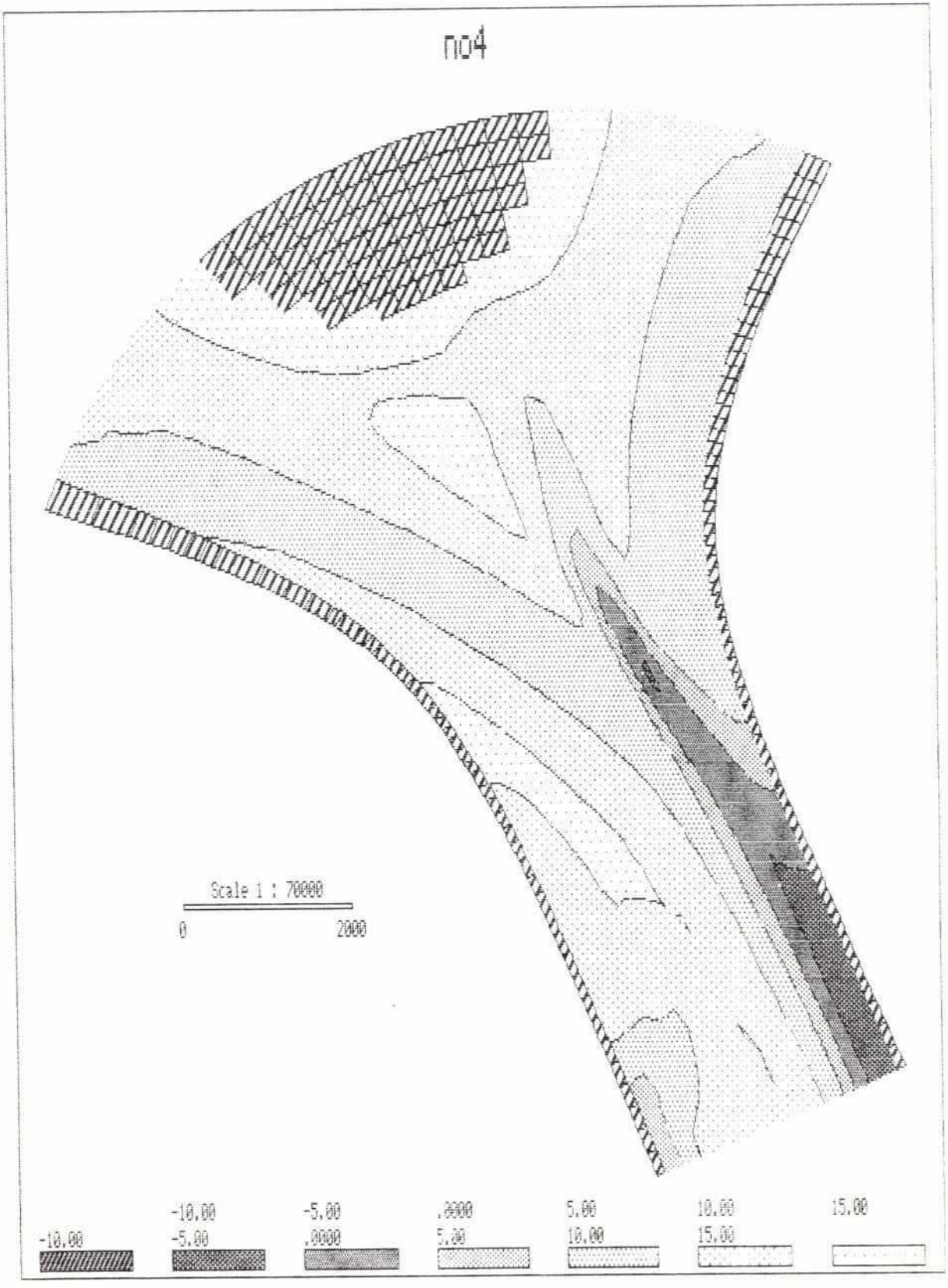

BRTS 2-D Numerical Modelling of Confluence Scour

Simulated Bed Level, Simulation 4

Vol.4 Part 11

Figure 4.4

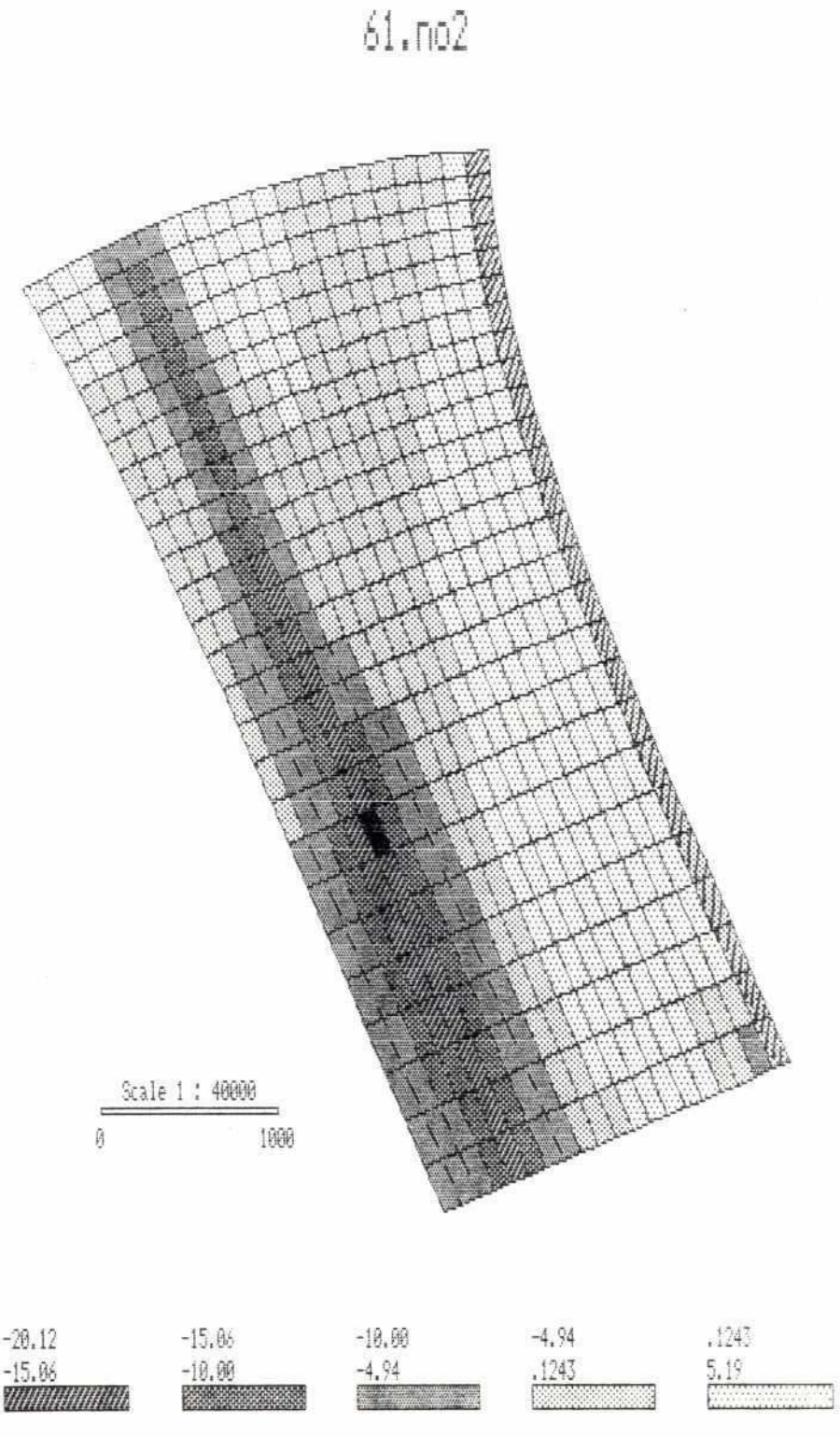

BRTS 2-D Numerical Modelling of Confluence Scour

Simulated Scour, Simulation 2

Vol.4 **Part 11**

Figure 4.5

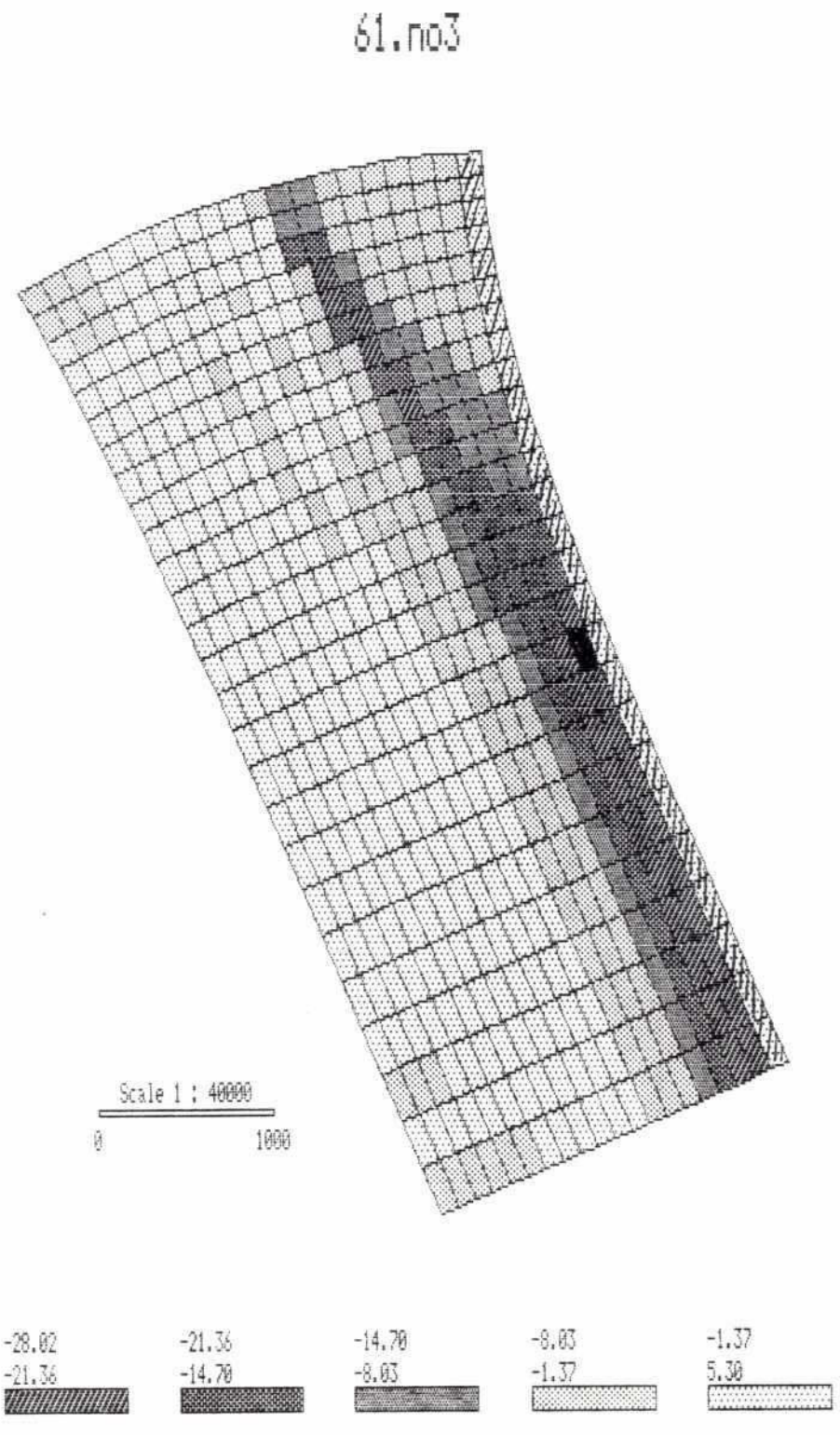

BRTS 2-D Numerical Modelling of Confluence Scour

Simulated Scour, Simulation 3

Vol.4 **Part 11**

Figure 4.6

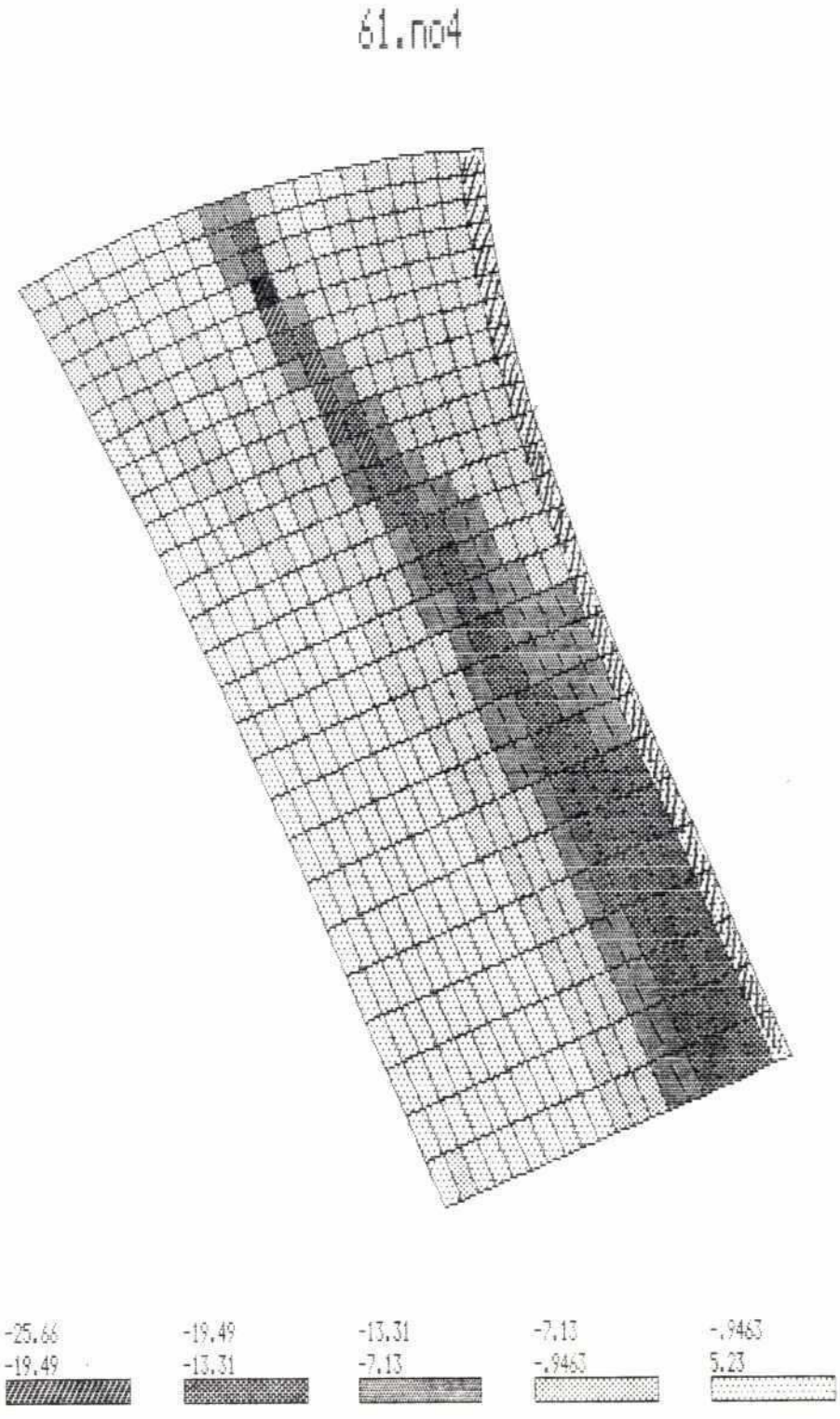

BRTS 2-D Numerical Modelling of Confluence Scour

Simulated Scour, Simulation 4

Vol.4 **Part 11**

Figure 4.7

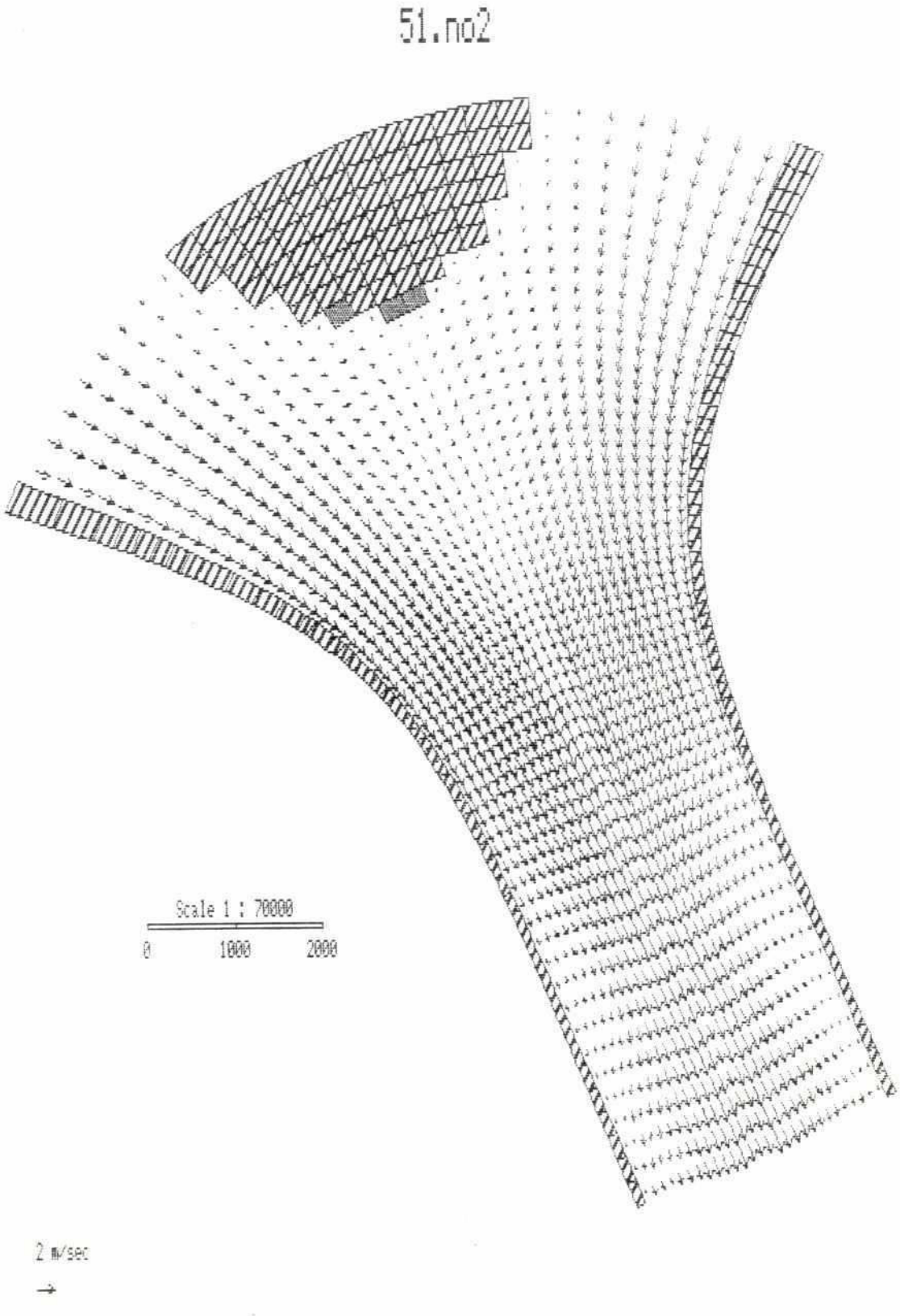

BRTS 2-D Numerical Modelling of Confluence Scour

Simulated Velocity, Simulation 2

Vol.4 Part 11

Figure 4.8

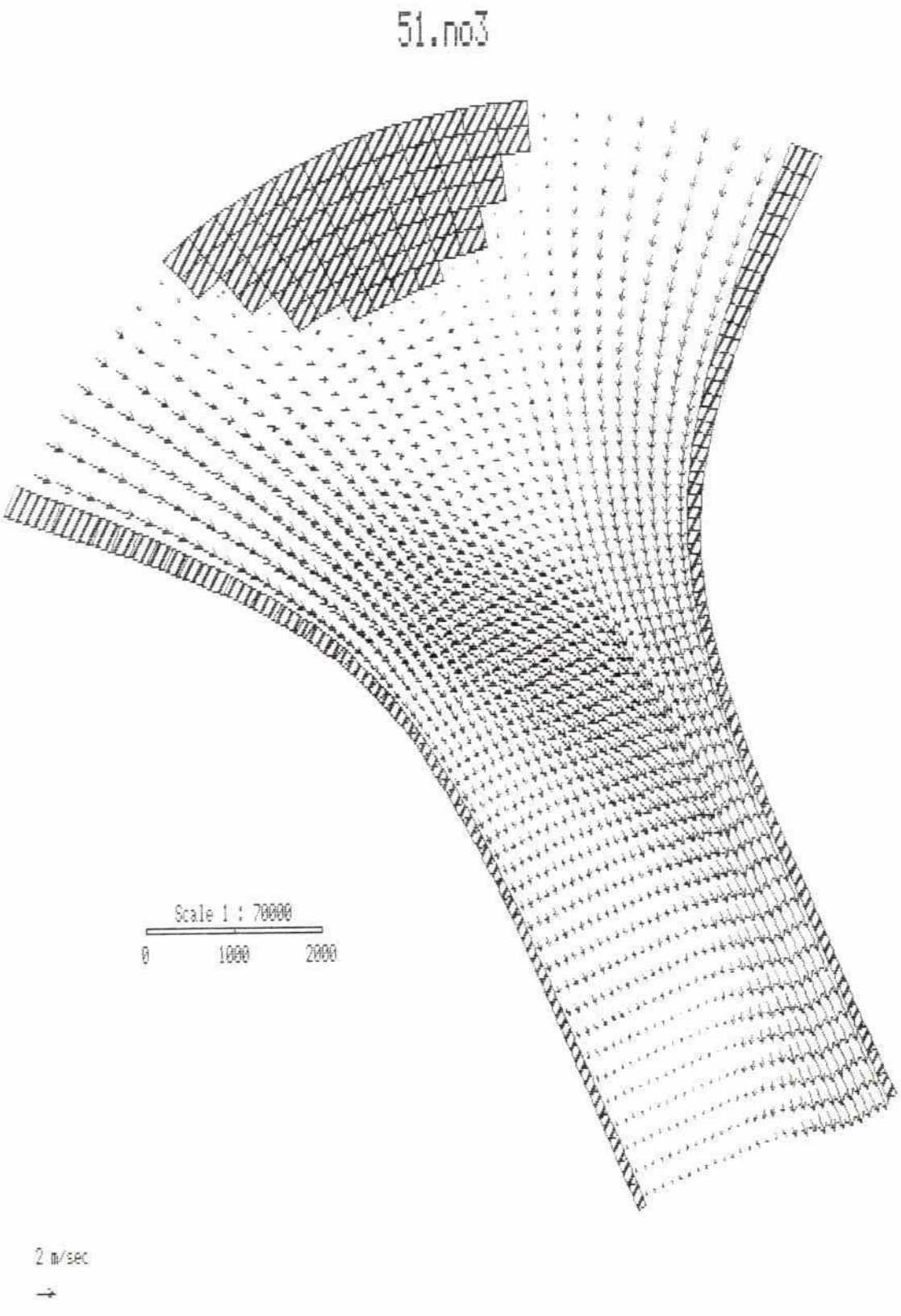

BRTS 2-D Numerical Modelling of Confluence Scour

Simulated Velocity, Simulation 3

Vol.4 Part 11

Figure 4.9

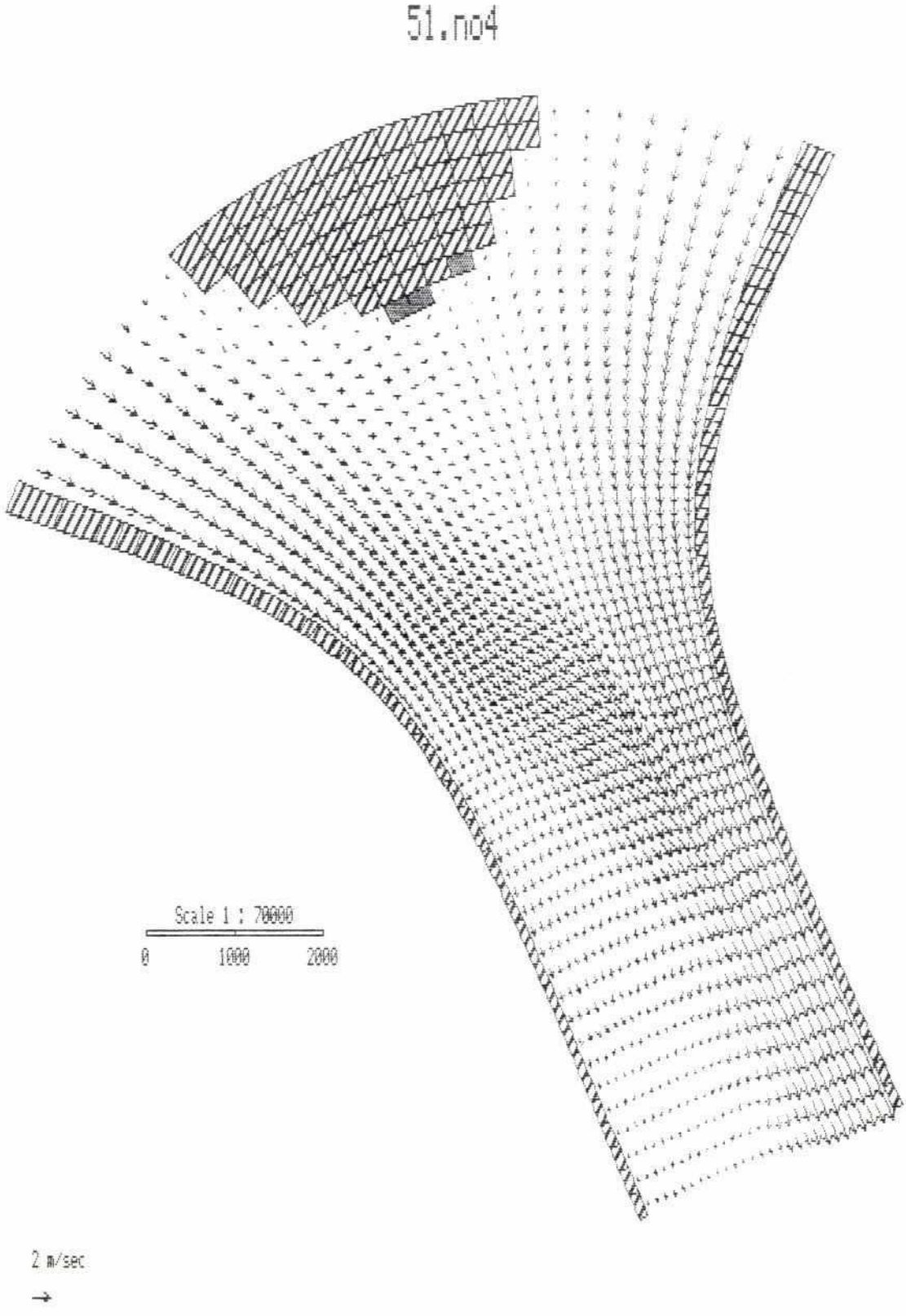

BRTS 2-D Numerical Modelling of Confluence Scour

Simulated Velocity, Simulation 4

Vol.4 Part 11

Figure 4.10

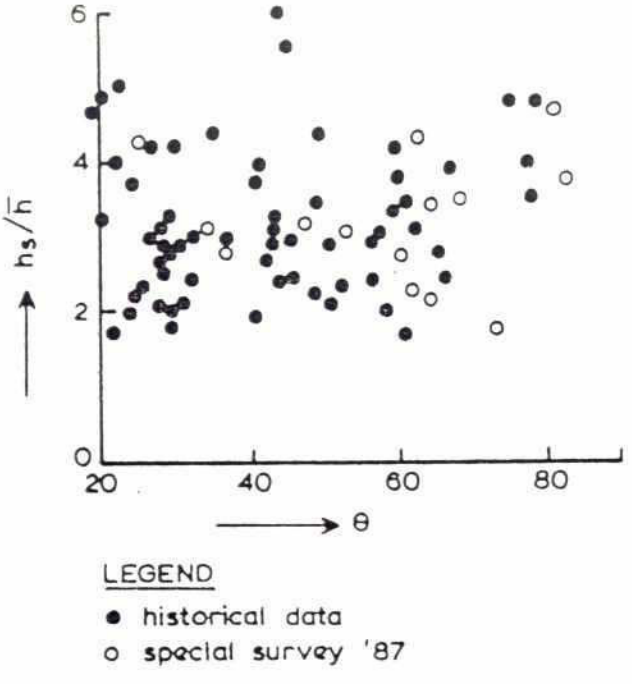

Figure 5.1(a) Confluence scour Jamuna River, all data

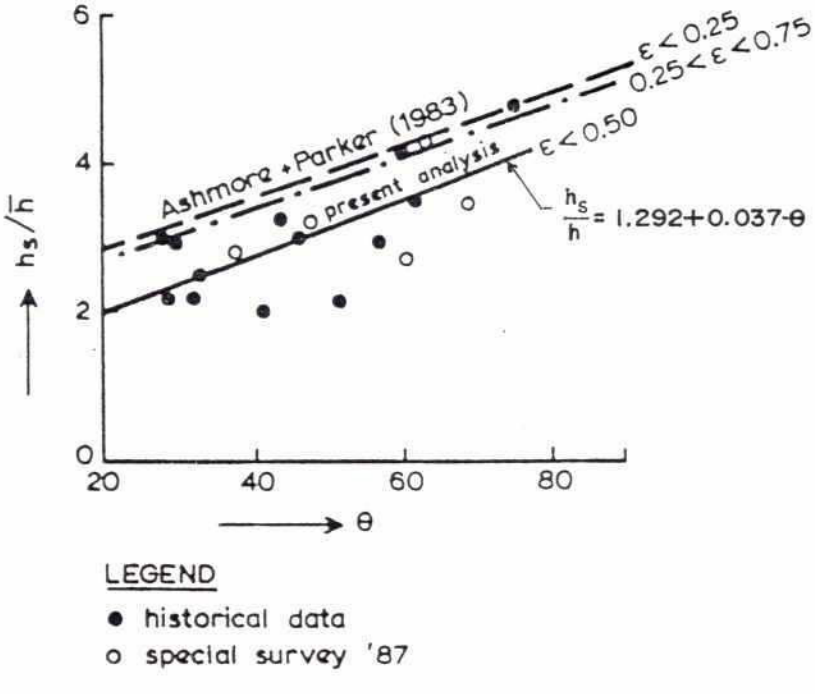

Figure 5.1(b) Tentative design curve confluence scour Jamuna River

Source : RPT/NEDECO/BCL

11 Bed Resistance

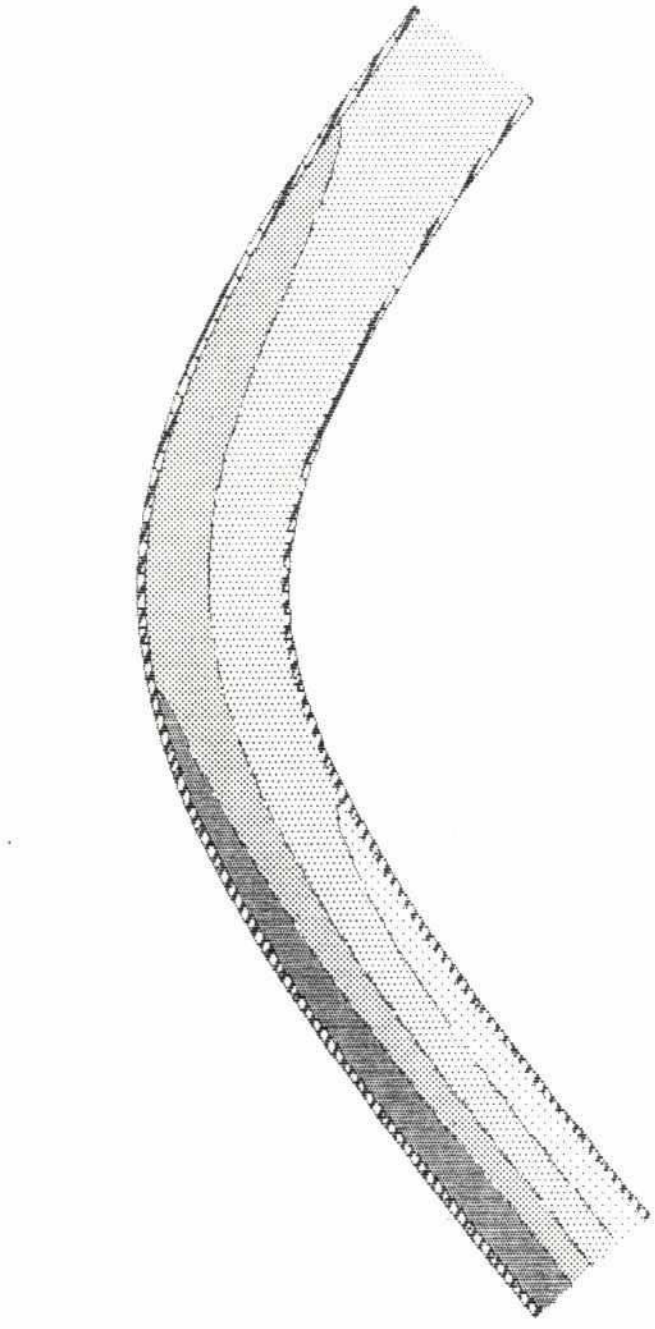

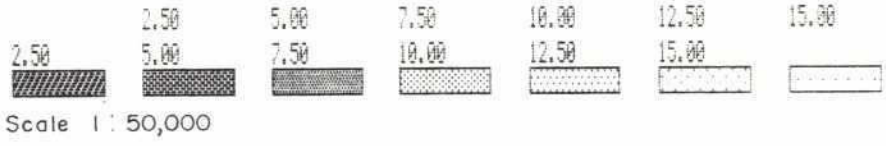

Scale 1 : 50,000

BRTS 2-D Numerical Modelling of River Bends

Simulated Bathymetry When the Bed Resistance is not Updated	**Vol.4** **Part 10** **Figure 2.7**

4. REFERENCES

Coleman, James M - Sedimentary Geology, Volume 3, August 1969 no 2/3, 1985/126

Halcrow/DHI/EPC/DIG - River Training Studies of Brahmaputra River First Interim Report, Technical Annexes, Annex 3: Mathematical Modelling, April 1991

Halcrow/DHI/EPC/DIG - River Training Studies of Brahmaputra River First Interim Report, Technical Annexes, Annex 1: Data Collection and Analysis, April 1991

Halcrow/DHI/EPC/DIG - River Training Studies of Brahmaputra River Working Paper on 2-D Modelling, December 1990

Halcrow/DHI/EPC/DIG - River Training Studies of Brahmaputra River Second Interim Report, Technical Annexes, Annex 1: River Survey, December 1991

Halcrow/DHI/EPC/DIG - River Training Studies of Brahmaputra River Second Interim Report, Technical Annexes, Annex 2: Mathematical Modelling, December 1991

Halcrow/DHI/EPC/DIG - River Training Studies of Brahmaputra River Second Interim Report, Technical Annexes, Annex 3: Morphology, December 1991

Rendel, Palmer and Tritton/NEDECO/BCL - Jamuna Bridge Project, Phase II, Study Feasibility Report, Volume II, Annex B: River Morphology, August 1989

FIGURES

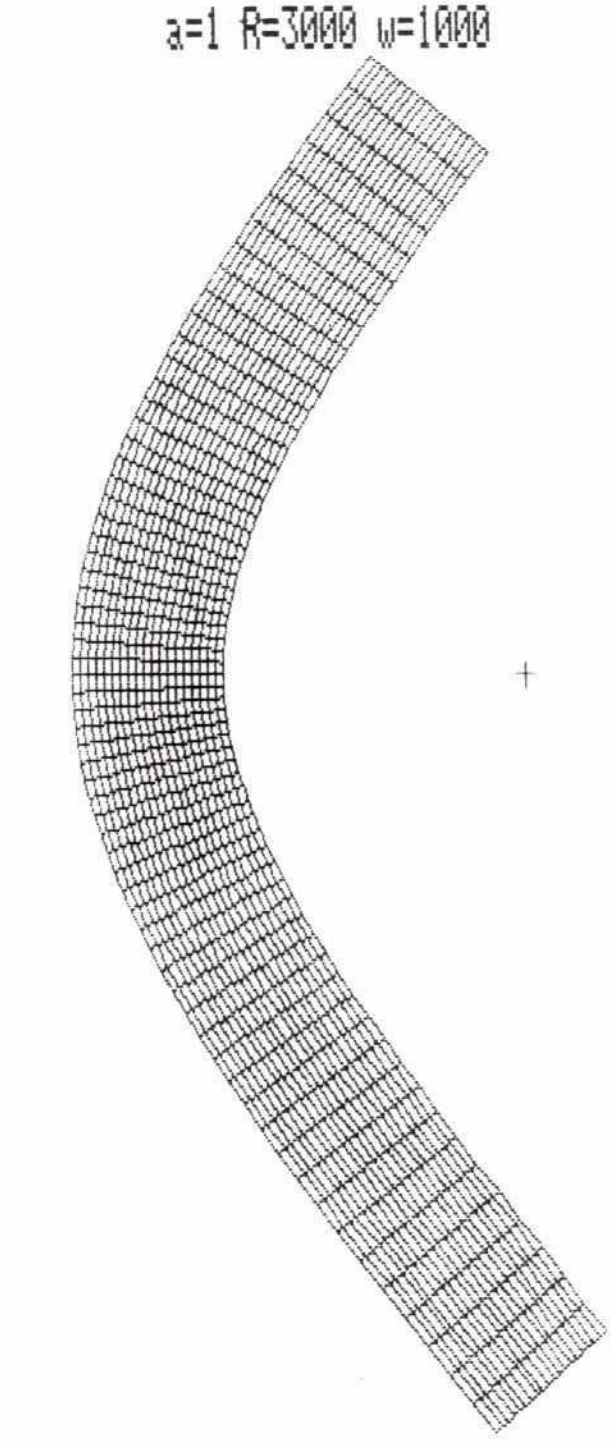

Scale 1 : 50,000

BRTS 2-D Numerical Modelling of River Bends

Computational Grid	Vol.4 Part 10
	Figure 1.1

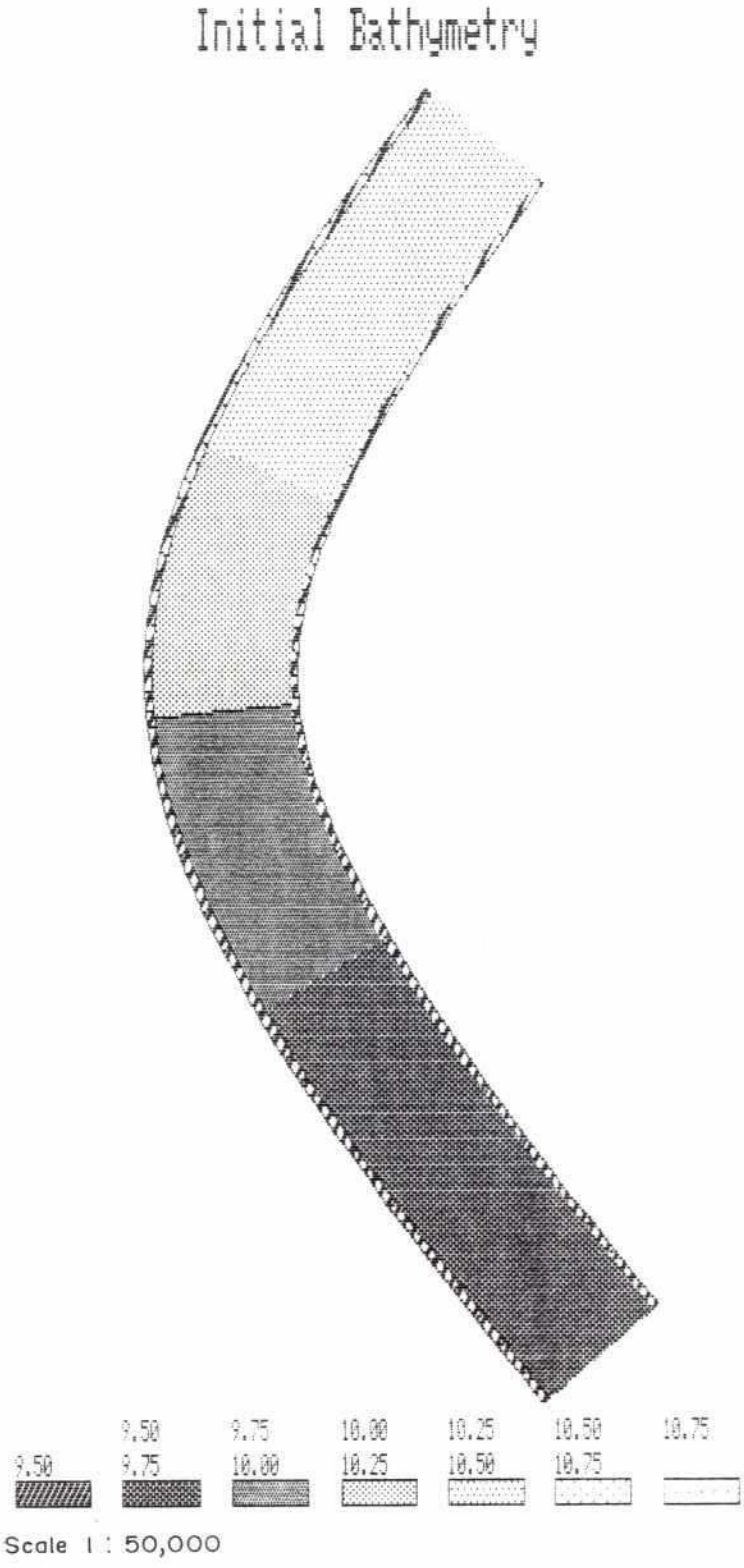

BRTS 2-D Numerical Modelling of River Bends

Start Bathymetry in all Simulations

Vol.4 Part 10

Figure 2.1

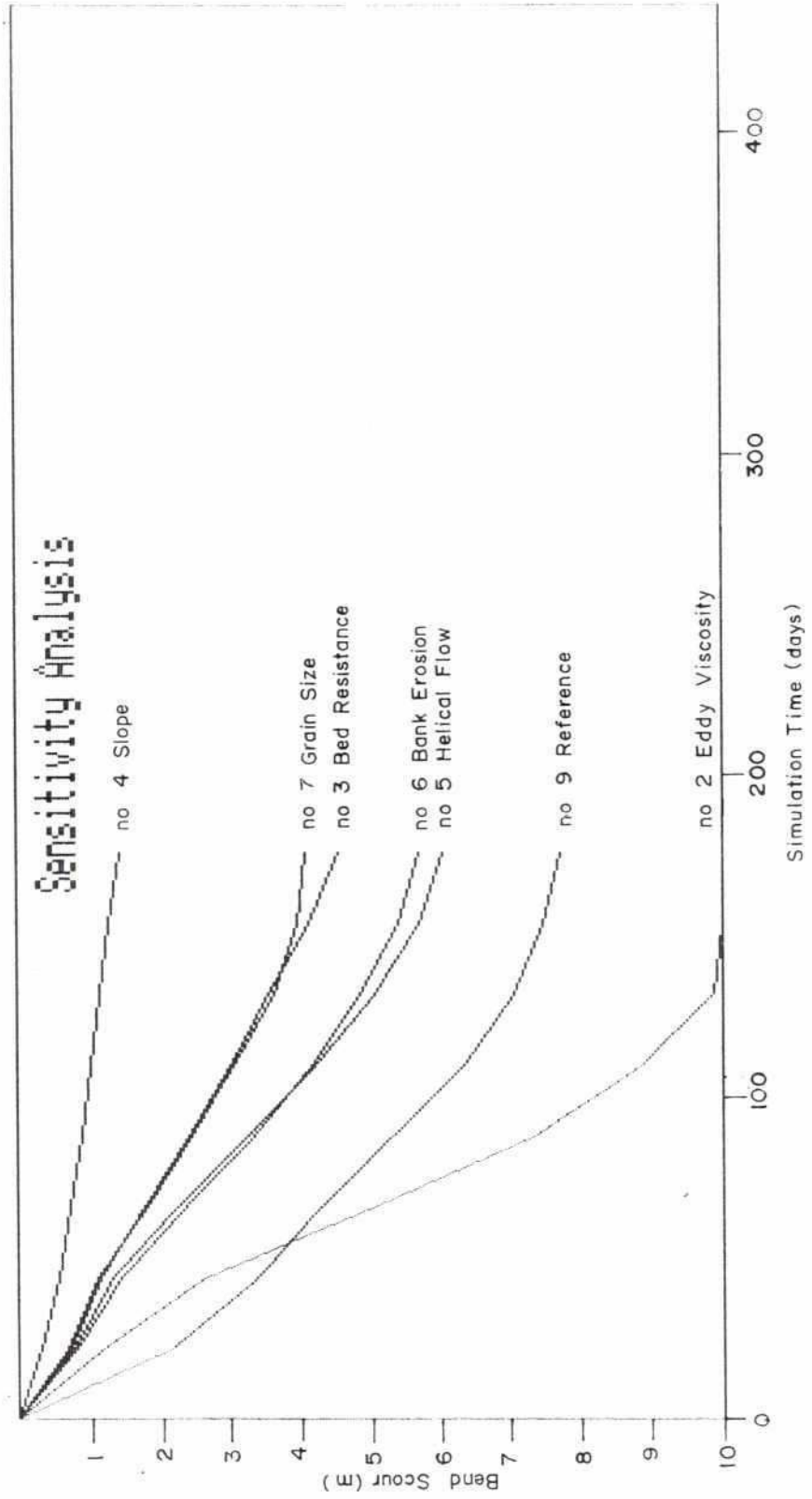

BRTS 2-D Numerical Modelling of River Bends

Time Series of Maximum Scour for Each Simulation	Vol.4 Part 10
	Figure 2.2

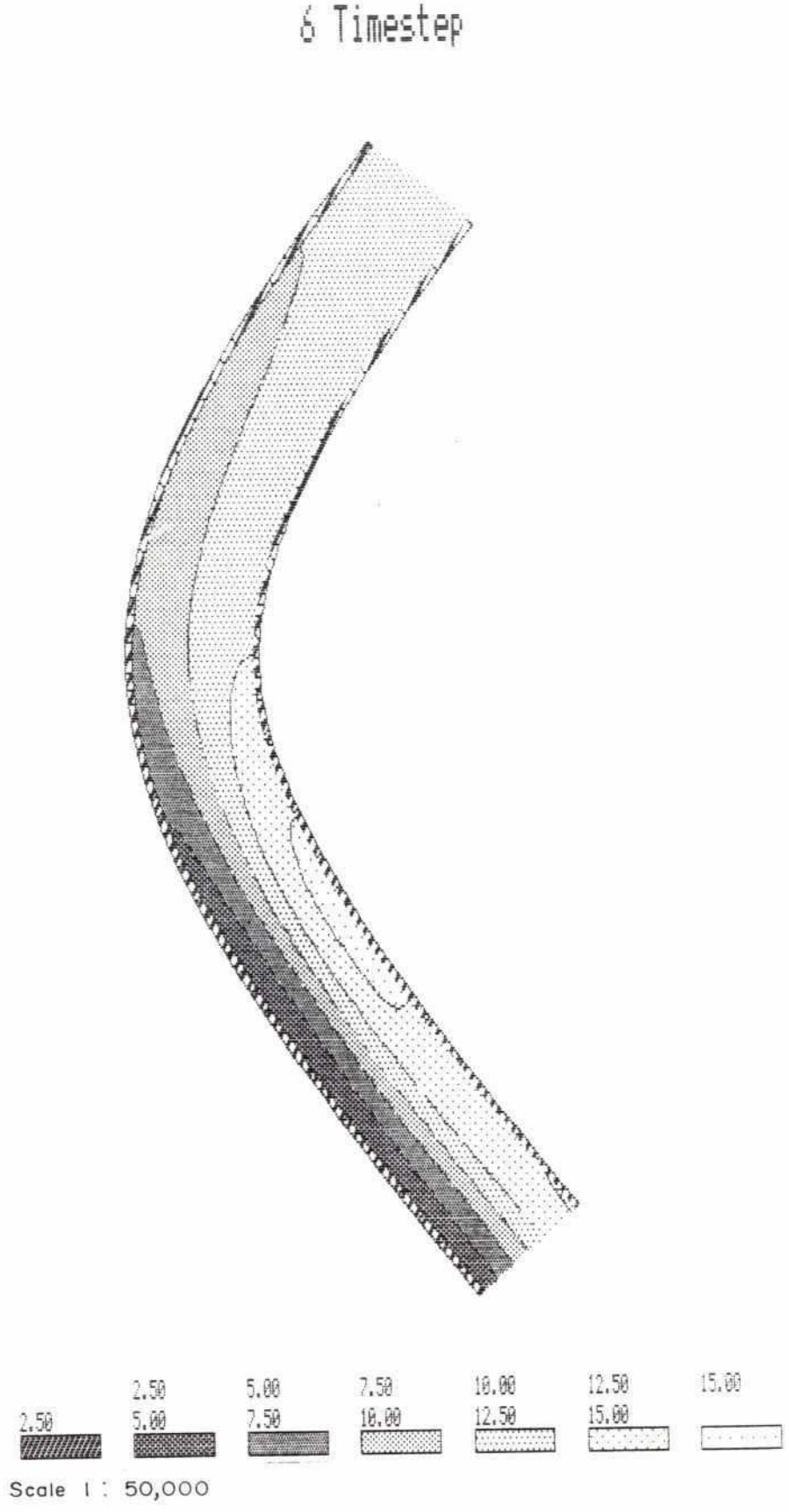

BRTS 2-D Numerical Modelling of River Bends

Simulated Bathymetry with Δt = 60 sec. Instead of Δt = 90 sec.

Vol.4 Part 10

Figure 2.3

5 Eddy Viscosity

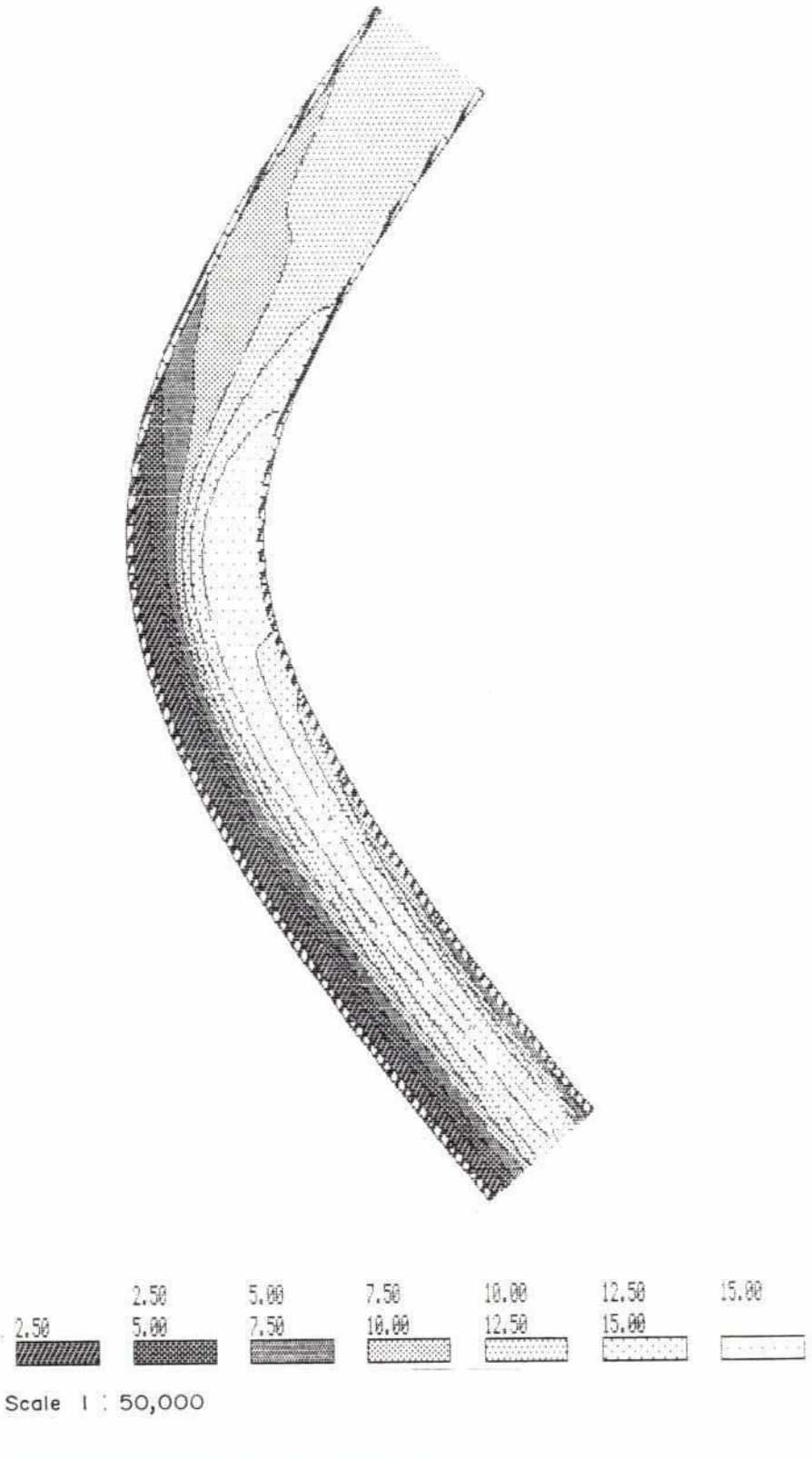

Scale 1 : 50,000

BRTS 2-D Numerical Modelling of River Bends

Simulated Bathymetry with Eddy Viscosity E = 5 m²/s instead of 20 m²/s	**Vol.4** **Part 10**
	Figure 2.4

Initial Bed Resistance (Chezy)

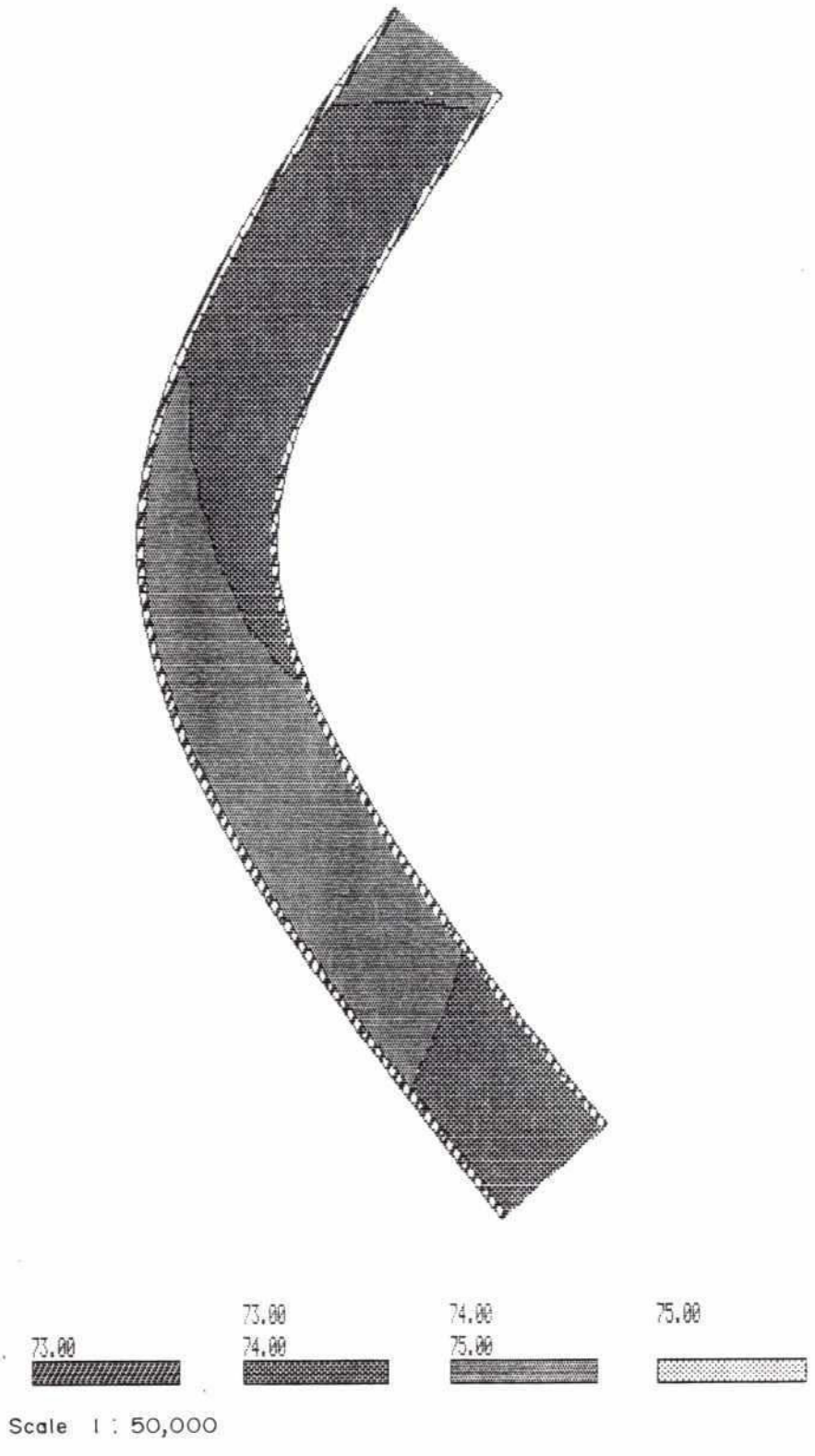

BRTS 2-D Numerical Modelling of River Bends

Bed Resistance, Chezy, at the Beginning of the Simulation	**Vol.4**	**Part 10**
	Figure 2.5	

Simulated Bed Resistance (Chezy)

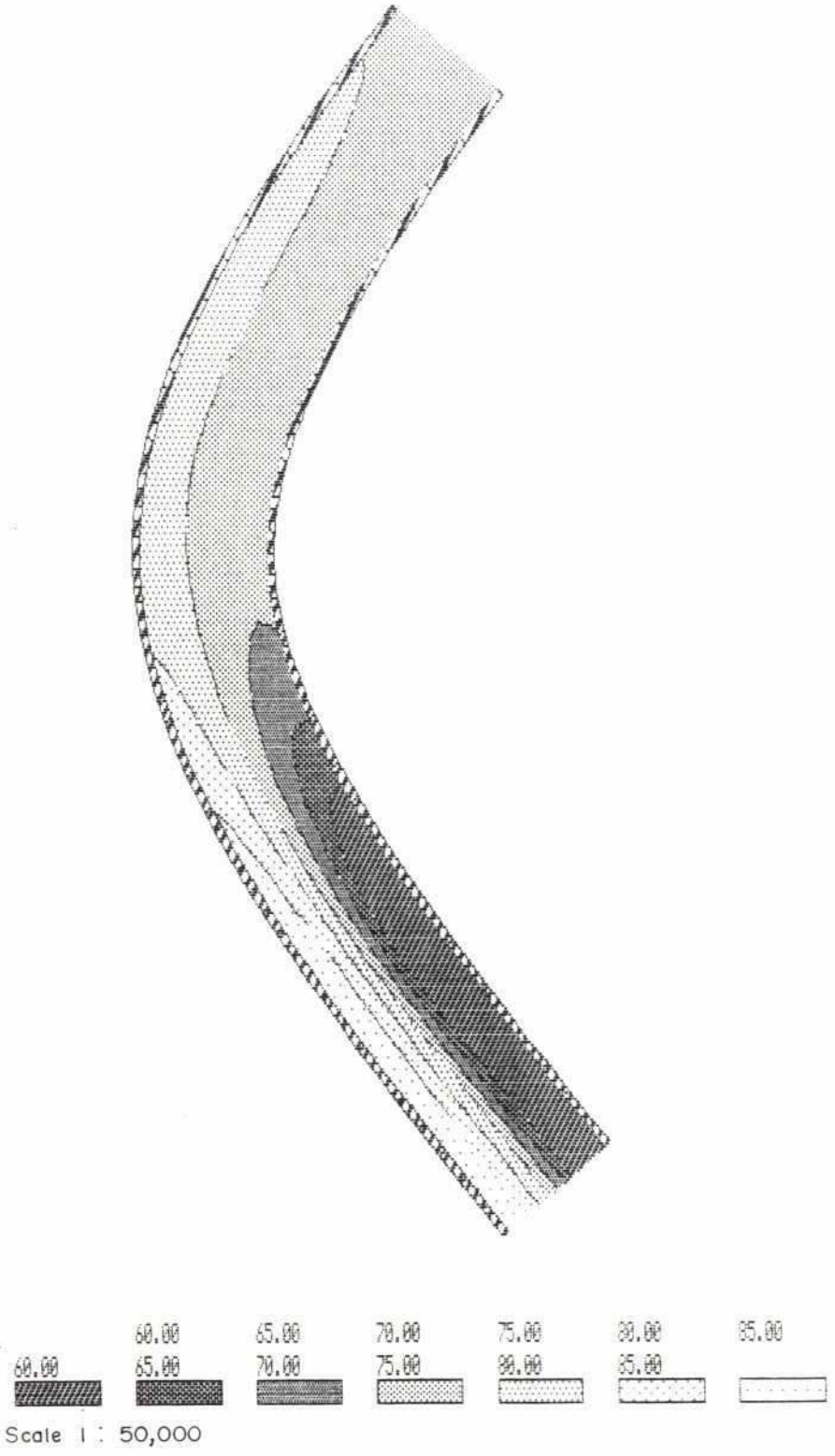

BRTS 2-D Numerical Modelling of River Bends

Simulated Bed Resistance at the End of the Simulation	**Vol.4** **Part 10**
	Figure 2.6

14 Slope

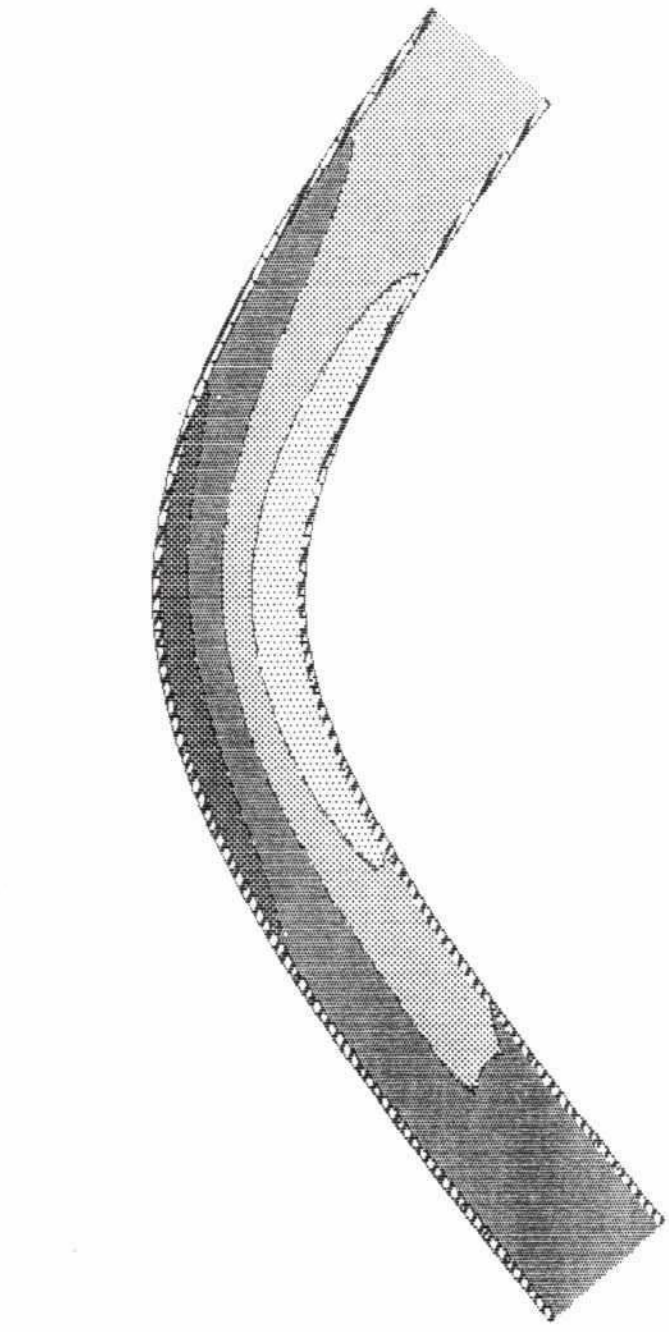

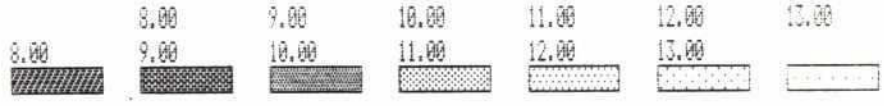

Scale 1 : 50,000

BRTS 2-D Numerical Modelling of River Bends

Simulated Bathymetry When the Slope is 7.10^{-5} instead of 11.10^{-5}	**Vol.4**	**Part 10**
	Figure 2.8	

8 Helical Flow

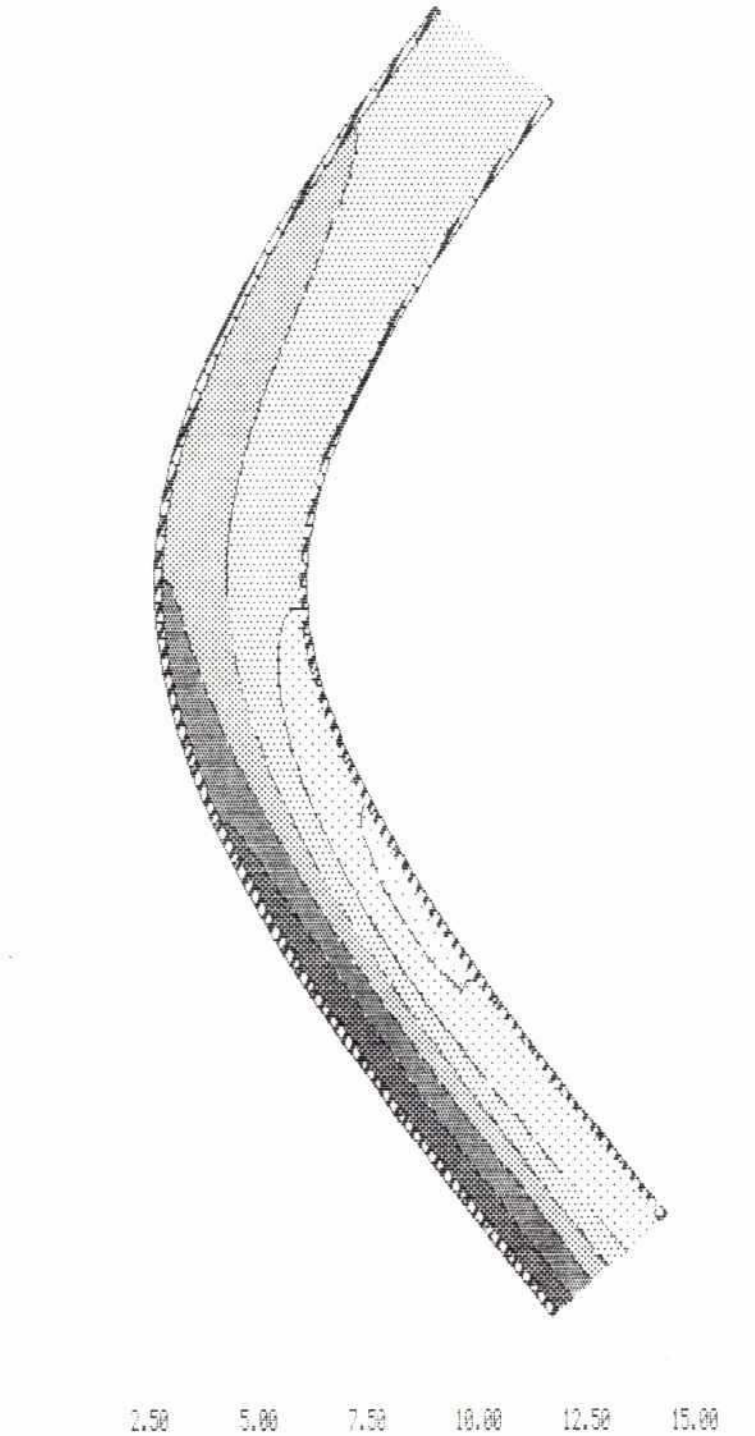

BRTS 2-D Numerical Modelling of River Bends

Simulated Bathymetry When the Helical Flow is Regulated	**Vol.4**	**Part 10**
	Figure 2.9	

9 Bank Erosion

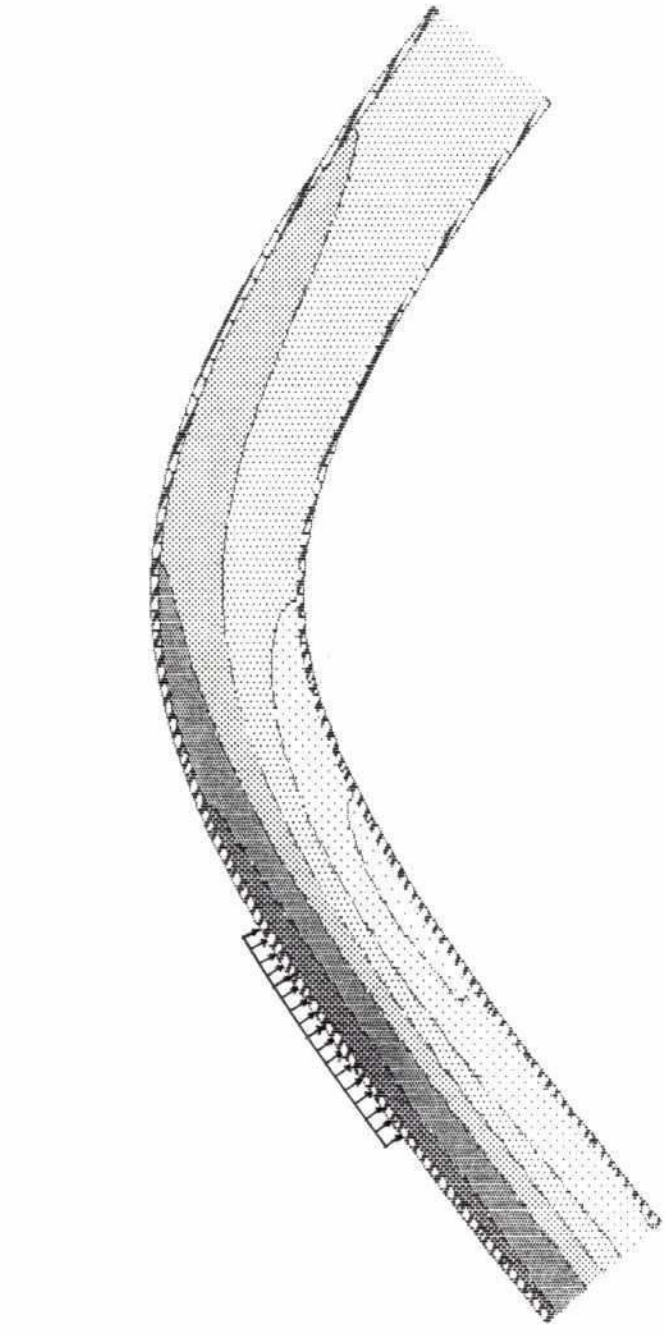

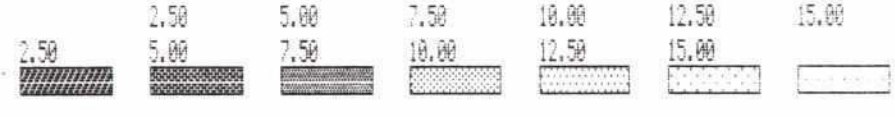

Scale 1 : 50,000

BRTS 2-D Numerical Modelling of River Bends

Simulated Bathymetry When Bank Erosion is Included	**Vol.4** **Part 10**
	Figure 2.10

12 Grain Size

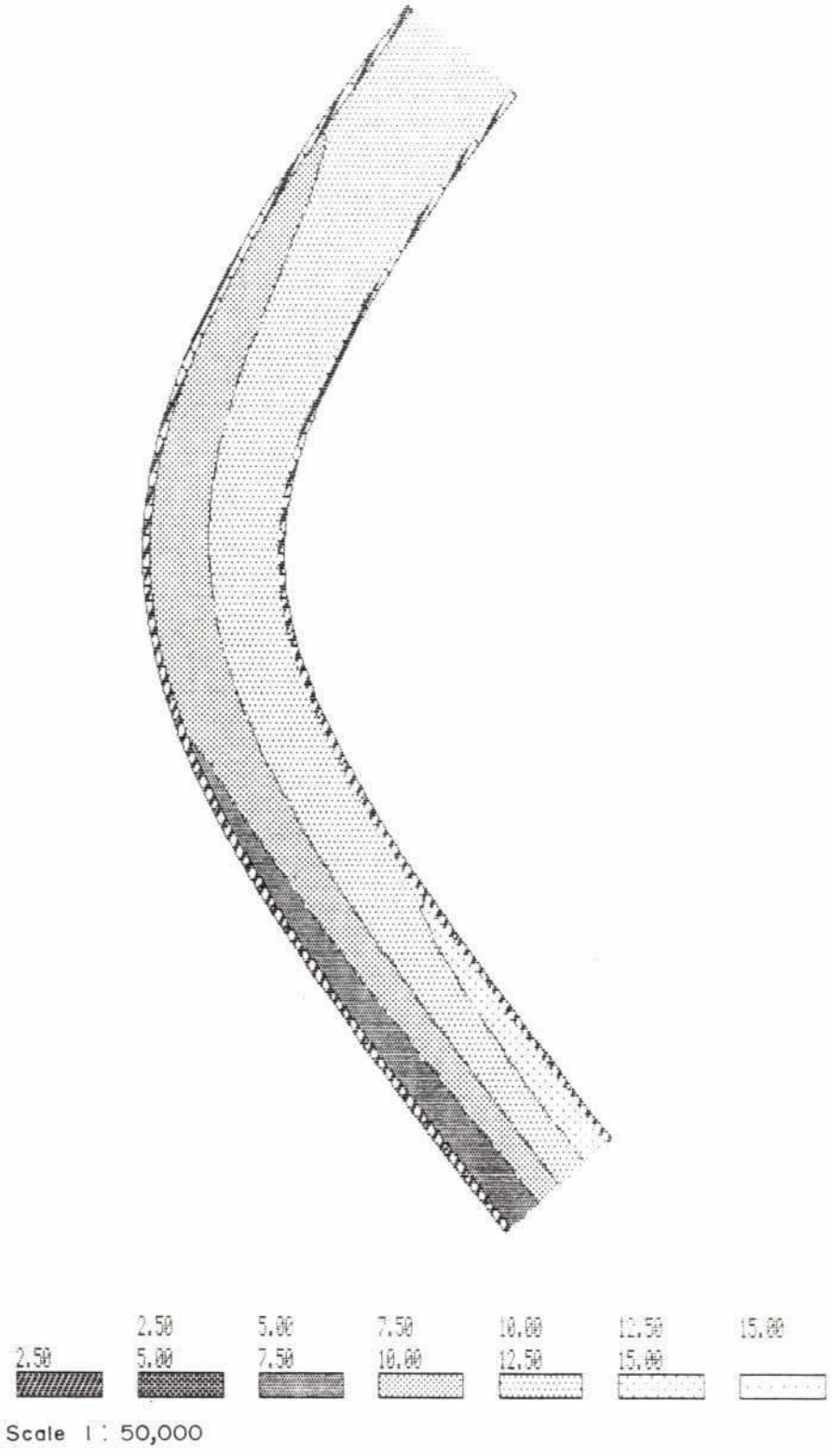

BRTS 2-D Numerical Modelling of River Bends

Simulated Bathymetry When the Grain Size of Sediment is Updated Continuously	Vol.4 Part 10
	Figure 2.11

Grain Size (mm)

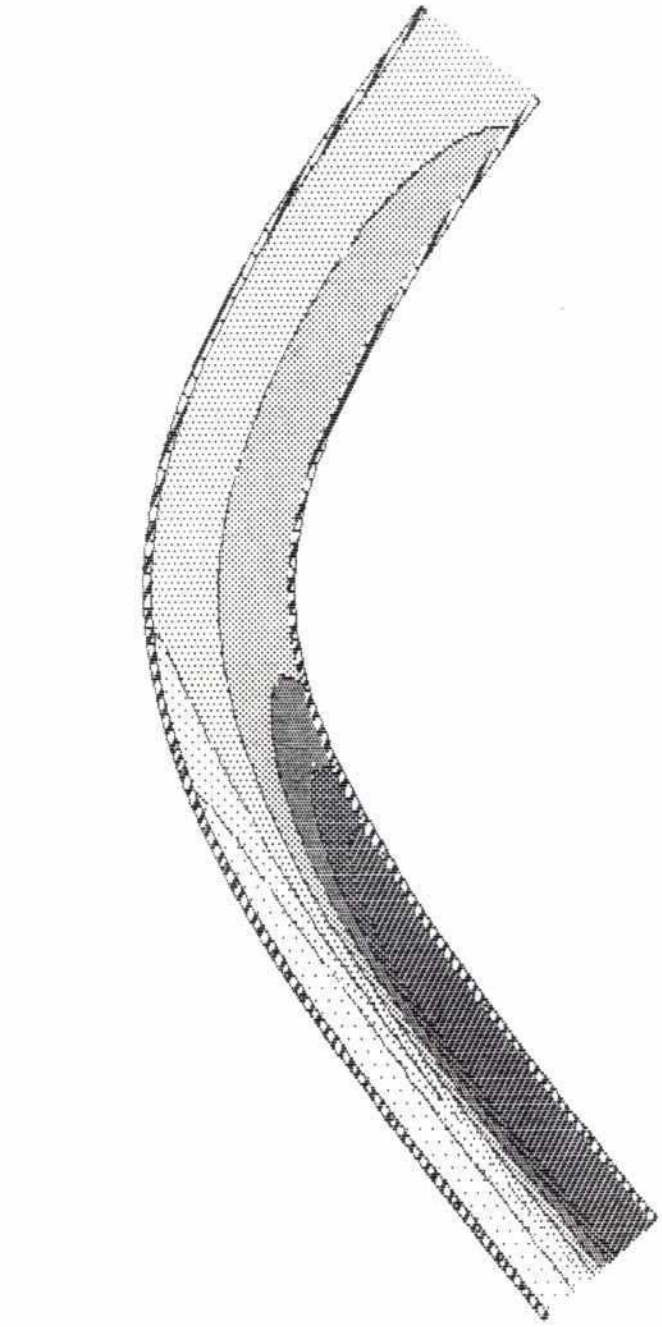

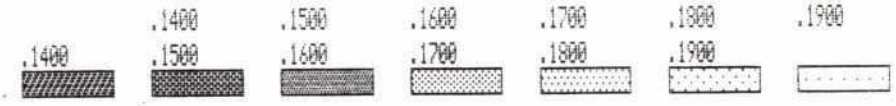

Scale 1 : 50,000

BRTS 2-D Numerical Modelling of River Bends

Simulated Grain Size Distribution

Vol.4 **Part 10**

Figure 2.12

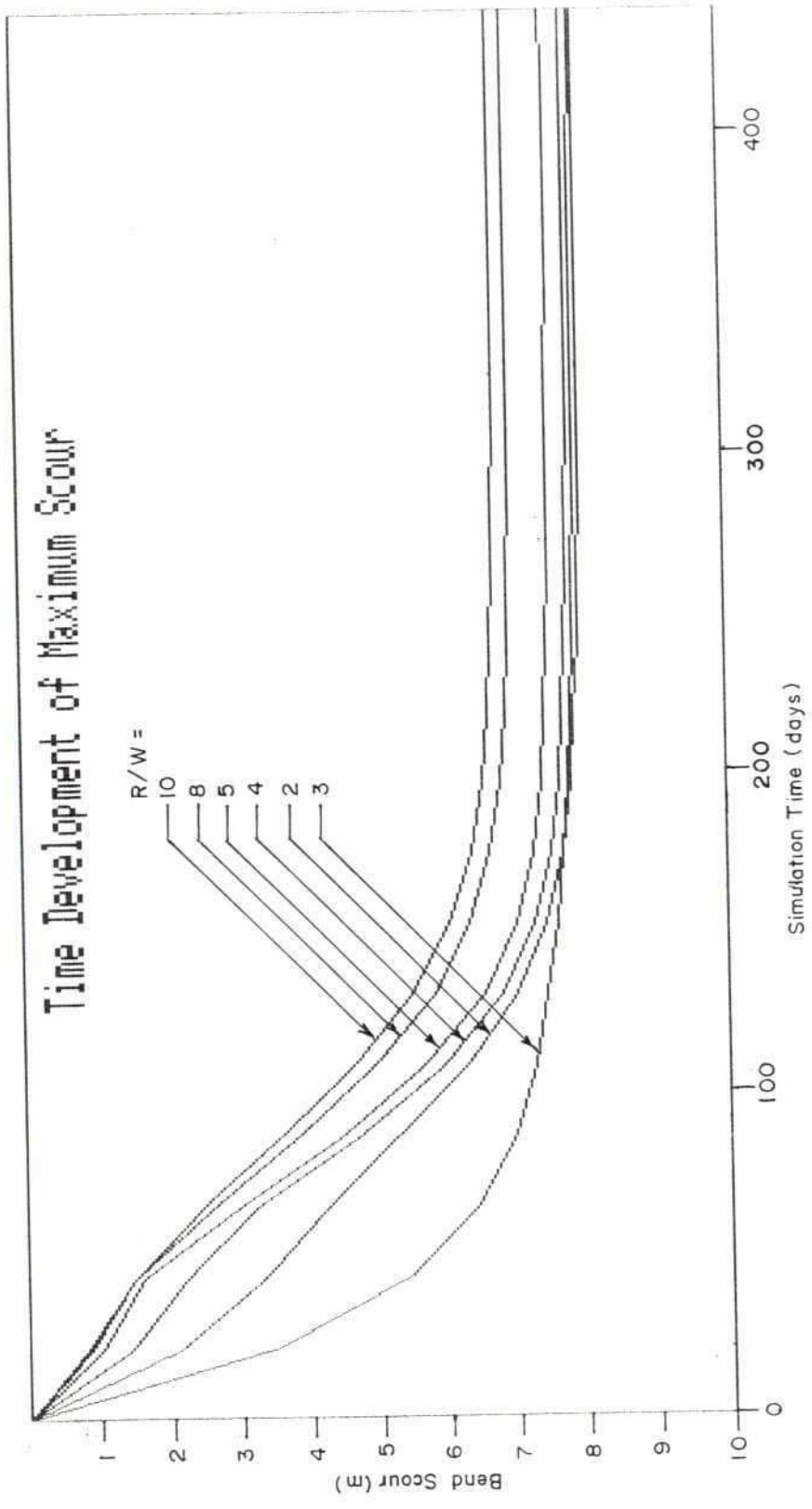

BRTS 2-D Numerical Modelling of River Bends

Time Series of Maximum Scour for Each Simulation	Vol.4 Part 10
	Figure 2.13

#21 N=20

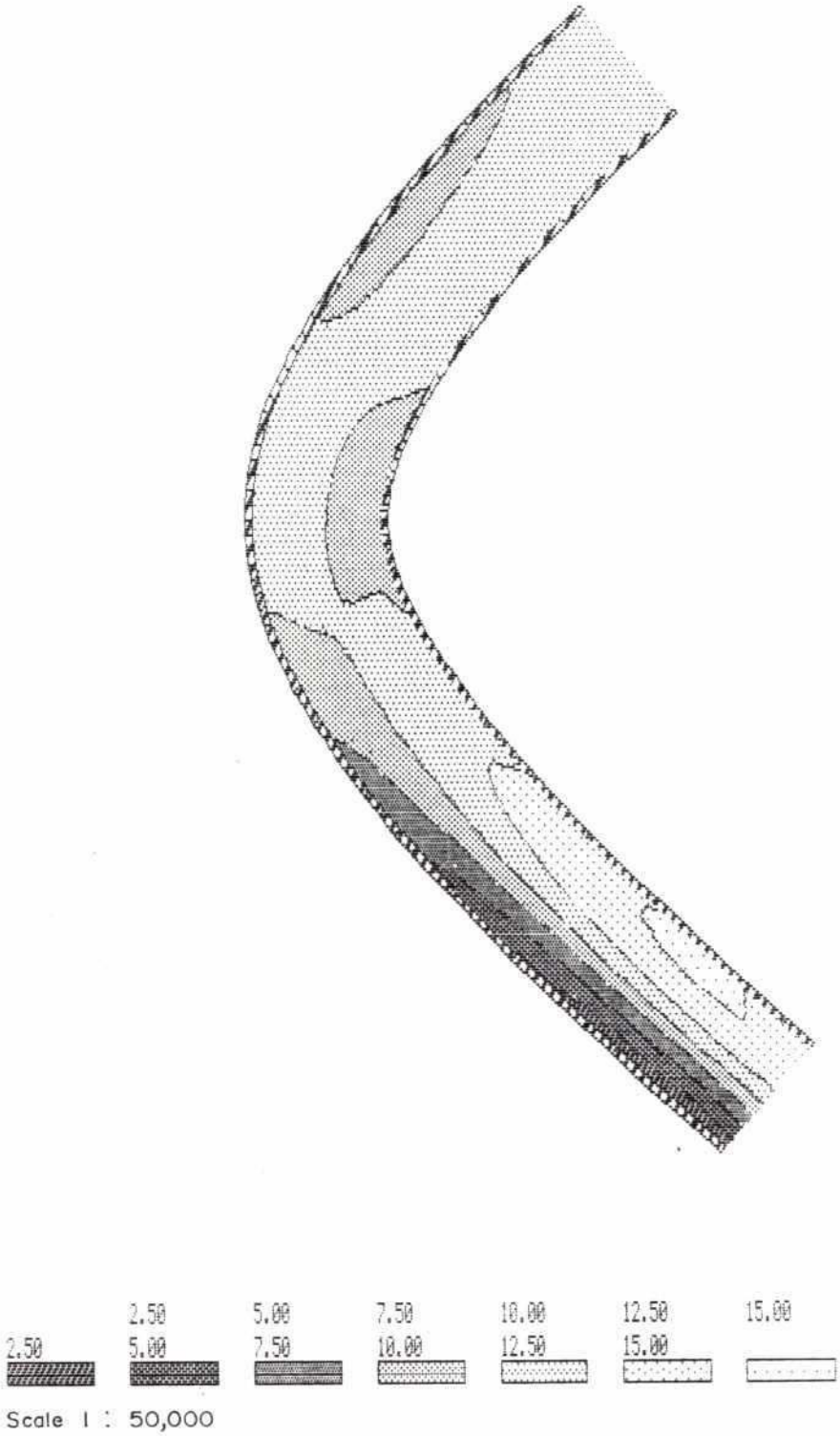

BRTS 2-D Numerical Modelling of River Bends

Simulated Bathymetry When R/W = 2

Vol.4 **Part 10**

Figure 2.14

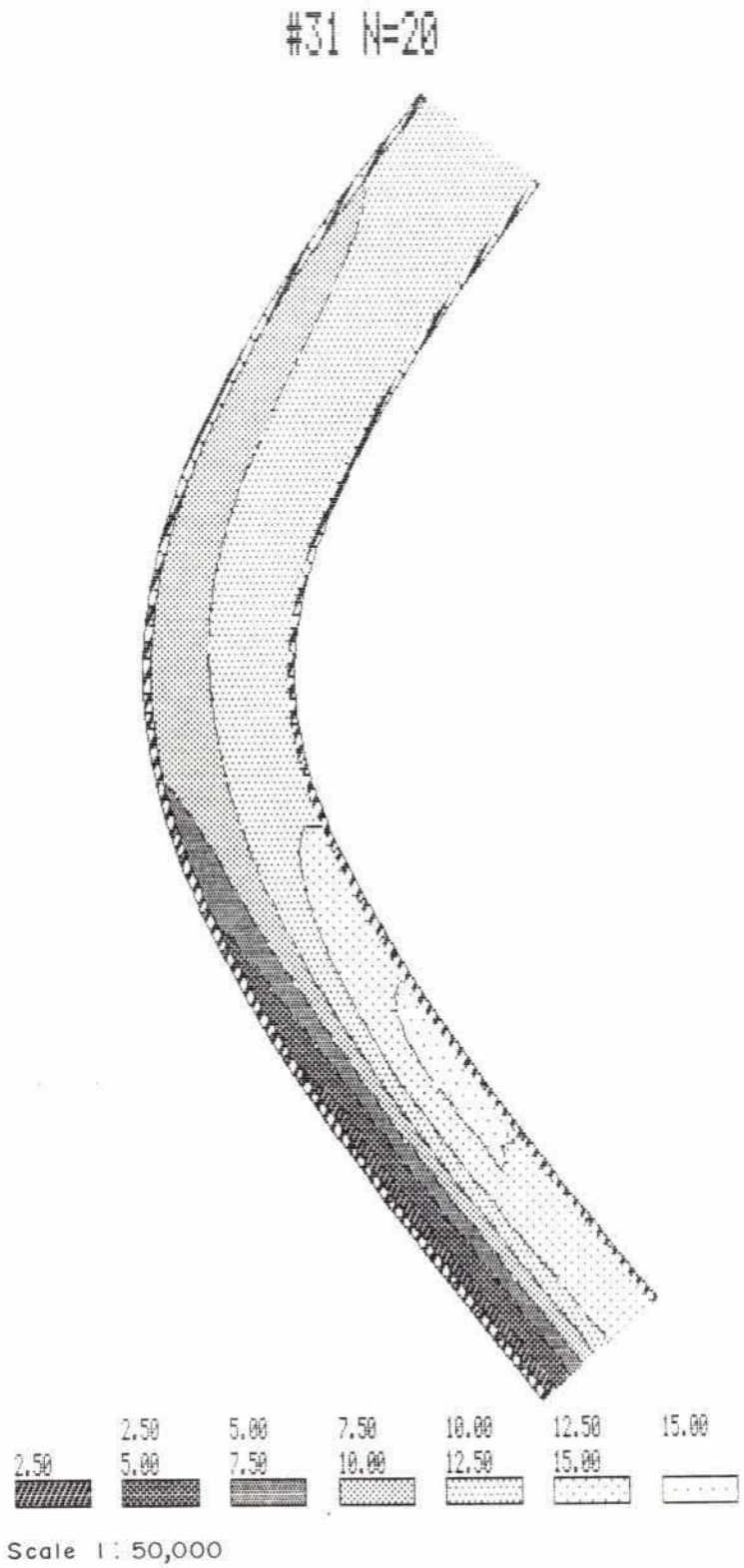

BRTS 2-D Numerical Modelling of River Bends

Simulated Bathymetry When R/W = 3

Vol.4 Part 10

Figure 2.15

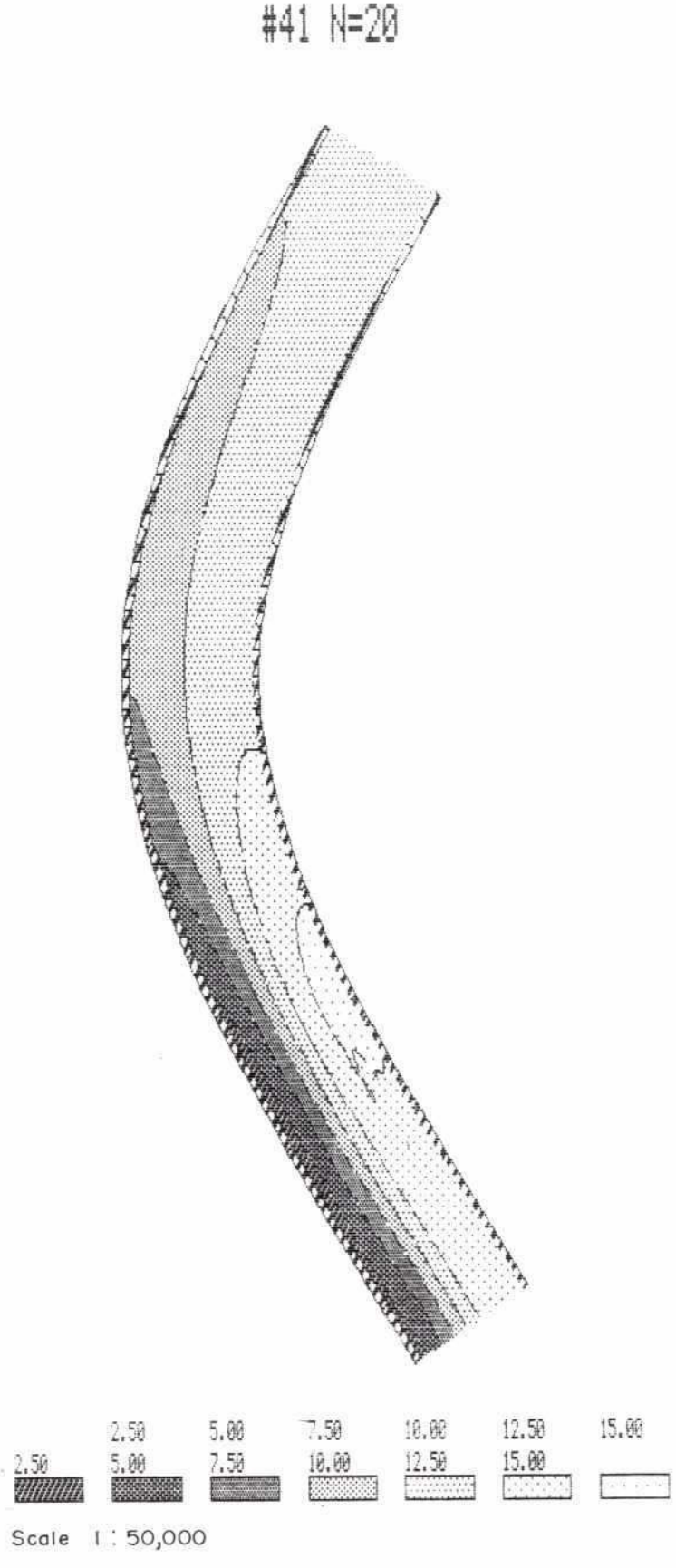

BRTS 2-D Numerical Modelling of River Bends

Simulated Bathymetry When R/W = 4

Vol.4 **Part 10**

Figure 2.16

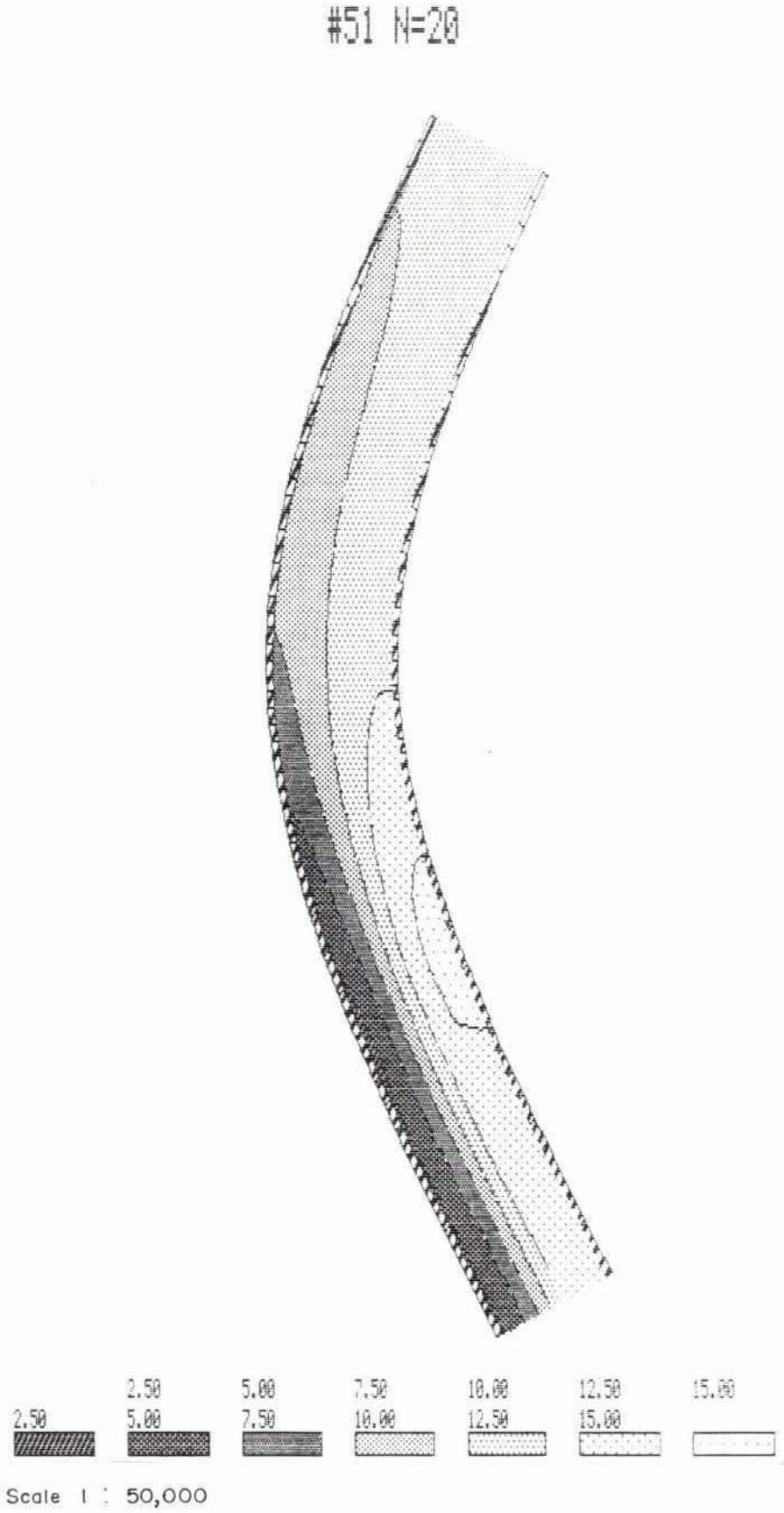

BRTS 2-D Numerical Modelling of River Bends

Simulated Bathymetry When R/W = 5

Vol.4 **Part 10**

Figure 2.17

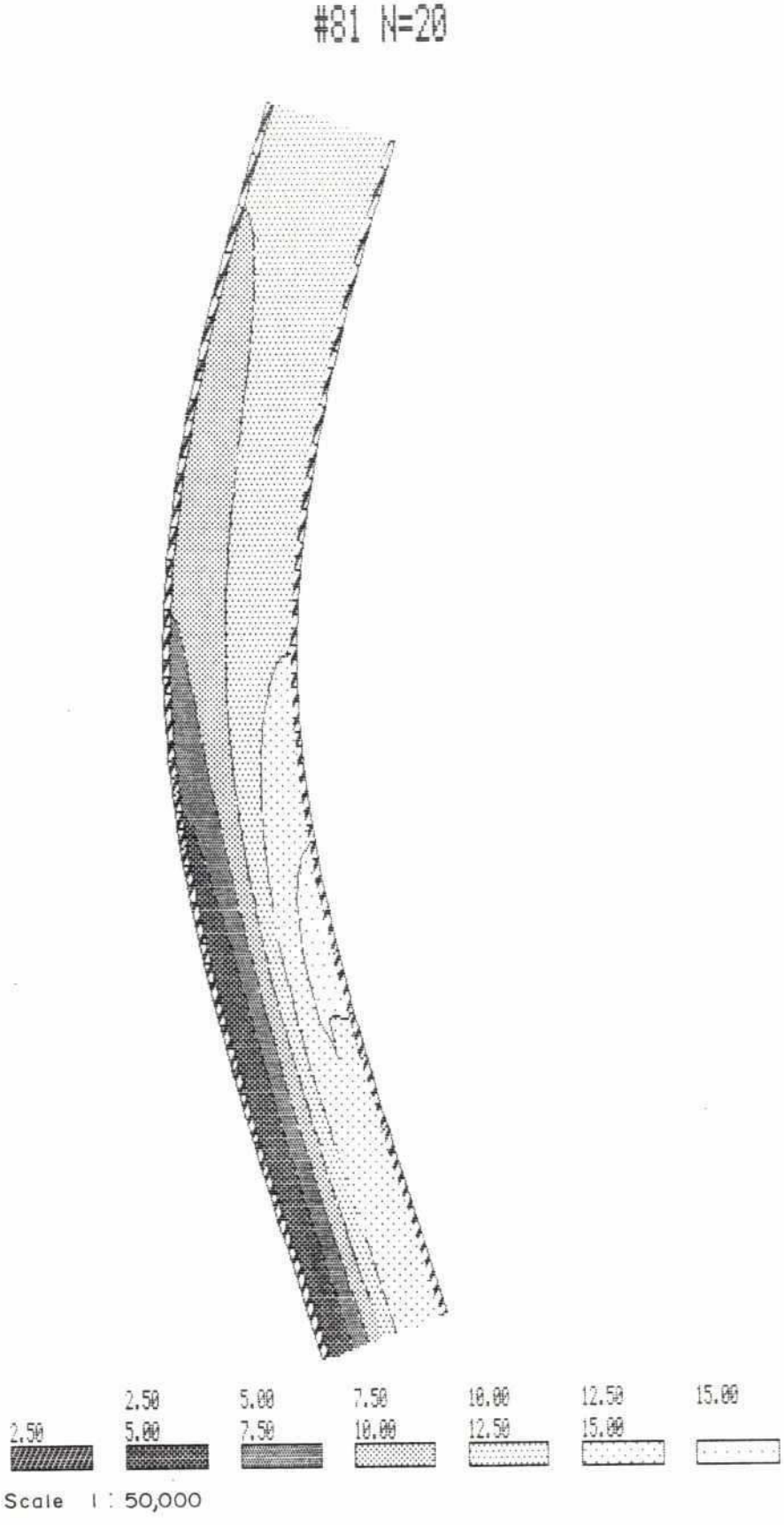

BRTS 2-D Numerical Modelling of River Bends

Simulated Bathymetry When R/W = 8

Vol.4 **Part 10**

Figure 2.18

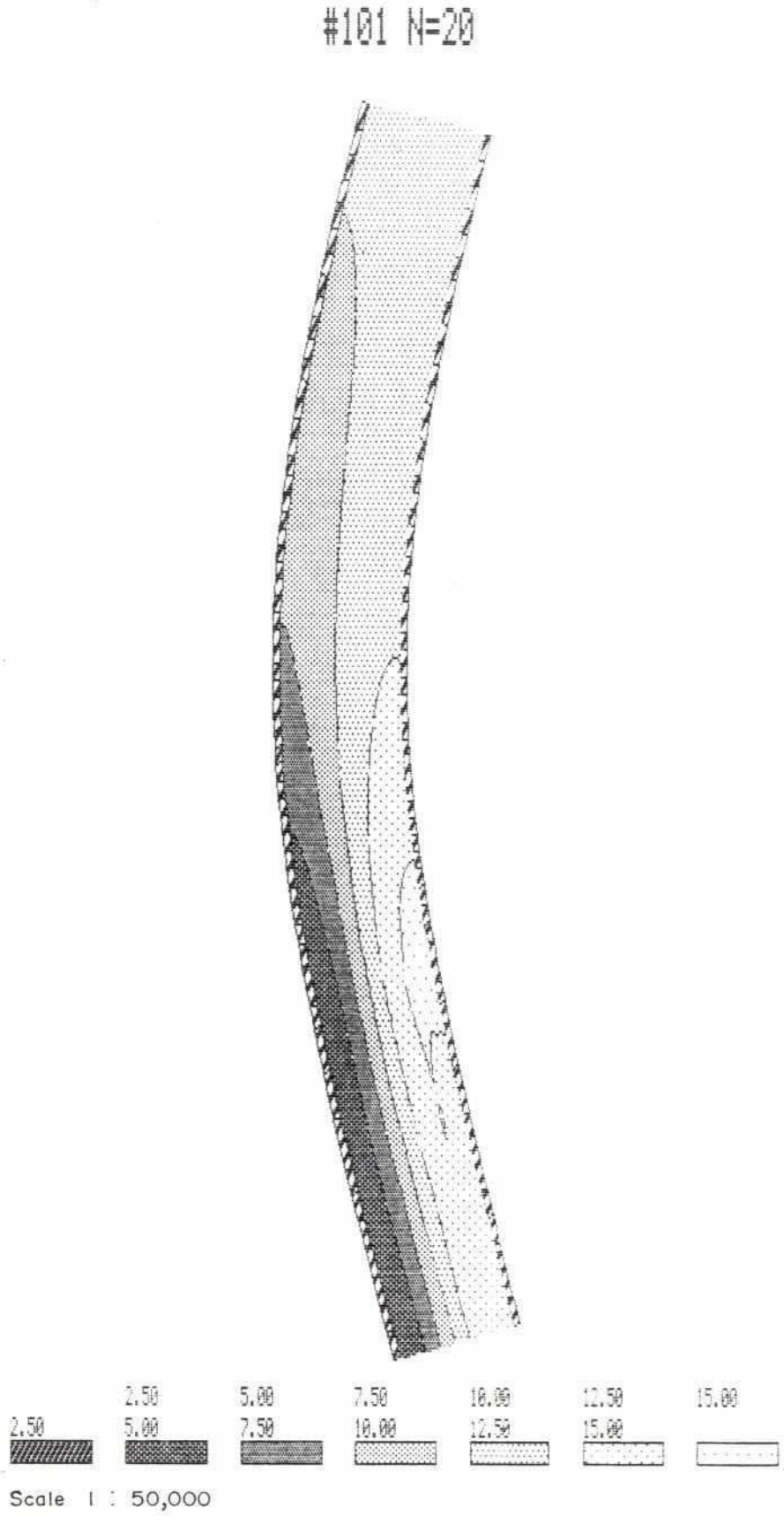

BRTS 2-D Numerical Modelling of River Bends

Simulated Bathymetry When R/W = 10

Vol.4 Part 10

Figure 2.19

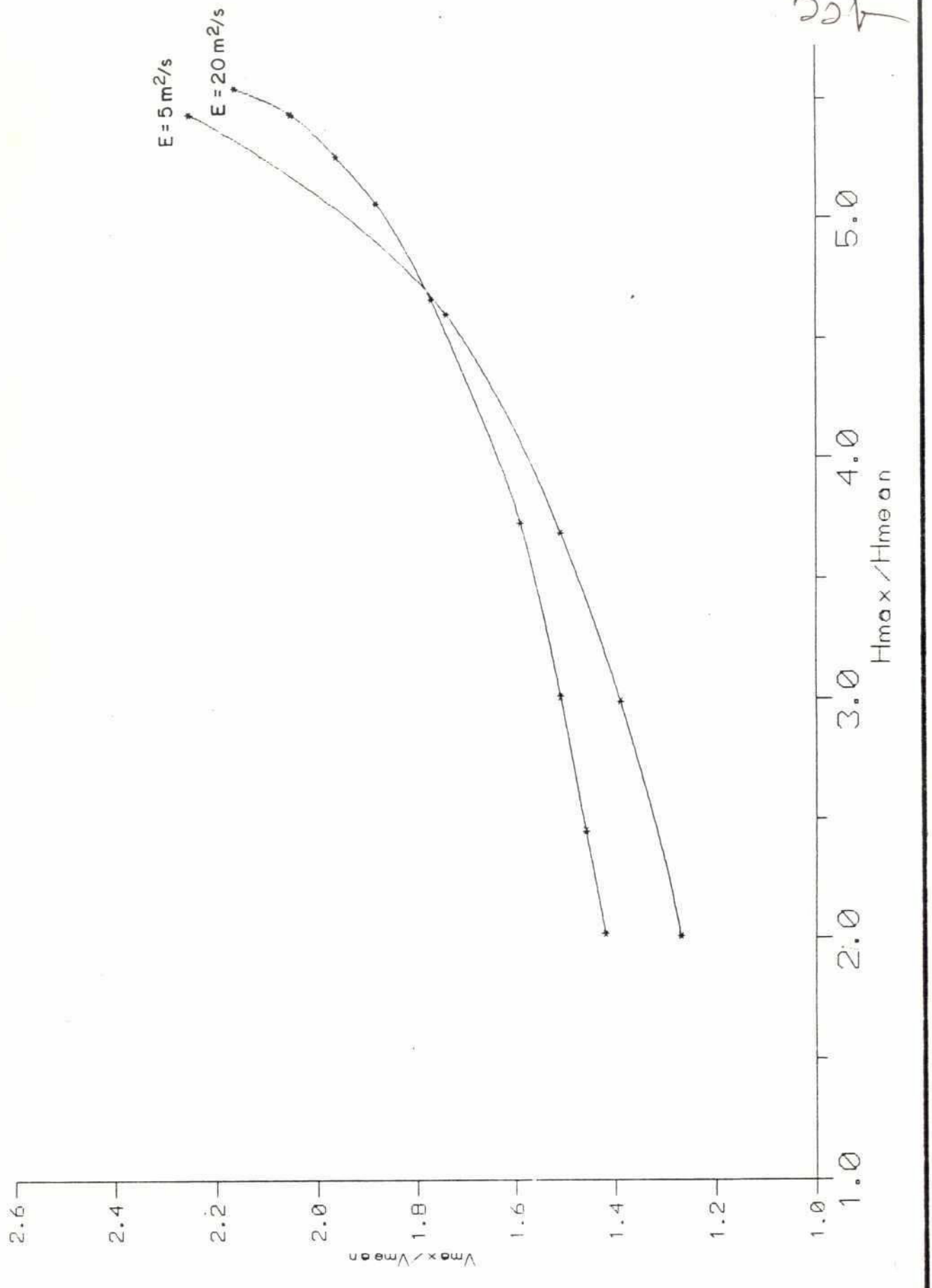

BRTS 2-D Numerical Modelling of River Bends

Simulated Relationship Between Dimensionless Depth and Velocity in a River Bend R/W = 3	Vol.4 Part 10
	Figure 2.20

Part 12

2-D Numerical Modelling of Flow and Scour Around a Groyne

HALCROW

RIVER TRAINING STUDIES OF THE BRAHMAPUTRA RIVER

REPORT ON MODEL STUDIES

PART 12 - 2-D NUMERICAL MODELLING OF FLOW AND LOCAL SCOUR AROUND A GROYNE

CONTENTS

FIGURES

1. OBJECTIVE

Physical models are used to estimate the velocity distribution and extension and magnitude of local scour around structures. The purpose of the present investigation was to study to what extent the two-dimensional depth-averaged mathematical model could satisfactorily simulate the velocities and scour around a groyne head and thereby complement the physical models for testing a variety of different scenarios in situations that, for reasons of scale, are not well suited to physical modelling.

2. APPROACH

A physical model of a simple layout of bathymetry (horizontal bed) and groyne (rectangular with vertical walls) was prepared in order to provide data for calibration of the 2-D model covering the same area at a similar scale. The influence of scale effects between physical model and prototype was avoided by setting up the 2-D model of the flume itself in the physical model. A comparison between observations in the physical model and 2-D simulations would then show whether the mathematical model is applicable in calculating local scour.

A model with a fixed bed, found by running the physical model until equilibrium was reached, was set up in order to compare measured and simulated velocities and to check the hydrodynamic modelling. Subsequently, a model with mobile bed was established so that sediment transport and development of scour could be simulated.

The scour simulation was repeated both in the physical model and in the 2-D model with another model where the groyne had side slope 1:2.

3. DESCRIPTION OF THE MODEL

3.1 The Flume

The measurements of the flume and the groyne are shown in the upper part of Fig. 3.1. At the beginning of the model test, the bed was plane with a water depth of 22.5 cm (15 m prototype in scale 1:66.7). The discharge was 0.424 m^3/s corresponding to a mean velocity of about 0.34 m/s (prototype velocity $0.34 \times 60.7^{1/2} = 2.8$ m/s). The bed consisted of fine sand from the Brahmaputra River with a grain diameter of 0.18 mm. The depth of the sand layer was more than 1.0 m.

3.2 Theoretical Considerations

Bed Resistance

The bed resistance is difficult to measure in the flume because the difference in water level between the upstream (u/s) and the downstream (d/s) end is very little and hard to measure with the required accuracy. However, it can be estimated from the theory by Engelund & Hansen together with an analysis of the observed bed forms. The principle of similarity (Engelund/Hansen 1967) is used. The bed shear stress is divided into skin shear stress originating from the roughness of the grains and into bed form shear stress related to the form drag caused by ripples and dunes:

$$\theta = \theta' + \theta'' \qquad (1)$$

The data from the Fort Collins test series provided the relationship between total shear stress θ and skin shear stress θ'.

$$\theta' = 0.06 + 0.4\,\theta^2 \qquad (2)$$

The latter is the portion of the total shear stress which causes the sediment grains to move.

The reduced water depth, which is simply a mathematical measure, is found through iteration of the following equations:

$$U'_* = \frac{V}{6 + 2.5 \ln (D/2.5\,d)} \qquad (3)$$

$$\theta' = \frac{U'^2_*}{(s - 1)\,g.d} \qquad (4)$$

$$D' = D.\frac{\theta'}{\theta} = D.\frac{\theta'}{\sqrt{\frac{(\theta' - 0.06)}{0.04}}} \qquad (5)$$

u_* = total bed shear velocity

u'_* = bed shear velocity originating from skin shear

V = depth averaged velocity

D = water depth

d = grain diameter

g = acceleration of gravity

s = relative density of sediment = 2.65

D' = reduced water depth

ν = kinematic viscosity, ~ 10^{-6} m^2/s

The start value should be D'= D. With V = 0.34 m/s, D = 0.225 m, d = 0.18 mm, s = 2.65, one finds by iteration:

$u'_* = 1.83\ 10^{-2}$ m/s

$u_* = 5.89\ 10^{-2}$ m/s

$\theta' = 0.115$

$\theta = 0.370$

D' = 0.0698 m

The friction factor ,f, is found by using the similarity principle:

$$f' = 2.\left(\frac{U'_*}{V}\right)^2 = 5.78.10^{-3} \qquad (6)$$

$$f = \frac{\theta}{\theta'}.f' = 1.85.10^{-2} \qquad (7)$$

$$C = \sqrt{\frac{29}{f}} = 33\ m^{0.5}/s \qquad (8)$$

The resistance formula for a rough bed is applied to estimate the corresponding roughness:

$$\sqrt{\frac{2}{f}} = 6 + 2.5.\ln\left(\frac{D}{k}\right) \qquad (9)$$

For f = $1.85\ 10^{-2}$ and D = 0.225 m, the equivalent roughness becomes:

k = 0.0387 m

which corresponds very well to the observed ripple height in the flume.

According to Engelund/Hansen, ripples occur when the sediment particle Reynolds number (ν is the kinematic viscosity)

$$R_* = \frac{U*d}{\nu} \qquad (10)$$

is less than about 10 (when d = 0.18 mm). In this case the Reynolds number is

$R_* = 10.6$

Hence, the bed seems to be on the limit between ripples and dunes.

Sediment Discharge

The critical bed shear stress for initiation of motion of the sediment is defined by Shields curve (Engelund/Hansen 1967). At $R_* = 10.6$, the critical shear stress is

$\theta_c = 0.035$

which is well below the effective skin friction = 0.115.

The criterion $w_s < 0.8\ u'_*$ says which fall velocity w_s a particle should have if it can go into suspension. The fall velocity is estimated from

$$W_s = \frac{(s-1)g.d^2}{18\nu} \approx 0.029\ m/s \quad for\ d = 0.18\ mm \qquad (11)$$

Furthermore, we have

$0.8\ u'_* = 0.015$ m/s

Hence, it can be concluded that the sediment transport will mainly be bed load.

The sediment transport rate is estimated from three different formulae.

Engelund/Hansen:

$$\phi = \frac{0.1}{f}\theta^{2.5} = 0.45 \qquad (12)$$

$$q = \phi\sqrt{(s-1)\ g\ d^3} = 4.4\ .10^{-6}\ m^2/s \qquad (13)$$

Meyer/Peter:

$$\phi = 8(\theta' - \theta_c)^{1.5} = 0.18 \qquad (14)$$

$q = 1.7.10^{-6}\ m^2/s$

Engelund/Fredsoe:

$$\phi = 5P(\sqrt{\theta'} - 0.7\sqrt{\theta_c}) = 0.32 \qquad (15)$$

$$p = (1 + (\frac{\frac{\pi}{6}\beta}{\theta' - \theta_c})^4)^{-0.25} = 0.305 \qquad (16)$$

$$q = 3.1 \cdot 10^{-6} m$$

The latter value of 3.1 x 10^{-6} m^2/s equals 3.1 x 10^{-6} $m^3/m/s$ x 5.5 m x 3600 s = 0.06 m^3/h (solid volume) or in the order in of 100 l/h. This appears in good agreement with observations in the model of the order of magnitude of sediment entering the sediment trap at the end of the flume.

3.3 Mathematical Description

The area was resolved in a space varying grid, see the lower part of Figure 3.1, with a minimum space step of 0.10 m at the groyne. The time step was 0.15 sec. The upstream boundary condition was a constant discharge of 424 l/s uniformly distributed over the width of the flume. At the d/s boundary, a constant water level of 0.225 m was applied (initial bed level = 0.000 m).

A Chezy Number of C = 33 $m^{0.5}/s$, determined from the analysis above, was used. The sediment transport rate is proportional to v^5/C^3 and, therefore, very sensitive to the value of C.

The description of exchange of momentum by the turbulence between grid cells becomes increasingly important when the space step is equal to or less than the depth. In models with large space steps, a constant eddy coefficient is normally applied. This was not adequate in this case. Therefore, the more advanced Smagorinsky formulation was utilized. It is a simplified turbulence model where the turbulence is assumed to be generated and dissipated at the same place. The coefficient C_s was determined by calibration and determines the so-called mixing length, $l = C_s \Delta X$, which is included in the expression for the eddy viscosity.

The Smagorinsky expression reads.

$$E = constant = l^2 \left(\left(\frac{\partial u}{\partial x} \right)^2 + \left(\frac{\partial v}{\partial y} \right)^2 + \frac{1}{2} \left(\frac{\partial u}{\partial y} + \frac{\partial v}{\partial x} \right) \right)^{\frac{1}{2}}$$

and $0 \leq C_s \leq 1.00$ (17)

The Engelund/Hansen formula was used to calculate sediment transport. Normally, this formula is quite accurate when the main part of the sediment load is bed load.

4. SIMULATION OF VELOCITY

The bathymetry shown in Figure 4.1 was how the bed in equilibrium looked in the physical model. Using this bathymetry, the velocity field shown in Figure 4.2 was simulated with the 2-D model. The separation point in the lee of the groyne was about one groyne length downstream. This fits very well with the observations in the physical model. In Figure 4.3, a contour plot of the simulated current velocity field is depicted.

The simulated and measured velocity across the flume is illustrated in Figures 4.4 to 4.7. The flow at the upstream end of the flume was not completely uniform, see Figure 4.4. The reason could have been that the bed shear stress was non-uniformly distributed over the width of the channel. However, the velocities were very much alike at the groyne and downstream of the groyne. Only at the tip of the structure, see Figure 4.5, the simulated velocity seemed to be underestimated in the 2-D model. The explanation is probably that the turbulence is very complex at this point and not adequately described in the 2-D model. The order of magnitude of the eddy in the flume was 10-20 cm and the space step in the 2-D model was 10 cm indicating that the eddy was difficult to model. The maximum simulated velocity was 0.45 m/s at the upstream corner of the groyne.

The first test showed that the 2-D model gives a fairly accurate representation of the flow velocity field compared with the observation in the physical model. The sediment transport was also simulated and it showed that the bed was almost in equilibrium in the 2-D model also. Figure 4.8 shows how the bed looked after an additional 2 hours of simulation with the 2-D model. When it is compared to the bathymetry in Figure 4.1, one finds that only minor erosion and deposition have taken place.

5. SIMULATION OF SCOUR

In the second simulation, the bed was horizontal at the beginning. The objective was to simulate the development of scour. Figure 5.1 shows the velocity field at the start. The velocity was nearly zero at the lee side of the groyne and far downstream.

The simulated sediment transport at the start of the simulation is shown in Figure 5.2. The highest rates occurred as expected at the tip of the groyne. The 2-D model simulated 4 hours real time which was the running time of the flume test.

The time development of the scour hole is depicted in Figure 5.3 for both the physical and the 2-D model. It is observed that the time scale for scour development was almost the same. The 2-D model, however, only simulated 12 cm of scour whereas the maximum scour in the flume was 42 cm.

After 4 hours, the simulated bathymetry was as shown in Figure 5.4. The bathymetry found in the physical model is shown in Figure 4.1. Maximum scour occurred at the upstream corner of the groyne in both models. The bar downstream of the groyne was not developed in the 2-D model. The influence from the groyne on the bed level reached the opposite wall in the 2-D model. This was not observed in the physical test flume. The observed scour hole in the physical model went all around the tip of the groyne whereas in the 2-D model, the scour hole was only on the upstream side. The main reasons for these discrepancies are considered to be:

- The vortices developed at the upstream corner of the groyne moved downstream with the flow in the physical model. They have the effect of enhancing erosion at the downstream corner of the groyne.

  In the Smagorinsky turbulence model used in the 2-D model, the eddies are not transported downstream. Hence, the turbulent energy behind the groyne inherent from the flow at the tip of the structure was not included in the 2-D model. As a result in the 2-D model, the water was more calm in the lee side whereas in the flume test, it was more turbulent.

- The shape of the equilibrium bed, see Figure 5.5, revealed the three-dimensional flow pattern at the groyne. A wedge formed bar was formed behind the groyne at the place where the bottom flow "crossed" the surface flow (see the sketch in Figure 5.6). Hence, the flow at the bottom downstream of the groyne was more directed inwards and the surface flow was directed outwards. This was also observed when small float track tests were carried out in the flume. The phenomenon is the equivalent of the "horse shoe" vortex effect associated with bridge piers.

- The 2-D model works with depth integrated equations and can hence not represent correctly this pattern of crossing flow. A fully 3-D model would be required for this simulation.

- The slope of the bed at the scour hole was at its maximum, the angle of repose of the sand. Thus, the sediment transport rate and direction was more complex here than can be described in the Engelund/Hansen model.

6. MODEL OF GROYNE WITH SIDE SLOPE

As described above the flow around the sharp corner of the vertical sided groyne was difficult to simulate accurately in the 2-D model. A new model with a rounded groyne nose and sloping sides was set up in the 2-D model and in the flume. It was anticipated that the 3-D current pattern would be less pronounced in the new model. Hence, the erosion and deposition should be better described in the 2-D model.

The initial bathymetry used in the 2-D model is shown in Figure 6.1. The selected grain size on the submerged part of the groyne was very coarse so that there would be no sediment transport there. The simulated velocity field is depicted in Figure 6.2 and the simulated bathymetry after four hours simulation time (real) is shown in Figure 6.3. The simulated bathymetry from the flume test is shown in Figure 6.4.

The simulated scour hole was in both cases of the same order of magnitude, 10-15 cm maximum scour. But the location of the scour hole was situated more upstream in the 2-D model than in the flume test.

The 2-D model simulation was more accurate for the groyne with side slope than the vertical sided groyne but in general the model cannot accurately simulate the flow pattern of 3-dimensional flow.

7. CONCLUSION

The 2-D model study and comparisons with the physical model tests of the same geometrical shape and for the same flow conditions have revealed that the 2-D model gives an accurate simulation of the flow field and associated scour only when the flow field is two-dimensional i.e. not with cross-flows as observed near the groyne nose in the physical model.

Fully 3-D models have been developed for simulation of fully three-dimensional flow. One such model is DHI's system 3. The models have not, however, yet been developed to cope with sediment transport and simulation of scour and deposition. For the present, therefore, the prediction and assessment of local scour around groynes and similar structures will still have to be based on physical models such as performed for the BRTS at River Research Institute. The physical model has the advantage of being able to reproduce accurately the complex 3-dimensional flow field near a groyne nose.

FIGURES

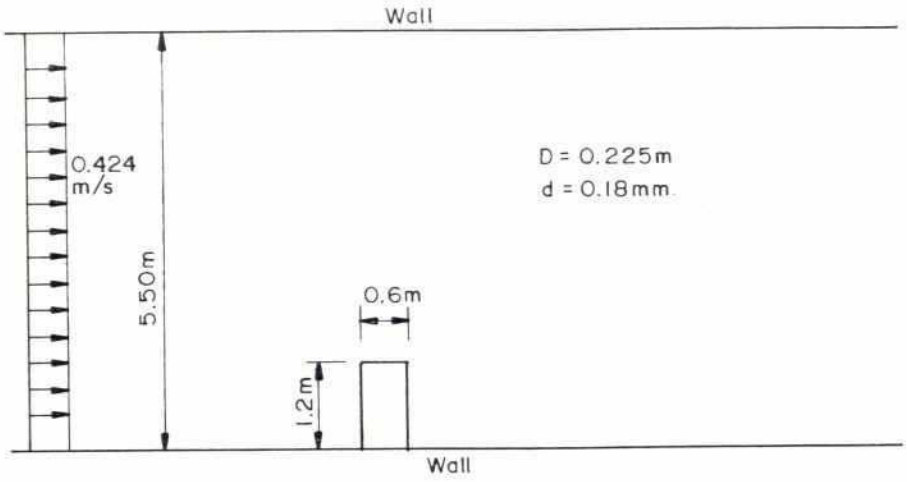

Key data of the flume test.

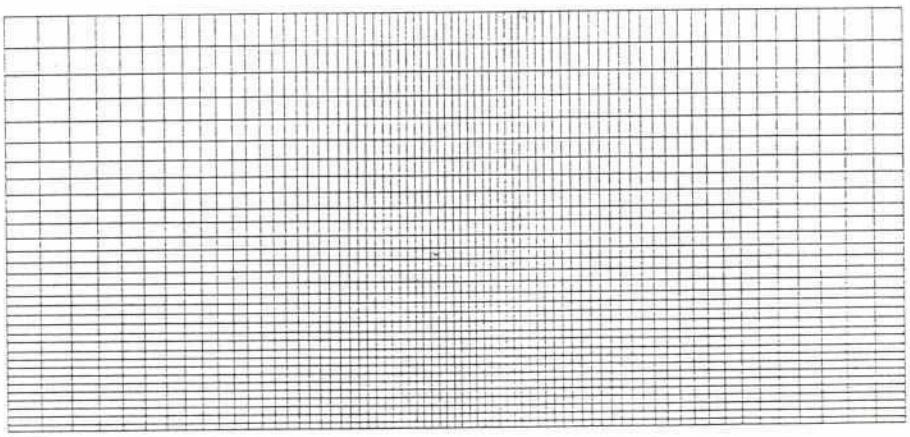

1:30000 / 1:100

Computational grid used in the 2-D model.

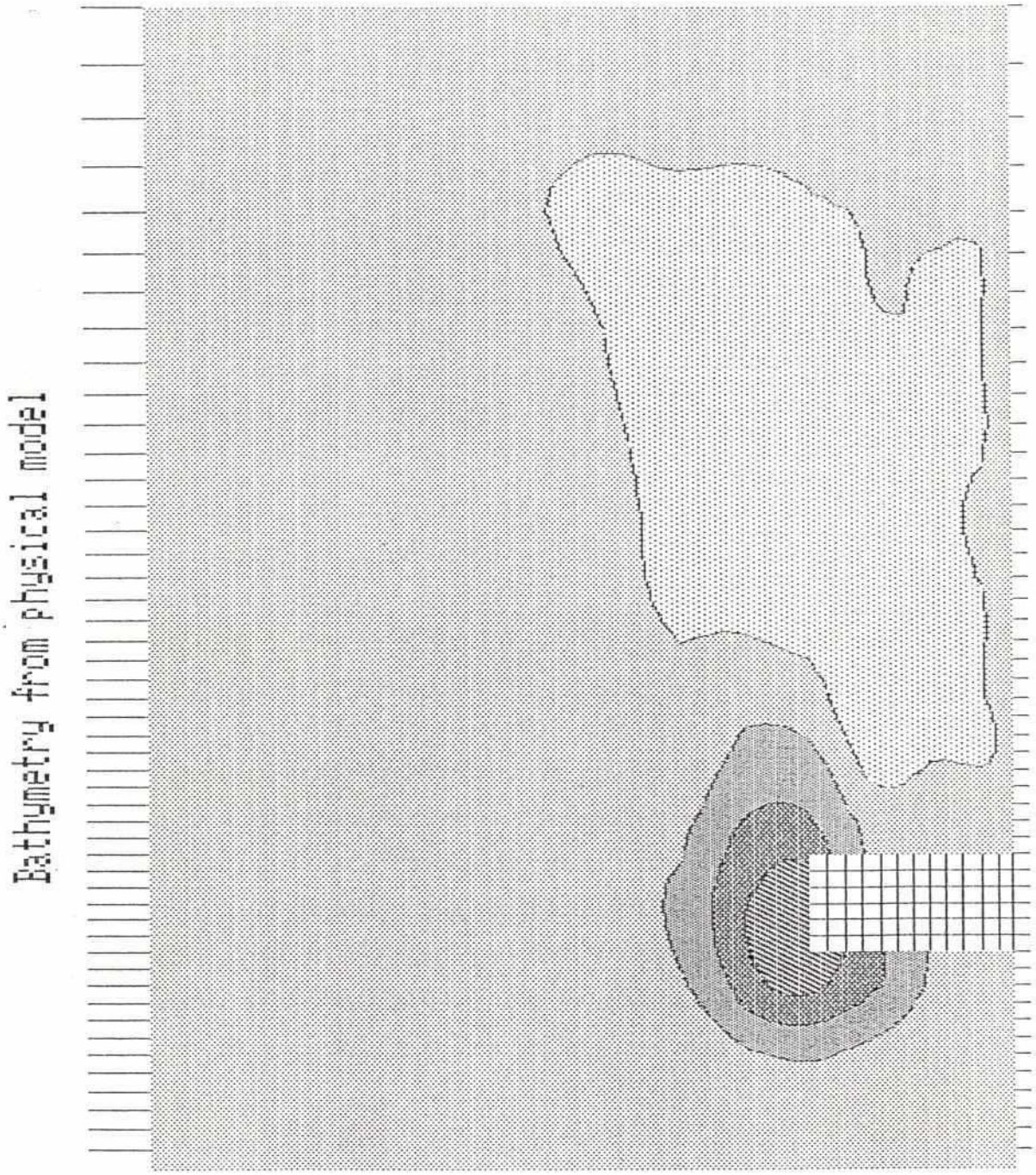

SCALE 1 : 40

BRTS 2-D Numerical Modelling of Flow and Scour Around a Groyne

Bathymetry of Equilibrium Bed in Flume Test	**Vol.4**	**Part 12**
	Figure 4.1	

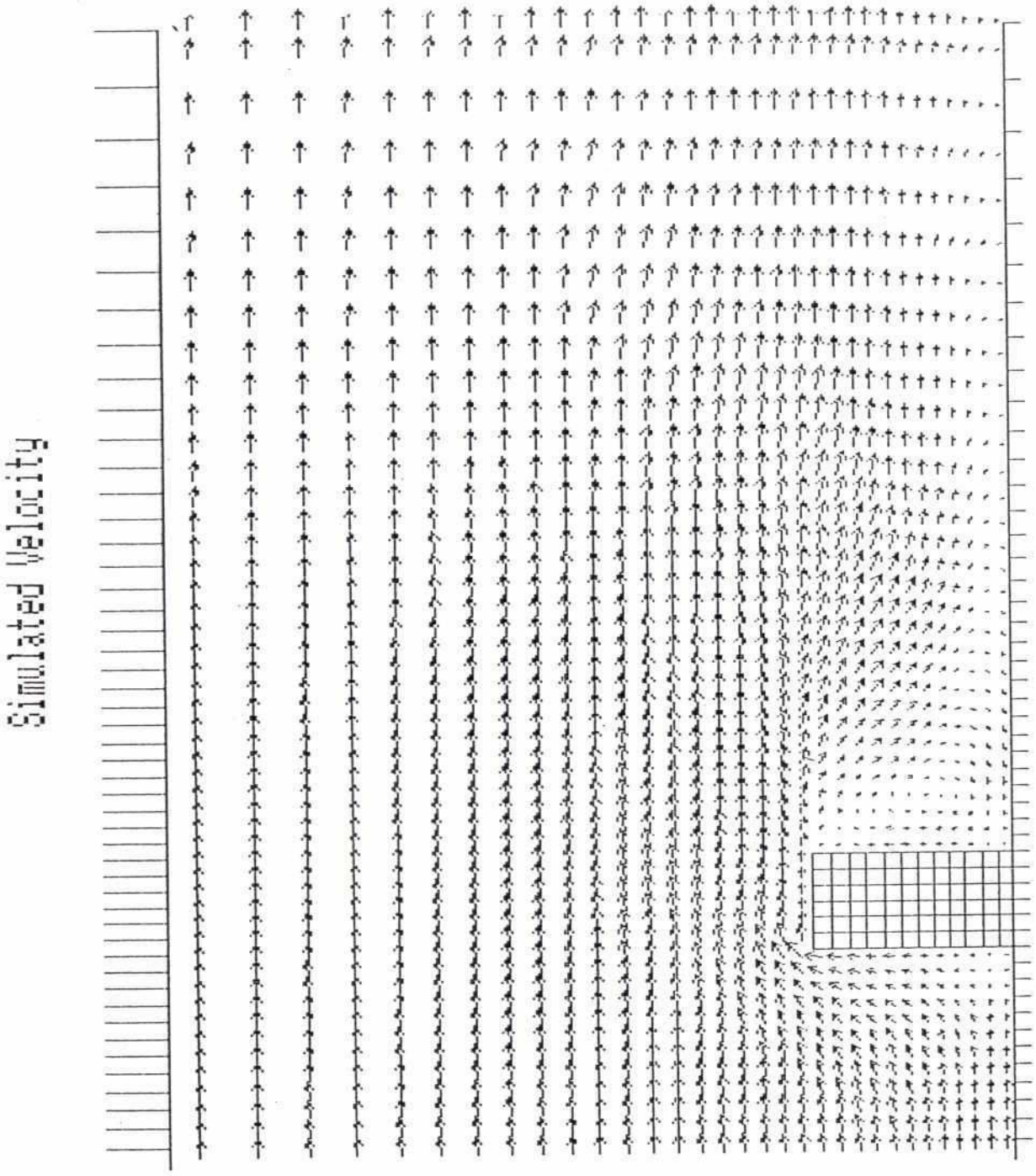

SCALE 1 : 40

BRTS 2-D Numerical Modelling of Flow and Scour Around a Groyne

Simulated Velocity Field with Equilibrium Bed

Vol.4 Part 12

Figure 4.2

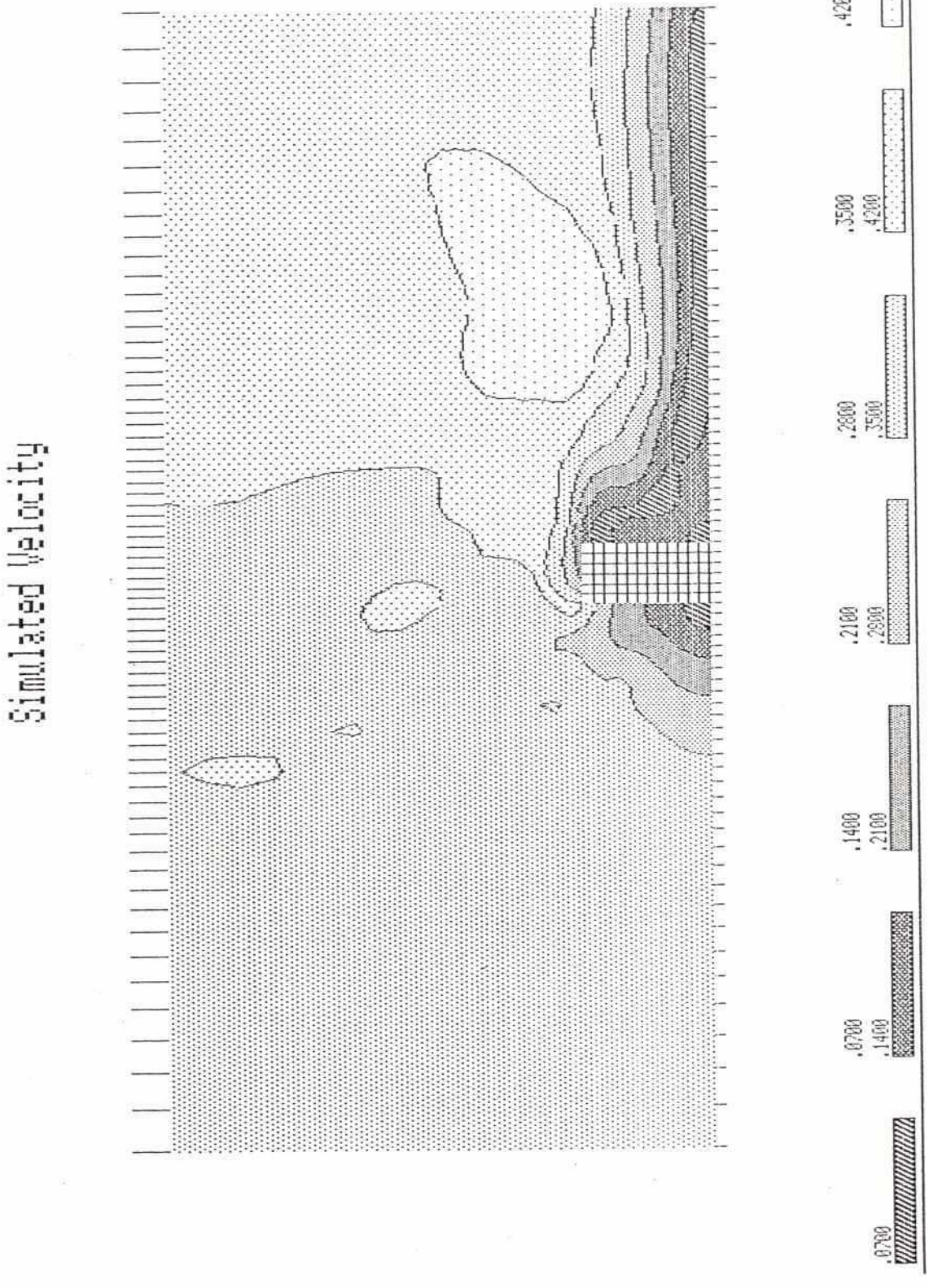

SCALE 1 : 60

BRTS 2-D Numerical Modelling of Flow and Scour Around a Groyne

Contour Plot of Simulated Velocity Field with Equilibrium Bed	Vol.4 Part 12
	Figure 4.3

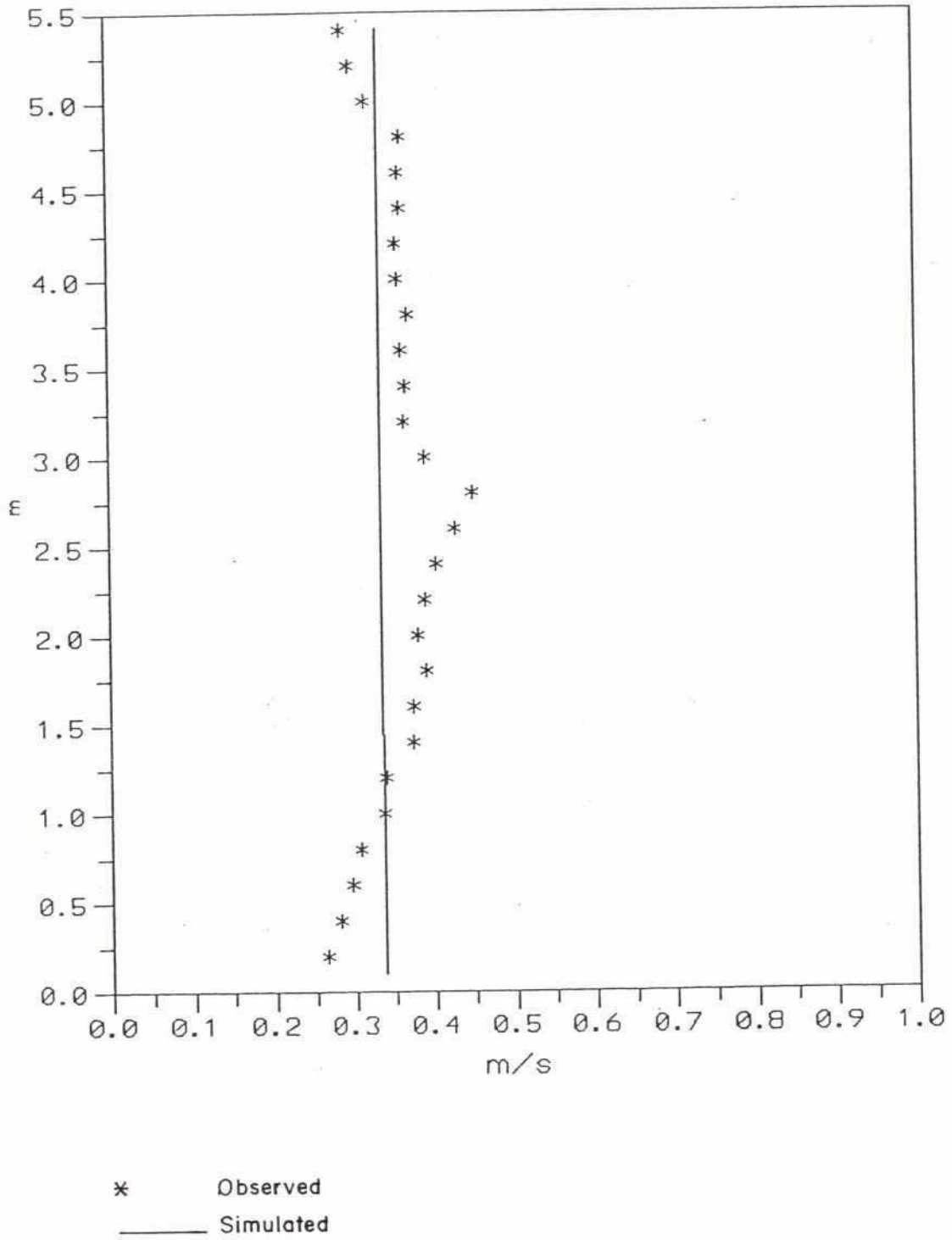

BRTS 2-D Numerical Modelling of Flow and Scour Around a Groyne

Velocity 6m Upstream of Groyne

Vol.4 Part 12

Figure 4.4

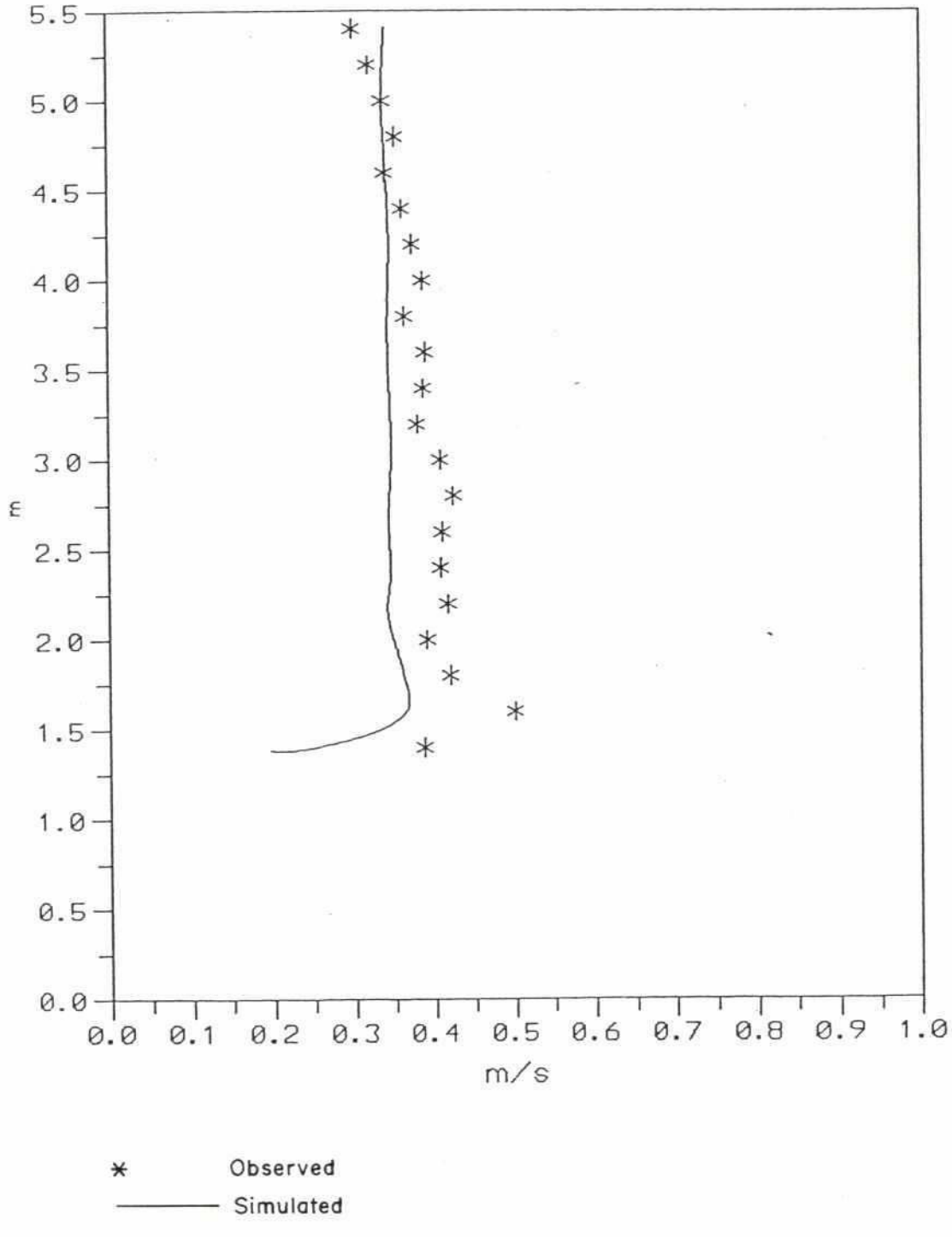

BRTS 2-D Numerical Modelling of Flow and Scour Around a Groyne

Velocity at the Groyne	**Vol.4** Part 12
	Figure 4.5

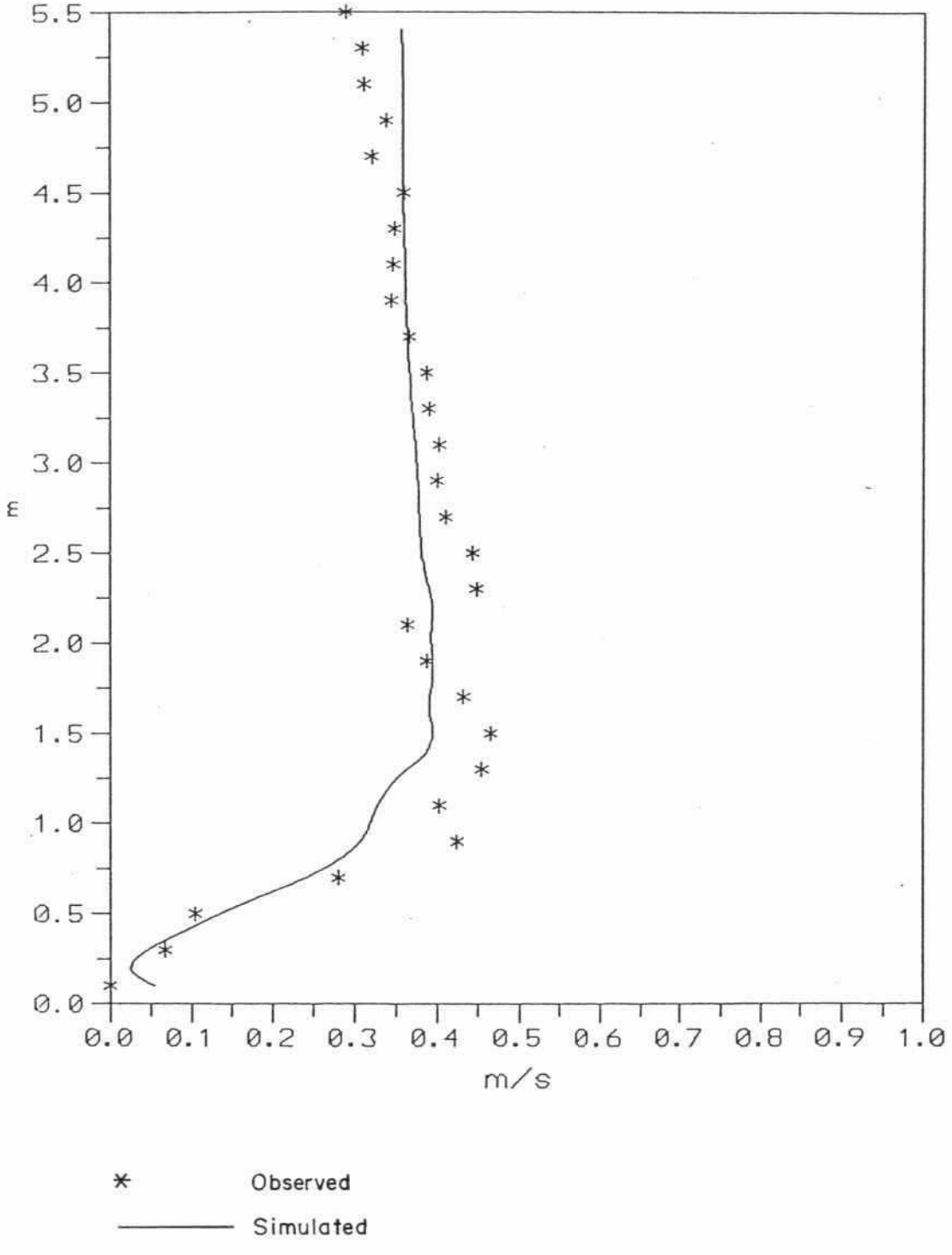

BRTS 2-D Numerical Modelling of Flow and Scour Around a Groyne

Velocity 1m Downstream of Groyne

Vol.4 Part 12

Figure 4.6

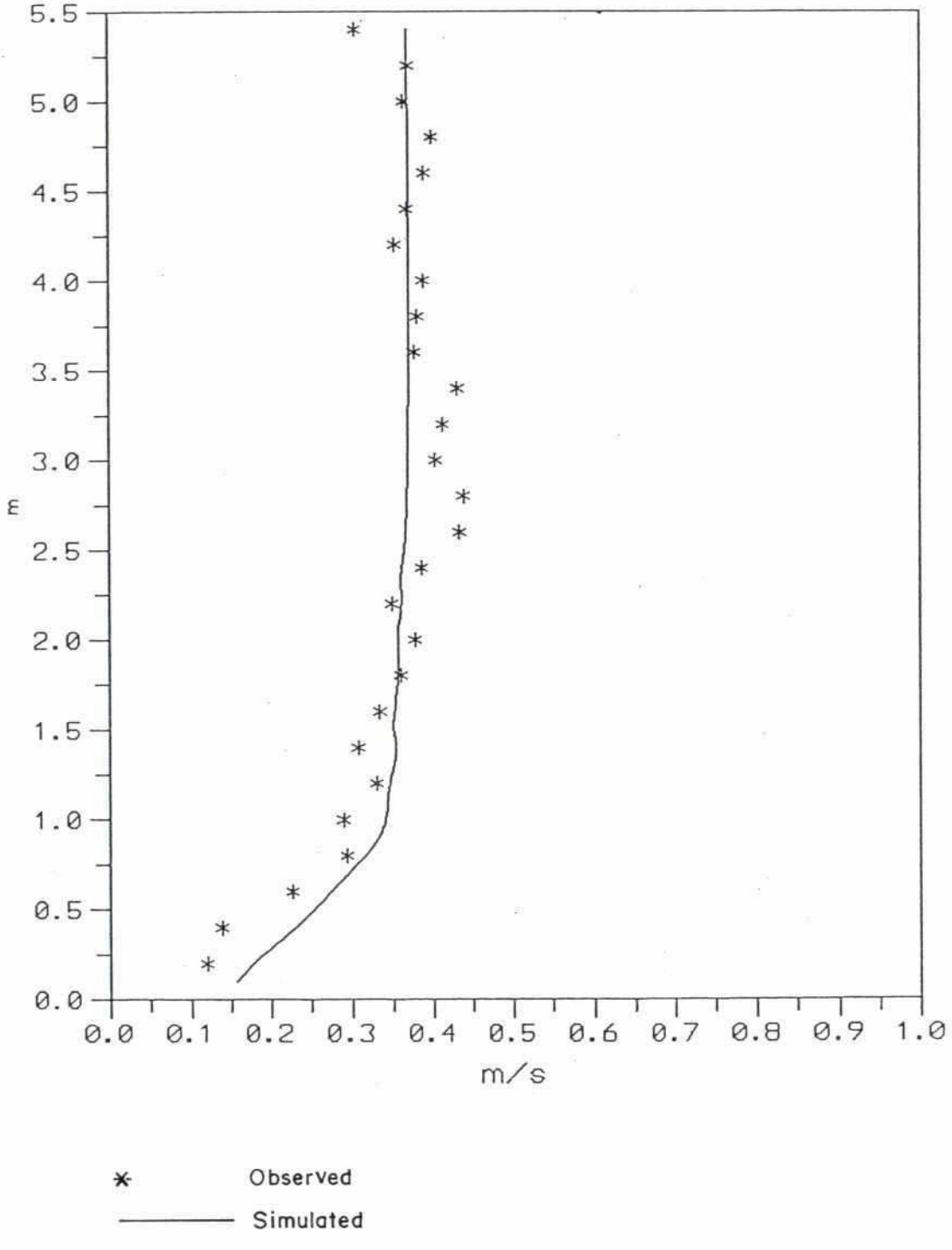

BRTS 2-D Numerical Modelling of Flow and Scour Around a Groyne

Velocity 6m Downstream of Groyne

Vol.4 Part 12

Figure 4.7

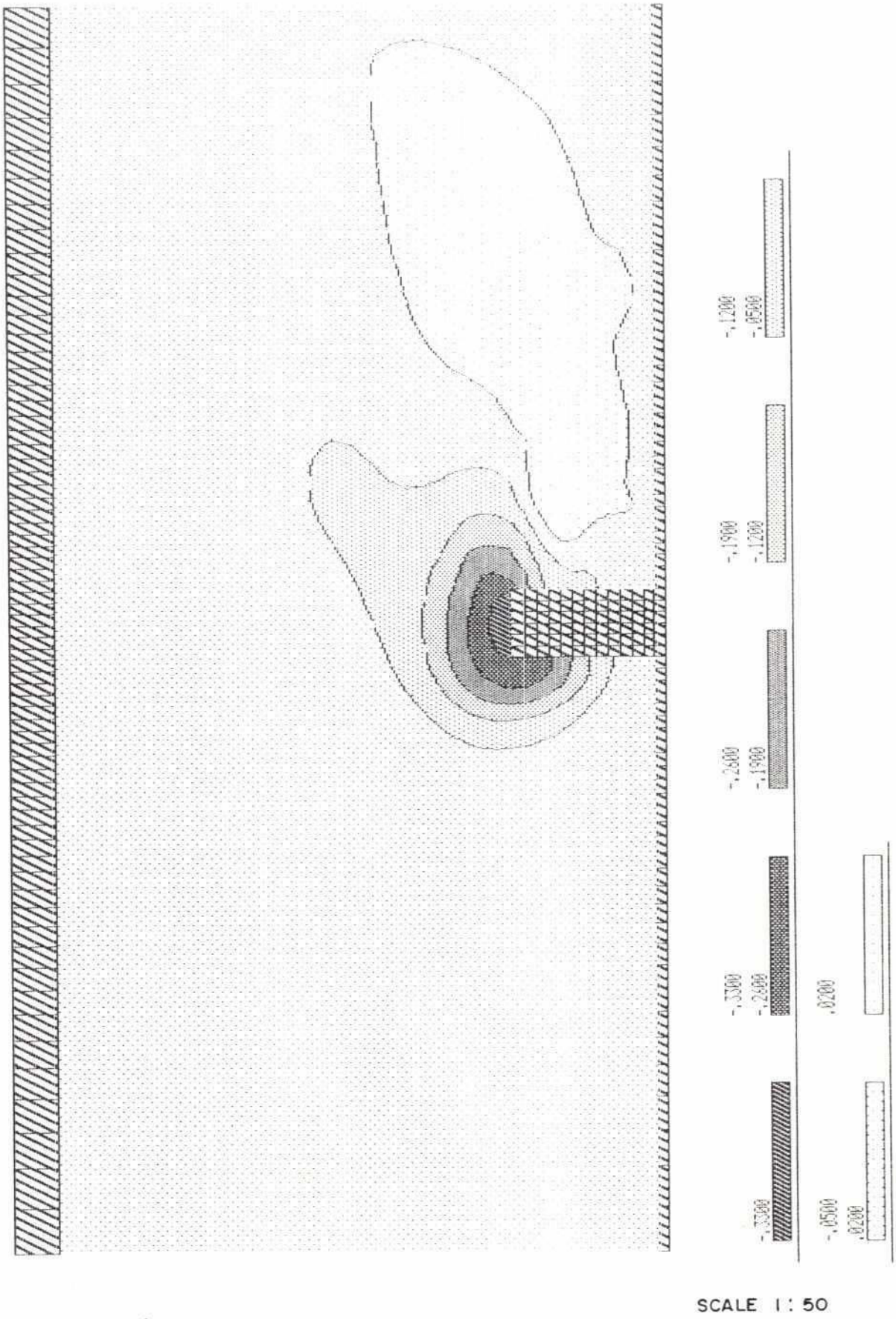

SCALE 1 : 50

BRTS 2-D Numerical Modelling of Flow and Scour Around a Groyne

Equilibrium Bed After Additional Two Hours Simulation	Vol.4 Part 12
	Figure 4.8

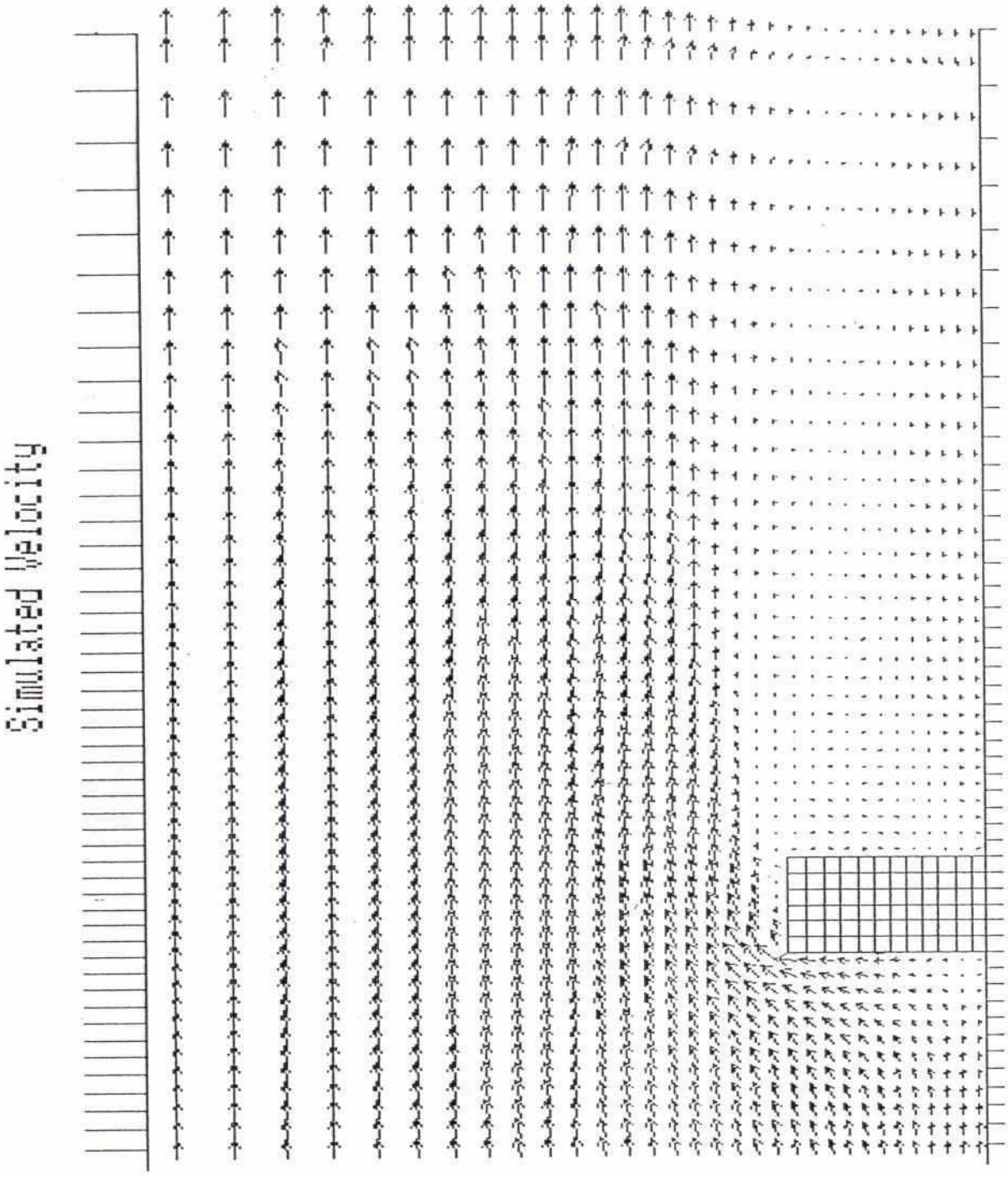

SCALE 1 : 40

BRTS 2-D Numerical Modelling of Flow and Scour Around a Groyne

Simulated Velocity Field with Plane Bed Initially	**Vol.4** **Part 12**
	Figure 5.1

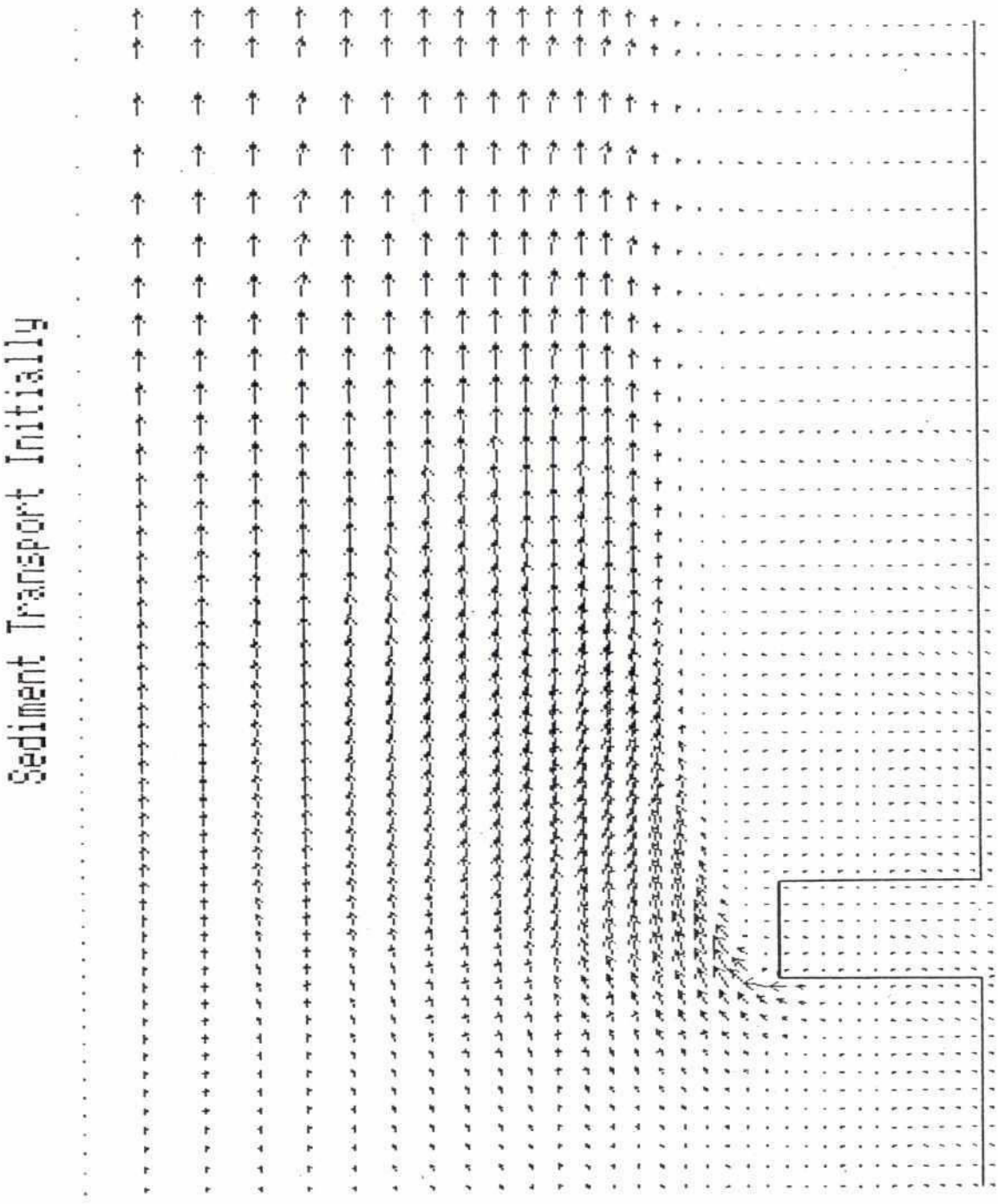

SCALE 1 : 40

BRTS 2-D Numerical Modelling of Flow and Scour Around a Groyne

Simulated Sediment Transport with Plane Bed Initially	**Vol.4** **Part 12**
	Figure 5.2

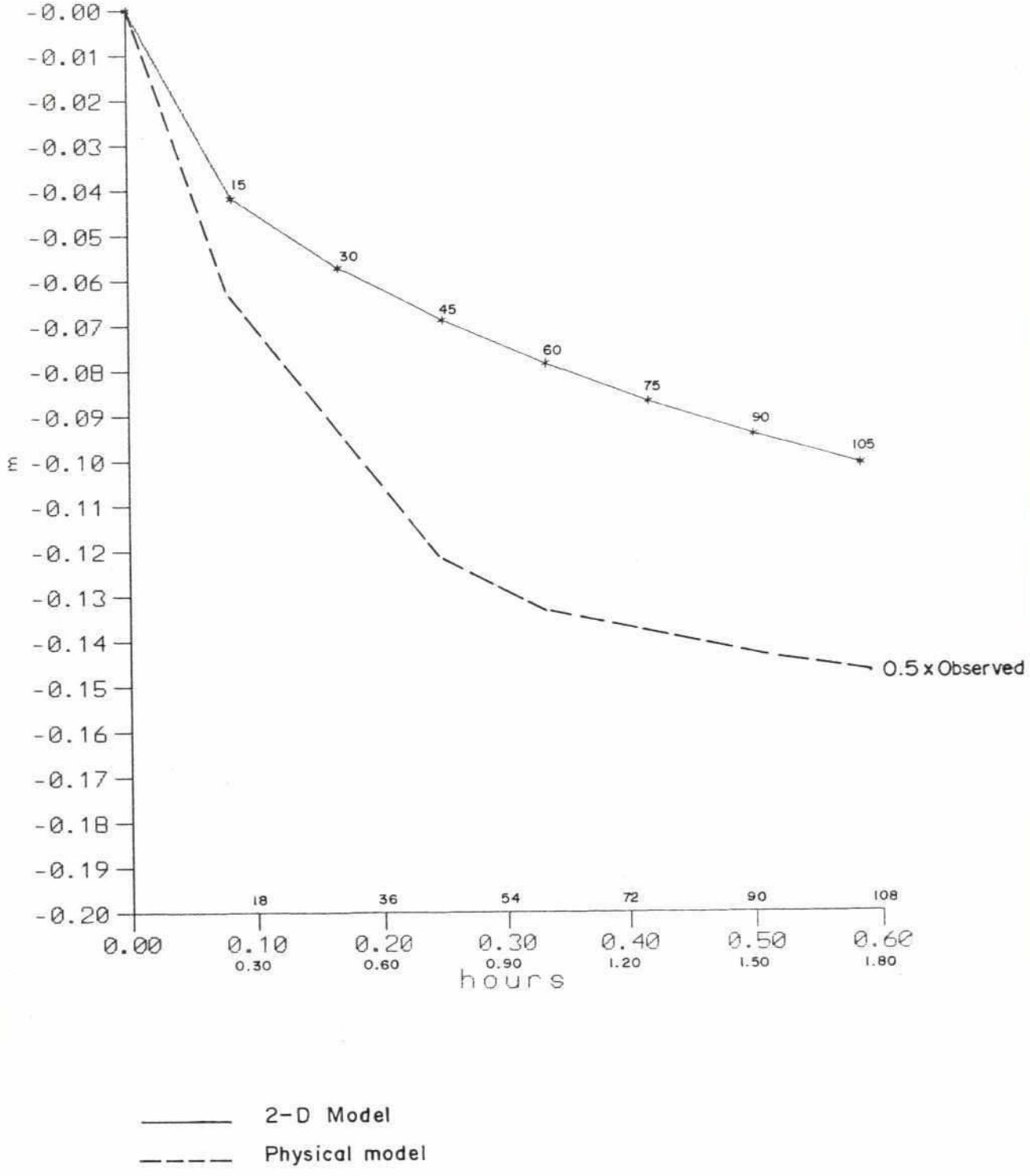

BRTS 2-D Numerical Modelling of Flow and Scour Around a Groyne

Time Development of Scour Hole	**Vol.4**	**Part 12**
	Figure 5.3	

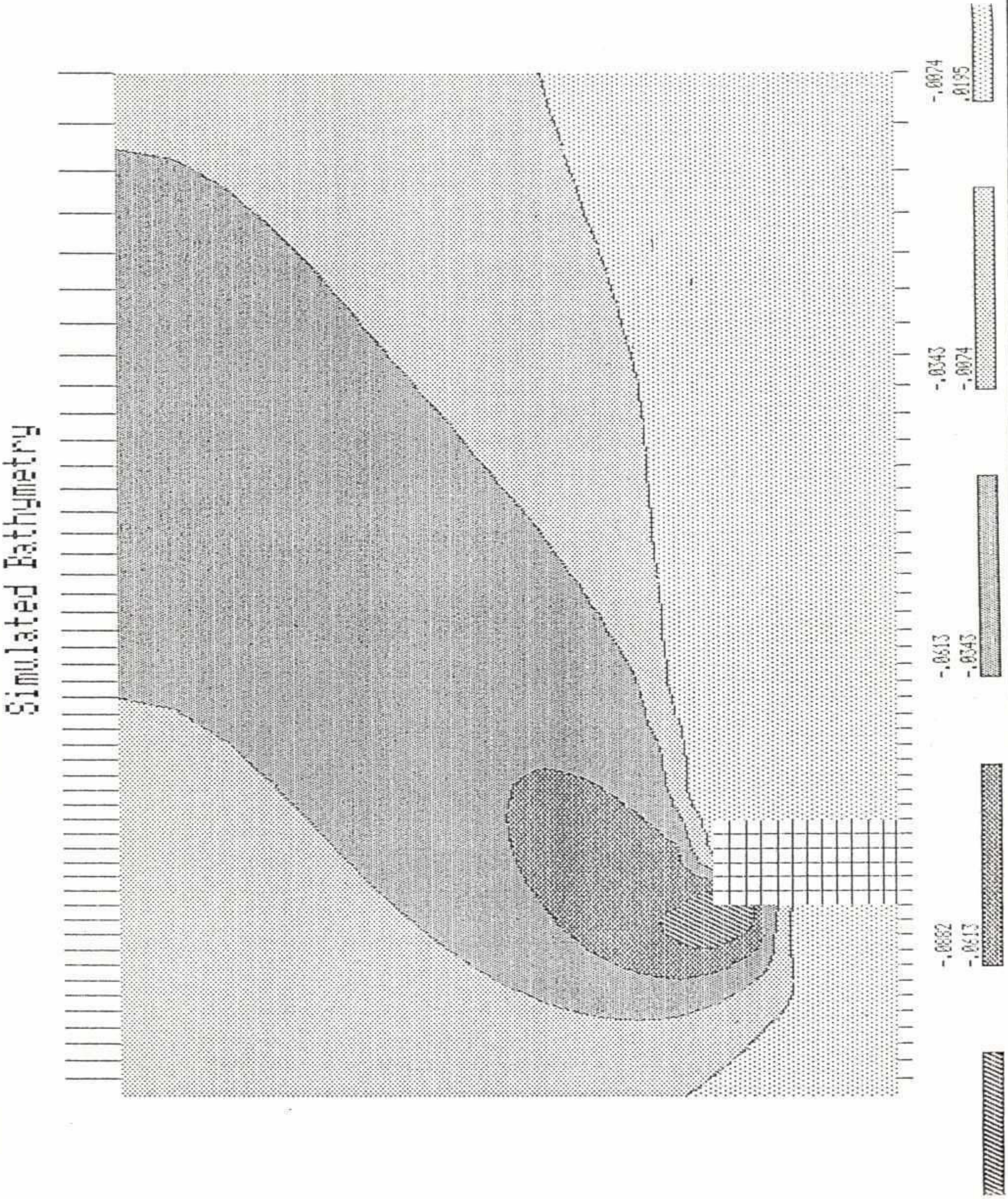

SCALE 1 : 40

BRTS 2-D Numerical Modelling of Flow and Scour Around a Groyne

Simulated Bathymetry	Vol.4 Part 12
	Figure 5.4

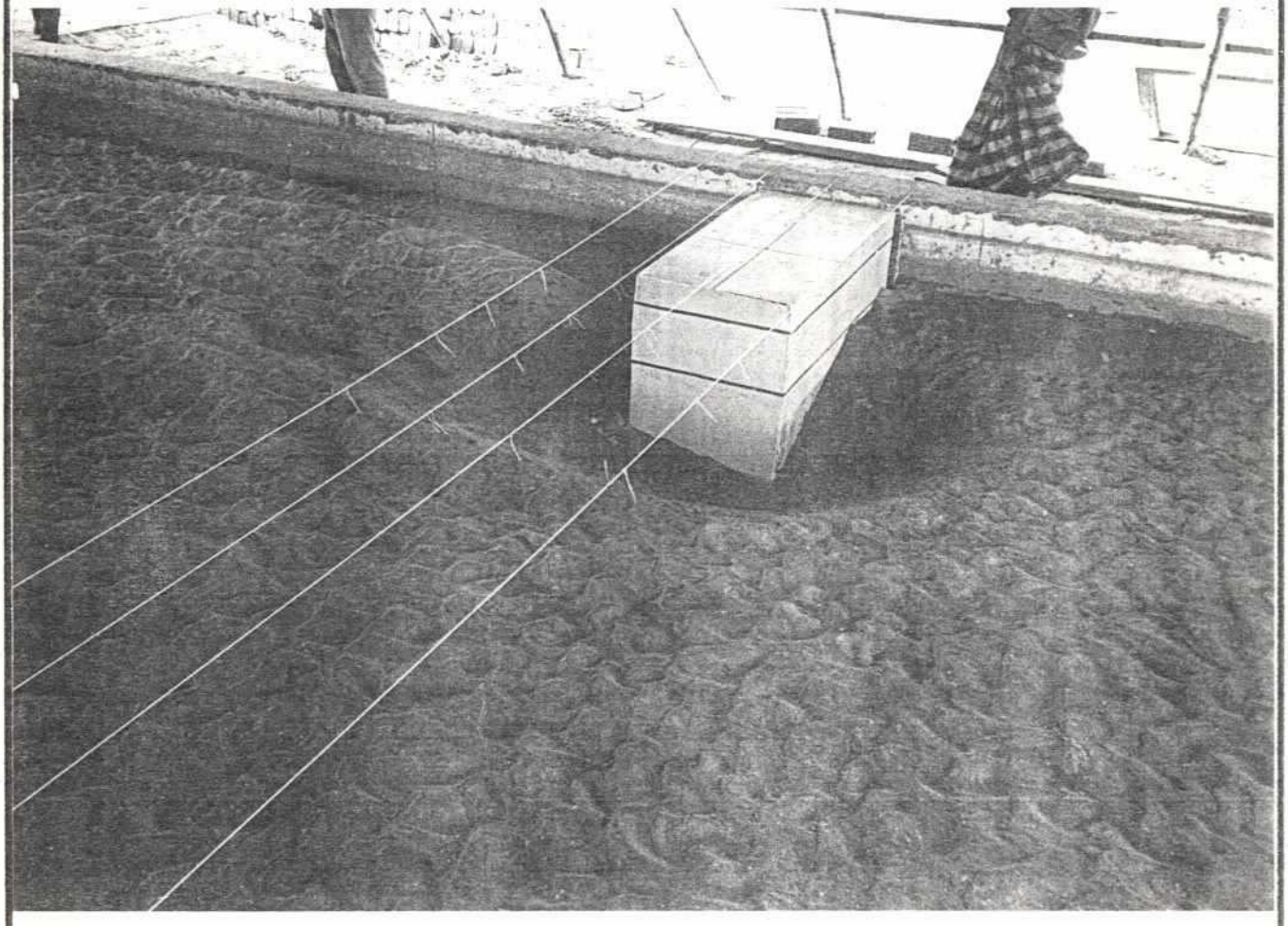

BRTS 2-D Numerical Modelling of Flow and Scour Around a Groyne

Photograph of Scour in Physical Model

Vol.4 Part 12

Figure 5.5

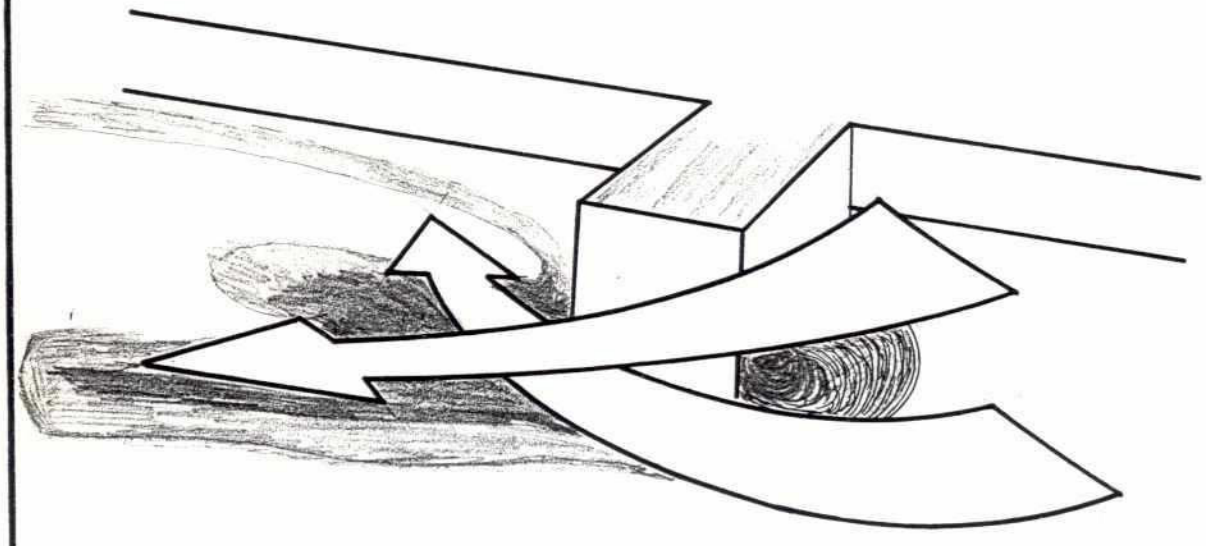

BRTS 2-D Numerical Modelling of Flow and Scour Around a Groyne

Sketch of 3-D Flow

Vol.4 Part 12

Figure 5.6

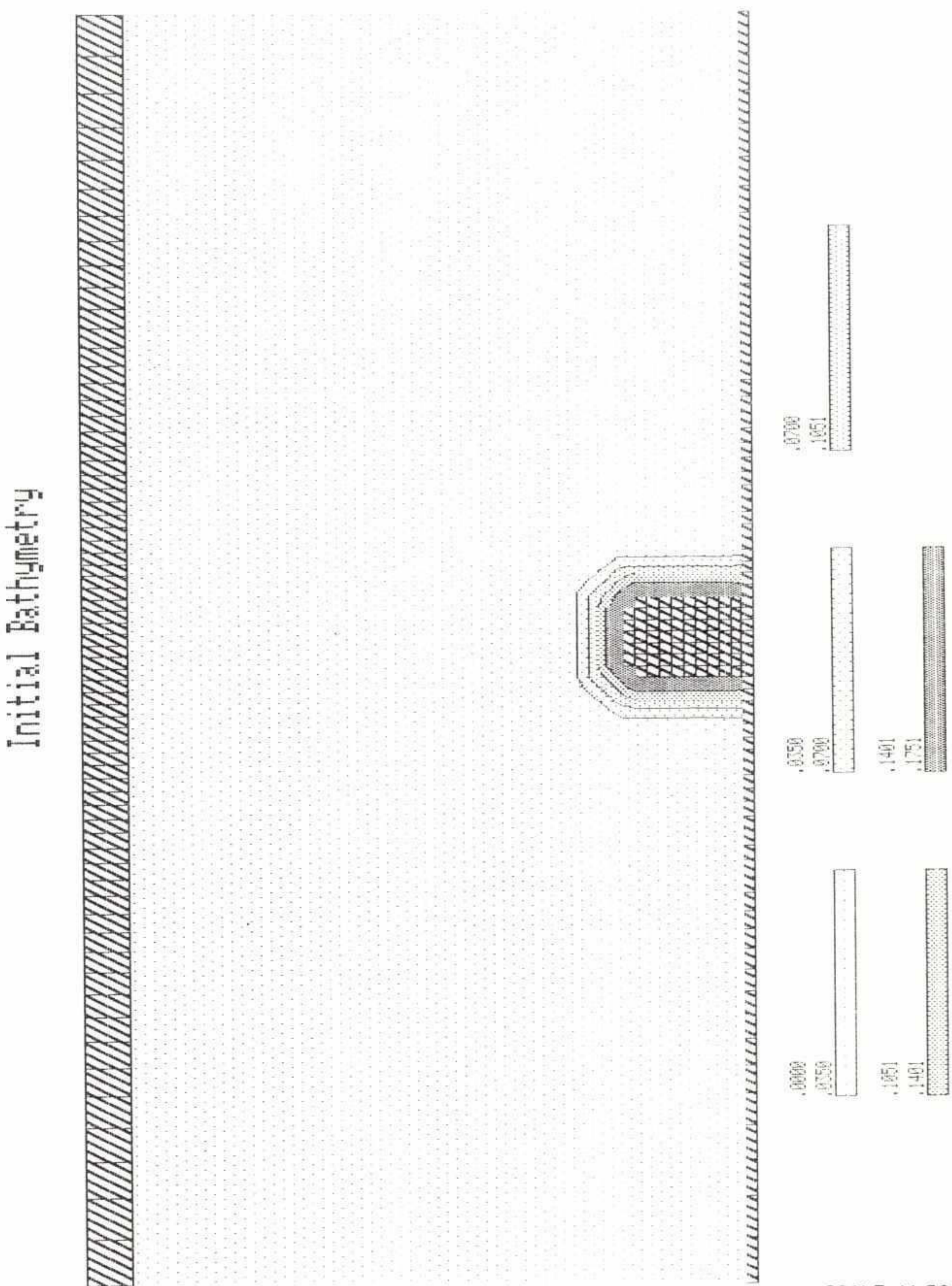

SCALE 1: 50

BRTS 2-D Numerical Modelling of Flow and Scour Around a Groyne

Initial Bathymetry in Model of Groyne with Side Slope	**Vol.4** **Part 12**
	Figure 6.1

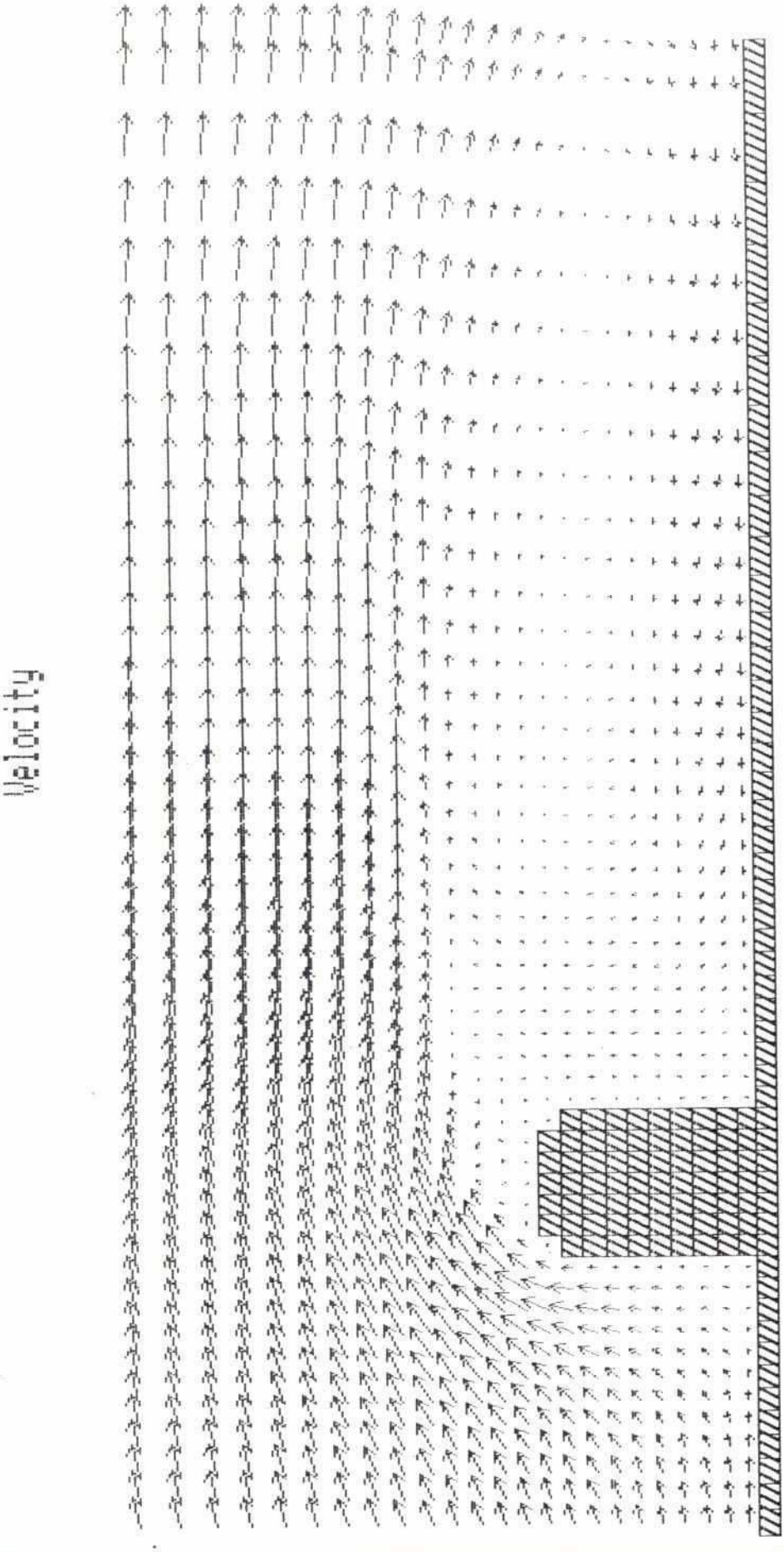

BRTS 2-D Numerical Modelling of Flow and Scour Around a Groyne

Simulated Velocity Field in the Model of Groyne with Side Slope

Vol.4 Part 12

Figure 6.2

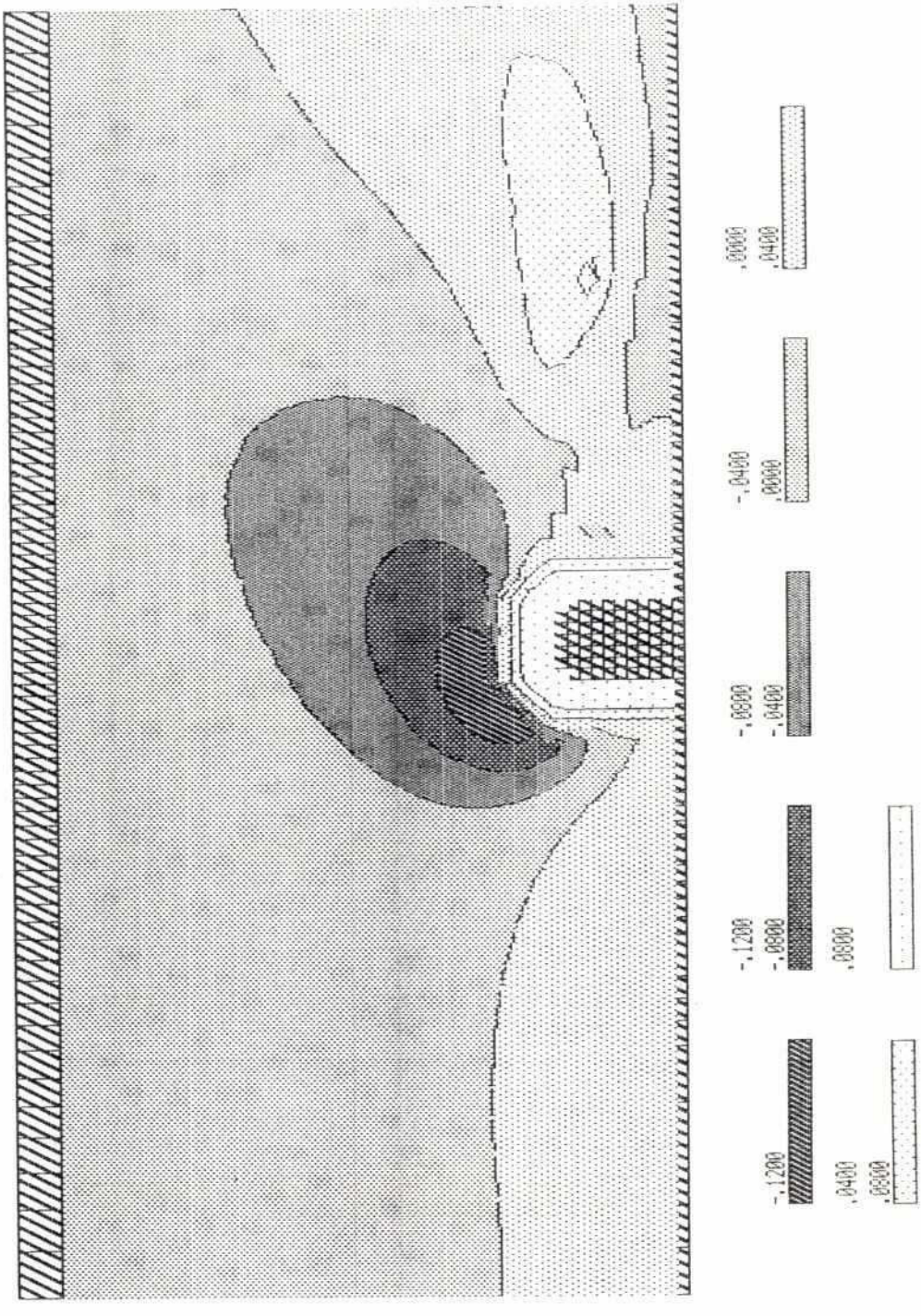

BRTS 2-D Numerical Modelling of Flow and Scour Around a Groyne

Simulated Bathymetry in 2-D Model	Vol.4 Part 12
	Figure 6.3

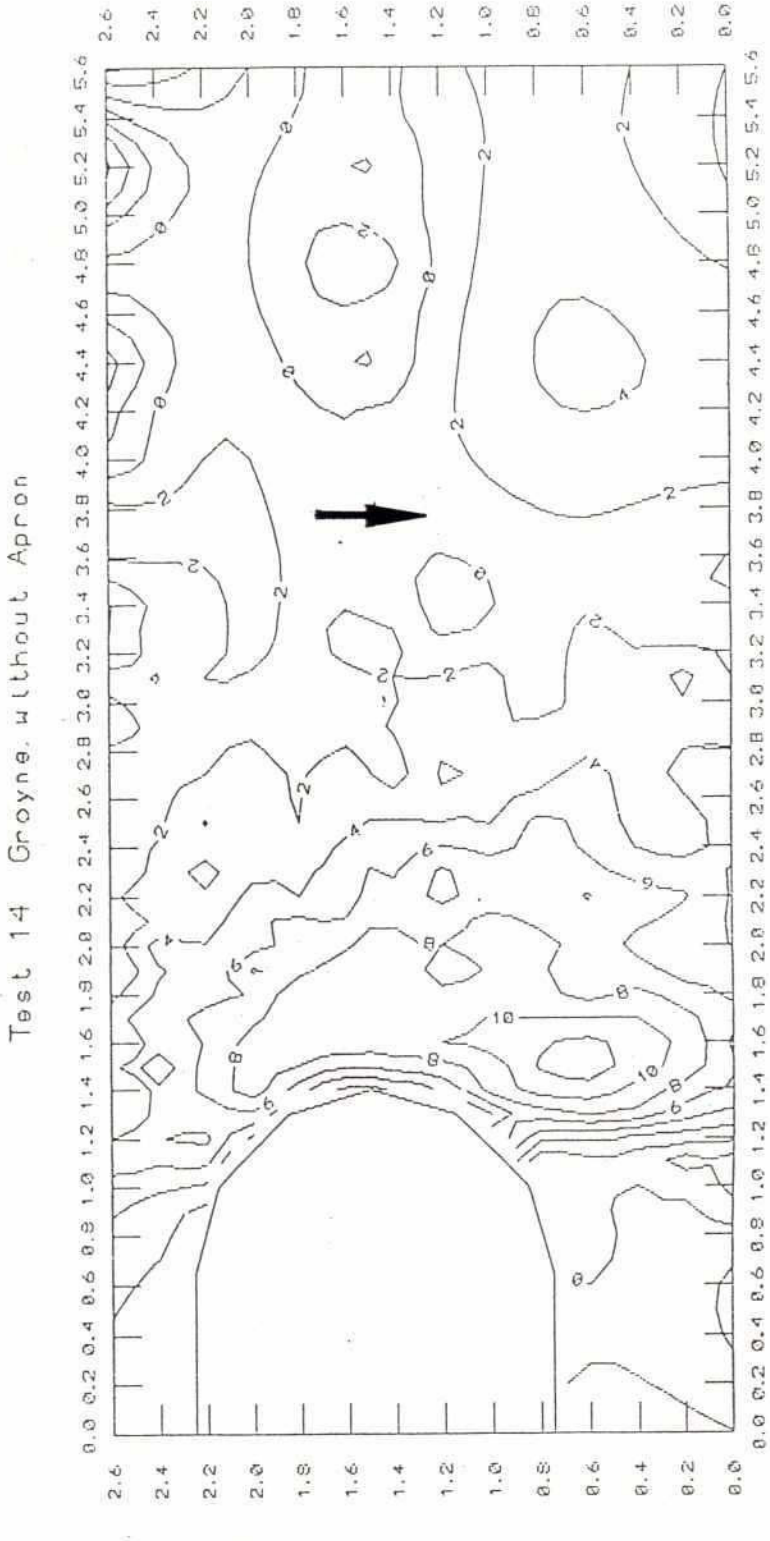

BRTS 2-D Numerical Modelling of Flow and Scour Around a Groyne

Simulated Bathymetry Around Groyne with Side Slope from Flume Test

Vol.4 **Part 12**

Figure 6.4

Part 13

2-D Numerical Modelling of Bifurcation and Stability of Anabranches

HALCROW

RIVER TRAINING STUDIES OF THE BRAHMAPUTRA RIVER

REPORT ON MODEL STUDIES

PART 13 - BIFURCATION ANALYSIS AND STABILITY OF ANABRANCHES

CONTENTS

FIGURES

1. OBJECTIVE

One of the objectives of the 2-D Numerical Modelling of the Brahmaputra was to analyse the development and decay of anabranches as described in "Working Paper on 2D-Modelling", BRTS (1990).

The first step in this analysis was to set up a very simple model of a channel dividing into two anabranches which then meet again 5 km further downstream. This study would indicate whether development of an anabranch can be controlled by dredging, and also how sensitive the processes are to change in flow distribution and angle of attack of the flow at the bifurcation point.

2. APPROACH

As the planform of the river is changing continuously and the anabranch problem is present at several locations along the river, it was decided that it was more appropriate to use a non site specific model which exhibits the same physical features as in nature. Typical values of width, depth, discharge and sediment load were found from available sources such as river surveys, aerial photographs, maps, satellite imagery and literature.

The hydrodynamic model and the sediment transport model were used separately in the first simulations in order to tune the model to represent the prototype satisfactorily. Following that, the two models were combined into the morphological model where the bed level is updated continuously. This model was used to:

- estimate the equilibrium bathymetry and establish a reference simulation for comparison with the simulations mentioned below

- analyse the effect of displacing sediment from one branch to another by running a simulation with increased bed level in one anabranch and decreased bed level in another anabranch initially

- analyse the effects of changing the flow direction at the bifurcation point by running a simulation with changed boundary conditions upstream.

3. DESCRIPTION OF THE NUMERICAL MODELLING PROGRAMME

The mathematical programme System 21 is described in the First Interim Report, Annex 3, Part 2, BRTS(1990). The hydrodynamic model, the sediment transport model and the large scale morphological model have been used in this study.

The hydrodynamic model is based on a two dimensional depth averaged system of equations (St Venant) discretisized into a curvilinear grid. In the sediment transport model, the helical flow which develops in bends is also taken into account.

The bed load of sediment is calculated explicitly with the Meyer-Peter & Muller, Engelund & Fredsoe or the van Rijn model where the transport rate is essentially a function of the bed shear stress and grain diameter. The slope of the bed is taken into account when the direction of the sediment movement is calculated.

The suspended load of sediment is computed by means of a depth averaged convection-dispersion model in which the vertical concentration profile of sediment and the vertical velocity profile (inclusive helical flow) is taken into account. The so-called equilibrium concentration which exists in steady, uniform flow is calculated by the equations of van Rijn or Engelund & Fredsoe. However, with the convection-dispersion model the time and space lag effect of sediment in suspension will be included.

The total load of sediment is calculated either as the sum of the bed load and the suspended load or by the equation of Engelund & Hansen.

The change in bed level is calculated by using the continuity equation for sediment. Spatial differences in sediment transport rate are counter- weighted by temporal changes in bed level. At the upstream boundary, the equilibrium concentration is applied and the upstream bed level can either be fixed or have a constant rate of change. The bed level is updated with a given timestep. Within each, quasi-steady hydrodynamic conditions are assumed.

The model operates with fixed banks. However, bank erosion can be simulated in an approximate manner by introducing inflow of sediment at various places in the model.

4. DESCRIPTION OF THE MODEL

4.1 Planform

The characteristic planform geometry used in the study has been estimated from aerial photos. Special emphasis has been put on the correct representation of the radius of curvature of the bends and the shape of the upper part of the char island at the bifurcation point. The report by Coleman (1969) on the Brahmaputra River has also been used.

The model geometry is shown in Figure 4.1. It is composed of two symmetrical anabranches which in fact represents an inherently unstable situation in the prototype. However, the main point of interest is to see how this symmetry is destroyed and how it can be controlled.

4.2 Cross Sections

The size and shape of the cross-sections depend on the water and sediment discharge, the sediment characteristics and the time history of the river bed development. The calibration and verification study of Test Area 1 and Test Area 2 showed that the latter has a major influence. The bathymetry behaves very dynamically and seems never to be in equilibrium locally. In this study, it is necessary to assume that the bathymetry is more or less in equilibrium (although unstable) from the beginning of the simulation. Hence an equilibrium bathymetry has to be estimated.

The river width W has been estimated from an empirical relationship used by RPT(1990) in the Jamuna Bridge Project study:

$$W = 16.1\ Q^{0.53}$$

The mean depth y has been derived as the natural depth for a given discharge Q and water surface slope I:

$$y = \left(\frac{Q}{C.W.I^{0.5}}\right)^{\frac{2}{3}}$$

In river bends, the secondary flow induced by the centripetal force will create a net transport of sediment from the outer to the inner bank. In a fully developed bend, this will be counter-weighted by the effect of gravity on the sediment grains moving on the sloping bed (the slope being in the transverse direction). This effect is described among others by Olesen(1987). The transverse slope can be estimated from the equation:

$$\frac{dz}{dn} = \frac{15u^2y}{R_s C^2 (S - 1) d_{50}}$$

u = velocity
y = horizontal coordinate
R_s = Raidus of curvature
C = Chezy Number
S = relative density of sand

d_{50} = grain size of sand

This has been used as a first estimate on the shape of the cross sections. The mean depth was maintained.

4.3 Hydraulic Parameters

The size of the model area has been "designed" for a discharge of 6000 m^3/s. Hence it only represents a small portion of total river width.

The surface slope has been set to be relatively steep at 10^{-4}. The mean velocity is about 2 m/s and the Chezy Number is 70 $m^{1/2}/s$. These values have been estimated from the experience gained from Test Area 1, see First Interim Report, Annex 3.

The model has been "calibrated" or tuned to comply with these natural conditions.

4.4 Sediment Parameters

A mean grain diameter of 0.15 mm was found in Test Area 1 and has also been used here. The sediment transport rate is in the order of 1.0×10^{-3} m^3/s per meter width with a mean velocity of 2 m/s. The fall velocity of grains is 0.02 m/s.

The van Rijn model for bed load and suspended load has been applied because the model performed well for Test Area 1 and 2, see Annex 1 to the Draft Final Report, "Analysis of Sediment Data".

5. RESULTS

The hydrodynamic model and the sediment transport model have been used separately in the first simulations. The velocity field for the equilibrium situation is shown in Figure 5.1. The corresponding sediment transport rate has been plotted in Figure 5.2. The two models have been combined into the morphological model where the bed level is updated continuously. This model has been used to

- estimate the equilibrium bathymetry
- analyse the effect of displacing sediment from one branch to another
- analyse the effect of changing flow direction at the bifurcation point

5.1 Equilibrium

Initially, the model was run with a horizontal bed level in the whole region in order to see whether erosion and deposition would take place at the right places. The simulated bathymetry after 8 days is shown in Figure 5.3. At cross section k=3 (see Figure 4.1), heavy confluence scour has taken place. At k=12, at the end of the long bends, bend scour is observed close to the outer banks and at k=35, just after the bifurcation point, bend scour has taken place on both sides of the char. The helical flow has changed direction in the middle of the model at k=23 although it is not fully developed. Based on these results, it is concluded that the model represents prototype dynamic conditions.

The equilibrium bathymetry takes a very long time to simulate. Instead, it has been estimated and tested in the model by simulating changes in bed level. By trial and error the bathymetry shown in Figure 5.4 was found. The mean bed level in the left and the right anabranch, respectively, along the thalweg has been calculated and is shown in Figure 5.5 and 5.6 at different times. The horizontal axis denotes the cross section k. Upstream of the bifurcation point ($k > 37$) and downstream of the confluence point ($k < 9$), the main branch has been split into two parts (in a left and a right part) in the symmetry line in the calculation of the mean bed level (the vertical axis). Four figures are shown: Mean bed level at time=0, 20, 40 and 80 days. Figure 5.5 and 5.6 shows that the bed level is more or less in equilibrium. At the confluence point (k=9) the bed level is 10.4 m and at the bifurcation point the bed level is 11.5 m. The variation in bed level along the thalwegs is caused by variation in width and by the slope of the water surface.

5.2 Moving Sediment From One Branch To Another

By dredging in one channel and filling up in another, it may be possible to create an enhancement effect with initiation of increased erosion in the first channel and accretion in the second.

With a big dredger with capacity 3,000 m^3/h working 8 h/day, it is possible during 1-2 months in the dry season to move about 1 million m^3 of sediment from one side of the char to another. Figure 5.7 and 5.8

show the areas where dredging is assumed and where dumping is taken place. Each computational cell is about 50m x 190m and the total volume moved is 71m x 50m x 190m = 675,000 m^3.

A simulation (G4) has been made with this new bathymetry and compared with the previous one in equilibrium (G3). In the right channel, there is a large bulk of sediment from section k=27 to 39 at the beginning of the simulation. Already, during the first 20 days large changes have taken place and the sediment has been moving downstream, see Figure 5.9. It seems to reach a stable bedlevel after 80 days where only a small part of the extra sediment has actually stayed in the channel, i.e. the mean bed level has not changed significantly. Figure 5.10 shows the changes in the left anabranch. The dredged hole with the deepest part at section 35 is migrating downstream also. Apart from the other channel, however, the bed level remains the same at the dredged spot. Eventually, after 80 days where the bedlevel seems to be stable, it has been lowered by about 1.5 m. The length of the anabranches is about 4 km. Thus the speed by which the changes of bedforms migrate is about 4000/80 = 50 m/day. This seems to be a fairly high value but not extraordinarily so when compared with the observed changes in Test Areas 1 and 2. Figure 5.11 shows the simulated bathymetry.

Then, does the dredging enhance erosion in the left channel and deposition in the right? In Figure 5.12 the discharge in the left and right anabranch is plotted as a function of time. The variation in time is caused by changes in the bedlevel and not by unsteadiness of the flow. The total discharge is 6,000 m^3/s and from the beginning there is a difference of 900 m^3/s. This difference increases to about 1,300 m^3/s after 80 days. The graph also reveals that a new equilibrium has still not been reached although the rate of change in discharge in each channel is decreasing. It is easily seen, however, that dredging has a catalytic effect.

5.3 Effect of Changing Flow Direction

In Figure 5.13 a new planform geometry is shown. The approach channel is curving at the bifurcation point and the flow at the upstream boundary has been concentrated more on the right side (at the outer bank of the bend). A calculation was performed to see how sensitive the bathymetry would be to such changes. A simulation (G5) was made and compared with the first simulation of equilibrium (G3), and the simulation with dredging (G4). Figure 5.14 shows the bathymetry after 80 days and in Figure 5.15 and 5.16 the longitudinal profiles of mean bed level at different times are shown. The changes in bathymetry are dramatic. The right anabranch silts up by 1-2 m and the left anabranch is eroded by about 1-2 m so that the total difference between the left and the right channel is about 3 m in mean bed level. The velocity after 80 days is shown in Figure 5.17. The angle at the bifurcation point is about 10 degrees from the symmetry line. Figures 5.15 to 5.17 indicate how the main thalweg will meander. It enters at the right bank, goes down the left anabranch and leaves again at the right bank.

In Figure 5.18 the difference in discharge through the left and the right channel is shown as a function of time. Initially, when the bathymetry has still not adapted to the new flow conditions, the discharge is almost equally distributed. It is a little higher in the right channel because the flow distribution at the upper boundary is

towards the right side. But this changes rapidly and after 25-30 days, the distribution of discharge is like the previous simulation. After 80 days, some equilibrium seems to have been reached when the discharge in the right channel is only 1200 m^3/s and the discharge in the left channel is 4800 m^3/s.

6. CONCLUSION

An equilibrium bathymetry was estimated and verified by simulating changes over 80 days. It has been shown that dredging can enhance the development of erosion in one channel and accretion in another. Changes in bathymetry happen quickly .When the discharge is plotted against time it is seen that the difference between the two channels gradually increases to a ratio 39:61 after 80 days. The migration speed of the change in bathymetry was found to be in the order of 50 m/day. The difference in mean bedlevel between the two channels was about 1.5 m.

A third simulation was run where the inflow conditions were changed instead. Compared to the previous run, the changes were much larger. The discharge distribution between the two channels went from 50%/50% to 19%/81%. The difference in mean depth between the left and the right channel was about 3 m.

The study has given some insight into morphological changes. Flow conditions change and then the bathymetry follows. It is much more difficult to change the bathymetry and "force" the flow conditions to change. Instead of dredging it seems more effective to try to change the upstream flow conditions and let the flow itself do the work.

7. REFERENCES

Coleman, James M - Sedimentary Geology, Volume 3, August 1969 no 2/3, 1985/126

Halcrow/DHI/EPC/DIG - River Training Studies of Brahmaputra River First Interim Report, Technical Annexes, Annex 3: Mathematical Modelling, April 1991

Halcrow/DHI/EPC/DIG - River Training Studies of Brahmaputra River First Interim Report, Technical Annexes, Annex 1: Data Collection and Analysis, April 1991

Halcrow/DHI/EPC/DIG - River Training Studies of Brahmaputra River Working Paper on 2-D Modelling, December 1990

Halcrow/DHI/EPC/DIG - River Training Studies of Brahmaputra River Second Interim Report, Technical Annexes, Annex 1: River Survey, December 1991

Halcrow/DHI/EPC/DIG - River Training Studies of Brahmaputra River Second Interim Report, Technical Annexes, Annex 2: Mathematical Modelling, December 1991

Halcrow/DHI/EPC/DIG - River Training Studies of Brahmaputra River Second Interim Report, Technical Annexes, Annex 3: Morphology, December 1991

Rendel, Palmer and Tritton/NEDECO/BCL - Jamuna Bridge Project, Phase II, Study Feasibility Report, Volume II, Annex B: River Morphology, August 1989

FIGURES

ANABRANCHES

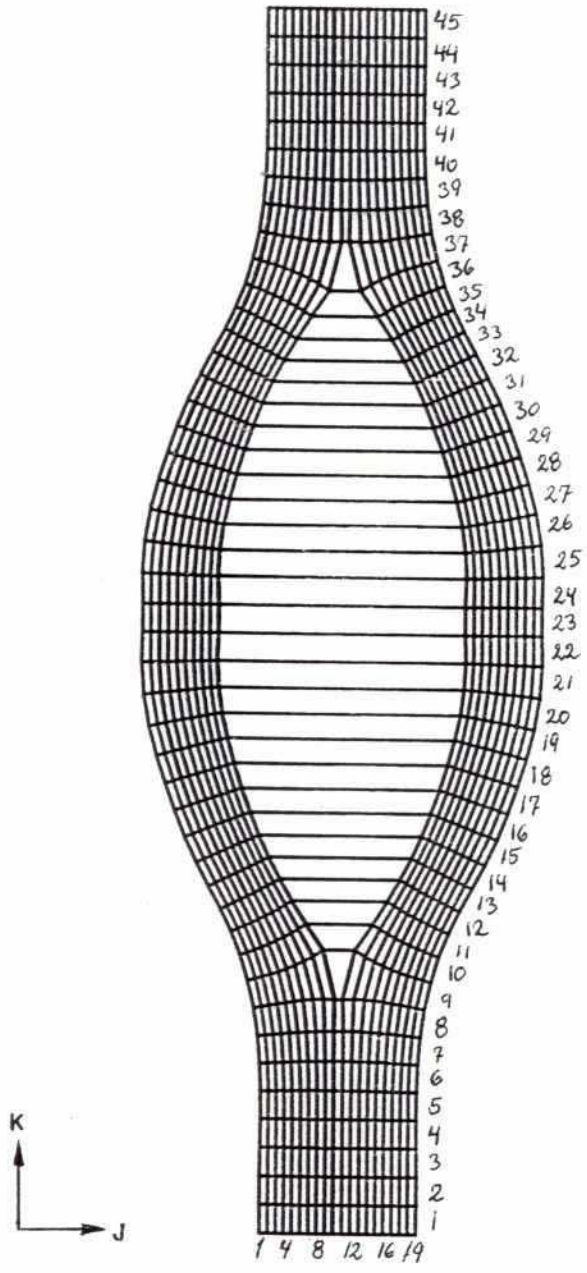

Scale 1 : 50,000

BRTS 2-D Numerical Modelling of Bifurcation and Anabranches

Model Geometry	Vol.4 Part 13
	Figure 4.1

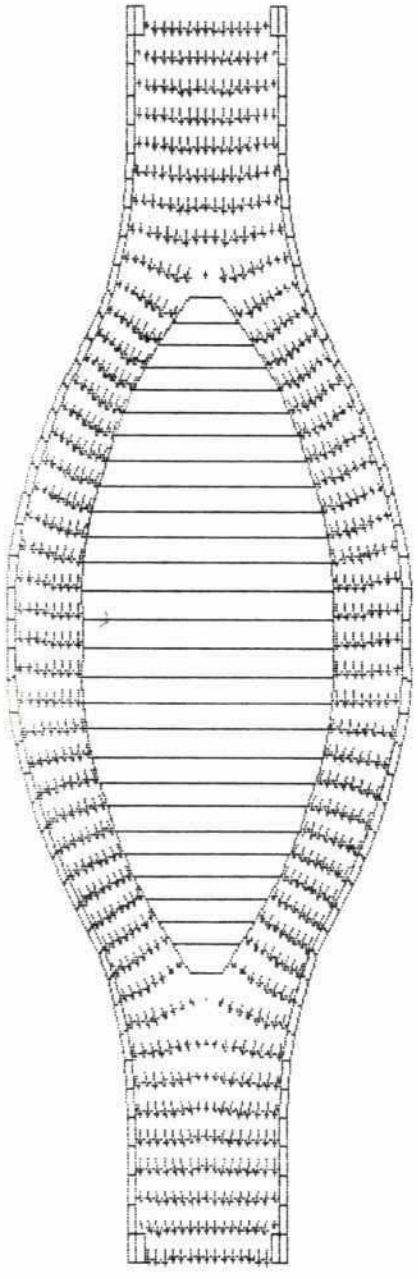

1 M/SEC

Scale 1 : 50,000

BRTS 2-D Numerical Modelling of Bifurcation and Anabranches

Simulated Velocity	Vol.4 Part 13
	Figure 5.1

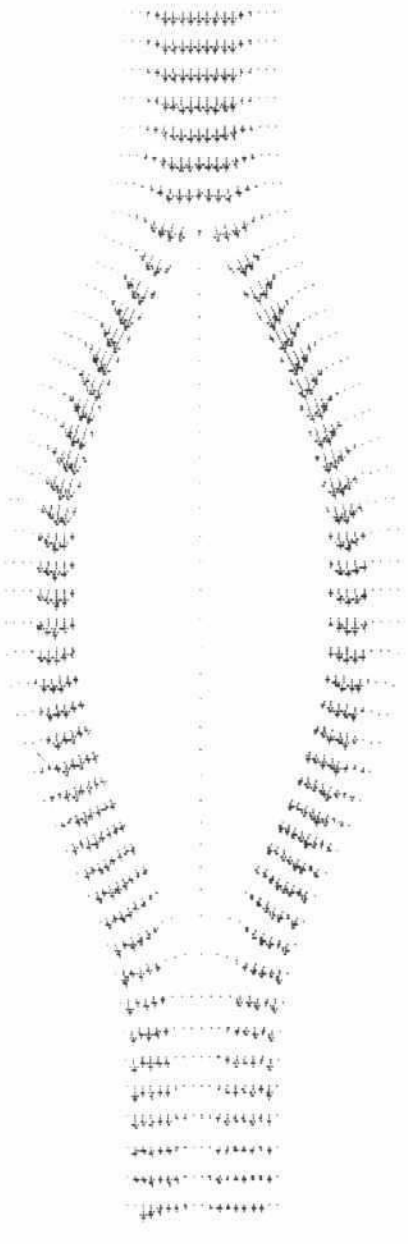

Scale 1 : 50,000

BRTS 2-D Numerical Modelling of Bifurcation and Anabranches

Simulated Sediment Transport Rate Per Unit Width	Vol.4 Part 13
	Figure 5.2

d1

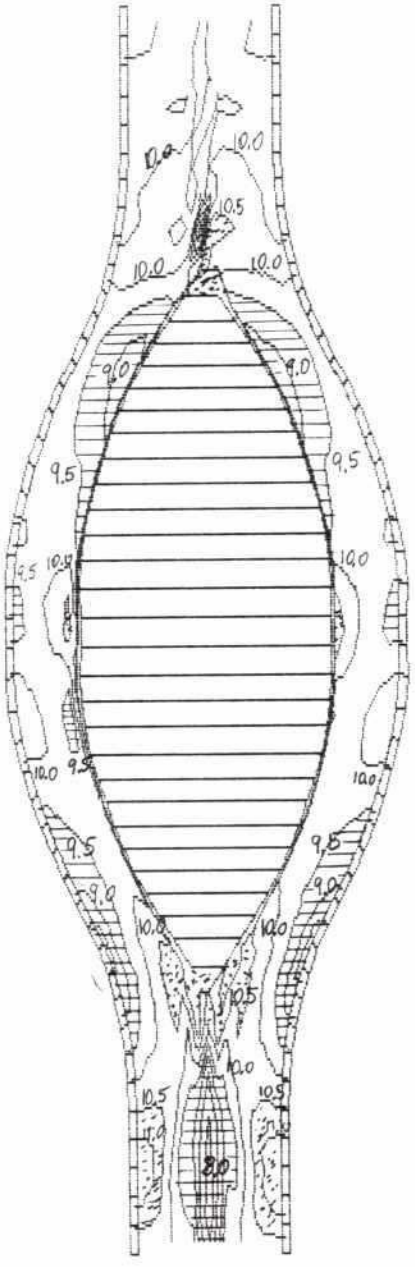

7.00 7.50 8.00 8.50 9.00 9.50 10.00 10.50

Scale 1 : 50,000

BRTS 2-D Numerical Modelling of Bifurcation and Anabranches

Simulated Bed Level After 8 Days with Initial Bed Level 10 m	Vol.4 Part 13
	Figure 5.3

93

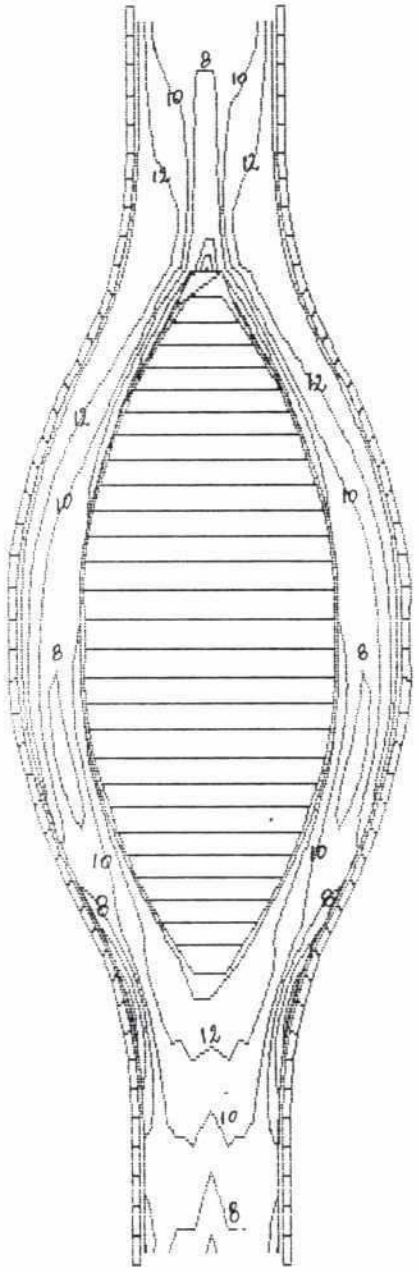

.0000 2.00 4.00 6.00 8.00 10.00 12.00

Scale 1 : 50,000

BRTS 2-D Numerical Modelling of Bifurcation and Anabranches

Simulated Bathymetry in Equilibrium	Vol.4 Part 13
	Figure 5.4

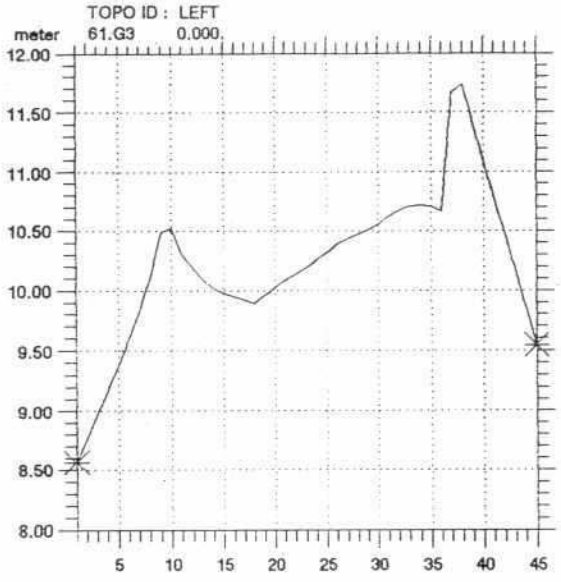

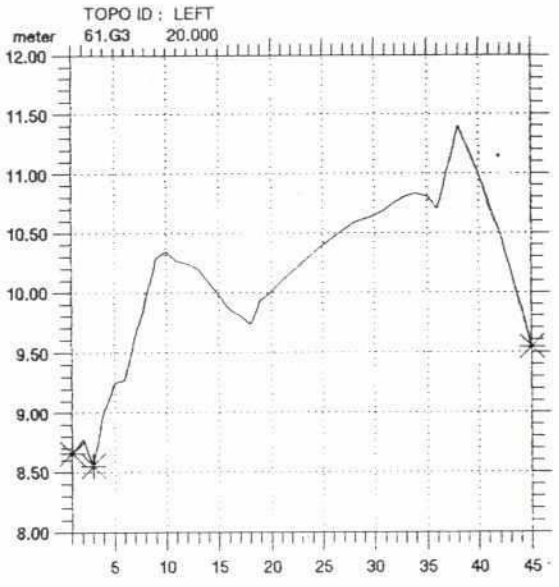

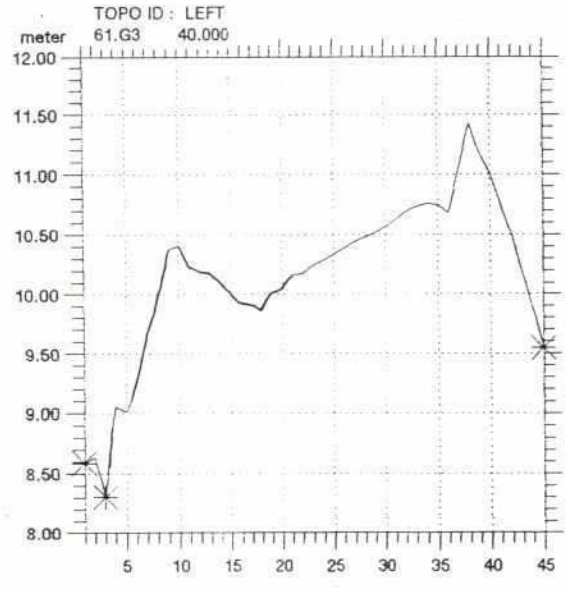

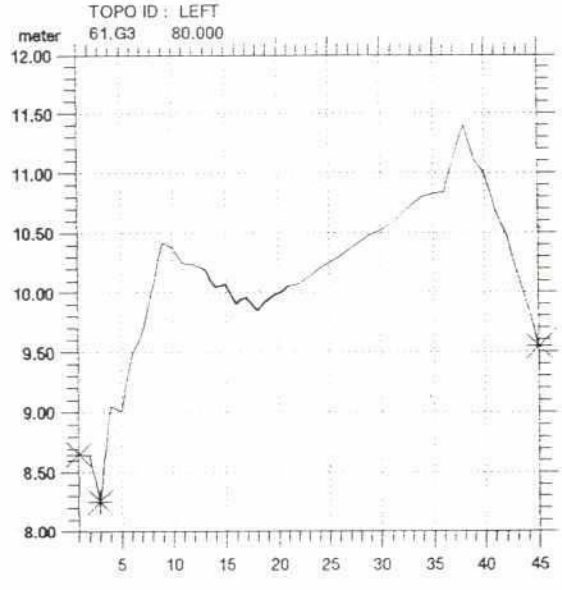

BRTS 2-D Numerical Modelling of Bifurcation and Anabranches

Mean Bed Level Along the Left (Eastern) Anabranch With Equilibrium Bathymetry After 0, 20, 40 and 80 Days	Vol.4 Part 13
	Figure 5.5

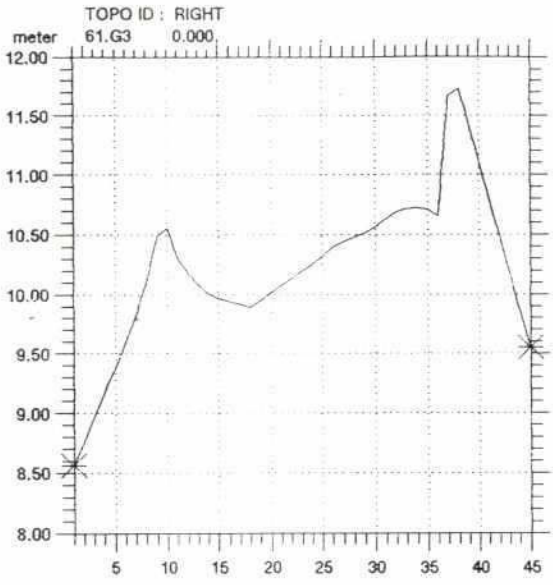

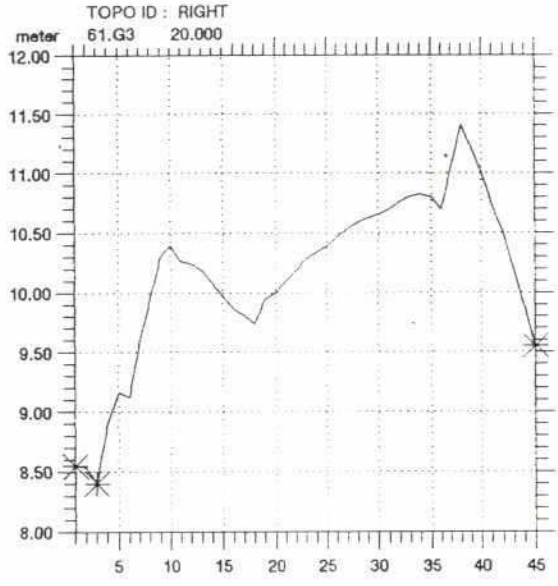

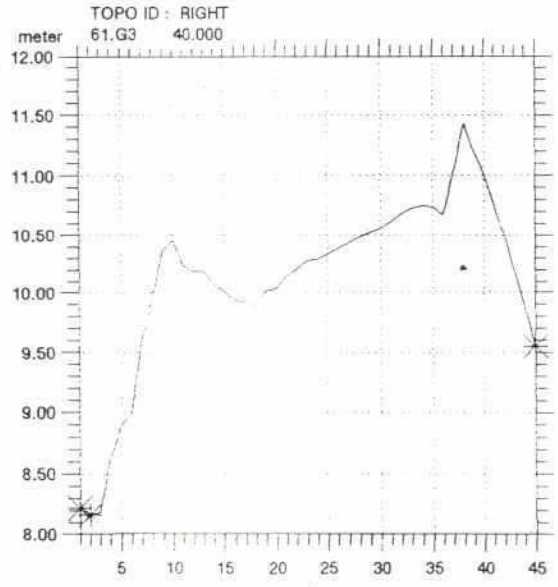

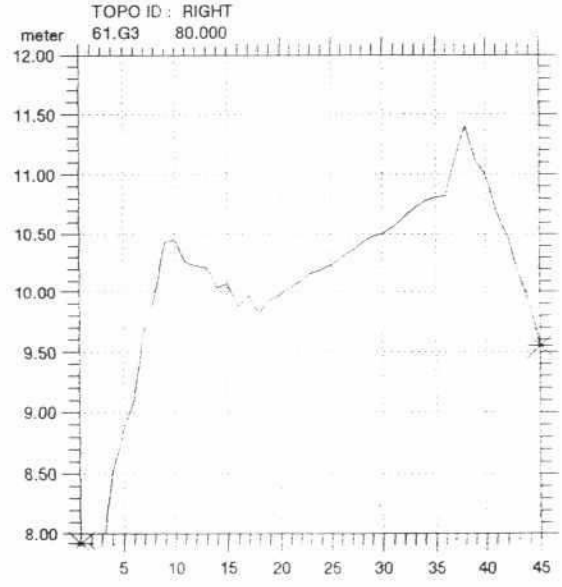

BRTS 2-D Numerical Modelling of Bifurcation and Anabranches

Mean Bed Level Along the Right Anabranch With Equilibrium Bathymetry After 0, 20, 40 and 80 Days	Vol.4 Part 13
	Figure 5.6

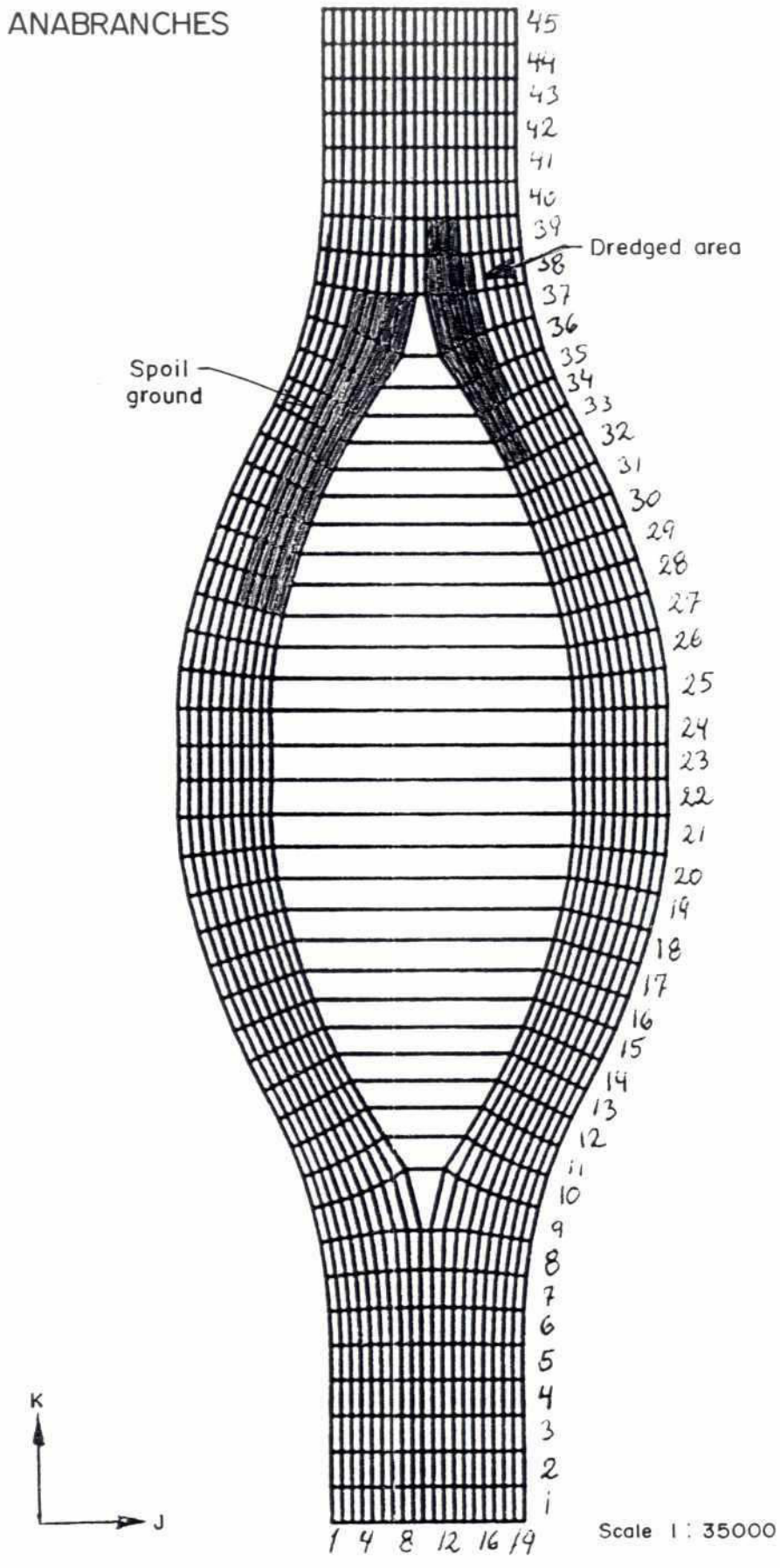

BRTS 2-D Numerical Modelling of Bifurcation and Anabranches

Location of Dredging and Spoil Ground

Vol.4 Part 13

Figure 5.7

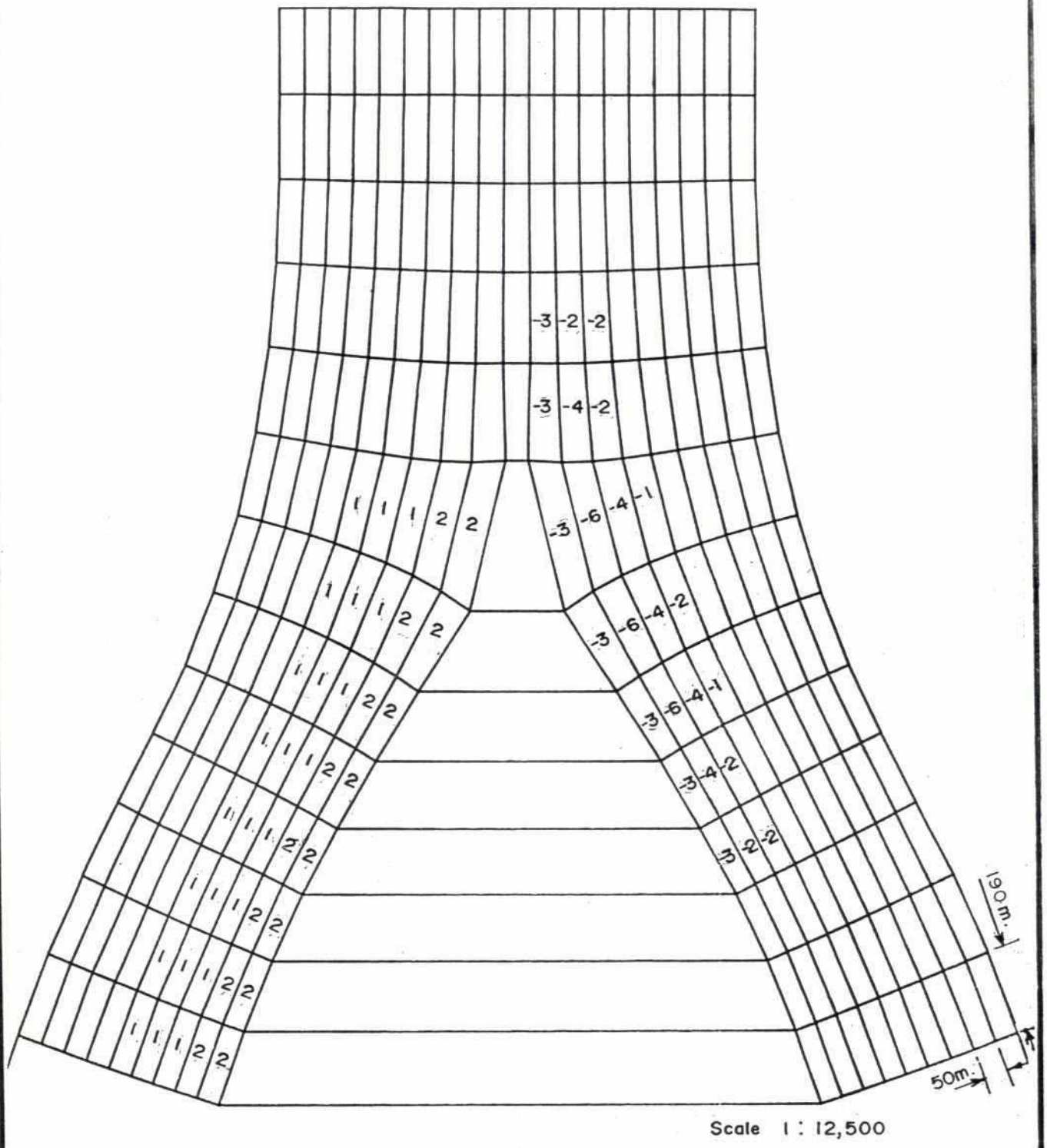

Scale 1 : 12,500

Note : Numbers represent depths in metres.

BRTS 2-D Numerical Modelling of Bifurcation and Anabranches

Definition of Dredging and Accretion in 50 x 190 m² Cells.	Vol.4 Part 13
	Figure 5.8

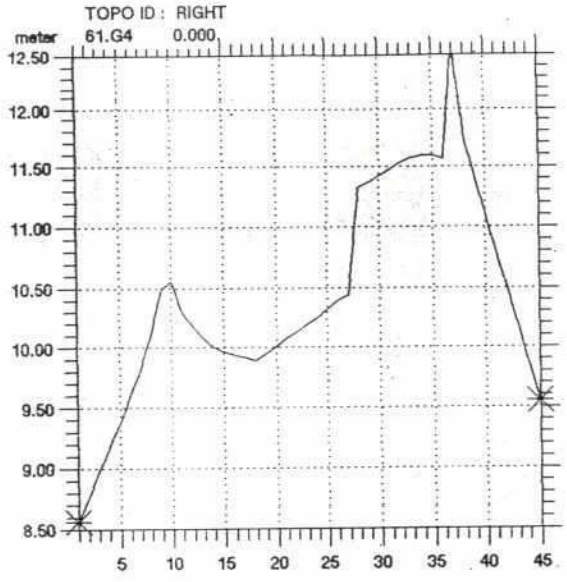

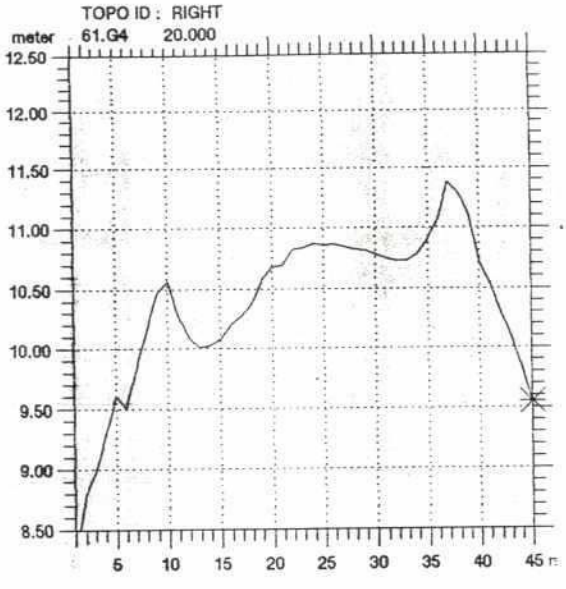

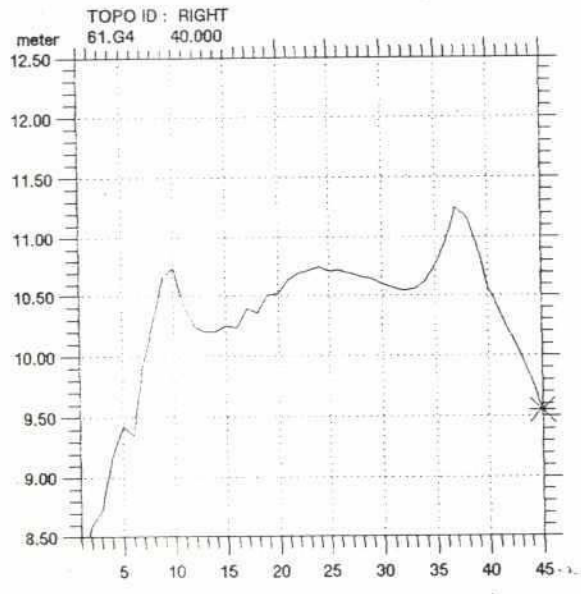

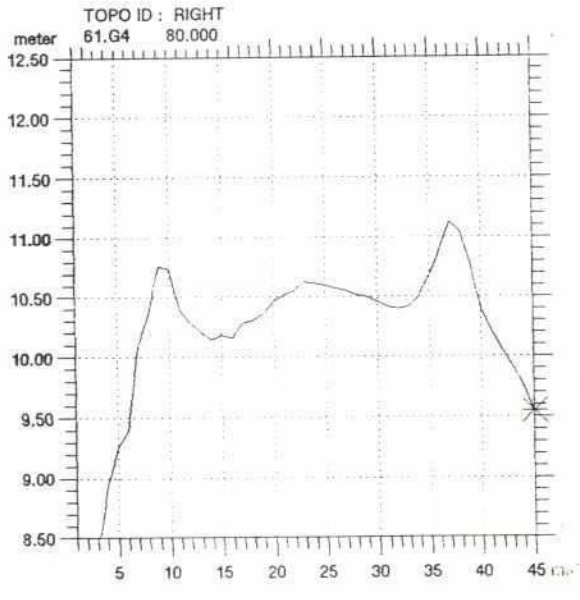

BRTS 2-D Numerical Modelling of Bifurcation and Anabranches

Mean Bed Level in Right Anabranch. Dredging Scenario	**Vol.4** **Part 13**
	Figure 5.9

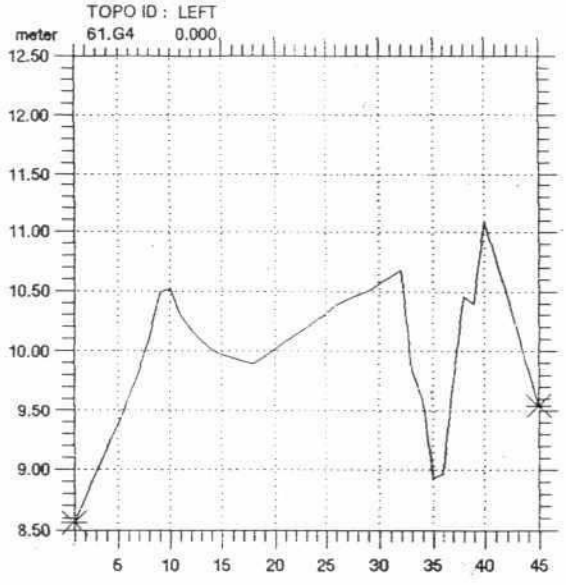
TOPO ID : LEFT
meter 61.G4 0.000
12.50
12.00
11.50
11.00
10.50
10.00
9.50
9.00
8.50
5 10 15 20 25 30 35 40 45

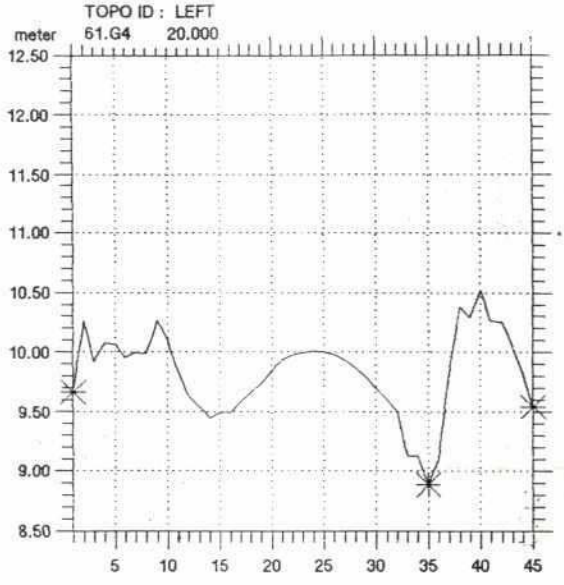
TOPO ID : LEFT
meter 61.G4 20.000
12.50
12.00
11.50
11.00
10.50
10.00
9.50
9.00
8.50
5 10 15 20 25 30 35 40 45

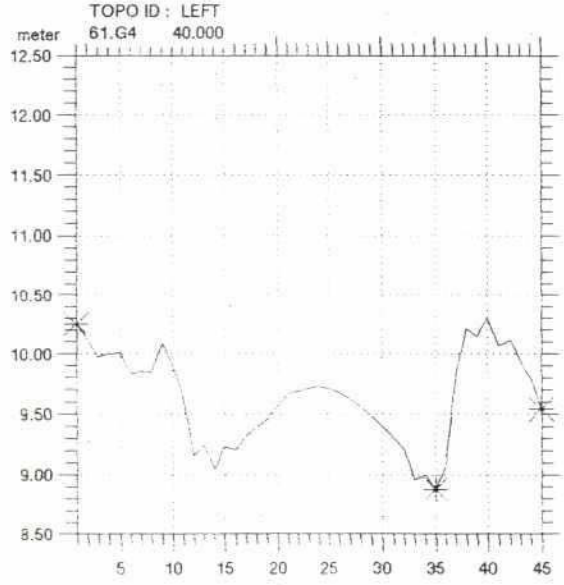
TOPO ID : LEFT
meter 61.G4 40.000
12.50
12.00
11.50
11.00
10.50
10.00
9.50
9.00
8.50
5 10 15 20 25 30 35 40 45

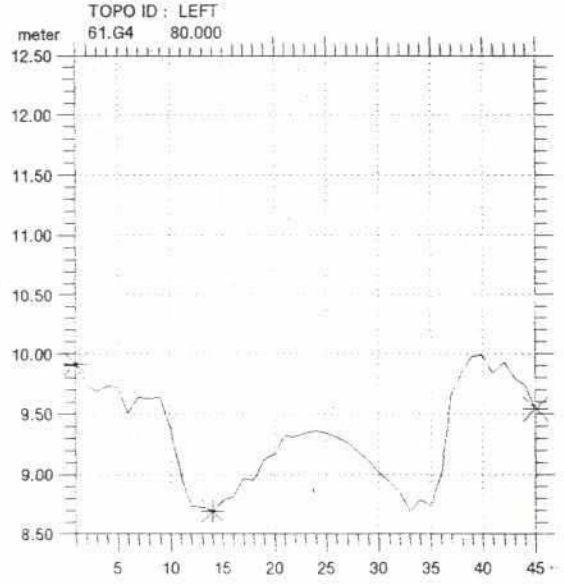
TOPO ID : LEFT
meter 61.G4 80.000
12.50
12.00
11.50
11.00
10.50
10.00
9.50
9.00
8.50
5 10 15 20 25 30 35 40 45

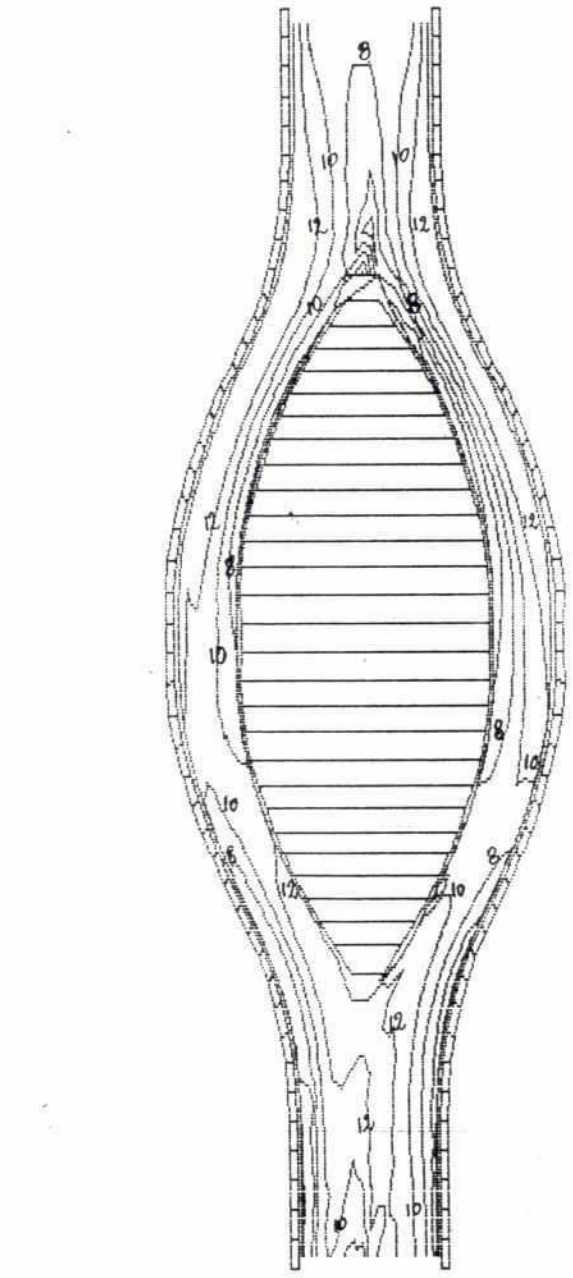

Scale 1: 50,000

BRTS 2-D Numerical Modelling of Bifurcation and Anabranches

Simulated Bathymetry in Dredging Scenario

Vol.4 Part 13

Figure 5.11

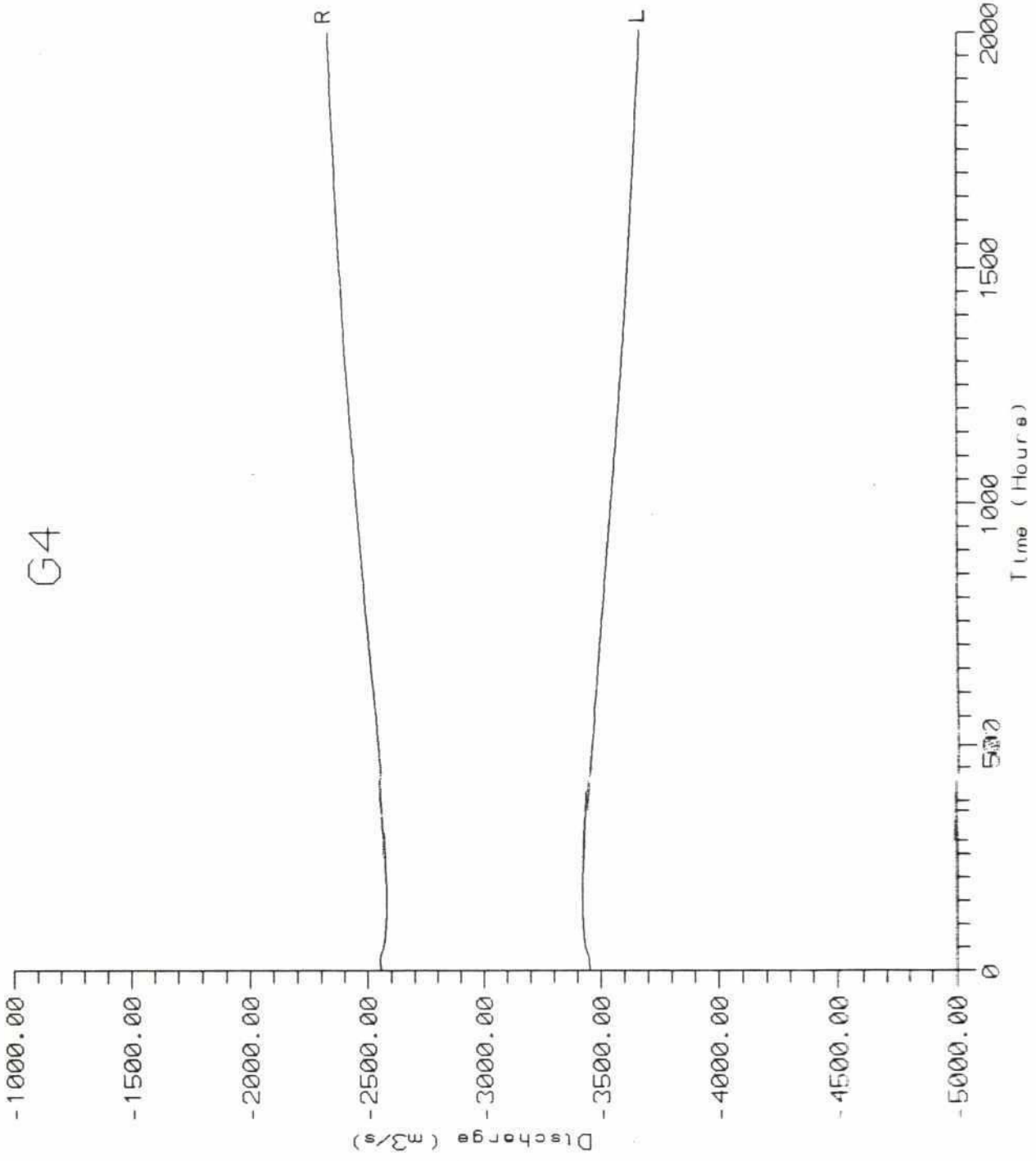

BRTS 2-D Numerical Modelling of Bifurcation and Anabranches

Simulated Discharge (Negative) in Left (L) and Right (R) Anabranch as a Function of Time. Dredging Scenario	Vol.4 Part 13
	Figure 5.12

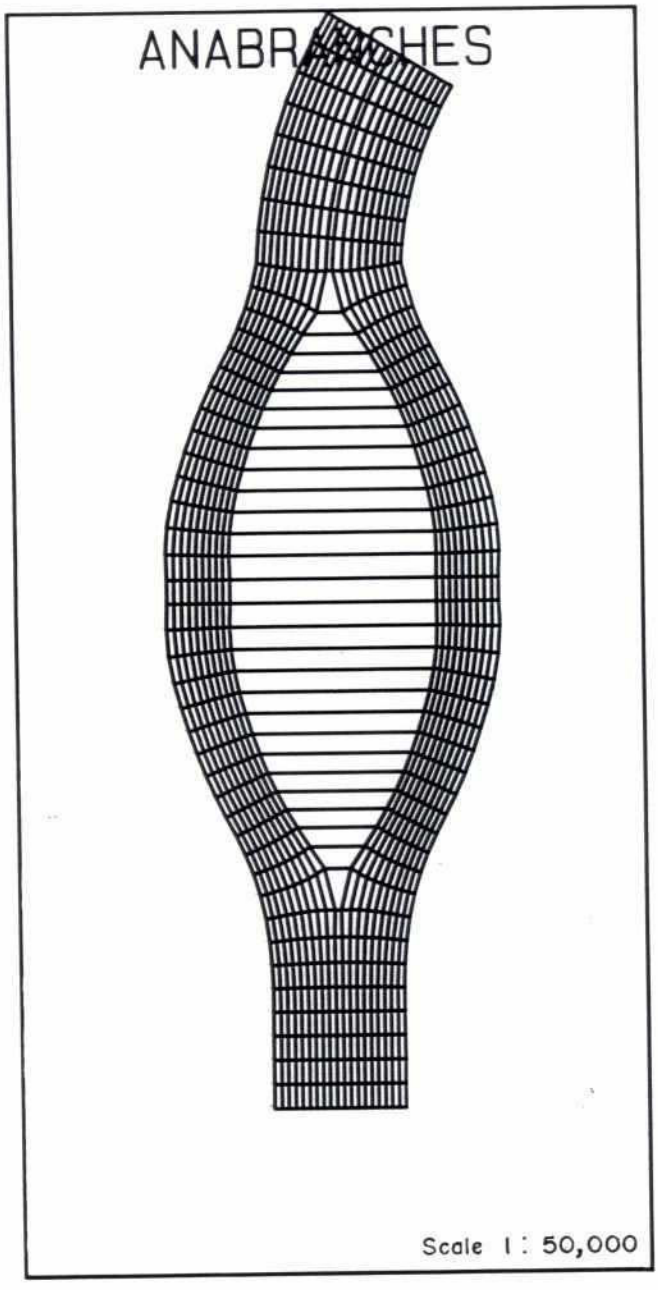

BRTS 2-D Numerical Modelling of Bifurcation and Anabranches

Model Set-Up for Curving Streamlines at Bifurcation Point	**Vol.4** **Part 13**
	Figure 5.13

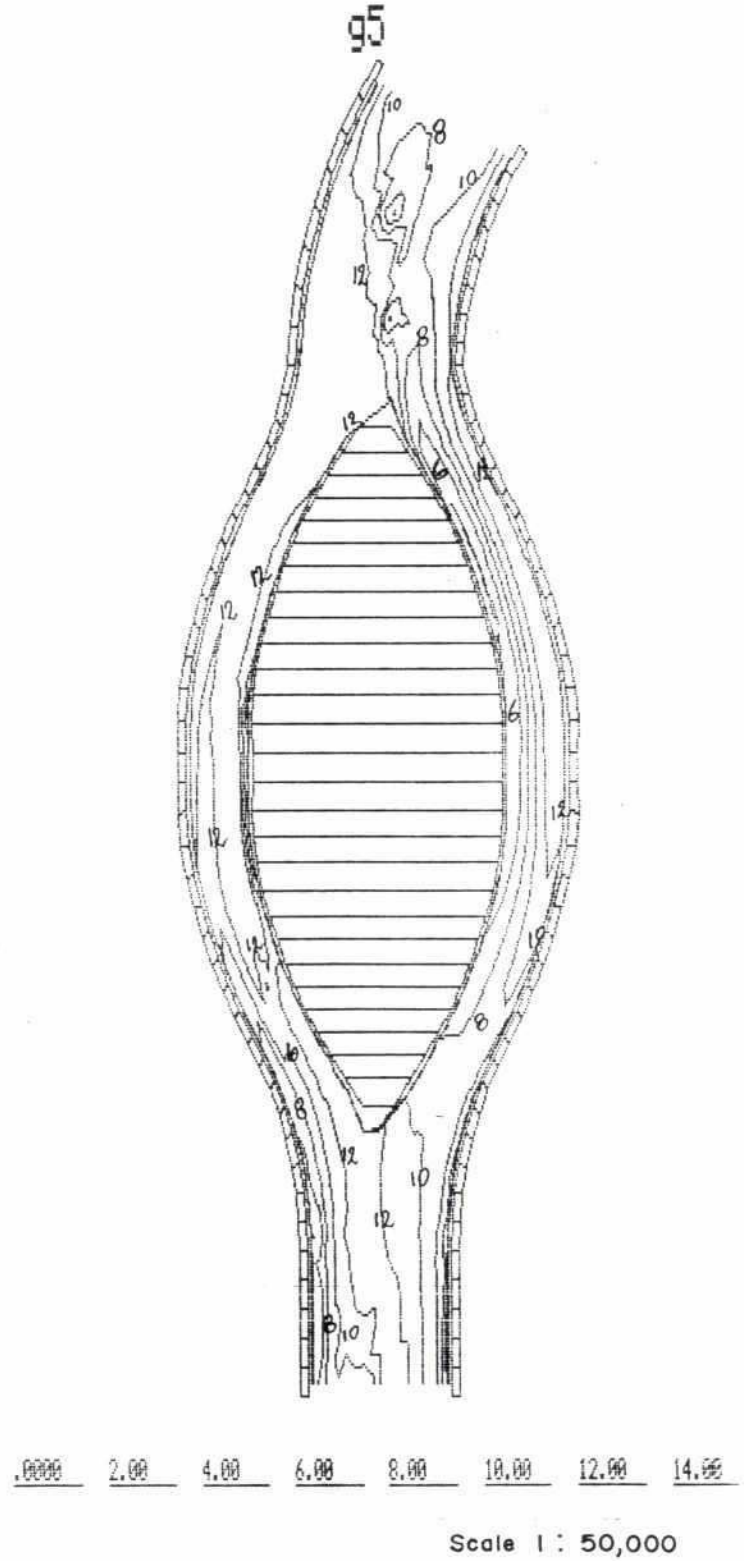

BRTS 2-D Numerical Modelling of Bifurcation and Anabranches

Simulated Bathymetry. Upstream Flow Scenario	Vol.4 Part 13
	Figure 5.14

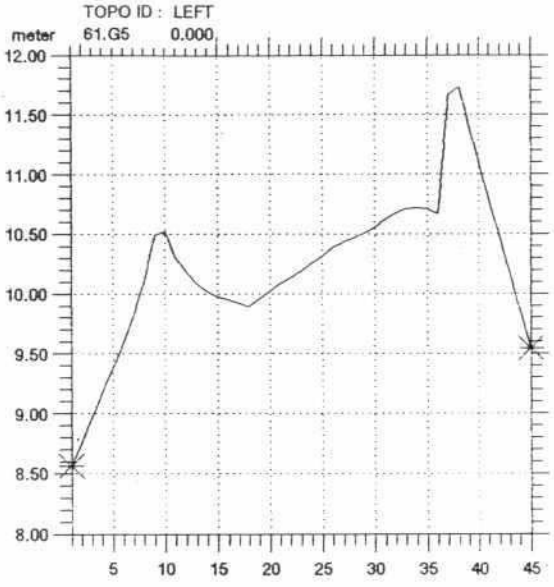

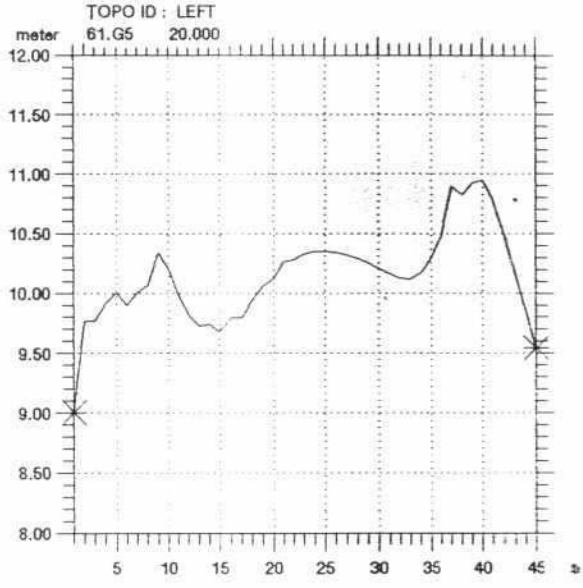

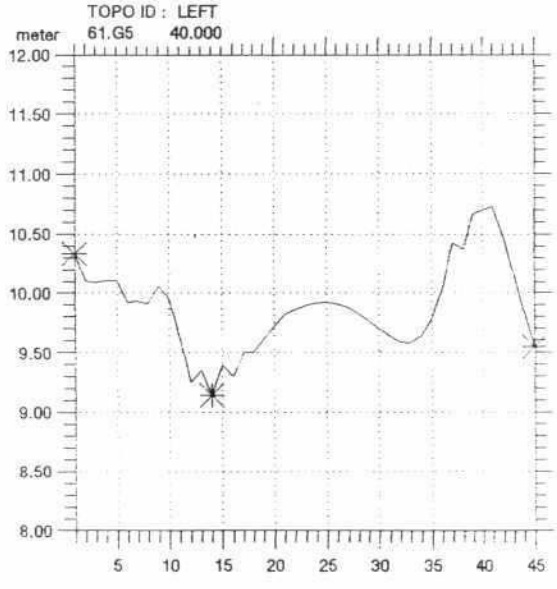

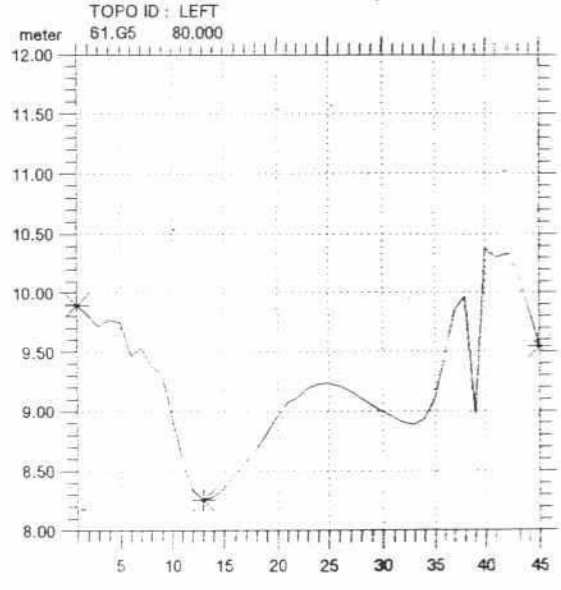

BRTS 2-D Numerical Modelling of Bifurcation and Anabranches

Mean Bed Level in Left Anabranch. Upstream Flow Scenario	**Vol.4** **Part 13**
	Figure 5.15

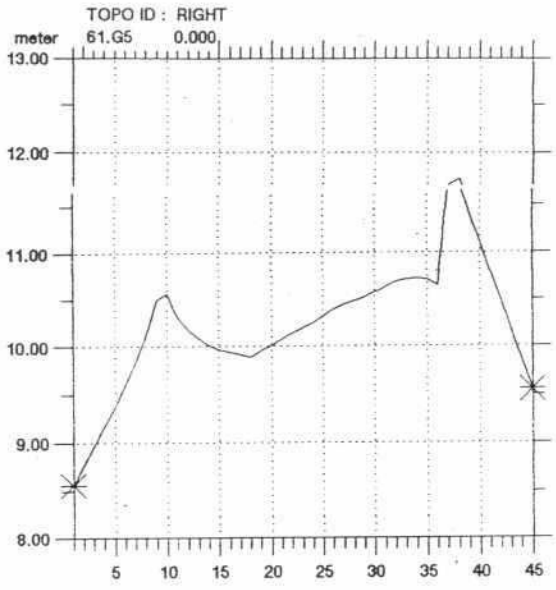

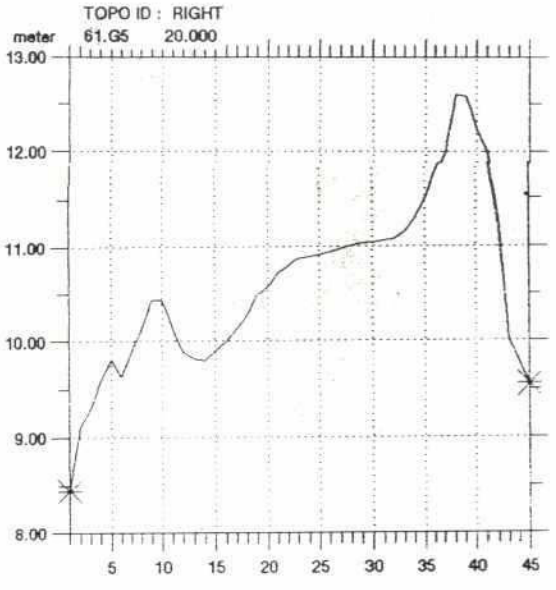

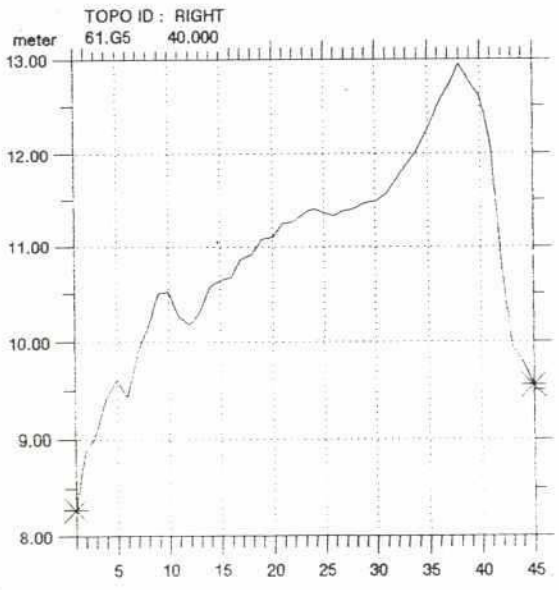

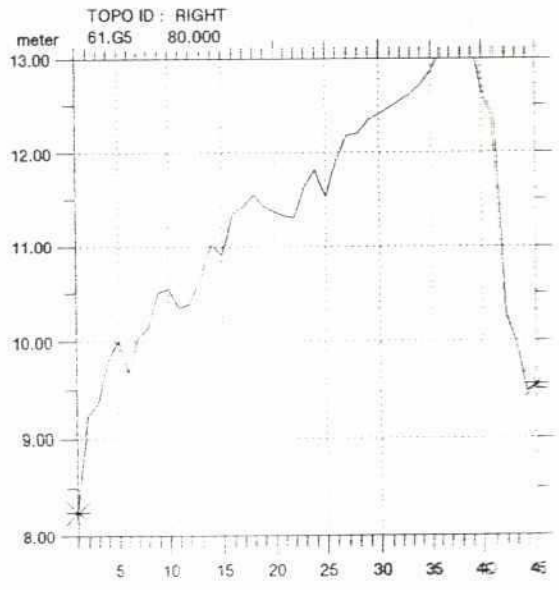

BRTS 2-D Numerical Modelling of Bifurcation and Anabranches

Mean Bed Level in Right Anabranch. Upstream Flow Scenario	**Vol.4** **Part 13**
	Figure 5.16

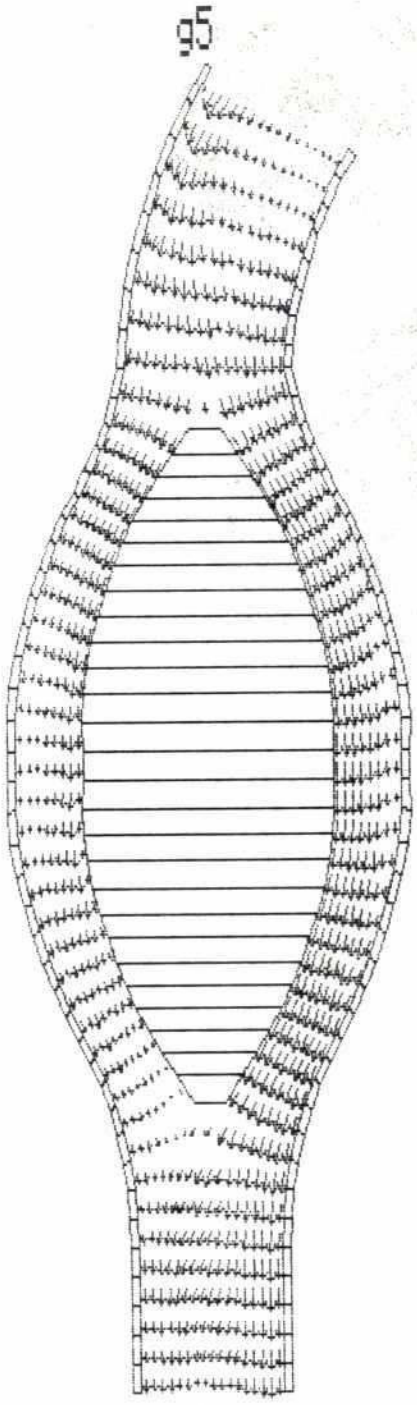

1 m/sec

Scale 1 : 50,000

BRTS 2-D Numerical Modelling of Bifurcation and Anabranches

Simulated Velocity. Upstream Flow Scenario

Vol.4 Part.13

Figure 5.17

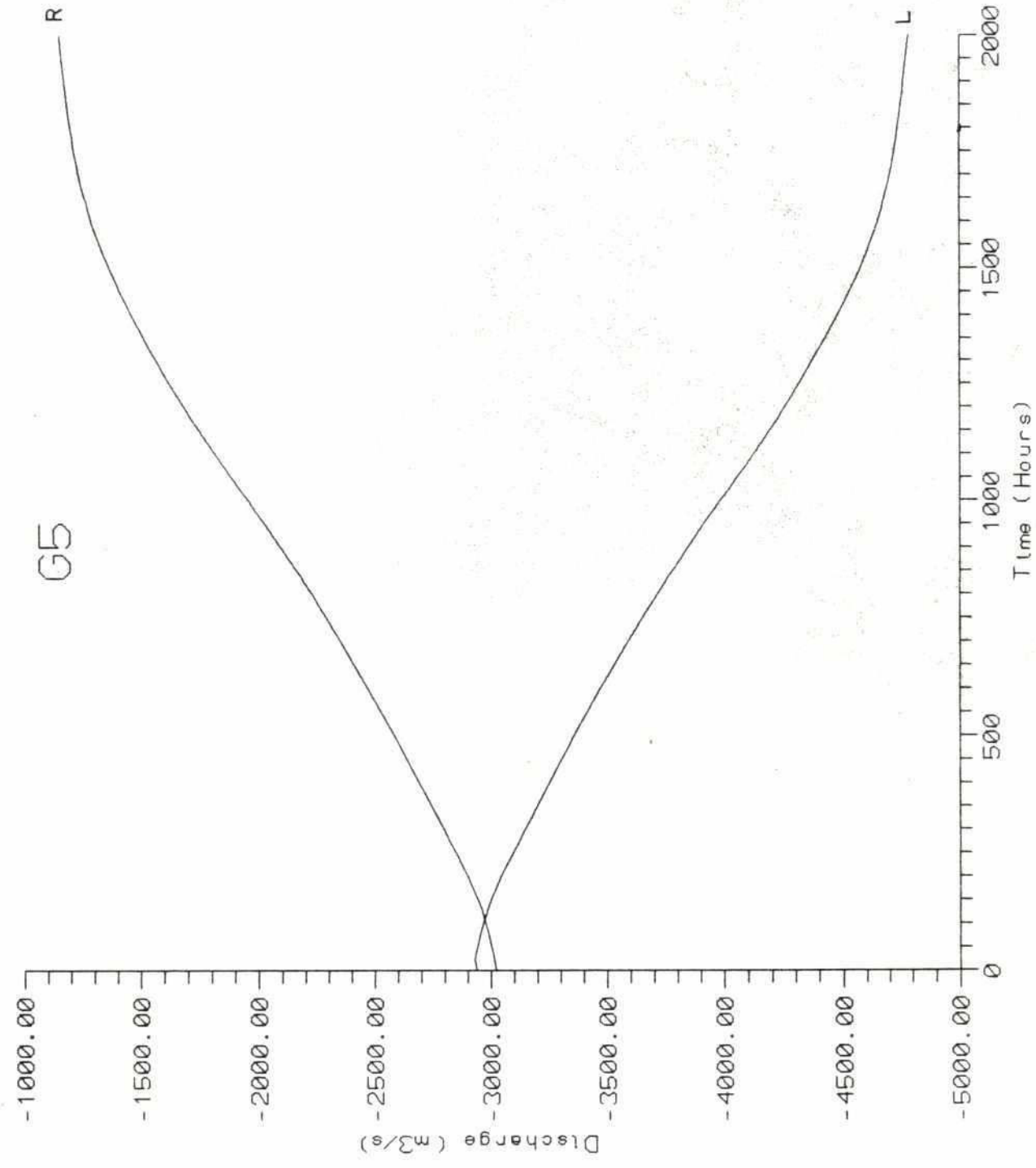

BRTS 2-D Numerical Modelling of Bifurcation and Anabranches

Simulated Discharge (Negative) in Left (L) and Right (R) Anabranch as a Function of Time, Upstream Flow Scenario ·	Vol.4	Part 13
	Figure 5.18	

Part 14

2-D Numerical Modelling of River Constriction Effects due to Jamuna Bridge Embankments

HALCROW

RIVER TRAINING STUDIES OF THE BRAHMAPUTRA RIVER

REPORT ON MODEL STUDIES

PART 14 - 2-D NUMERICAL MODELLING OF RIVER CONSTRICTION EFFECTS DUE TO JAMUNA BRIDGE EMBANKMENTS

CONTENTS

TABLES

FIGURES

1. INTRODUCTION

1.1 Background

The BRTS Terms of Reference require the Consultant to consider the consequences of intervention, including the construction of the Jamuna Bridge, on the conditions along the right bank of the river. Discussion with the JMB Authority and their Consultants revealed that a final decision on the length of the bridge had not been made but that the minimum width between abutments being considered was 4,600 m and this might be increased by 10 percent or more.

The local constriction of the river in this way also represents one form of node stabilisation that might be undertaken as a part of a major river training programme. The principle is therefore of relevance to the master plan study irrespective of the final decision with regard to the bridge.

1.2 Objective

The objective of the 2-D model study was to investigate, in more detail than could be achieved with the 1-D model, how the water levels between the bridge and Sirajganj would be affected by different degrees of constriction such as might be imposed by the construction of approach embankments for the Jamuna Bridge or a major river node stabilisation. The morphological sub-models allow the hydrodynamic conditions to be simulated both immediately following construction and after the river bed has adjusted to the new situation.

1.3 Approach

For convenience, the Jamuna Bridge was taken as a representative example in order to assess the relationship between water level rise and the degree of constriction. Three different distances between bridge abutments were simulated: 5,600, 4,600 and 3,600 m. Since the actual bed conditions at the time of construction cannot be predicted, in each case the starting bed topography was taken to be that of July 1990, for which good survey data are available from BRTS river survey programme. This year is appropriate for the purpose as it is representative of a typical hydrological year.

To simulate a complete hydrological time series would have involved computer run time that was incompatible with the study time scale. The approach adopted, therefore, was first to run the model with a fixed bed and a steady discharge of 102,250 m^3/s, representing the peak flow of an event of approximately 100 year return period, in order to assess the maximum water level rise that could occur should such an event follow immediately after the construction of the constriction.

The bed morphology was then adjusted, to take into account the new flow conditions after completion of the constriction, by running both hydrodynamic and morphological elements of the model for a discharge of 38,000 m^3/s, representing the river's dominant discharge. Since it is the dominant discharge that is responsible for the majority of sediment transport over a period of time, and the discharge to which the river channel morphology is adjusted, the bed morphology attained in this way

may be considered representative of average conditions.

The third step was to rerun the model with the adjusted bed morphology but with the 100 year discharge. This simulates the water level surface that may be expected to arise with the passage of the design flood after the river bed has settled down to the new regime.

The procedure was then repeated for the other two constriction widths.

1.4 Description of the Model

The hydrographic survey and 2-D modelling of Test Area 1 was described in the First Interim Report. The location of the proposed Jamuna Bridge is covered within this Test Area. Hence the calibrated 2-D model from Test Area 1 was used for the study.

In order to improve the performance of the model when the Jamuna Bridge guide bunds are included, some modifications of the original Test Area 1 model have been implemented:

- The northern boundary of the model area has been moved further to the north in order to allow the inflow of water to adapt to the changed bathymetry with the bridge included. The influence of inaccuracies in boundary conditions was thereby reduced.

- The top of the sand bar at the southern boundary of Test Area 1 has been defined as the water level at dominant discharge.

This is consistent with maps of from the morphological studies and improves model stability.

When the water levels were simulated with the bridge guide bunds introduced in the model area, the following assumptions applied:

- The tender drawings (RPT/NEDECO/BCL 1990) show that extensive bank protection works will be constructed at the abutments on each side. These were represented by changing the land boundaries in the model area.

- The back water effect of the bridge piers in the middle of the river is small compared to the influence of the major abutments. Hence the bridge piers were neglected in this analysis.

- The bathymetry is changing and the bank lines are shifting continuously. The banklines used for this simulation approximate to the July 1990 banklines, as shown in Figure 1.1.

- The bridge guide bunds were in each case placed symmetrically around the river centerline.

- During the 100 year return period peak flow, the flood plains adjacent to the river will be inundated. These were not included in the Test Area 1 model and were not included in this model either. The significance of the flood plains on

water levels and sediment transport will be relatively small and may be assessed qualitatively.

1.5 Boundary Conditions

For each scenario, two different flow events have been simulated: the dominant discharge (with respect to morphological changes) and the maximum discharge from a 100 year return period event. The derivation of the two discharges is set out in the BRTS Second Interim Report. The corresponding water levels at the downstream boundary have been found by simulating the events with the calibrated MIKE 11 1-D model. The discharge of water into the model at the upper boundary has been distributed over the width of the river by relating the flux to the depth according to Manning's resistance formula:

$$P = \text{constant} \times h^{5/3}$$

where p is flux (discharge per unit width) and h is the local depth.

The water level at the southern boundary was assumed to be constant over the whole width of the river. Some sensitivity runs to test this assumption were carried out.

The boundary conditions for the two design events are shown in Table 1.1.

Table 1.1: Applied Boundary Conditions

	Dominant Discharge	100 Year Discharge
DISCHARGE UPSTREAM Sirajganj	38,000 m^3/s	102,250 m^3/s
WATER LEVEL DOWNSTREAM Shahapur	12.50 m	13.78 m

The bed resistance was taken as the same as that found from calibration of the model on Test Area 1:

$$C = 74 \times (h/h_o)^{0.25} \quad m^{1/2}/s$$

where C is the Chezy Number, h is the local depth and h_o is the overall mean depth.

In reality, the depth will change from one scenario to another and thus the spatial distribution of C will vary, although the mean value will be the same. The effect of updating the Chezy Number with the morphological changes was checked and it was concluded that in this case a constant Chezy Number could legitimately be used

For sediment transport, the van Rijn model was applied using a mean

sediment grain size of 0.15 mm, and a fall velocity of 2 cm/s, as determined during the calibration of the Test Area 1 model (see the BRTS First Interim Report).

2. THE RESULTS OF THE SIMULATIONS

Two sets of model runs were carried out: 100 years discharge with fixed bed and both dominant and 100 year discharge with dynamic morphology. See Tables 2.1 and 2.2.

In the latter case the simulations were continued until equilibrium was reached.

Table 2.1: Simulations of Water Levels with 100 year Discharge.

BRIDGE SPAN m BATHYMETRY	5,600 model run	4,600 reference	3,600
Initial Bathymetry	1	4	7
Modified by dominant Discharge	2	5	8
Modified by 1 in 100 year Discharge	3	6	9

Table 2.2: Bed Levels with Dominant and 100 Year Discharge

BRIDGE SPAN (m) FLOW CONDITIONS	5,600 model run	4,600 reference	3,600
Dominant Discharge	10	12	14
100 Year Discharge	11	13	15

The initial bathymetry was used in simulations 1, 4 and 7 to assess the immediate impact of the bridge. The simulated bathymetry from 10 was used in 2, from 12 in 5, from 14 in 8 and so on. Simulations 2, 5 and 8 show the effect of the bridge after the bathymetry has been eroded by the dominant discharge. Runs 3, 6 and 9 produce the water levels after the bathymetry has been shaped by the 100-year discharge.

The computational grid is depicted in Figure 2 and the initial bathymetry in Figure 2.2.

Scour

Figure 2.3 shows an example of the simulated erosion pattern (run 13), also the area in which mean and maximum depth have been measured, as shown in Tables 2.3 and 2.4. For the initial bathymetry the mean bed level was 6.79 m. The real time simulation period differs between the simulations with dominant discharge and simulations with 100 year discharge, as shown in Table 2.5.

The sediment transport is about 20 times larger in the simulation with the 100 year discharge than in the simulation with dominant discharge. Thus the time before equilibrium is reached will decrease correspondingly provided that the boundary conditions are fixed.

Table 2.3: Minimum Bed Level in Meters inside the Area Shown in Figure 2.3

BRIDGE SPAN FLOW CONDITIONS	5,600	4,600	3,600
Dominant Discharge	0.81	-4.67	-5.41
1 in 100 year Discharge	0.32	-4.95	-7.27

Table 2.4: Mean Bed Level in Meters

BRIDGE SPAN FLOW CONDITIONS	5,600	4,600	3,600
Dominant Discharge	6.55	6.16	5.49
1 in 100 year Discharge	6.04	5.11	3.65

Table 2.5: Simulation Time in Days

BRIDGE SPAN CONDITIONS [m]	5,600	4,600	3,600
Dominant Discharge (days)	100	100	100
1 in 100 year Discharge (days)	13	13	14

The results can be verified by use of a simplified formula to estimate the increase in depth when the width is reduced. It is derived from the equation of continuity of water and sediment:

$$Z = h_1 . (1-(W_1/W_2)^{1-1/b})$$

where h_1 is the mean depth at cross-section 1, (6.5 m for dominant discharge, 7.8 m for 100 year discharge)

W_1 is the width at cross-section 1,

W_2 the width at cross-section 2, Z the difference in depth (and

bed level) between cross-section 1 and 2,

and b is the exponential power (between 3 and 5) in the simplified sediment transport equation $S = a \times u^b$.

By using h_1 = 7.8 m, W_1 = 4,600 m, W_2 = 3,600 m, b = 3.5 one finds Z = 1.48 m.

This agrees well with the simulated value, Z = 5.11 - 3.65 = 1.46 m.

Water Levels

The water levels were simulated by using the 100 year discharge. Figure 2.4 shows the simulated water level in run 4 using the initial bathymetry. In the north west corner the slope of the water surface is very high across the river, which causes considerable differences in water level between the right and the left bank. This is mainly due to the strong current combined with the high curvature of the streamlines in this corner, as illustrated in Figure 2.5, which is a plot of the velocity vectors. When the adjusted bathymetries were used instead, the simulations showed this large super-elevation in water level due to centrifugal effects decreased.

This shows that substantial super-elevation can occur under adverse combinations of bed morphology and high discharge but that it will reduce with time.

Table 2.6 contains the simulated water levels at five representative locations, as shown in Figure 2.4.

Table 2.6: Simulated Water Levels in Meters above PWD Datum

BRIDGE SPAN (m) BATHYMETRY	Location	5600	4600	3600	Description
Fixed Initial Bathymetry	A	15.62	16.04	16.65	Sirajganj
	B	15.29	16.07	16.59	Bridge, RB
	C	14.75	14.78	15.19	Shahapur
	D	14.90	15.05	15.91	Bhuapur
	E	14.82	14.98	16.02	Bridge, LB
Modified by Dominant Discharge	A	15.41	15.56	15.92	Sirajganj
	B	15.24	15.52	15.90	Bridge, RB
	C	14.69	14.78	15.05	Shahapur
	D	14.90	15.02	15.51	Bhuapur
	E	14.83	14.97	15.59	Bridge, LB
Modified by 100 Year Discharge	A	15.28	15.32	15.22	Sirajganj
	B	15.11	15.25	15.16	Bridge, RB
	C	14.60	14.63	14.56	Shahapur
	D	14.82	14.84	14.90	Bhuapur
	E	14.74	14.79	14.95	Bridge, LB

The locations are 4 km upstream of the bridge on the right bank (A), at the bridge on the right bank (B), 4 km downstream of the bridge on the right bank (C), 4 km upstream of the bridge on the left bank (D), at the bridge on the left bank (E).

The difference in maximum water level between the three constriction scenarios is listed in Table 2.7. The mean value over the entire cross-section 4 km upstream and at the bridge is also shown.

Table 2.7: Difference in Simulated Water Level Between the Three Scenarios, in Meters

BRIDGE SPAN BATHYMETRY	Location	4600 -5600	3600 -5600	3600 -4600	Description
Fixed Initial Bathymetry	A	0.42	1.03	0.61	
	B	0.78	1.30	0.52	
	C	0.03	0.44	0.41	
	D	0.15	1.01	0.86	
	E	0.16	1.20	1.04	
	mean A,D	0.29	1.02	0.73	4 km upstream
	mean B,E	0.47	1.25	0.78	at the bridge
Modified by Dominant Discharge	A	0.15	0.51	0.36	
	B	0.28	0.66	0.38	
	C	0.09	0.36	0.27	
	D	0.12	0.61	0.49	
	E	0.14	0.76	0.62	
	mean A,D	0.14	0.56	0.43	4 km upstream
	mean B,E	0.21	0.71	0.50	at the bridge
Modified by 100 Year Discharge	A	0.04	-0.06	-0.10	
	B	0.14	0.05	-0.09	
	C	0.03	-0.04	-0.07	
	D	0.02	0.08	0.06	
	E	0.05	0.21	0.16	
	mean A,D	0.03	0.01	-0.02	4 km upstream
	mean B,E	0.10	0.13	0.04	at the bridge

The constriction effect is most pronounced when the initial bathymetry is used. In that case the increase in water level at the bridge by going from a bridge span of 5,600 to 4,600 m is 0.78 m at the right bank, 0.16 m at the left bank and 0.47 m on the average across the river. At Sirajganj (A) the difference is 0.42 m and at Bhuapur (D) the difference is 0.15 m. The difference between the right and the left bank is due to the location of the abutments in relation to the main flow.

If the bridge span is reduced to 3,600 m the increase in water level compared to the bridge span of 5,600 m will be of the same order of magnitude on both the left and the right bank: 1.2-1.3 m at the bridge, 1.03-1.01 m at Sirajganj and Bhuapur.

This first simulation represents the severe case of a 100 year flood event occurring immediately after completion of the bridge, i.e the immediate effect of the bridge. If the bathymetry is in morphological equilibrium with the new land boundaries (simulations 2, 5 and 8), the water level will drop at the upstream end because the hydraulic resistance decreases. The difference between the three scenarios will then only be about half of the differences using the initial

bathymetry. For example: The mean difference at the bridge between spans of 5,600 m and 4,600 m is now 0.21 m instead of 0.47 m and between 5,600 m and 3,600 m span it is 0.71 m instead of 1.25 m.

At the other extreme, if it is assumed that the bed level has found its equilibrium during a 100 year flood event (simulations 3, 6 and 9), the difference in water level at the bridge will be 0.10 m between 5,600 m and 4,600 m span and 0.13 m between 5,600 m and 3,600 m span. This should be regarded as a lower bound for the increase in water level, while the simulations with the initial bathymetry produce an upper bound.

Velocity

Table 2.8: Maximum and Mean Velocity in the Simulations

BRIDGE SPAN / BATHYMETRY		5,600 m	4,600 m	3,600 m
Initial	Max	3.66	5.21	5.04
Bathymetry	Mean	2.31	2.73	3.03
Ratio		1.58	1.91	1.67
Modified by	Max	3.12	3.83	3.84
Dominant Discharge	Mean	2.21	2.34	2.47
Ratio		1.41	1.64	1.55
Modified by	Max	3.09	3.72	3.89
100 Year Discharge	Mean	2.09	2.19	2.17
Ratio		1.48	1.70	1.79

The maximum velocity is an important parameter for the design of the bank stabilisation works in the initial bathymetry cast, the mean velocity increase from 2.31 m/s with a 5,600 m span to 2.73 m/s with a 4,600 m span and 3.03 m/s with a 3,600 m span. The increase relative to the 5,600 m scenario is 18 percent and 31 percent respectively. If the bathymetry formed by dominant discharge is used, the increases reduce to 6 percent and 12 percent respectively

Effect of Flood Plains

The effect of the flood plains was not included in the simulation, with steady flow, the effect on water level and velocity in the main channel is negligible if there is no conveyance of water over the flood plains. However, even though the resistance to flow is very high on flood plains, some conveyance will take place there. With the construction of the road embankments perpendicular to the stream direction on both sides of the bridge, this will be prevented. Thus, some additional rise in water level can be expected when more flow is forced through the main channel.

The impact of reducing flood plan storage and conveyance has been evaluated separately using the 1-D model.

Sensitivity Runs

The sensitivity of simulated water levels to the cross-slope of the downstream water level boundary was checked. It was found that if the water level varied 0.30 m between the left and the right banks, the difference in water level between the two banks at the upstream boundary would be reduced by about 0.10 m, that is from 0.87 m to 0.77 m in case of a fixed bed run 1. The difference between the scenarios would however, remain unchanged. The sensitivity run showed that the large difference in water level is primarily not a product of inaccurate boundary conditions but a result of the complex hydraulic conditions.

Simulations 3 and 9 were repeated with the resistance number being updated for the new bathymetry. The mean value of the Chezy Number remained the same but the spatial distribution was different. In both simulations, the difference in water level was less than 0.04 m from the earlier runs. Hence, the updating of the bed resistance has a small effect and can be sensibly ignored for the purpose of these simulations.

3. 1-D MORPHOLOGICAL MODELLING OF THE EFFECT OF JAMUNA BRIDGE EMBANKMENTS

The 1-D morphological model (see details in Volume 3, Part 8) has been used to make an assessment of how the proposed narrow option of the Jamuna Bridge affected a flood such the 1988 flood. The distance between the abutments was taken as 3500 m so that the effect of scouring could be seen for the maximum constriction.

Several model runs were made for the simulation period 1 April 1988 to 31 March 1989. The first baseline simulation (No. 1) was for establishing the modelled water levels for the existing topography (i.e. no Jamuna Bridge). The next run (No. 2) was carried out with the bridge in place but without allowing any bed movement (i.e. a fixed bed model). Runs Nos. 3, 4 and 5 were carried out with the fully mobile bed model but with the simulation starting with three different sets of initial conditions. Run No. 3 was begun from the existing bed profile. Run No. 4 was started from the bed profile arrived at by running the morphological (mobile bed) model for five monsoons (1965-1969 inclusive). Run No. 5 was started with the bed profile reached after a 100 monsoon simulations (1965-1989 inclusive repeated four times). The results are presented in tabular form for the increase of the maximum water level above that reached in simulation No. 1 for the existing conditions.

Table 3.1: Results of 1-D Morphological Modelling of the Effect of Jamuna Bridge on the Water Level at the Bridge Axis and Upstream

Simulation No.	Scenario	Increase of Maximum Water Levels (m)		
		Bridge Axis	Sirajganj	Kazipur
1	Present response to 1988 Flood	0.00	0.00	0.00
2	Fixed Bed Model with Narrow Jamuna Bridge	0.58	0.65	0.28
3	Mobile Bed: 1988 Flood in First Year	0.36	0.35	0.14
4	Mobile Bed: 1988 Flood after Five Years	0.31	0.31	0.14
5	Mobile Bed: 1988 Flood after 100 Years	0.33	0.34	0.19

The figures presented show very clearly that scouring at the bridge reduces the maximum rise in the water level by nearly 50 percent. It also shows that these beneficial effects of scouring come into play so quickly that almost the full effect is felt even when the flood arrives in the very first year after the construction of the bridge.

4. INTERPRETATION AND CONCLUSIONS

The primary objective of the study was to evaluate the relative impact of different degrees of channel width constriction on the water levels upstream of the restricting structure.

The simulations have shown the importance of taking into consideration the changes in the bed bathymetry in the vicinity of a major constriction, such as the proposed Jamuna Bridge, when estimating post construction water levels. They have also graphically illustrated the quite significant differences in water level that can occur between left and right banks when the main flow follows a strongly curving path, which in this case was enhanced by the presence of the constriction, and therefore the need to take into consideration 2-D effects. The maximum difference of level between the two banks that was recorded during the simulations was of the order of 0.6 m for the 100 year flow and adjusted average bed morphology.

With any mobile bed river the water level for any given discharge will vary according to the bed topography at the time, which in turn is dependent on the preceding flow conditions. In the case of the construction of an artificial constriction, such as the Jamuna Bridge, this variability is accentuated. The worst case would be the occurrence of a high return period flood soon after the completion of the constriction and before the river bed has had time to adjust to the new dominant flow conditions. The least impact would result from a severe flood following another unusually high flow season.

In order to evaluate this possible range of circumstances, simulations were carried out firstly using typical bathymetry prior to construction, secondly the bedform after construction and adjustment of the channel geometry to the river's dominant shape forming discharge and finally with the bed scoured by the passage of a 100 year flood.

The inference from the 1-D hydrodynamic modelling (Part 7 of this report) is that the water levels at Sirajganj resulting from the 1988 flood would have been approximately 0.4 m higher after construction of Jamuna Bridge (4600 m opening) than before. Chapter 3 of this part of the report indicates that this value would be nearly halved within a year of construction. In other words, in a 100 year flood, the effect of the Jamuna Bridge embankments, after the bed has had time to adjust to the new situation, would be to cause a rise in water level at Sirajganj of the order of 0.2 m.

The effect of increasing the width between the bridge abutments to 5,600 m is to reduce the post-construction design water level 4 km north of the bridge by between 0.29 m and 0.14 m, the greatest impact being on the worst case scenario of a design flood occurring soon after construction.

Narrowing the opening to 3600 m has a relatively greater effect with an increase in water level 4 km north of the bridge of between 0.73 m and 0.43 m more than the increase for the 4600 m opening. This is consistent with the conclusion that the 4600 m opening should be considered as a practical minimum.

The timescale for reaching morphological equilibrium with the a steady dominant discharge is of the order of 100 days. Therefore in practice

the new regime is likely to be established within two years of completion of the bridge embankments.

The passage of a 100 year flood will result in considerable additional scour at the bridge and if this were to fully develop the rise in water level due to the bridge could be as little as 0.10 m. However the estimated time for such a development is about 14 days and it is the maximum water levels that arise when the flood first peaks that are critical for the design of flood embankments and river training works.

The simulation also provided data on the mean sectional velocity and the maximum point value in addition to the scour pattern around the abutments. The ratio of maximum to mean velocity ranged from 1.4 to 1.9 with the highest velocities occurring around the upstream nose of the right bank stabilised abutment. In the extreme (3600 m opening) scenario a maximum depth averaged velocity of 5.2 m/s was simulated. This dropped to 3.8 m/s for the 4,600 m opening once the bed morphology had adjusted. Increasing the opening to 5,600 m resulted in a very significant reduction in both mean and maximum velocities.

The 2-D model does not replicate the local scour due to 3-D effects and thus cannot fully reproduce the scour associated with structural intervention. The pattern of bed erosion shown in Figure 2.3 does however illustrate the general pattern. It is of note that deep scour is indicated along both banks downstream of the bridge but particularly on the right bank. This implies that fairly rapid bank erosion must be expected in these reaches following completion of the embankment works, or even during their construction once they start deflecting the flow.

FIGURES

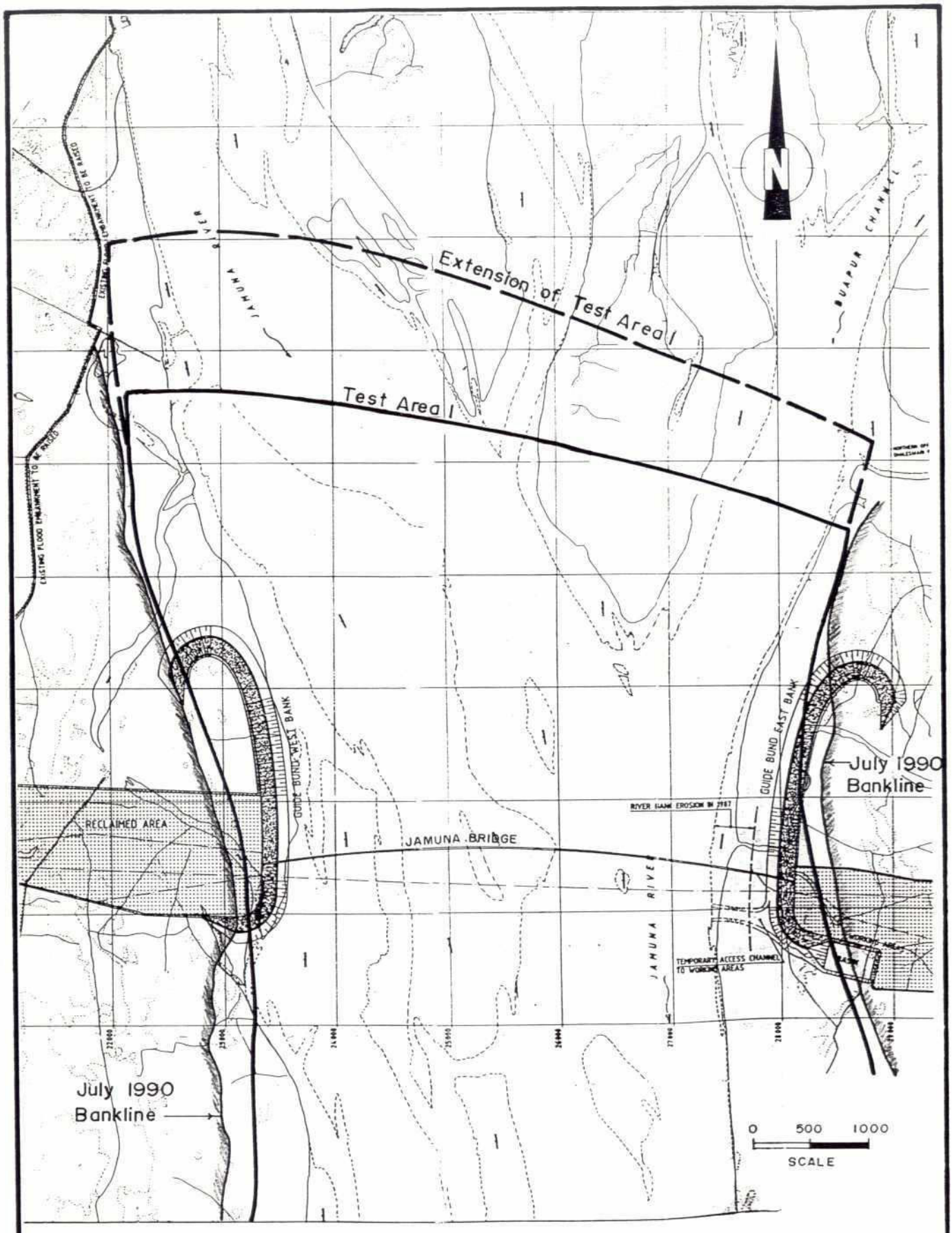

Source: JMB Phase II Study - Feasibility Report - Volume II - Figure no. D1 (RPT/NEDECO/BCL) based aerial photography of February 1987.

BRTS 2-D Numerical Modelling of River Constriction Effects

Layout of Jamuna Bridge Embankments	**Vol.4** **Part 14**
	Figure 1.1

Computational Grid

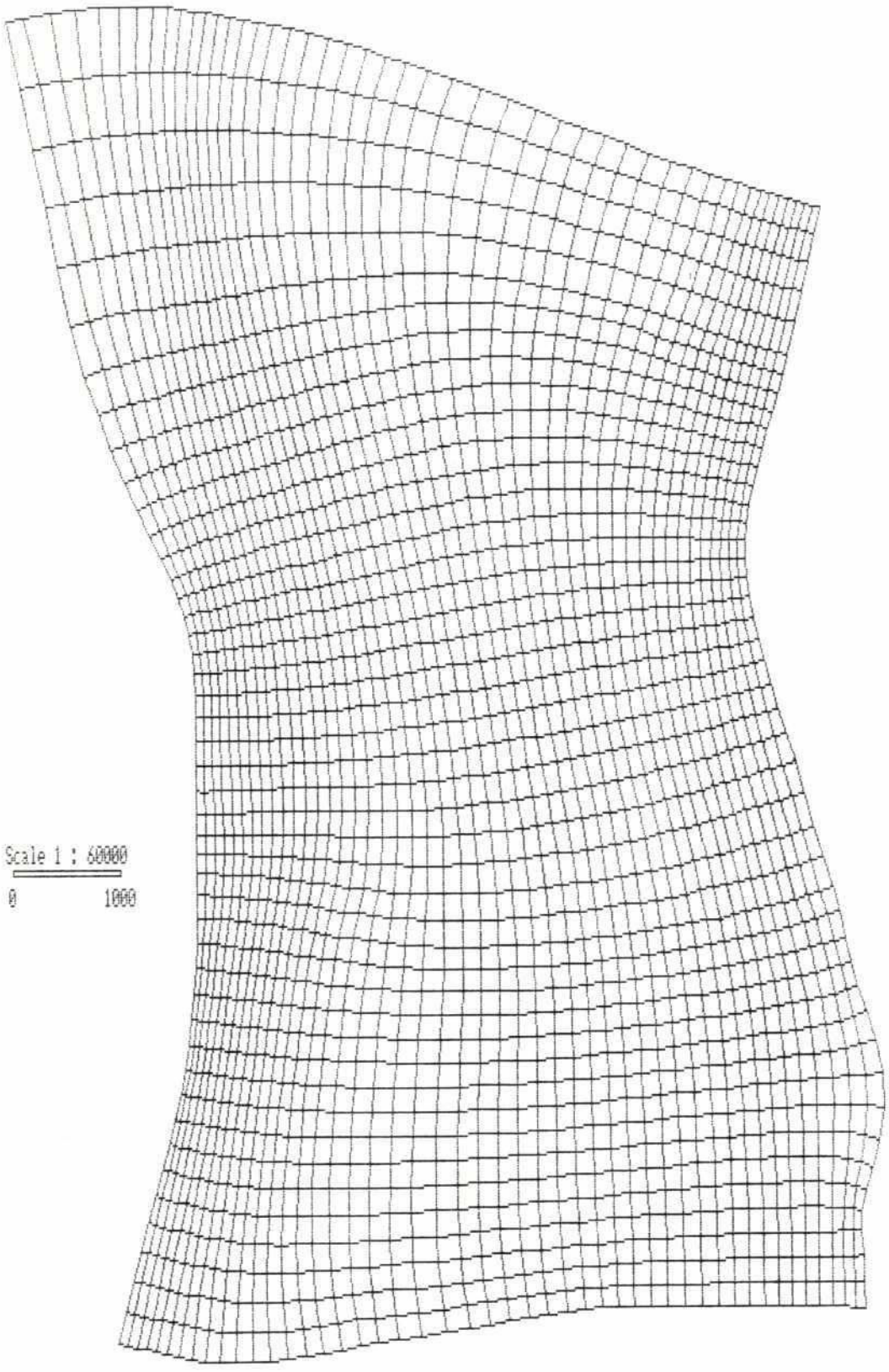

BRTS 2-D Numerical Modelling of River Constriction Effects

Computational Grid	**Vol.4** Part 14
	Figure 2.1

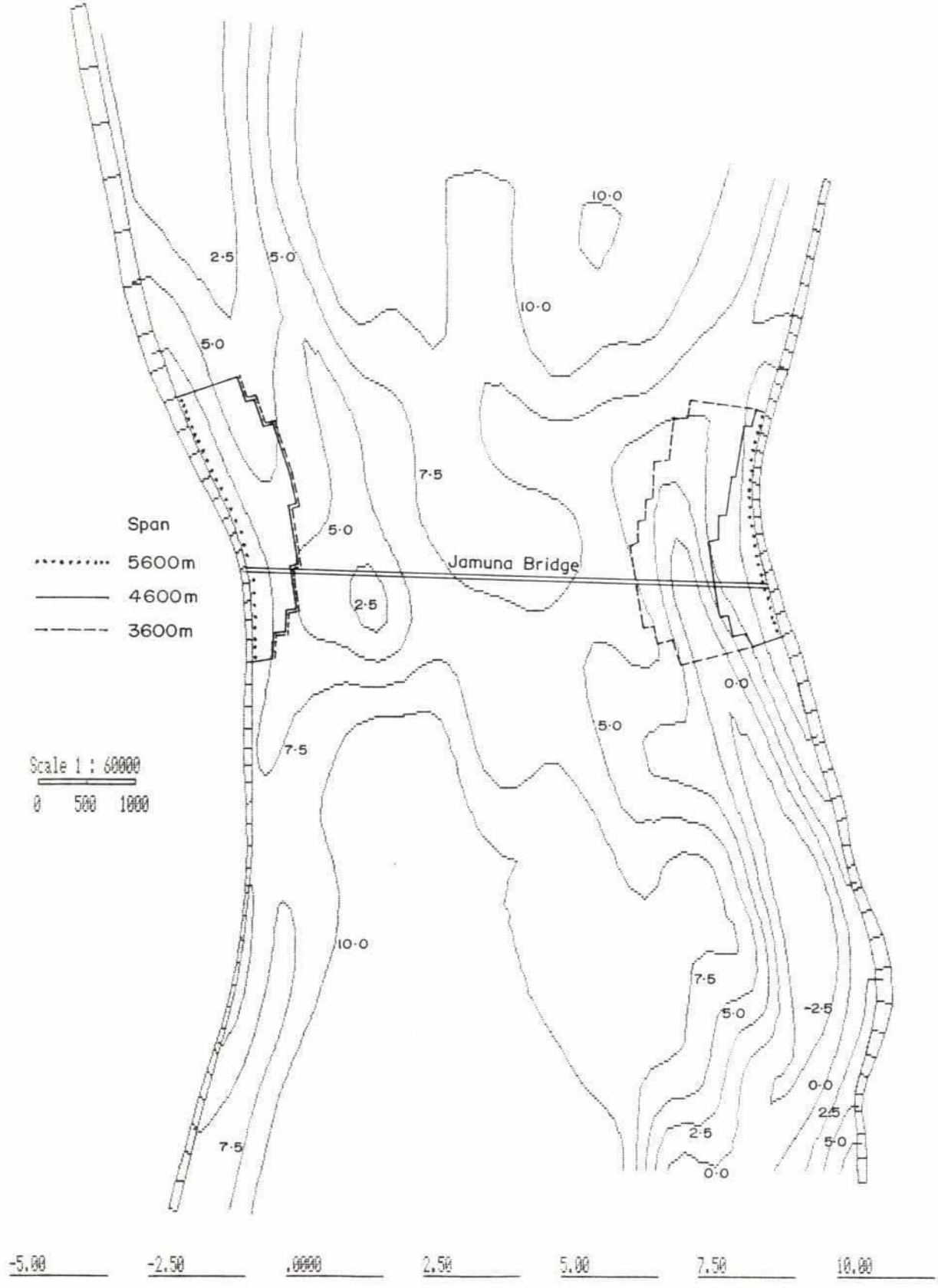

BRTS 2-D Numerical Modelling of River Constriction Effects

Bathymetry Surveyed by BRTS in July 1990, Test Area 1

Vol.4 Part 14

Figure 2.2

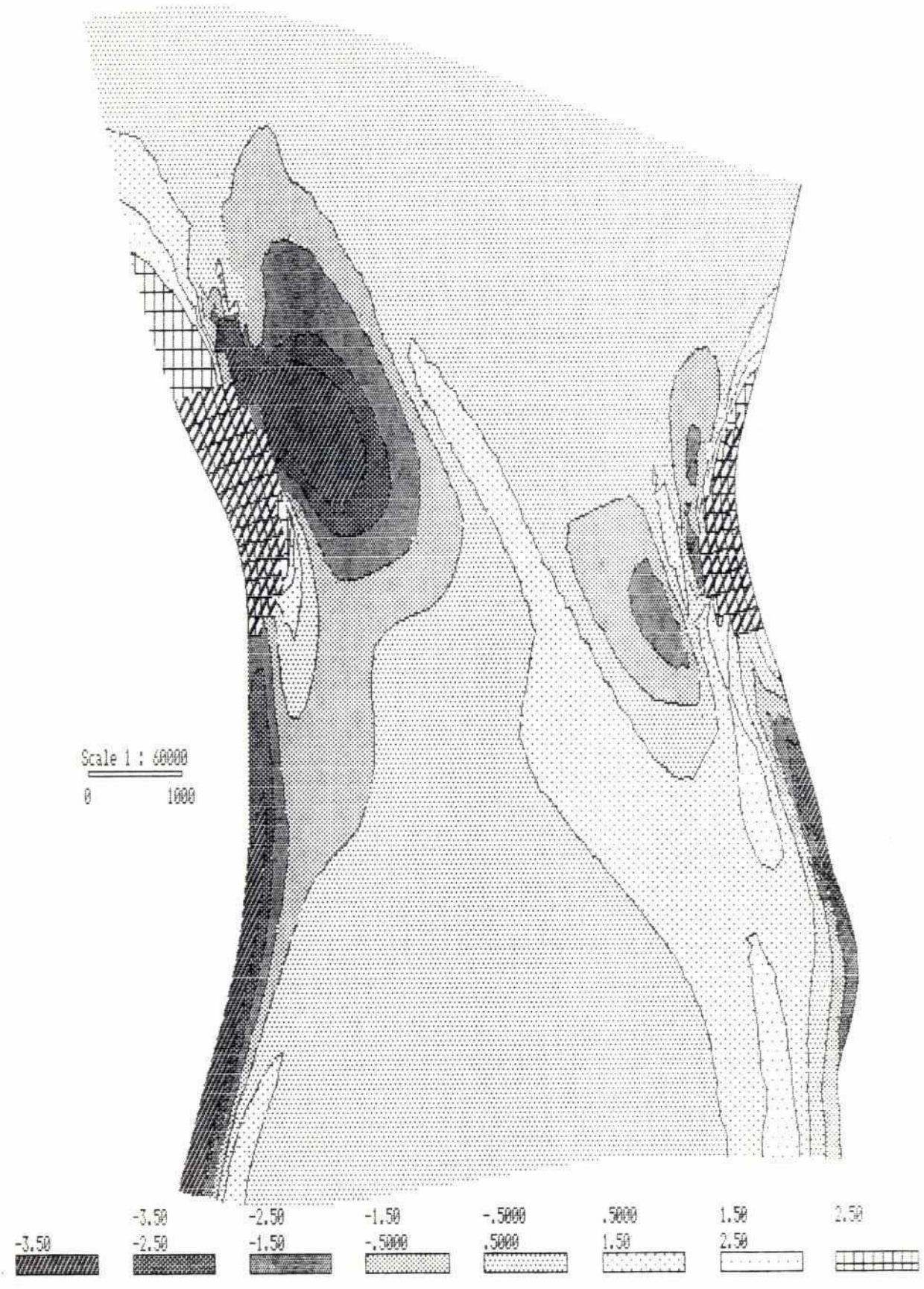

BRTS 2-D Numerical Modelling of River Constriction Effects

Additional Erosion/Deposition Caused by Bridge, 100 Year Discharge	Vol.4 Part 14 Figure 2.3

Jamuna Bridge, 100 Year

20f

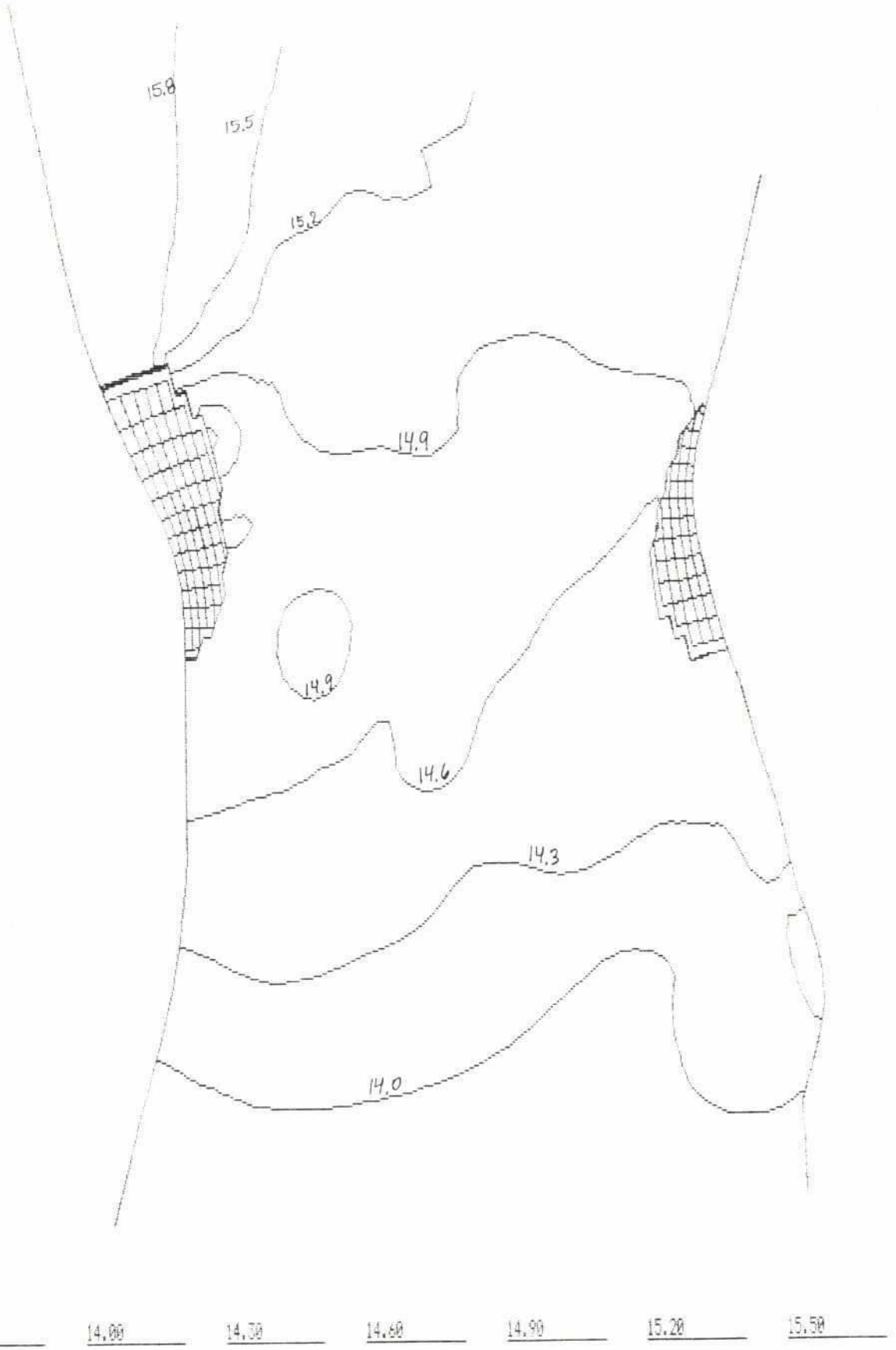

BRTS 2-D Numerical Modelling of River Constriction Effects

Simulated Water Level, 100 Year Discharge with Jamuna Bridge included	**Vol.4**	**Part 14**
	Figure 2.4	

Jamuna Bridge, 100 Year

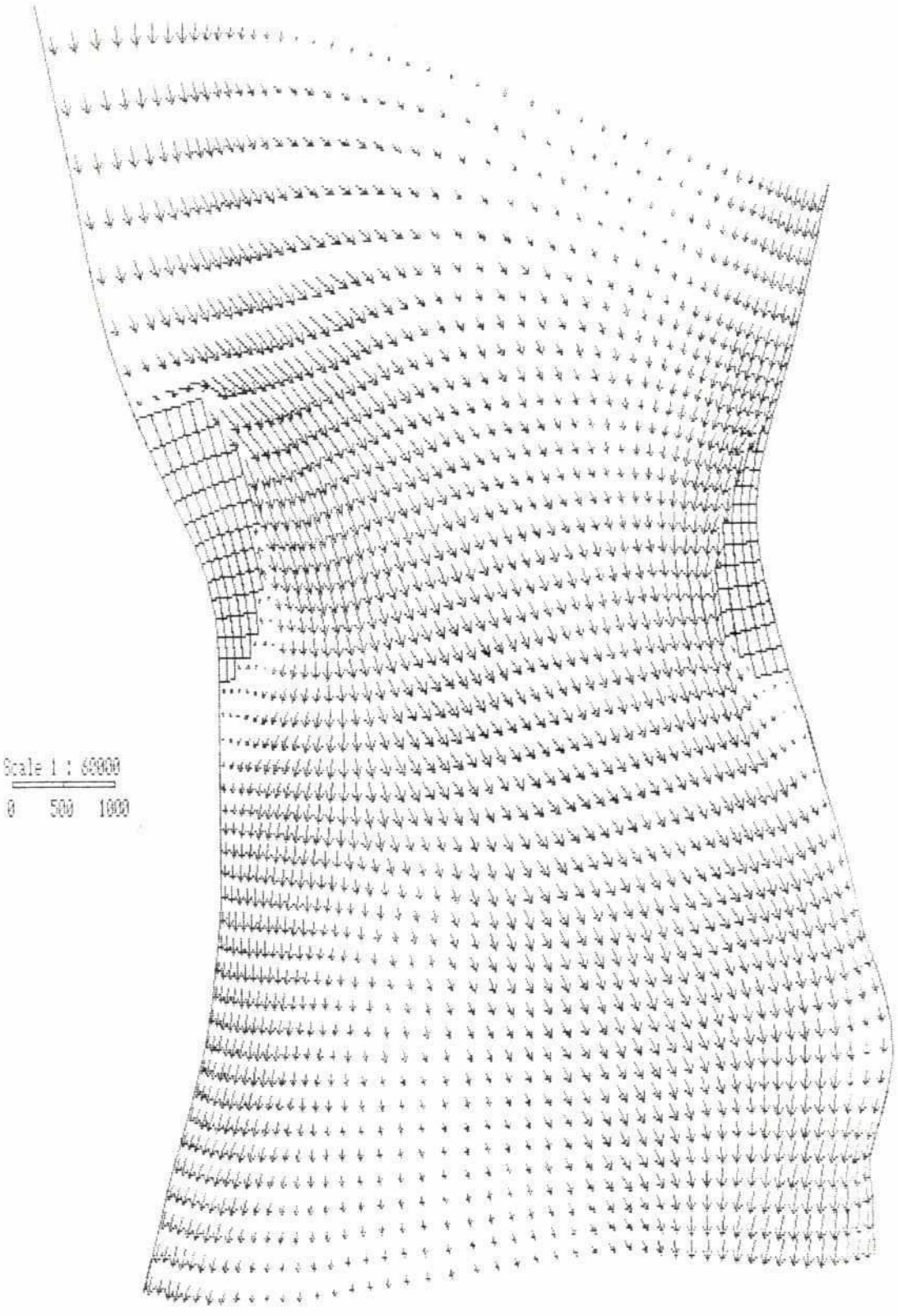

BRTS 2-D Numerical Modelling of River Constriction Effects

Simulated Velocity, 100 Year Discharge	Vol.4 Part 14
	Figure 2.5